

**NBSIR 87-3640**

# Investigation of L'Ambiance Plaza Building Collapse in Bridgeport, Connecticut

Center for Building Technology  
National Engineering Laboratory  
National Bureau of Standards  
Gaithersburg, MD 20899



QC

100

DEPARTMENT OF COMMERCE

NATIONAL BUREAU OF STANDARDS

.U56

#87-3640

1987

C.2



**NBSIR 87-3640**

NBSC  
QC100  
.1156  
N. 87-3640  
1987  
C-2

# **Investigation of L'Ambiance Plaza Building Collapse in Bridgeport, Connecticut**

---

Charles G. Culver  
Charles F. Scribner  
Richard D. Marshall  
Felix Y. Yokel  
John L. Gross  
Charles W. Yancey  
Erik M. Hendrickson

Center for Building Technology  
National Engineering Laboratory  
National Bureau of Standards  
Gaithersburg, MD 20899

Sponsored by:

Occupational Safety and Health Administration  
U.S. Department of Labor  
Washington, DC 20001

Issued September 1987



---

**U.S. DEPARTMENT OF COMMERCE, Clarence J. Brown, Acting Secretary**  
**NATIONAL BUREAU OF STANDARDS, Ernest Ambler, Director**



## ABSTRACT

Results from an investigation to determine the cause of the collapse of the L'Ambiance Plaza building on April 23, 1987 are presented. The building was being constructed using the lift-slab method; collapse occurred during construction. The investigation included on-site inspections immediately following the collapse, review of eyewitness accounts of the collapse, review of project documentation, laboratory and field tests and analyses of the structure. Several potential failure mechanisms were investigated. The most probable cause of the collapse was determined to be loss of support at a lifting jack in the west tower during placement of an upper level package of three floor slabs. The loss of support was likely due to excessive deformation of the lifting angle in a shearhead followed by a lifting nut slipping off the lifting angle of the shearhead. The postulated failure mechanism was duplicated in laboratory experiments. The local failure propagated as loads were redistributed. The remaining jack rods along column line E supporting the package of floor slabs slipped off the lifting angles and the slabs failed in flexure and shear. These slabs fell causing the lower level slabs to fail.

Keywords: building; collapse; concrete; construction failure; lift-slab construction; post-tensioned concrete; progressive collapse.

## EXECUTIVE SUMMARY

On April 23, 1987, the L'Ambiance Plaza building under construction in Bridgeport, Connecticut, collapsed killing 28 construction workers. This was the largest loss of life in a U.S. construction accident since 51 workmen were killed in the collapse of a reinforced concrete cooling tower under construction at Willow Island, West Virginia, in 1978.

On April 24, 1987, the Occupational Safety and Health Administration, Department of Labor, requested that the National Bureau of Standards (NBS) carry out an investigation of the failure to determine the most probable cause of the collapse. NBS conducted an investigation under the terms of an Interagency Agreement established between OSHA and NBS in 1973. Under this agreement, NBS conducts scientific and technical investigations in connection with failures under the jurisdiction of OSHA.

The NBS investigation commenced immediately upon arrival of NBS personnel on the site on April 24, 1987. Data were collected and assessments made of the nature of the failure of various elements of the structure during and subsequent to the rescue efforts. In addition to observations from the on-site inspection, the NBS team in carrying out its investigation used:

- (1) information on the collapse obtained from interviews of survivors and eyewitnesses
- (2) project documentation including design specifications, plans, shop drawings, construction records, testing laboratory reports and project correspondence
- (3) laboratory tests of samples removed from the collapsed structure
- (4) data obtained from a subsurface investigation at the site after the collapse, and
- (5) analytical studies, including computer analyses.

L'Ambiance Plaza was being constructed using the lift-slab method. The floor and roof slabs were cast one on top of the other at ground level. The floor slabs were two-way post-tensioned flat plates. After post-tensioning, the slabs were lifted by hydraulic jacks and secured to the columns. The building was to be a 13-story structure with three levels of a five level parking garage located under the building. It consisted of two offset rectangular towers, designated in this report as the east tower and the west tower. At the time of the collapse, erection of the slabs was over half complete. The collapse occurred during placement of wedges under a package of three slabs being parked in a temporary position during erection of the building. In the collapse, all the floor slabs fell trapping the workmen involved in the lifting operation and those on the lower floors engaged in other phases of the construction.

A number of possible mechanisms which may have initiated the collapse were considered in carrying out the investigation. These included: (1) lateral instability (2) individual column instability, (3) floor slab failure, (4) weld failure, (5) foundation failure, (6) failure due to lateral soil pressure and (7) loss of support of floor slab. Field observations, eyewitness accounts,

laboratory tests and analytical studies were used to assess the likelihood of each failure mechanism.

Based on the results of the investigation, NBS concludes that:

1. The most probable cause of the collapse was failure of the lifting system in the west tower during placement of a package of three upper level floor slabs. The failure most probably began below the most heavily loaded jack (column E4.8) or an adjacent jack (column E3.8). Excessive deformations occurred in the lifting angle of the shearhead at the location of the initial failure. This was followed by one of the jack rods in the lifting assembly slipping off the lifting angle in the shearhead supporting the package of three slabs. This failure mechanism was duplicated in laboratory experiments. The local failure propagated as loads were redistributed and the remaining jack rods along column line E slipped off the lifting angles and the package of three slabs failed in flexure and shear. These slabs fell, causing the lower level slabs to fail. This resulted in the collapse of the entire west tower. Consequently, the east tower collapsed due to one or more of the following factors: (a) forces transmitted to it by the west tower collapse, (b) damage to the post-tensioning tendons caused by falling debris from the west tower, or (c) lateral instability caused by falling debris from the west tower.
2. The quality of materials in the structure was generally in accordance with the project plans and specifications and did not play a significant role in initiating the collapse.
3. There were a number of deviations from the project plans and specifications in the structure as built, but these did not play a significant role in initiating the collapse.
4. It is unlikely that the horizontal jack used to plumb the structure initiated the collapse.
5. The reserve capacity against lateral instability was small. It does not appear, however, that lateral instability was the initial cause of the collapse. Inadequate resistance to lateral instability may have caused the collapse of the east tower.
6. It is unlikely that lateral earth pressure acting against the basement wall on the north side of the structure caused the building to collapse.
7. It is unlikely that differential foundation settlements caused the building to collapse.

ABSTRACT . . . . .	iii
EXECUTIVE SUMMARY . . . . .	iv
1. INTRODUCTION . . . . .	1
1.1 BACKGROUND . . . . .	1
1.2 OBJECTIVE AND SCOPE OF THE INVESTIGATION . . . . .	1
1.3 ORGANIZATION OF THE REPORT . . . . .	2
2. CONDUCT OF THE INVESTIGATION . . . . .	5
2.1 SITE INVESTIGATION . . . . .	5
2.2 LABORATORY TESTS . . . . .	5
2.3 WITNESS INTERVIEWS . . . . .	6
2.4 REVIEW OF DOCUMENTS . . . . .	6
2.5 SUBSURFACE INVESTIGATIONS . . . . .	6
2.6 ANALYTICAL STUDIES . . . . .	6
3. DESCRIPTION OF THE STRUCTURE AND CONSTRUCTION . . . . .	8
3.1 INTRODUCTION . . . . .	8
3.2 DESCRIPTION OF THE STRUCTURE . . . . .	8
3.3 LIFT SLAB CONSTRUCTION DETAILS . . . . .	9
3.4 CONSTRUCTION SCHEDULE . . . . .	12
4. DESCRIPTION OF COLLAPSE . . . . .	26
4.1 INTRODUCTION . . . . .	26
4.2 ACTIVITIES PRECEDING COLLAPSE . . . . .	26
4.3 EYEWITNESS ACCOUNTS OF COLLAPSE . . . . .	27
4.4 OBSERVATIONS OF DEBRIS . . . . .	30
4.4.1 Overall Collapse . . . . .	30
4.4.2 Floor Slabs . . . . .	32
4.4.3 Shearheads . . . . .	33
4.4.4 Welds . . . . .	34
4.4.5 Additional Observations . . . . .	35
4.4.6 Detailed Observations of Stage IV Columns-West Tower . . . . .	35
4.4.7 Summary . . . . .	37
5. LABORATORY TESTS . . . . .	81
5.1 INTRODUCTION . . . . .	81
5.2 TESTS OF CONCRETE SPECIMENS . . . . .	81
5.2.1 Sampling and Testing Procedures . . . . .	81
5.2.2 Results of Tests . . . . .	82
5.2.3 Comparison of Strengths of Core Samples and of Quality Control Samples . . . . .	82
5.3 TESTS OF STEEL SPECIMENS . . . . .	83
5.3.1 Sampling and Testing Procedure . . . . .	83
5.3.2 Results of Tests . . . . .	84
5.3.3 Comparison of Results with ASTM Standards and Mill Tests . . . . .	85
5.4 TESTS OF WELDMENTS . . . . .	85
5.4.1 Sampling and Testing Procedure . . . . .	85
5.4.2 Results of Strength Tests . . . . .	87
5.4.3 Metallography Results . . . . .	88
5.4.4 Fractography Results . . . . .	89
5.5 AUXILIARY TESTS . . . . .	91
5.5.1 Introduction . . . . .	91
5.5.2 Tests of Post-tensioning Strands . . . . .	91
5.5.2.1 Sampling and Testing Procedure . . . . .	91



5.5.2.2	Results of Tests . . . . .	92
5.5.2.3	Comparison of Results with ASTM A 416 . . . . .	93
5.5.3.	Tests of Jack Rods . . . . .	93
5.5.3.1	Sampling and Testing Procedure . . . . .	93
5.5.3.2	Results of Tests . . . . .	94
5.5.3.3	Metallography Results . . . . .	94
5.5.4	Tests of Shearheads . . . . .	95
5.5.5	Lifting Assembly . . . . .	97
5.6	SUMMARY . . . . .	102
6.	SUBSURFACE EXPLORATION . . . . .	147
6.1	INTRODUCTION . . . . .	147
6.2	EXPLORATION PROCEDURES . . . . .	148
6.3	EXPLORATION RESULTS . . . . .	149
7.	STRUCTURAL ANALYSIS . . . . .	154
7.1	INTRODUCTION . . . . .	154
7.2	FLOOR SLABS . . . . .	154
7.2.1	Computer Model . . . . .	154
7.2.2	Results of Analyses . . . . .	155
7.3	COLUMN INSTABILITY . . . . .	159
7.4	LATERAL LOAD ANALYSIS . . . . .	160
7.4.1	Introduction . . . . .	160
7.4.2	Frame Stability . . . . .	160
7.4.3	Horizontal Jacking Load . . . . .	164
7.4.4	Earth Pressure . . . . .	165
7.4.5	Wind Loading . . . . .	170
7.5	DIFFERENTIAL FOUNDATION SETTLEMENTS . . . . .	170
8.	EVALUATION OF CONSTRUCTION PRACTICES . . . . .	201
8.1	INTRODUCTION . . . . .	201
8.2	COMPARISON WITH PROJECT SPECIFICATIONS . . . . .	201
8.2.1	Construction Materials . . . . .	201
8.2.2	Foundations . . . . .	201
8.2.3	Column Sections . . . . .	202
8.2.4	Lateral Bracing . . . . .	202
8.2.5	Welding . . . . .	203
8.2.6	Post-Tensioning Tendon Detail . . . . .	204
9.	ANALYSIS OF COLLAPSE . . . . .	206
9.1	INTRODUCTION . . . . .	206
9.2	REVIEW OF POTENTIAL FAILURE MECHANISMS . . . . .	206
9.3	PROBABLE CAUSE OF COLLAPSE . . . . .	209
9.4	PROBABLE SEQUENCE OF COLLAPSE . . . . .	211
10.	CONCLUSIONS . . . . .	222
11.	ACKNOWLEDGEMENTS . . . . .	225
12.	REFERENCES . . . . .	226
	APPENDICES	
Appendix A	Detailed Observations of Stage IV Columns West Tower . . . . .	228
Appendix B	Geotechnical Engineering Investigation . . . . .	236
Appendix C	Resistance Criteria for Columns and Floor Slabs . . . . .	307



## 1. INTRODUCTION

### 1.1 BACKGROUND

At approximately 1:30 p.m. on April 23, 1987, the L'Ambiance Plaza, a residential apartment building under construction in Bridgeport, Connecticut collapsed, killing 28 construction workers. This was the largest loss of life in a U.S. construction accident since 51 workmen were killed in the collapse of a reinforced concrete cooling tower under construction at Willow Island, West Virginia in 1978 [1].

L'Ambiance Plaza was being constructed using the lift-slab method. In lift-slab construction, floor and roof slabs are cast one on top of the other at ground level. The floors are usually two-way post-tensioned flat plates of either regular or lightweight concrete. After post-tensioning, the slabs are lifted to their final positions by hydraulic jacks and are secured to the columns. By casting the slabs at ground level, lift-slab construction can eliminate 90 percent of the formwork required for cast-in-place construction and reduces labor requirements [15]. Cost savings and speed of construction are two primary advantages claimed for lift-slab construction [3].

L'Ambiance Plaza was to be a 13-story building with three levels of a five-level parking garage located under the building. A sketch of the building is shown in figure 1.1.1. At the time of the collapse, erection of the slabs was over half complete; i.e., three levels of the parking garage and three to six levels of the towers were in place. The collapse occurred while a group of three slabs was being placed in temporary position. In the collapse, all the floor slabs fell, trapping the workmen involved in the lifting operation and those on the lower floors engaged in other phases of the construction.

An investigating team from the Occupational Safety and Health Administration (OSHA) was on site shortly after the collapse. On April 24, 1987, OSHA requested technical assistance from the National Bureau of Standards (NBS) in investigating the collapse. A team of engineers from NBS arrived on the site of the collapse at 6:00 p.m. that same day.

### 1.2 OBJECTIVE AND SCOPE OF THE INVESTIGATION

NBS carried out the investigation for the Occupational Safety and Health Administration under the terms of an Interagency Agreement established between OSHA and NBS in 1973. Under this agreement, NBS conducts scientific and technical investigations in connection with failures under the jurisdiction of OSHA. The objective of the NBS investigation was to determine the most probable physical cause of the collapse. The study did not include evaluation of the design of the completed structure.

The NBS investigation commenced immediately upon arrival of the team on the site on April 24, 1987. Data were collected and assessments made of the nature of the failure of various elements of the structure while the rescue efforts proceeded. Special efforts were made to ensure that the investigation did not interfere with these rescue efforts. In addition to the on-site inspection, the NBS team in carrying out its investigation used: (1) information on the

collapse obtained from interviews of survivors and eyewitnesses, (2) project documentation including design specifications, plans, shop drawings, construction records, testing laboratory reports and project correspondence, (3) laboratory tests of samples removed from the collapsed structure, (4) data obtained from a subsurface investigation at the site after the collapse, and (5) analytical studies.

### 1.3 ORGANIZATION OF THE REPORT

This report is organized in 12 Chapters and Appendices:

Chapter 2 describes the procedure followed by the NBS team in conducting the investigation. The procedure included on-site investigations, laboratory tests, witness interviews, review of project documentation, subsurface investigations and analytical studies.

Chapter 3 describes the general layout of the structure, the structural elements involved in lift-slab construction, and the status of construction at the time of the collapse. A description of the jacking system used to erect the building and its operation are included.

Chapter 4 summarizes construction activities preceding the collapse. The configuration of the structure at the time of the collapse and eyewitness accounts of the sequence of events associated with the collapse are presented. Detailed observations of the debris and the performance of the structural components in the collapse are summarized.

Chapter 5 describes the NBS laboratory testing program and the test results. The program included tests of the construction materials and tests of structural components and subassemblies.

Chapter 6 describes the procedures used and results obtained from subsurface explorations conducted to explore the in-situ conditions with respect to support of the footings and backfill conditions behind a basement wall.

Chapter 7 presents the results of analytical studies conducted to evaluate the loads on the structure during erection. Deformations and stresses in the floor slabs and support reactions for the lifting jacks and columns were determined. Column stability, frame stability, effects produced by a horizontal jack used to plumb the building, effects due to earth pressure on a basement wall and wind loads were analyzed.

Chapter 8 presents a comparison of the results of the laboratory tests and field tests with the project specifications.

Chapter 9 addresses the collapse of the structure. A number of possible failure scenarios are reviewed. The probable cause of the collapse is identified and the sequence of events in the collapse is presented.

Chapter 10 presents the conclusions reached by the NBS investigation team.

Chapter 11 includes acknowledgements of individuals providing assistance in the investigation.

Chapter 12 lists the references cited in the text.

The Appendices present material used in conducting the investigation. Detailed observations of the condition of the columns in the upper portion of the west tower, data collected in the subsurface exploration and resistance criteria used in analyzing the performance of the columns and floor slabs are included.

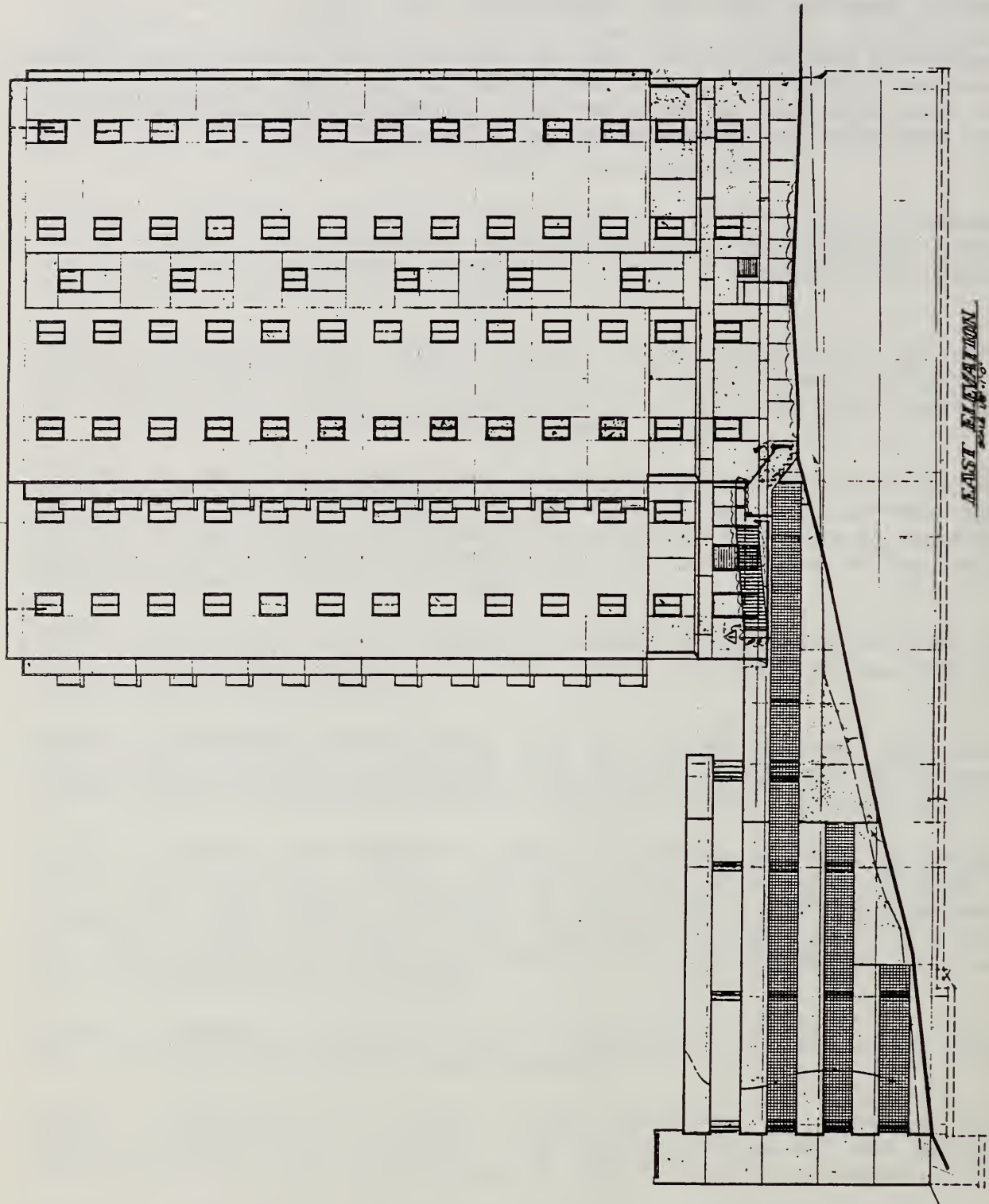


Figure 1.1.1 Proposed L'Ambiance Plaza Building

## 2. CONDUCT OF THE INVESTIGATION

### 2.1 SITE INVESTIGATION

The initial on-site phase of the investigation was conducted from April 24 through May 1, 1987. During this period data were collected on the collapsed structure. Photographs and video tape records were made as the rescue efforts proceeded and as debris was removed from the site. Sketches were made of the pattern of deformation of the columns and the orientation of the collapsed floor slabs. Detailed measurements were also made of several columns as they were removed from the debris. Several floor slabs at different levels in the building were identified as they were removed from the debris in order that core samples could be taken later.

The debris removed from the site was transported by the City of Bridgeport to a landfill at Seaside Park in south Bridgeport. Samples of the construction materials were collected on April 29-30 and transported to the National Bureau of Standards on May 1 for testing. The materials included: (1) concrete core samples from the floor slabs and shear walls (taken at both the landfill and at the building site), (2) portions of columns and portions of columns containing splices and weld blocks\* (3) post-tensioning strand from the floor slabs and unused strand at the site, (4) one large and one small hydraulic jack, jack rods, nuts and end fittings, (5) several shearheads and wedges and (6) a large portion of a floor slab with the shearhead and post-tensioning strand intact.

Subsequent visits were made to the building site and the landfill during the months of May, June, July and August to collect additional data and material for testing. Elevations at the column locations were measured after the debris was removed to determine whether settlement of the footings had occurred. Additional measurements were made of the columns and welding details, including both shop and field welds. Samples of several weld fractures were also taken for laboratory analysis.

### 2.2 LABORATORY TESTS

Two types of laboratory tests were conducted. The first included standard tests for evaluating material properties and welding details. Compression tests and splitting tensile tests were conducted on the concrete cores. Tensile tests, metallographic and chemical analyses, hardness tests and fracture analyses were conducted on the column steel and weldments. Tensile tests were also conducted on the post-tensioning strand.

The second type of test involved individual components and assemblies of the lifting system. Tensile tests were carried out on the jack rods and attachments. Load tests were conducted on the shearhead-column assembly and the lifting assembly (jack, jack rods and attachments, shearhead).

---

\* Terminology used in this report follows that used in the L'Ambiance Plaza project documentation

### 2.3 WITNESS INTERVIEWS

Witness statements obtained by the Bridgeport City Police in the first few days following the collapse and by the Connecticut State Police and OSHA staff over the next several weeks were reviewed. Witnesses included construction workers on the site at the time of the collapse, eyewitnesses in the vicinity of the site at the time of the collapse and other parties with information related to the construction. A total of 48 statements were reviewed. OSHA arranged for the NBS staff to reinterview a number of the witnesses to clarify points made in their original statements and to obtain additional information not included in the initial interviews.

### 2.4 REVIEW OF DOCUMENTS

Following the collapse, the State of Connecticut seized a variety of documents from the construction site. Copies of these documents were provided to NBS by the Connecticut Department of Public Safety. This material included: (1) the daily construction logs, (2) testing laboratory reports, (3) project correspondence and (4) design and construction drawings. Copies of the project specifications and the architectural, structural and mechanical-electrical drawings were obtained from the City of Bridgeport. Wind speed data and temperature records were obtained from the weather station at the Bridgeport airport. Additional material obtained by OSHA as the investigation proceeded included pre-collapse photographs of the structure, mill test reports and the construction log of the lifting subcontractor.

### 2.5 SUBSURFACE INVESTIGATIONS

Subsurface investigations were conducted at the building site between May 27 and June 17 after the majority of the debris had been removed. The objective of these investigations was to evaluate the in-situ condition of the foundations and the backfill behind the retaining wall on the north side of the building. Soil borings were taken in the fill material behind the retaining wall and core borings were taken at a select number of column footings. The core borings penetrated directly through the column footings, the underlying soil, weathered or fractured rock, and into underlying bedrock deposits. Test pits were dug adjacent to a few footings in order to permit visual inspection of the footings and the supporting soil or rock. One test pit was dug behind the retaining wall to retrieve soil samples for testing. In-situ tests included standard penetration tests and pressuremeter tests. Laboratory studies included routine classification tests and direct shear tests on re-constituted soil samples.

### 2.6 ANALYTICAL STUDIES

The structure was analyzed for loadings encountered during erection. Loadings induced by a number of possible conditions that could have precipitated collapse of the structure were also studied.

Structural analyses were performed to determine deformations, stresses and support reactions for the floor slabs. Stability of the individual columns was analyzed. A two-dimensional analysis of the structural framing system and a



simplified column model were used to analyze the lateral stability of the structure. Effects produced by a hydraulic jack used to plumb the building during erection were also determined. Lateral displacements, internal forces, and the ability of the structure to resist these lateral forces resulting from earth pressure on a basement wall were evaluated. The effect of wind loads and differential foundations settlements on the performance of the structure were also considered.

### 3. DESCRIPTION OF THE STRUCTURE AND CONSTRUCTION

#### 3.1 INTRODUCTION

This chapter describes the structure and summarizes the construction schedule for erection of the structural system. A description of the jacking system and its operation during lifting of the slabs is included.

#### 3.2 DESCRIPTION OF THE STRUCTURE

A plan view showing the column layout and shearwall locations is given in figure 3.2.1. The structural system consisted of steel columns (W and HP shapes) and two-way unbonded post-tensioned concrete flat plates with shearwalls at four perimeter and four interior locations. The building consisted of two offset rectangular towers, each 112 ft (34 m) by 62 ft (19 m) in plan. These towers will be referred to in this report as the east tower and the west tower.

An elevation view of the west tower is shown in figure 3.2.2. The perimeter shearwalls are not shown. The status of construction and position of the floor slabs at the time of collapse are discussed in Chapter 4. The floor level designations in figure 3.2.2 are those used in the plans and will be used throughout this report. Levels C, D and E are the parking garage. The story heights were the same throughout the height of the building except at level C and at ground level. The column schedule is given in table 3.2.1.

Each tower of the building was erected independently. The slabs of the two towers were connected by cast-in-place reinforced concrete pour strips in the center portion of the building. The pour strips were cast after the corresponding lift slabs in the two towers of the building were secured in their final position.

The three levels of parking garage were below ground level on the north side of the building. A basement wall extended from level E to level C. This wall was in contact with the floor slab at these levels and transmitted lateral soil pressure to the structure. The interior and perimeter shearwalls terminated at level 11. The shearwalls were connected to the floor slabs by reinforcing bars which protruded from the precast lift slabs and were embedded into the cast-in-place shearwalls.

The floor slabs were 7-in (178 mm) thick two-way unbonded post-tensioned flat plates. Regular weight concrete was used throughout. The location of the post-tensioning tendons is shown schematically in figure 3.2.3. Pipe chase openings shown are for a typical floor. At each line in the figure, there were a number of tendons. The tendons in the north-south direction were approximately uniformly spaced over the length of the slab. In the east-west direction, the tendons were banded generally following the column lines. Due to the presence of the elevator shaft, the tendons along column line E in the west tower were splayed as shown in figure 3.2.3. It should be noted that the centroids of the banded tendons, particularly those at the exterior column lines, do not coincide with the column centerlines. A note on the tendon layout drawing indicated the stressing end and dead end were reversed on some of the transverse tendons (north-south direction) from that shown in figure

3.2.3. This would not be expected to have any influence on the performance of the floor slabs. A nominal amount of bonded reinforcement was used in the vicinity of the columns and shearwalls.

The building was supported by spread footings which, in accordance with the plans, were to rest on the underlying bedrock. A plan view of the footings showing the footing size and elevation (referenced to the ground floor elevation) is given in figure 3.2.4. Figure 3.2.5 shows a typical detail of an interior column footing.

The footings were designed for a  $7 \text{ ton/ft}^2$  (670 kPa) bearing pressure and varied in size in accordance with the supported load. Along the basement walls on the north and east side of the building the columns and walls were supported by combined footings. The shearwalls were supported by combined rectangular footings, which also supported adjacent columns and basement walls, and in one case an adjacent elevator shaft.

### 3.3 LIFT SLAB CONSTRUCTION DETAILS

The lift-slab construction process used at L'Ambiance Plaza consisted of casting floor slabs at ground level, raising those floor slabs to the desired elevation using hydraulic jacks, and fixing the floor slabs in position mechanically. The casting of floor slabs one on top of another on a slab on grade was straightforward. This procedure eliminated the need for shoring or other formwork underneath each slab, and required only that a side form for the slabs be constructed.

Floor slabs were raised to the desired elevation using a system of hydraulic jacks, threaded jack rods and attachments, and welded steel collars called shearheads which were cast into the concrete floor slab at each column. A sketch of a typical jack with attachments is shown in figure 3.3.1. The details of a typical shearhead are shown in figure 3.3.2. Each jack consisted of an upper and lower crossarm separated by a hydraulic cylinder. The hydraulic cylinder and lower crossarm were an integral unit which sat directly on the column top. The upper arm supported two jack rods which were attached in turn to the floor slabs through the shearhead.

In the lifting operation, a hydraulic jack was mounted on the top of each column (24 columns in the east tower and 25 columns in the west tower). A separate power unit and control console was provided for each tower and the lifting and positioning of the floor slabs in each tower consisted of independent operations. The nominal load capacity of each jack was 150 kips (667 kN), but for the four columns with the heaviest sections in each tower, "super jacks" with a capacity of 300 kips (1334 kN) were used. These larger jacks were fitted with a bearing plate and were installed on columns B9, B10, D9 and D10 in the east tower and on columns E3, E3.8, G3 and G4 in the west tower. Although a 150 kip (667 kN) jack is described below, the essential features and mode of operation apply equally to the 300 kip (1334 kN) jacks. Each jack was connected to its console with two hoses, one for extending the jack and one for retracting the jack. All jacks connected to a given console operated at the same line pressure.

Lifting of floors was accomplished by raising the jacks and jack rods in 1/2-in (12.7 mm) increments. At the start of each increment, or lifting cycle, the upper crossarm of the jack was forced upward 5/8 in (15.9 mm), the maximum stroke of the hydraulic piston. As each jack was being raised, a hydraulic actuator (not shown in figure 3.3.1) and chain drive rotated a holding nut downward on each jack rod to keep the nut in contact with the bottom crossarm. This provided a positive mechanical support of the jack rods to prevent the slabs from dropping in the event of a hydraulic system malfunction. When the jack reached its maximum travel and the bottom holding nuts had been turned snug against the lower crossarm, the piston was retracted. The hydraulic actuator and a second set of chain drives rotated an upper set of take-up nuts down the jack rods to keep them in contact with the upper crossarm.

When the hydraulic piston had been fully retracted and the take-up nuts turned snug against the upper crossarm, the lifting cycle was complete. Although the stroke of the piston was 5/8 in, 1/8 in of travel was lost in each cycle because of slack between the nuts and crossarms. As a result, the floor slab was lifted only 1/2 in during each cycle of lifting. A system of electrical interlocks prevented the jacks from being cycled if either the holding or take-up nuts had not followed and maintained contact with the crossarms. This system prevented the floor slabs from being raised more than 1/2 in differentially between any two jacks. The cycle of lifting was repeated until the slabs were close to the desired elevation for parking. When operating in the automatic mode, lifting rates of approximately 5 ft (1.52 m) per hour were normal.

Once the slabs had been placed approximately at the desired elevation for parking (mechanical attachment to the columns), the jacks could be valved for local control so that the shearhead and floor slab at each column location could be raised or lowered to exactly the desired elevation. The floor slabs were then mechanically attached, either permanently or temporarily, to the columns.

Slabs were attached to the columns through the shearheads by blocks welded to the external faces of the column flanges and by steel wedges placed between these blocks and the lower face of the shearheads. An isometric view of a typical permanent connection of a slab to a column and the nomenclature of the components of the connection are shown in figure 3.3.3. The seal block shown in figure 3.3.3 was present only at those locations where the slab was to be attached permanently to the column.

The parking of a slab at a desired elevation was done by three workers who moved as a team from column to column and fixed the slab at the desired elevation. At each column, one worker observed the elevation of the lower surface of the slab from beneath the slab. A second worker, located at the lifting jack, responded to signals from the first worker, and raised or lowered the jack until the floor was in the desired position. At that time, the first worker and a helper would place a wedge between the weld block and the bottom face of the shearhead on each side of the column. After the load was transferred to the wedges, a welder fixed each wedge in place temporarily with two tack welds, one between the wedge and the column at each end of the wedge.

When a pair of wedges at a column had been inserted and tack welded, the jack rods were lowered for attachment to another package of slabs and the jacking

process was repeated. To facilitate lowering of the jack rods and to make other operations easy, split- or swing-nuts were used to transfer loads from the jack crossarms to the jack rods. Under load, the nuts were enclosed in chain-driven sockets. Raising these sockets released the nuts, allowing the jack rods to be moved up or down quickly. The nominal jack rod length is 28 ft (8.53 m) and for the lower packages of slabs it was necessary to add extension rods as shown in figure 3.3.1.

Slabs could be parked either temporarily or permanently, depending on the schedule of lifting. If the slab was to remain in its parked position only temporarily, wedges would be held in position only by tack welds and by friction. However, if the slab was to be parked permanently, the connection between the slab and column was strengthened. In the latter case, fillet welds were applied between the wedges and all adjacent surfaces of the columns, weld blocks, and shearheads. The top faces of the shearhead were welded to the seal blocks to further stiffen the connection, and concrete was placed in the cavity (referred to on the project as a "beam pocket" despite the fact that no beam was present) between the shearhead and column.

Columns and floor slabs were erected in stages. The first step in the construction of the east and west towers consisted of setting the stage I columns on their foundations. Shearheads were then lowered onto the column sections in preparation for the casting of floor slabs.

Slabs were cast one on top of the other on the slab on grade (level E), each subsequent slab using the previously-cast slab as its bottom form. After they had been finished, the top surfaces of the slabs were sprayed with a bond breaker to prevent them from bonding to the following slab.

After the slabs had been cast and had reached the appropriate strength, they were post-tensioned. The column sections for stage IV and above were stacked on the top slab along with the power units, operating console and gantry. After jacks had been placed on top of the stage I columns, lifting of slabs was begun. The sequence of lifting required that up to three slabs be lifted at one time. A group of two or three slabs that was to be lifted at one time was referred to as a "package" of slabs. This report will refer to these groups of slabs by the levels of the floor slab separated by virgules. For example, the group of slabs that consisted of slabs for levels 9, 10, and 11 will be referred to as "9/10/11." When more than one slab was lifted at once, jack rods and lifting nuts were attached to the bottom slab in the package. The upper slabs in a package of slabs were supported only by the lowest slab in the package and were not directly attached to the lifting rods.

Erection of the floor slabs began with the lifting of the package 12/roof in the east tower on 02/10/87. With the exception of the first and last package of two floor slabs in each tower, all packages consisted of three floor slabs. The column height for stage I was 31'-2" (9.5 m). Subsequent column extensions of 15'-3" (4.65 m), 17'-4" (5.28 m) and 19'-9" (6.02 m) were added to reach stage IV at the time of the collapse. Because of their weight, the stage II and stage III column extensions were placed using a truck crane. The sequence of lifting floor slabs and extending columns is shown in figure 3.3.4.

After the lifting was completed for a stage, the column extensions for the next stage were installed. To accomplish this, one jack was removed from a column top and placed horizontally on the top slab using the service gantry. A column extension was then positioned with the gantry and welded in place. The jack on an adjacent column was then removed and placed on the extended column and the process continued until all columns were extended and all jacks were in place to commence another lift.

### 3.4 CONSTRUCTION SCHEDULE

The schedule followed by the contractor in building the structural system is summarized in table 3.4.1. The dates and descriptions of activities listed in the table were extracted from the general contractor's daily log. In certain instances this information was supplemented with data obtained from the daily log of the lift-slab subcontractor. An attempt has been made to limit the description to activities directly related to construction of the building structural system.

Using the two daily logs, it was possible to reconstruct with reasonable certainty the schedule for adding column sections and for lifting floor slabs. Less clear was the actual schedule followed in the placement of shearwalls, the final welding of wedges to the columns and shearheads, and grouting of the shearhead cavities. Table 3.4.1 begins on October 1 with erection of the 1st stage columns in the east tower and ends with the building collapse on April 23 at approximately 1:30 p.m. The table does not include the schedule for construction of the footings or construction of the retaining wall along the north side of the building.

TABLE 3.2.1

TOWER COLUMN SCHEDULE

Column	LC	TA 12A 12B 12F 12H 12J 12K	7F	6A, 11A, 7D, 11D, 2C, 4BC, 2D, 6G	6C, 5	2H 5H 11F	10A 3C 30C	9A	6-ES	3H 4H 10F	7D 3E 3B-E	11B 11D 2E 2G	8B 5G	10B 10D 3G, 4G	1E 1G	8D	8F	9D	7F	4B-E
ROOF	W10x42	HP10x42	HP10x42	HP12x53	HP12x53	HP12x53	HP12x53	HP12x53	HP12x53	HP12x53	HP12x53	HP12x53	HP12x53	HP12x53	HP12x53	HP12x53	HP12x53	HP12x53	HP12x53	HP12x53
TWELFTH LEVEL	W10x42	HP10x42	HP10x42	HP12x53	HP12x53	HP12x53	HP12x53	HP12x53	HP12x53	HP12x53	HP12x53	HP12x53	HP12x53	HP12x53	HP12x53	HP12x53	HP12x53	HP12x53	HP12x53	HP12x53
ELEVENTH LEVEL	W10x42	HP10x42	HP10x42	HP12x53	HP12x53	HP12x53	HP12x53	HP12x53	HP12x53	HP12x53	HP12x53	HP12x53	HP12x53	HP12x53	HP12x53	HP12x53	HP12x53	HP12x53	HP12x53	HP12x53
TENTH LEVEL	W10x42	HP10x42	HP10x42	HP12x53	HP12x53	HP12x53	HP12x53	HP12x53	HP12x53	HP12x53	HP12x53	HP12x53	HP12x53	HP12x53	HP12x53	HP12x53	HP12x53	HP12x53	HP12x53	HP12x53
NINTH LEVEL	W10x42	HP10x42	HP10x42	HP12x53	HP12x53	HP12x53	HP12x53	HP12x53	HP12x53	HP12x53	HP12x53	HP12x53	HP12x53	HP12x53	HP12x53	HP12x53	HP12x53	HP12x53	HP12x53	HP12x53
EIGHTH LEVEL	W10x42	HP10x42	HP10x42	HP12x53	HP12x53	HP12x53	HP12x53	HP12x53	HP12x53	HP12x53	HP12x53	HP12x53	HP12x53	HP12x53	HP12x53	HP12x53	HP12x53	HP12x53	HP12x53	HP12x53
SEVENTH LEVEL	W10x42	HP10x42	HP10x42	HP12x53	HP12x53	HP12x53	HP12x53	HP12x53	HP12x53	HP12x53	HP12x53	HP12x53	HP12x53	HP12x53	HP12x53	HP12x53	HP12x53	HP12x53	HP12x53	HP12x53
SIXTH LEVEL	W10x42	HP10x42	HP10x42	HP12x53	HP12x53	HP12x53	HP12x53	HP12x53	HP12x53	HP12x53	HP12x53	HP12x53	HP12x53	HP12x53	HP12x53	HP12x53	HP12x53	HP12x53	HP12x53	HP12x53
FIFTH LEVEL	W10x42	HP10x42	HP10x42	HP12x53	HP12x53	HP12x53	HP12x53	HP12x53	HP12x53	HP12x53	HP12x53	HP12x53	HP12x53	HP12x53	HP12x53	HP12x53	HP12x53	HP12x53	HP12x53	HP12x53
FOURTH LEVEL	W10x42	HP10x42	HP10x42	HP12x53	HP12x53	HP12x53	HP12x53	HP12x53	HP12x53	HP12x53	HP12x53	HP12x53	HP12x53	HP12x53	HP12x53	HP12x53	HP12x53	HP12x53	HP12x53	HP12x53
THIRD LEVEL	W10x42	HP10x42	HP10x42	HP12x53	HP12x53	HP12x53	HP12x53	HP12x53	HP12x53	HP12x53	HP12x53	HP12x53	HP12x53	HP12x53	HP12x53	HP12x53	HP12x53	HP12x53	HP12x53	HP12x53
SECOND LEVEL	W10x42	HP10x42	HP10x42	HP12x53	HP12x53	HP12x53	HP12x53	HP12x53	HP12x53	HP12x53	HP12x53	HP12x53	HP12x53	HP12x53	HP12x53	HP12x53	HP12x53	HP12x53	HP12x53	HP12x53
FIRST LEVEL	W10x42	HP10x42	HP10x42	HP12x53	HP12x53	HP12x53	HP12x53	HP12x53	HP12x53	HP12x53	HP12x53	HP12x53	HP12x53	HP12x53	HP12x53	HP12x53	HP12x53	HP12x53	HP12x53	HP12x53
GROUND LEVEL	W10x42	HP10x42	HP10x42	HP12x53	HP12x53	HP12x53	HP12x53	HP12x53	HP12x53	HP12x53	HP12x53	HP12x53	HP12x53	HP12x53	HP12x53	HP12x53	HP12x53	HP12x53	HP12x53	HP12x53
LEVEL 'C'	W10x42	HP10x42	HP10x42	HP12x53	HP12x53	HP12x53	HP12x53	HP12x53	HP12x53	HP12x53	HP12x53	HP12x53	HP12x53	HP12x53	HP12x53	HP12x53	HP12x53	HP12x53	HP12x53	HP12x53
LEVEL 'D'	W10x42	HP10x42	HP10x42	HP12x53	HP12x53	HP12x53	HP12x53	HP12x53	HP12x53	HP12x53	HP12x53	HP12x53	HP12x53	HP12x53	HP12x53	HP12x53	HP12x53	HP12x53	HP12x53	HP12x53
LEVEL 'E'	W10x42	HP10x42	HP10x42	HP12x53	HP12x53	HP12x53	HP12x53	HP12x53	HP12x53	HP12x53	HP12x53	HP12x53	HP12x53	HP12x53	HP12x53	HP12x53	HP12x53	HP12x53	HP12x53	HP12x53
BASE PLATE	W10x42	HP10x42	HP10x42	HP12x53	HP12x53	HP12x53	HP12x53	HP12x53	HP12x53	HP12x53	HP12x53	HP12x53	HP12x53	HP12x53	HP12x53	HP12x53	HP12x53	HP12x53	HP12x53	HP12x53

\* Indicates grade 50, A572 steel; all other columns are A36 steel.

TABLE 3.4.1BUILDING ERECTION SEQUENCE

<u>RPT</u> <u>NO.</u>	<u>DATE</u>	<u>ACTIVITY</u>
075	10/01/86	Erect columns east wing
076	10/02/86	Erect columns east wing
077	10/03/86	Erect columns west wing
078	10/06/86	Plumb columns
080	10/08/86	Grout base plates east wing
081	10/09/86	Place slab on grade east wing
082	10/10/86	Grout base plates west wing, place slab on grade east wing
088	10/17/86	Place slab on grade west wing
096	10/28/86	Place "D" level east wing
097	10/29/86	Place "D" level west wing
098	10/30/86	Place "C" level east wing
099	10/31/86	Place "C" level west wing
100	11/03/86	Place "GND" level east wing
101	11/04/86	Place "GND" level west wing
103	11/06/86	Place "1st" level east wing
104	11/07/86	Place "1st" level west wing
106	11/11/86	Pour cancelled due to forecast of snow/sleet/rain
107	11/12/86	Place "2nd" level east wing
110	11/17/86	Place "2nd" level west wing
111	11/18/86	Place "3rd" level east wing
112	11/19/86	Pour cancelled due to snow
113	11/20/86	Place "3rd" level west wing
114	11/21/86	Place "4th" level east wing
117	11/25/86	Pour cancelled due to rain
118	11/26/86	Pour cancelled due to rain
120	12/01/86	Place "4th" level west wing
121	12/02/86	Place "5th" level east wing. Meeting with rep from W.R. Grace concerning slow set of yesterdays pour.
122	12/03/86	Pour cancelled due to rain
123	12/04/86	Place "5th" level west wing
124	12/05/86	Place "6th" level east wing
126	12/08/86	Place "6th" level west wing
127	12/09/86	Pour cancelled due to snow/sleet/rain
128	12/10/86	Place "7th" level east wing
129	12/11/86	Concrete plant breakdown, one load on job, pour cancelled
131	12/15/86	Place "7th" level west wing
132	12/16/86	Place "8th" level east wing
133	12/17/86	Place "8th" level west wing
136	12/22/86	Place "9th" level east wing
137	12/23/86	Place "9th" level west wing
140	12/29/86	Place "10th" level east wing
141	12/30/86	Place "10th" level west wing
142	12/31/86	Place "11th" level east wing
143	01/02/87	Work cancelled due to snow/rain
146	01/07/87	Place "11th" level west wing



147 01/08/87 Place "12th" level east wing  
148 01/09/87 Place "12th" level west wing  
150 01/13/87 Place "Roof" level east wing  
152 01/15/87 Place "Roof" level west wing  
156 01/21/87 Begin prestressing operation  
164 02/02/87 Lift column steel onto roof slabs  
165 02/03/87 Lift column steel onto roof slabs  
170 02/10/87 STAGE I LIFT - ROOF/12 east wing  
171 02/11/87 Park ROOF/12 east wing, lift 11/10/9 east wing  
172 02/12/87 Park 11/10/9 east wing, lift ROOF/12 west wing  
173 02/13/87 Blocking and welding on slabs east wing  
174 02/16/87 Lift 8/7/6 (Notes say 7/6/5) east wing  
175 02/17/87 Park 8/7/6 east wing, park ROOF/12 west wing  
176 02/18/87 Lift 5/4/3 (Notes say 2/1) east wing, lift 11/10/9 west wing  
177 02/19/87 Park 5/4/3 east wing, park 11/10/9 west wing  
178 02/20/87 Lift 8/7/6 west wing, lift 2/1/GND east wing  
179 02/23/87 Work cancelled due to snow  
180 02/24/87 Park 8/7/6 west wing, lift 5/4/3 west wing, park 2/1/GND east wing, lift C/D east wing  
181 02/25/87 Lock D east wing, park 5/4/3 west wing  
182 02/26/87 Lift and lock C east wing, lift and park 2/1/GND west wing  
183 02/27/87 Lock C east wing, set Stage II columns east wing (Notes say west wing)  
184 03/02/87 Lift C/D west wing, lock D west wing, weld columns east wing  
185 03/03/87 Lift and lock C west wing, weld columns east wing  
186 03/04/87 Set Stage II columns west wing, weld columns east wing. Observed "stress cable lifting thru the concrete slab" on D level  
187 03/05/87 Set Stage II columns west wing, weld columns east and west wings  
188 03/06/87 Weld columns east and west wings  
189 03/09/87 STAGE II LIFT - ROOF/12 east wing, weld columns west wing. "Hollow spots" reported in E level, Col. 12, garage  
190 03/10/87 Lift ROOF/12 east wing. "Building being leveled off with cables on east end."  
191 03/11/87 Placed shearwalls on D and E levels at following locations: C-3, A&B-8, G&H-2, H-4&5, F-8&9, A&B-11  
Lift and park ROOF/12 east wing. Place pour strips on D level.  
192 03/12/87 Lift and park 11/10/9 east wing, weld columns west wing. Large amount of hydraulic oil near Col. 2G, level D  
194 03/16/87 Lift and park 8/7/6 east wing  
195 03/17/87 Lift and park ROOF/12 west wing, lift and park 5/4/3 east wing  
196 03/18/87 Lift and lock GND east wing, lift 11/10/9 west wing. Laying in concrete block on C level.  
197 03/19/87 Lift and park 2/1 and lock GND east wing, lift and park 11/10/9 west wing. "West end - leveled off building steel"  
198 03/20/87 Set Stage III columns east wing, lift and park 8/7/6 west wing  
199 03/23/87 Lift 5/4/3 west wing, weld column splices east wing  
200 03/24/87 Park 5/4/3 and lift 2/1/GND west wing, weld column splices east wing, lock GND west wing  
201 03/25/87 Lock GND west wing, lift and lock 1 west wing

202 03/26/87 STAGE III LIFT ROOF/12 east wing. Set Stage III columns west wing. Placed shearwalls at level D on 8 line, 11 line and F line east wing. Placed elevator shearwall at level E.

203 03/27/87 Set Stage III columns west wing, park ROOF/12 east wing

204 03/30/87 Lift and park 11/10/9 east wing. Leveling off east wing. Weld column splices west wing. Lift and park 8,7,6 east wing.

205 03/31/87 Place shearwall at C-3 and shearwall on A line between lines 8 and 9

206 04/01/87 Lift and park 5/4/3 east wing, complete welding of column splices west wing.

207 04/02/87 Start STAGE III lifting, west wing

208 04/03/87 Lift 11/10/9 west wing, set STAGE IV columns east wing, placed shearwalls at interior of building on level C, park 11/10/9 west wing

211 04/08/87 Park 11/10/9 and lift 8/7/6 west wing

212 04/09/87 Lift and park 8/7/6 west wing, finish welding column splices east wing

213 04/10/87 Lift and park 5/4/3 and lock 3 west wing

214 04/13/87 Lift and lock 2 and set STAGE IV columns west wing

215 04/14/87 Set STAGE IV columns west wing, STAGE IV LIFT ROOF/12 east wing

216 04/15/87 Set STAGE IV columns west wing

217 04/16/87 Lift and park 11/10/9 east wing, fill column pockets on level 2 east and west wings, placed elevator shearwall from level D to level C

218 04/20/87 Lifting 8/7/6 east wing, fill column pockets 1/GRD. Place shearwalls GND floor to 1st floor.

219 04/21/87 STAGE IV LIFT ROOF/12 west wing, park 8/7/6 east wing

220 04/22/87 Lift 4th floor east wing. Park ROOF/12 west wing.

221 04/23/87 Lift 5th floor into permanent position on east wing. Park 11,10,9 west wing and guy west wing. Place shearwalls from 1st floor to 2nd floor. Building collapsed at 1:30 p.m.

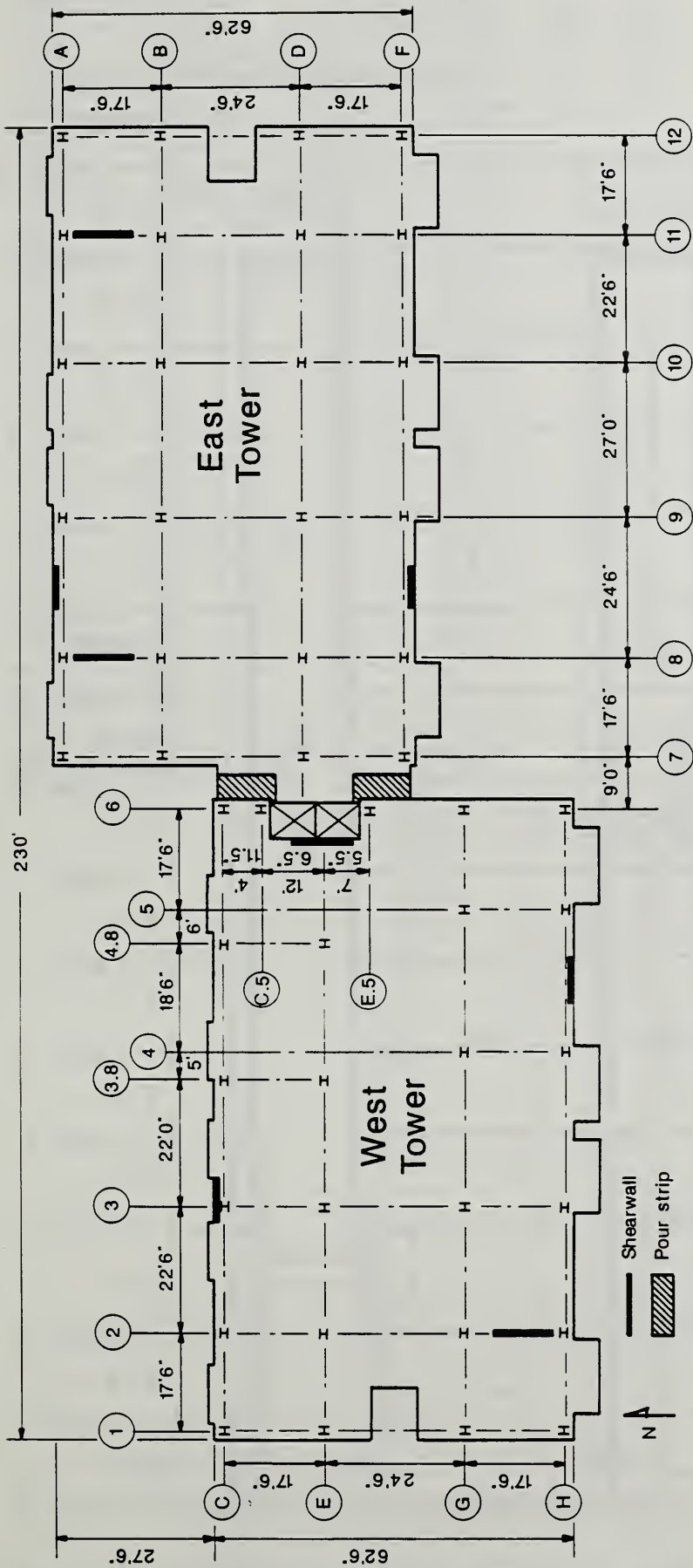


Figure 3.2.1 Plan view showing column layout and shearwall locations

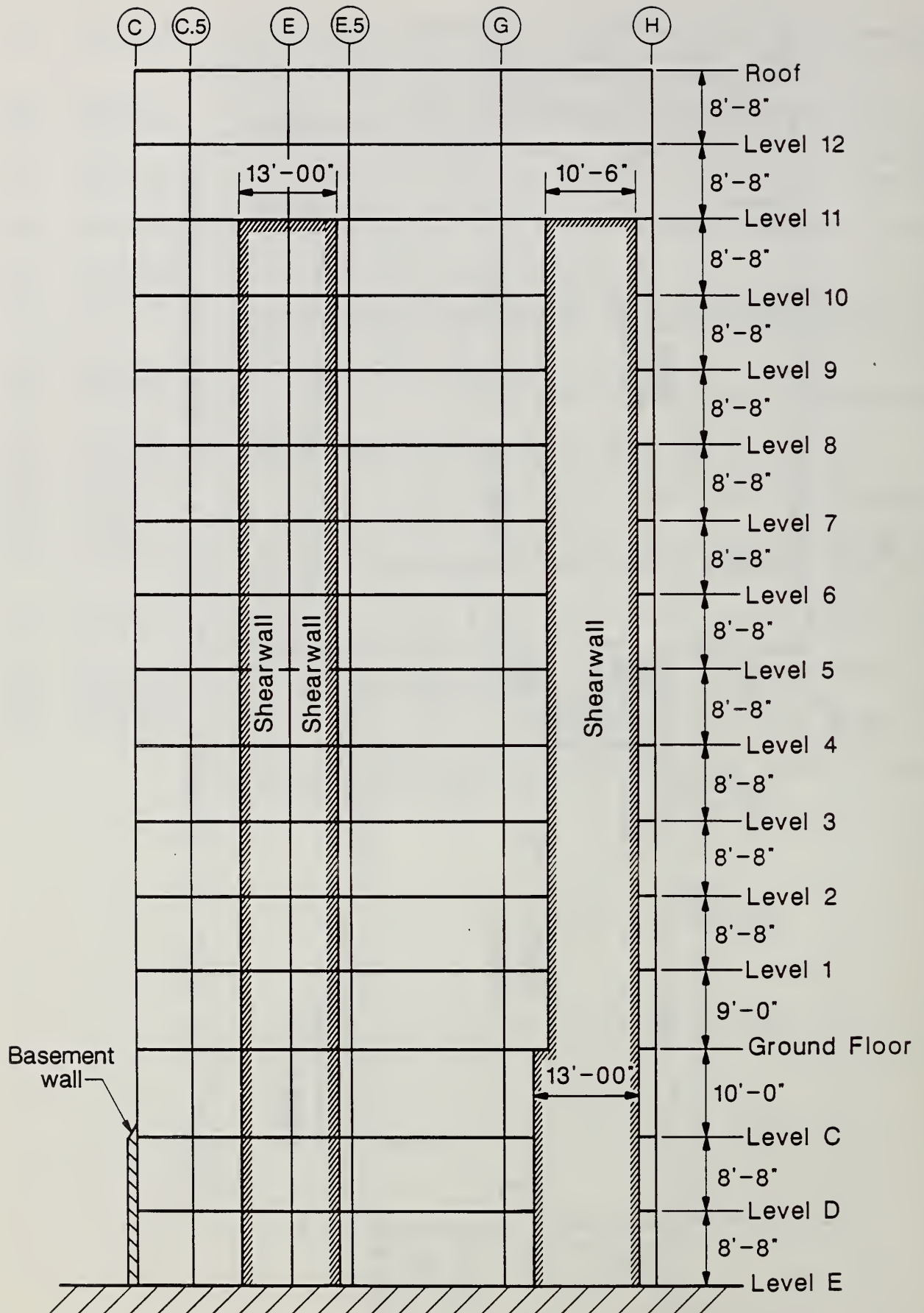


Figure 3.2.2 Elevation of West tower - Viewed from the West

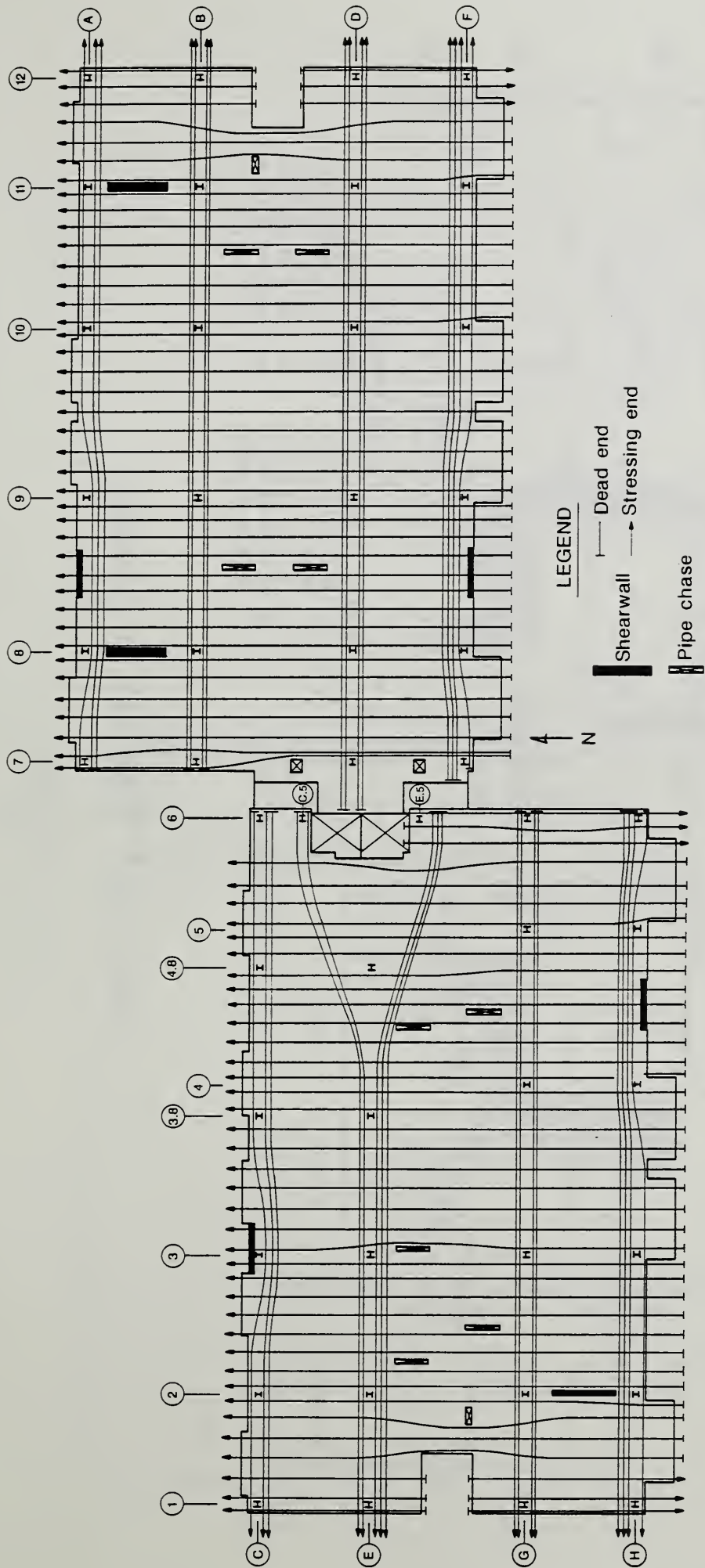


Figure 3.2.3 Location of post-tensioning tendons

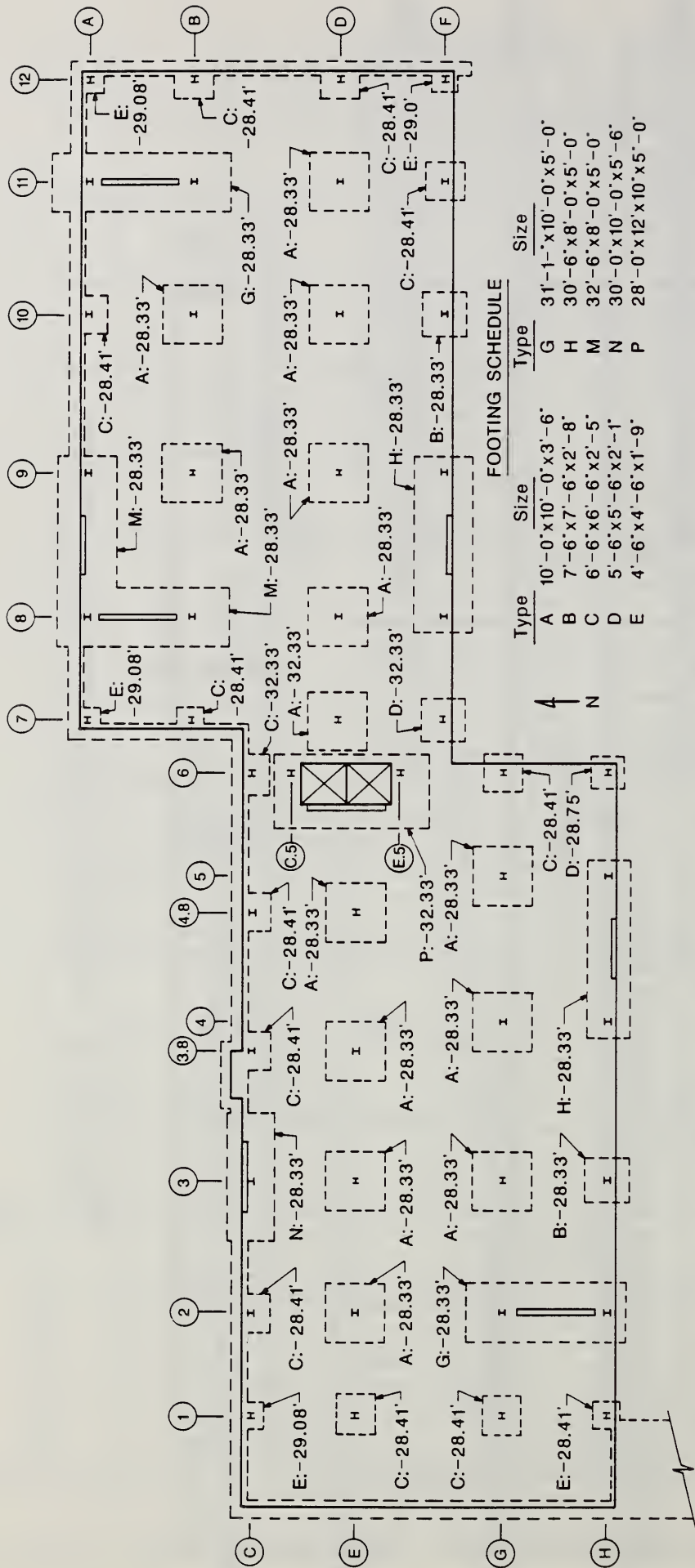


Figure 3.2.4 Plan view of footings

# TYPICAL INTERIOR COLUMN

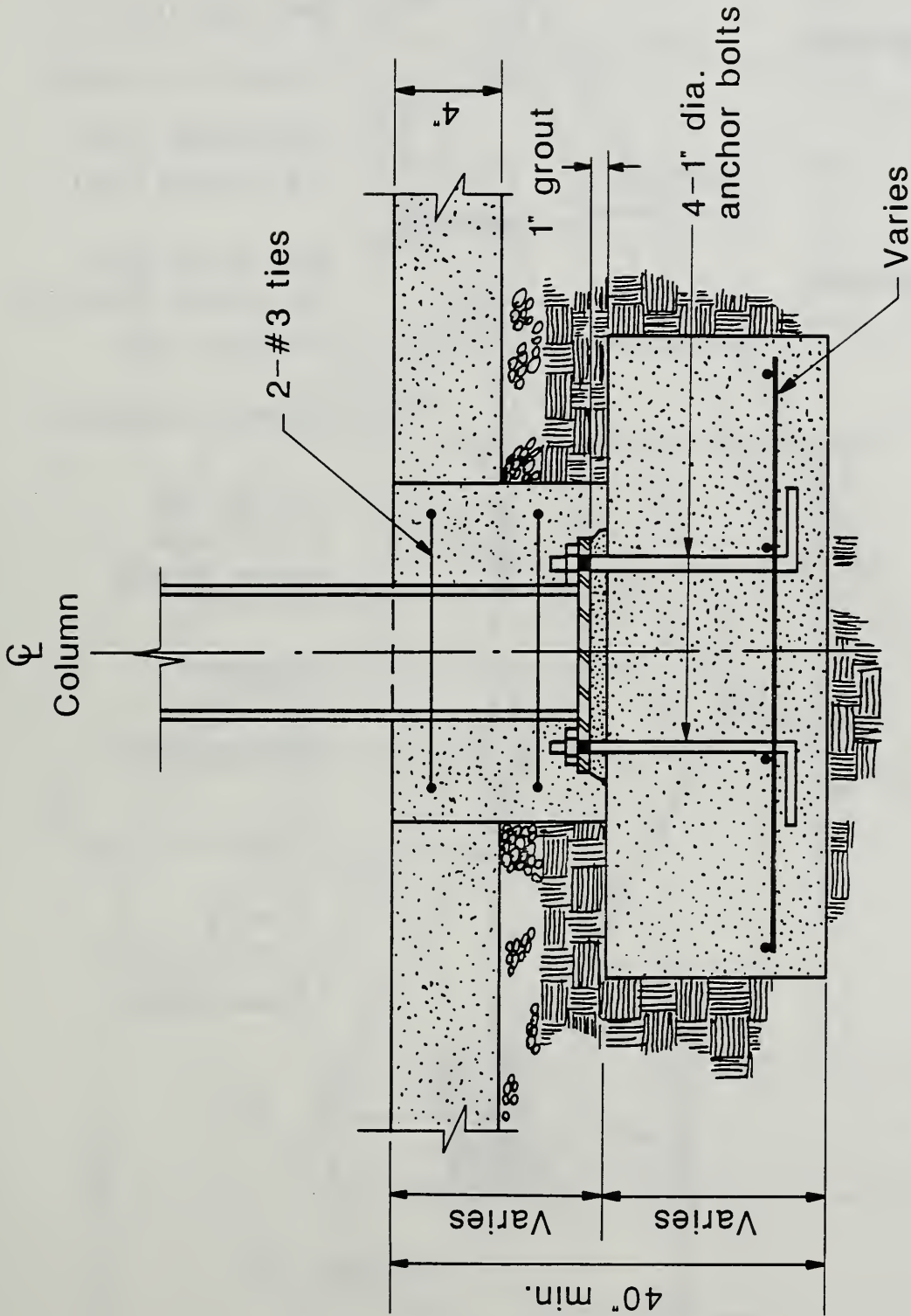


Figure 3.2.5 Typical detail of interior column footing

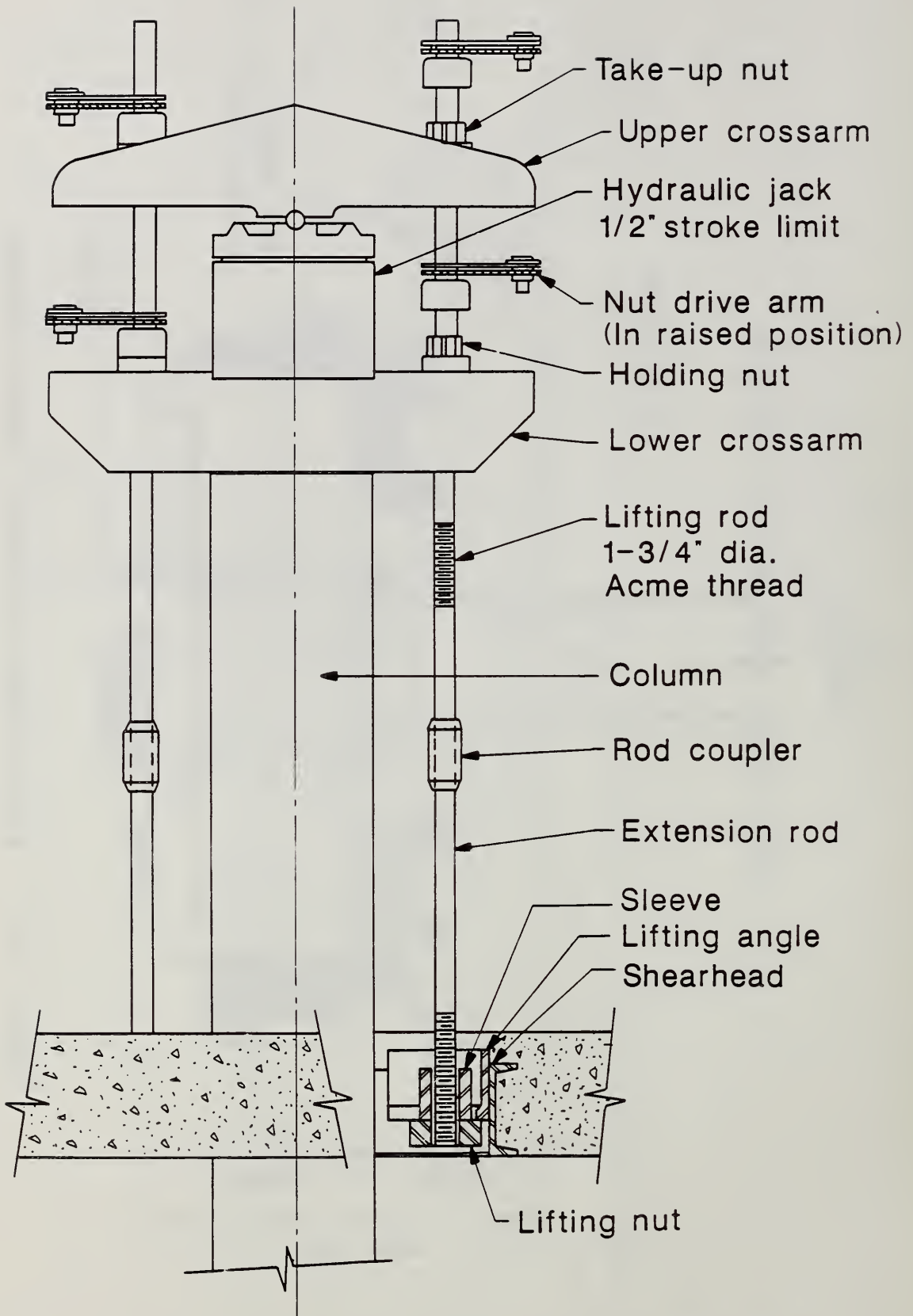


Figure 3.3.1 Lifting assembly, 150 kip jack



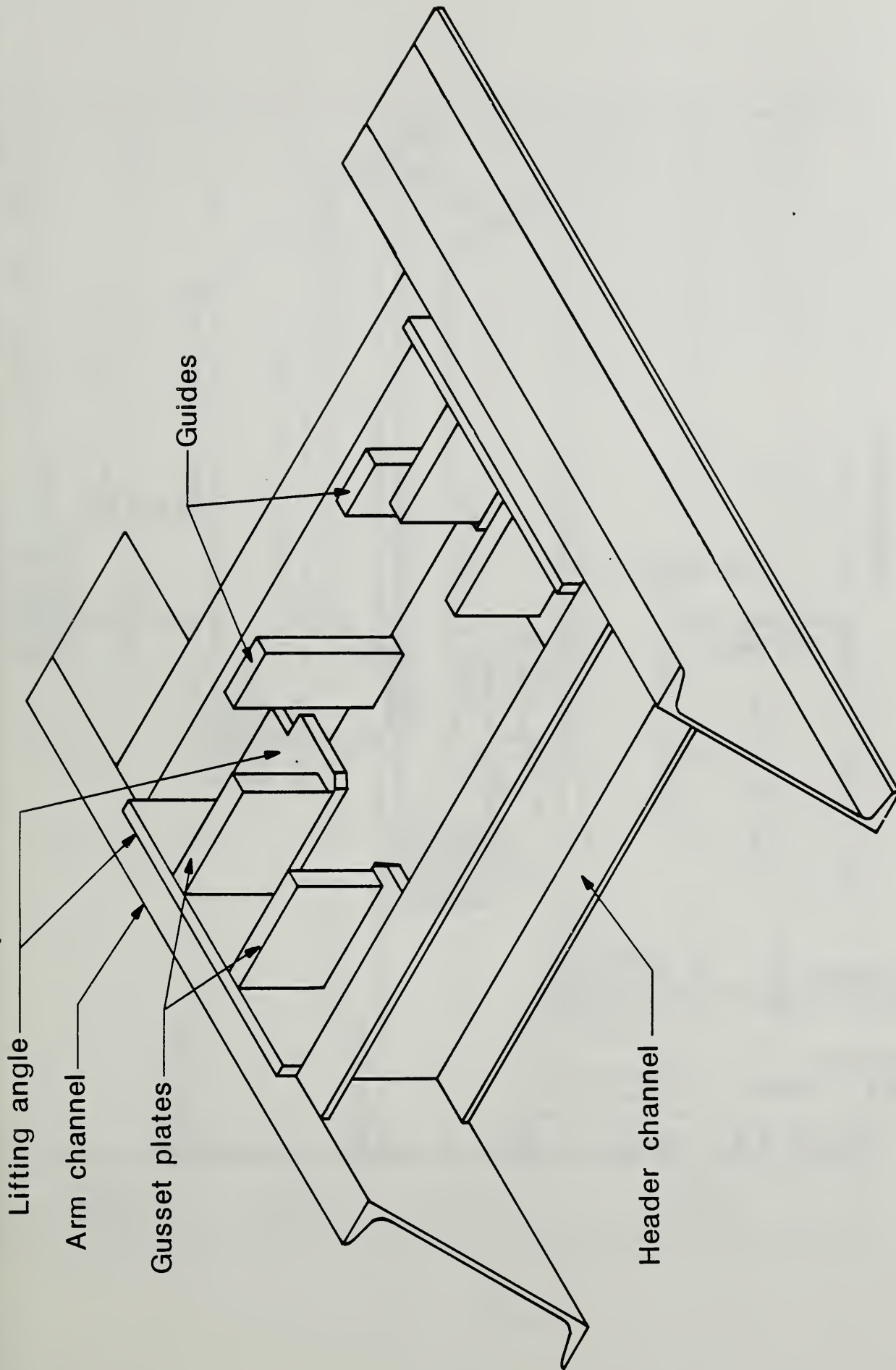


Figure 3.3.2 Shearhead detail

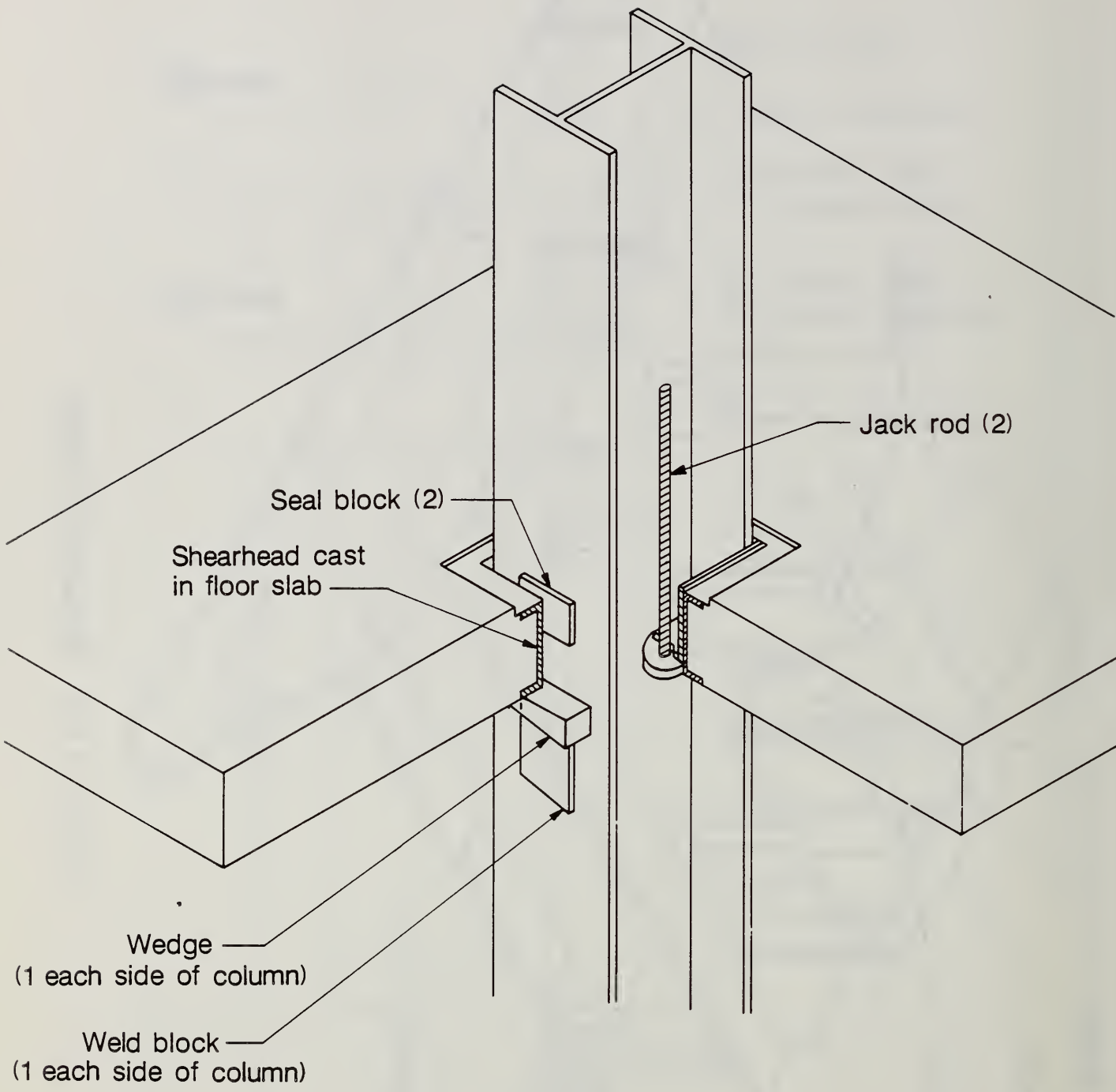


Figure 3.3.3 Detail of slab to column connection

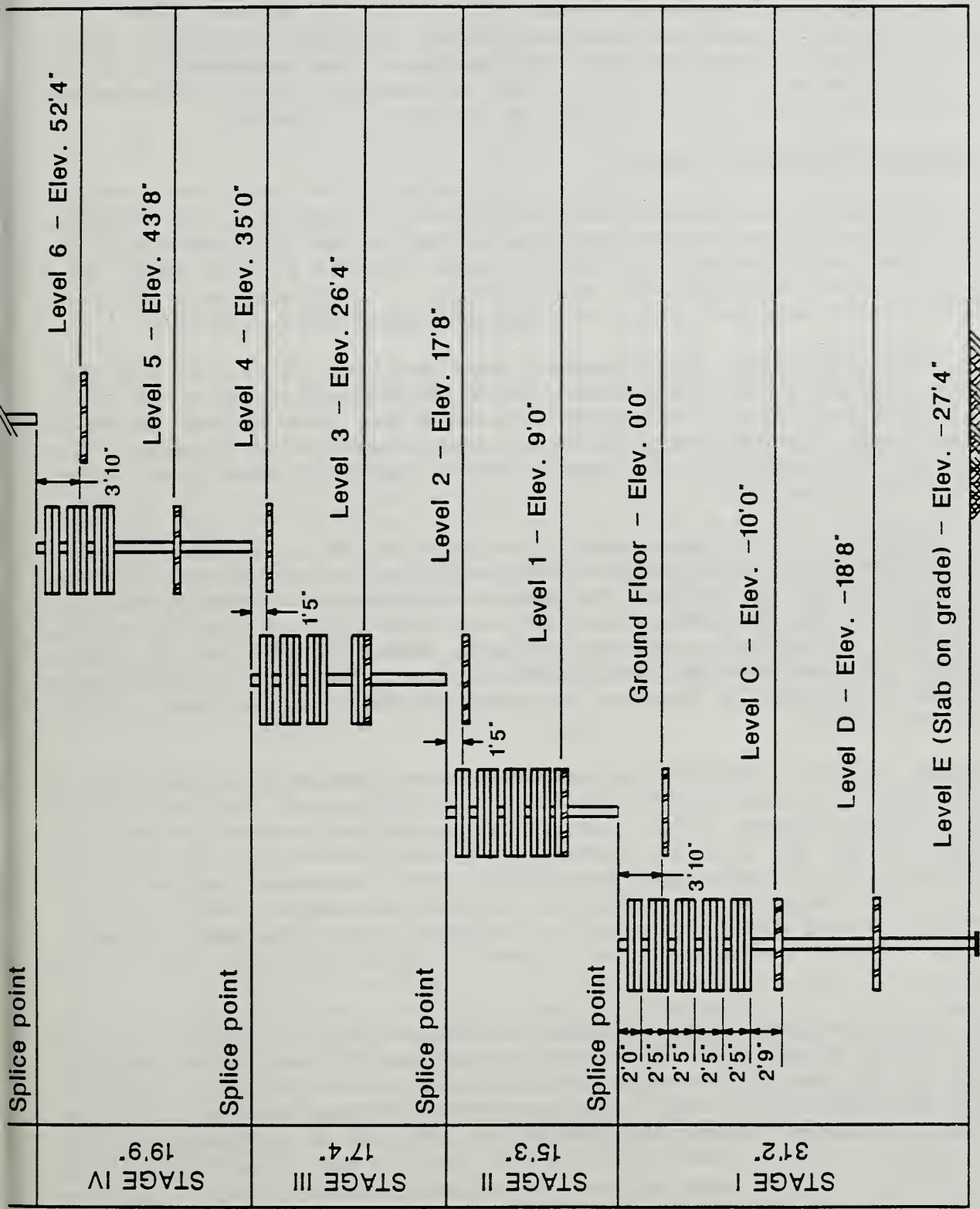


Figure 3.3.4 Lift slab sequence

## 4. DESCRIPTION OF COLLAPSE

### 4.1 INTRODUCTION

Construction activities preceding the collapse, eyewitness accounts of the sequence of events associated with the collapse, and descriptions of the debris are presented in this chapter. This information was used in determining the most probable cause of the collapse as described in Chapter 9.

### 4.2 ACTIVITIES PRECEDING COLLAPSE

Several construction operations were in progress on the day of the collapse. Some of these activities involved portions of the project unrelated to the two building towers which actually collapsed. Level A of the parking garage south of the east tower was being cast and finished. A retaining wall was being backfilled at the northeast corner of the east tower.

Workmen were installing nonstructural items in both towers of the main structure. Electricians were installing electrical services on the lower floors of the west tower. Plumbers were installing pipe hangers and waste water lines and carpenters were installing nonstructural steel studding in the west tower. It is unlikely that any of these activities contributed to the collapse of the structure.

Several structural operations were in progress in both the east and west towers. Concrete was being placed in shearwall forms between ground level and level 1 at the south side of both the east and west towers. Concrete was also being placed in the shearwall at the elevator shaft between level C and the ground level. In addition, concrete was being placed in the cavities between the columns and shearheads on levels 2 and 3. Masons had just finished placing pour strips to connect the floors of the east and west towers at level 2 at the time of the collapse.

Potentially critical construction procedures being conducted on the 23rd of April included lifting of the floor slabs and securing these slabs with wedges in both the east and west towers. The lifting operation in the east tower had progressed to the end of stage IV while in the west tower stage IV was about half complete. On the morning of the 23rd of April, the level 5 floor slab of the east tower was raised to its final position and wedges were installed. These wedges, having been tack-welded in position as they were placed initially, were being welded permanently to the columns and shearheads when the collapse occurred.

Erection operations were being conducted in the west tower at the time of the collapse. The roof and level 12 floor slabs had been lifted to their temporary positions at the top of the stage IV column sections on the 21st of April. The slabs for floor levels 9/10/11 had been raised to their temporary position in the fourth stage of lifting by approximately 11:30 a.m. on the morning of April 23rd. A 12-ton (107 kN) capacity hydraulic jack had been placed between the slabs at level 11 of the east and west towers approximately 4 ft (1.2 m) from column line C to adjust laterally the position of the floors that were being lifted. Figure 4.2.1 is a schematic representation of the state of construction

of floor slabs, shearwalls, and cavities around the columns at the time the collapse occurred. As shown in this figure, shearwalls on the north side of the east and west towers had been cast prior to the day of the collapse and had developed some portion of their design strength. Shearwalls on the south side of the east and west towers had been cast between the ground level and level 1 on the day of the collapse and had not developed significant strength at the time of the collapse.

At the time of the collapse, workmen were installing wedges to hold slabs 9/10/11 in this position temporarily. Wedges had been installed along column lines G and H and an ironworker (#14 in figure 4.3.1) was installing temporary wedges at column E4.8. A floor plan of the west tower showing the locations and sequence for which wedges had been installed to support the group of slabs for levels 9/10/11 is shown in figure 4.2.2.

#### 4.3 EYEWITNESS ACCOUNTS OF COLLAPSE

Descriptions of the collapse were provided by 45 individuals who were on the site or nearby. Fourteen of these individuals were in the structure at the time of the collapse and 31 were at various locations around the structure. Three other individuals who were not on the jobsite at the time of the collapse were interviewed to obtain general information about construction procedures used at the jobsite. Most witnesses who were in the structure at the time of the collapse had a limited view of the structure and were not in a position to see all aspects of the collapse, but saw only the failure of members in their immediate vicinity. This section will summarize the general observations of witnesses and then consider in detail the descriptions of key aspects of the event given by four eyewitnesses. The locations of fourteen individuals who were known to have been in the vicinity of the structure at the time of the collapse and who could describe the event in some detail are shown in figure 4.3.1. Other witnesses in the structure were not in a position to observe the initiation or progression of the collapse.

Descriptions of the collapse varied somewhat in detail. This is inevitable in such situations because of the suddenness of the event and, particularly in this case, because of the relatively short amount of time from the start of the failure to its conclusion. Many witnesses could not accurately describe what they saw because of their lack of familiarity with construction techniques and equipment. Some witnesses, for example, referred to the boom of a concrete pumper truck as a crane.

Witnesses disagreed as to the activities they recalled seeing in progress just prior to the collapse. Two individuals indicated they saw cranes working at the site and that steel column sections were being welded on top of existing columns on the east tower. Other witnesses could not recall specifically what workmen were doing, if anything, on the roofs of the buildings prior to the collapse. The construction manager at the jobsite indicated that no cranes were on the site on the day of the collapse and no column extensions were being erected.

In general, all witnesses agreed that the collapse was extremely rapid. Estimates of the time from initiation of failure (the point at which their

attention was first drawn to the structure by noise) to the time at which the collapse was complete ranged between 2 and 10 seconds. The majority of witnesses stated that the collapse took place within a time span of approximately 5 seconds. Note the time required for a particle to fall from a height of 81.5 ft (24.8 m), the height of the roof slab above level E, under the force of gravity is 2.25 sec. Apparently the lower level floor slabs offered minimal resistance to the debris from above as the failure progressed vertically. Almost all witnesses indicated they first noticed the failure because of a loud noise. Descriptions of the character of the noise varied from one witness to another. The majority of witnesses reported hearing a single initial noise, which was followed by a general rumbling as slabs fell and the collapse took place. This initial noise was variously described as a loud snap, crack, or boom, which some likened to the bang of a hinged tailgate of a dump truck, a spring breaking on a big truck, or a piece of metal snapping under pressure. Others were aware of only the general sound of the collapse itself, which they described as the sound of a large jet, a rumble, or the sound of an earthquake or thunder. They did not specifically mention hearing a single individual noise which might have accompanied the failure of a single component at the beginning of the failure.

Two witnesses believed the building might have been swaying prior to the collapse, and one individual who had passed the construction site frequently in the days prior to the collapse stated he believed he could detect a slight swaying motion of the building in response to wind loads. Winds were light and variable on the day of the collapse, with sustained winds of approximately 12 knots (6.2 m/s) ESE as measured by the National Weather Service Office (NWSO) at the Sikorsky Memorial Airport, Bridgeport, Connecticut. A copy of the NWSO stripchart for April 23 was obtained from the National Climatic Data Center. The stripchart indicates peak winds of 20 knots (10.3 m/s) from 12 Noon to 1 p.m. (LST). The Sikorsky Memorial Airport is approximately 5 miles (8 km) southeast of the site of the collapse.

Almost all witnesses of the collapse indicated that they did not see the building moving prior to the collapse. None of the workmen who had been in the building and who escaped the collapse reported any swaying or unusual motion of the building.

The majority of witnesses indicated they believed the collapse started in the west tower. Only one witness indicated that the east tower began to collapse first. As a testimony to the speed of the collapse and to the shock it instilled in observers, this witness related in one interview that the west tower collapsed first and in a subsequent interview that the east tower failed first. Of the workmen who were in the building at the time of the collapse, all who could determine the location of the first sound of the failure said the failure appeared to start high in the structure in the west tower.

Additional eyewitness accounts of the early stages of the collapse will be discussed in Chapter 9. The testimony of one of the survivors of the collapse was considered particularly valuable. Just prior to the collapse, an ironworker (#14, figure 4.3.1) was installing wedges at column E4.8 underneath slabs 9/10/11, the package of slabs which had been raised to its temporary parking position in stage IV of the lifting sequence on the morning of April 23rd.

The witness stated that he "heard a loud noise... like steel breaking under pressure," which he believed came from within 25 ft (7.6 m) of where he was working, either directly above him or toward the center of the slab in the vicinity of column E3.8. He then noticed that the floor slab directly over his head "was cracking just like ice breaking." The floor slabs above him then collapsed, pushing him between the uprights of the scaffolding on which he was standing. Protected somewhat by the scaffolding, he was carried down with the collapsing structure and later rescued. He was the only survivor of the men working in that area at the time of the collapse.

Three descriptions of the overall collapse were essentially similar. One of these accounts was given by the operator of a concrete pump truck parked at the southeast corner of the west tower (#3 in figure 4.3.1). The attention of the operator was directed toward the building because of his need to respond to signals of workmen who were removing a hose used for placing concrete in shearwall forms within the building. The operator stated that he was first made aware of some problem in the structure by a loud, metallic noise that he described as being similar to the noise which could be made by the breaking of a leaf spring on a truck. The noise seemed to come from the southwest corner of the west building near the top of the slabs which were located in their temporary positions (levels 9/10/11 and 12/roof). The operator reported that he turned immediately toward the sound and saw the corners of the two uppermost slabs start to move downward until they struck the slabs immediately below them, at which time the fall of the slabs slowed momentarily. The collapse then spread eastward and northeastward throughout the uppermost slabs of the west tower and then the entire building collapsed vertically. He reported that the east tower collapsed as a result of being struck by sections of the collapsing west tower and as a result of being linked to the west tower at several locations.

A second description of the collapse seemed to agree in general with the report given by the operator of the pump truck. A construction contractor who had stopped on a nearby roadway because of a minor motor vehicle accident witnessed the event from a distance of approximately 100 yards (91.4 m) (#4 in figure 4.3.1). He indicated that he glanced at the building several times to observe the operations being conducted as he was waiting for police to deal with the accident. His attention was then drawn to the building by a loud, sudden noise which he described as either a crack, boom, or snap, stressing that the sound was sharp rather than muffled. He related that he then saw the west region of the top slabs of the west tower drop down to the lower floors. The failure then appeared to progress from the west side of the west tower eastward, enveloping all of the west tower to the extent that the slabs appeared to be dropping vertically at some point in the failure. At some point that he could not describe definitely, the east tower became involved in the collapse as a result of either impacts from debris falling from the west tower or from other factors unknown. The east tower then collapsed completely. The witness stated that the total amount of time required for the collapse seemed to him to be no more than 5 seconds.

The Connecticut state policeman (#11 in figure 4.3.1) who was controlling traffic at the scene of the motor vehicle accident mentioned above also witnessed the collapse. This witness stated that he first heard three loud booms like explosions. As he turned to look in the direction of the noises,

he saw the west tower collapsing straight down. The west tower then keeled over eastward into the east tower, causing the top floors of the east tower to snap and fall onto the floors below. The east tower then fell slightly eastward and collapsed completely.

#### 4.4 OBSERVATIONS OF DEBRIS

Observations of the debris provide insight into the pattern of collapse of the structure. This insight is helpful in identifying the sequence of collapse and possibly the point of initiation of the failure. The information presented in this section will be used in subsequent sections of the report in connection with analysis of the structure and the explanation of the most probable cause of the failure.

##### 4.4.1 Overall Collapse

An overview of the collapsed structure is shown in figure 4.4.1. The photograph was taken approximately two hours after the collapse and prior to any significant amount of debris removal in the rescue operation. The undamaged columns in the foreground are for the parking garage which had not been erected at the time of the collapse. Two distinct heaps of debris, one the east tower and one the west tower, are clearly visible. The clear area between the heaps of debris in the photograph is the service core between the two towers. In each tower, the columns are draped over the pile of concrete floor slabs. It appears that the slabs collapsed near the center of each tower, pulling the columns inward.

##### Column Bending

The collapse toward the center of each tower produced inelastic bending of the upper portions of the perimeter columns. Column C3, a perimeter column on the north side of the west tower, is shown in figure 4.4.2. Note the column bending at level 1 in this case is about the strong axis of the column. The deformation of column E1, a perimeter column on the west side of the same tower is shown in figure 4.4.3. Significant inelastic action and formation of a plastic hinge occurred in the upper portions of the column near level 1. Bending occurred over the lower three stories about an axis approximately midway between the principal axes of the column.

##### Lower Story Lateral Displacement

The lower stories of each tower did not exhibit any significant overall lateral displacement although there was some localized lateral displacement. The lower two levels (level E and level D) of the columns on the east edge of the east tower (column line 12) shown in figure 4.4.4, for example, are essentially vertical. The shearwalls in place at the lower levels provided some lateral support. The north face of the shearwall between column lines 8 and 9 and oriented in the east-west direction is shown in figure 4.4.5. The orientation of the cracks indicates the wall was subjected to a shear force directed from west to east.



## Torsional Deformations

Several of the columns twisted significantly. Column C3.8, for example, shown in figure 4.4.6 twisted approximately 25 degrees. The pattern of twisting of the columns is shown in figure 4.4.7. The twists given are approximate and represent visual estimates made at the site prior to removal of the columns. Several columns were removed before estimates could be obtained.

Figure 4.4.7 shows twists of as much as 60 degrees occurred. For some columns, twists in opposite directions occurred at different levels. Column C6, for example, twisted counterclockwise up to level D, then clockwise with increasing magnitude at levels 1, 2, 3 and 4. At the lower levels in some cases, there was no column twist. Column C3, for example, did not twist up to the ground level. As indicated, some of the twisting of column B12 was elastic rather than inelastic. Observations of a series of photographs of this column showed that some of the initial counterclockwise twist between levels D and C was recovered as the debris was removed.

In general there does not appear to be a consistent pattern to the twists in figure 4.4.7. Observed twists in the lower levels (level E to level C) of the east tower, however, are all counterclockwise. Also there are no significant differences between twists in the east versus the west tower. For example, columns E1 and G1 on the west edge of the building twisted counterclockwise, whereas column C2 on the north edge twisted clockwise. A similar situation occurred in the east tower with columns A10, B12, and D12. This lack of any pattern consistent with rigid body twisting of the slabs indicates the slabs generally did not remain intact during the collapse of the building.

## Floor Slab Orientation

The orientation of floor slab segments in the debris provides an indication of the manner in which the building collapsed. Figure 4.4.8 shows the orientation of the lower level floor slabs at the northwest corner of the west tower. The photograph was taken after the upper level slabs had been removed. Approximately seven slabs are visible. Note the slab segments to the left of the center of the photograph (between column lines C and E) are essentially horizontal. The slab segments on the right are at an angle of approximately 60 degrees with the horizontal. Clearly these slabs did not remain intact as the building collapsed. The slabs broke and the individual segments fell separately. The pattern in figure 4.4.8 would indicate the lower seven or eight levels of slabs broke in the vicinity of column line E during the collapse.

The upper level floor slabs at the northwest corner of the west tower are shown in figure 4.4.9. Eight slabs are visible in the photograph. The slabs are oriented approximately vertically. The plastic hinge in column E1 (the kink in the center of the photograph) is at level 1, which is located at approximately mid-height of the column in place at the time of collapse (column up to level 6). Apparently during the collapse, portions of the upper level slabs fell with the columns, rotating as the columns deformed and bent toward the center of the building.

The orientation of the lower level slabs in the center portion of the west tower near the perimeter shearwall on the south side is shown in figure 4.4.10. Again the eight lower level slabs are horizontal and the remaining eight slabs are essentially vertical.

The horizontal orientation of the lower level slabs and the more nearly vertical orientation of the upper level slabs was also apparent in the center portion of the east tower as shown in figure 4.4.11.

The upper level slabs at the southeast corner of the east tower fell in a fashion similar to that of the slabs on the northwest corner of the west tower. This is apparent in figure 4.4.12. In this case some of the slabs actually rotated beyond the vertical position and landed upside down. The two slabs in the lower right portion of the figure are in this position.

### Collapse Pattern

To more clearly visualize the overall collapse pattern of the structure, the composite sketches of the deformed shapes of the columns in each tower in figures 4.4.13 and 4.4.14 were prepared. Three views are shown for each tower. Photographs of the columns taken prior to removal from the collapsed structure were used to produce these sketches. The columns shown are not complete in every case since portions were removed as the rescue operation proceeded. Displacements were estimated at the various floor levels. Column segments between floor levels and/or plastic hinges are indicated as undeformed elements. Column A7, for example, in the northwest corner of the east tower (figure 4.4.14) has nine elements representing level E through level 6.

Referring to figure 4.4.13, for the west tower, note that there is no indication of any consistent translation or rotation in which the structure deformed as a unit. It appears that each column deformed independently and the floor slabs broke early in the collapse sequence. The upper level slabs caused the columns to deflect toward the center of the building as these slabs fell. Figure 4.4.1 clearly illustrates this behavior.

The lower levels of the columns remained relatively straight and in most cases vertical. Significant deformations or buckling of the columns in general occurred at the ground level or level 1. This was the case for columns C1, C2, C3, C.5, C6, E3, G1, H1, H2 and H5. This would be expected since the floor slabs at level D, level C and ground level were fully welded in place. Note that column C3 at the shearwall on the north side of the west tower remained vertical up to level 1. There was some twisting of the columns around the perimeter of the building at the lower levels.

The deformed shapes of the columns in the east tower shown in figure 4.4.14 indicate the mode of collapse in the two towers was similar.

### 4.4.2 Floor Slabs

The condition of the collapsed floor slabs in the vicinity of the shearheads near the top of a column is shown in figure 4.4.15. The behavior noted in Section 4.4.1 in which the upper level slabs fell with the columns, rotating as

the columns deformed, is apparent in the photograph. The slabs are completely separated from the shearheads and are aligned in a nearly vertical position. The post-tensioning strands are clearly visible.

Typical crack patterns and broken floor slabs are shown in figures 4.4.16 and 4.4.17. Note the slabs broke into a number of small pieces. This would be expected once the post-tensioning is lost due to the lack of conventional reinforcing steel except in the vicinity of the columns.

#### 4.4.3 Shearheads

The deformations of the shearheads that occurred at various levels in the structure during the collapse are shown in the stack of shearheads in figure 4.4.18. The position of the shearheads in the photograph was not changed as the debris was removed. Note that sixteen shearheads came to rest at level E. The ten shearheads which had been located in the upper levels of the structure were relatively undamaged. Similar conditions were observed at most locations throughout the structure. This indicates that the shearheads in the upper levels of the building were not subjected to forces large enough to induce substantial inelastic deformations during the collapse. Two possible explanations are: (a) the post-tensioning in the slabs could have been lost early in the collapse and the slabs broke away from the shearheads, and/or (b) the wedges supporting the upper level slabs could have been dislodged or the weld blocks on the columns could have sheared off.

Although welds at the weld blocks failed, this occurred only in a few cases. These were confined to the lower levels of the structure. The crack pattern in the slabs discussed in Section 4.4.2 suggests that the post-tensioning was lost. The deformed shapes of the columns in figures 4.4.13 and 4.4.14 discussed in Section 4.4.1 support this conclusion. The wedges had to be dislodged for the shearheads to come together as shown in figure 4.4.18. One would have expected to see some concrete remaining partially intact around the shearheads due to the presence of the reinforcing steel in the vicinity of the columns. If only the wedges had been dislodged and the post-tensioning not lost, one would have expected to see considerable scoring along the length of the columns as the floor slabs fell and the shearheads scraped the column. This was generally not the case. Scoring due to movement of the shearheads down the columns was observed in only a limited number of cases. Clearly, the wedges supporting the slabs in the upper levels were dislodged and the post-tensioning was lost early in the collapse.

The deformations of the lower six shearheads in figure 4.4.18 indicate they were subjected to considerable force during the collapse. It would appear that the slabs in the lower levels remained whole or portions of the slabs remained attached to the shearheads because of the conventional bonded reinforcing. Enough force was transmitted to the shearheads to cause the shearhead to fail, to cause a punching shear type failure of the slab or to fail the welds between the weld block and the column or the welds between the wedges and the weld blocks. Each of these conditions occurred. Figure 4.4.19 illustrates a situation where the shearhead failed. Although the welds to the wedge and the column held, the shearhead was literally torn apart. Failure of the weld block welds and the welds of the wedges are discussed in Section 4.4.4.

The locations of the shearheads along the height of the columns throughout the structure are shown in figure 4.4.20. In general, shearheads on the perimeter columns remained in place at the floor levels as the building collapsed. On the interior columns, however, the shearheads were dislodged and came together as shown in figure 4.4.18. Apparently the concrete slabs broke away from the shearheads around the perimeter leaving the shearheads in place. At the interior columns, the slabs exerted sufficient force to fail the shearhead-column connection. There was more conventional reinforcing in the slab at the interior columns than at the perimeter columns and it was located on all four sides of the column.

The shearhead detail at what would appear to be a corner column is shown in figure 4.4.21. Only one such shearhead detail, however, was found. Note the post-tensioning tendons were run through the channel sections comprising the shearhead rather than over the shearhead. This was probably due to the need to locate the post-tensioning tendons at mid-depth of the slab.

#### 4.4.4 Welds

The performance of the welds varied throughout the structure. In some cases the welds remained intact without signs of distress while in other cases the welds failed. The performance of a column splice weld is shown in figure 4.4.22. Despite the apparently high forces exerted on the column section and the severe deformations illustrated in figure 4.4.22, the column splice weld remained intact.

The variation in performance of the welds at the shearhead - column connection is illustrated in figures 4.4.23-27. In some cases, as shown in figure 4.4.23, the welds remained intact. There were no apparent deformations of the elements of the connection and it is not clear to what force the connection was subjected. The welds on the weld block shown in figure 4.4.19 remained intact, although the failure of the shearhead suggests that considerable force was applied to the weld block.

Some welds failed on the weld blocks as shown in figures 4.4.24, 4.4.25 and 4.4.26. The wedges were fully welded and these connections were obviously at slabs in the building which were in their final locations rather than parked temporarily. In the latter case, the wedges were only tack welded. Note the rotation of the wedge in figure 4.4.25. Note also the small shim on the bottom of the wedge. In all three figures, the wedge had pulled away from the column flange and the weld block. The welds do not appear to have fractured but rather the wedge separated from the weld, probably due to the lack of fusion.

Failure of a weld on a weld block is shown in figure 4.4.27. A crack in the column flange can be seen at the top of the weld block (to the right in the photograph). This crack propagated under the weld block and through the weld block weld about half way down the weld block. Note the separation of the upper portion of the weld block from the column flange. Again there appears to be a lack of fusion between the weld and weld block at this location.

A weld for a wedge under one of the upper level slabs which was parked temporarily prior to being lifted to its final position is shown in figure 4.4.28. Note in this case the wedge was welded to the column at each end with a small tack weld. The wedge was not welded to the weld block or shearhead. This was done for ease of removal of the wedge prior to lifting the slab to its final position. In several cases these tack welds were extremely small. They were difficult to see and barely perceptible to the touch as a raised portion on the flange.

#### 4.4.5 Additional Observations

Additional observations during the on-site investigation included the performance of the perimeter walls at the garage levels and the performance of the jack rods used to lift the slabs.

The perimeter wall on the north side of the building was below ground level. This basement wall extended from level E to level C in the parking garage. The wall was in contact with the floor slabs at these levels. The retaining wall on the west side of the buildings was not in contact with the structure. A photograph taken on May 1, 1987 of the basement wall on the north side of the east tower, viewed from the east end, is shown in figure 4.4.29. Note that the wall appears straight. Figure 4.4.30 presents a similar view taken on July 22, 1987 after the rescue operations were complete and much of the debris removed. There is a noticeable lateral displacement or bowing along the length of wall. Evidence of movement of the retaining wall was also observed on the surface of the backfill, which exhibited two parallel tension cracks in the direction of the wall extending over the entire length of the wall (figure 4.4.31). Either the wall was damaged during the collapse or by surcharge loads and vibrations during removal of the debris.

Many of the jack rods used to lift the slabs were cut with an acetylene torch during removal of the debris. Three fractured jack rods were found in the debris at the landfill and one fractured rod was removed from the jack at column A9 in the east tower. The jack locations of the rods from the debris could not be determined. These three rods were approximately 3 to 5 ft (0.9 to 1.5 m) in length. The fractures indicated the rods were subjected to bending and axial load. Results from metallographic tests of the fracture surface are presented in Section 5.5.3.

#### 4.4.6 Detailed Observations of Stage IV Columns - West Tower

As debris was removed from the construction site, an effort was made to identify column sections at the Seaside Park landfill. Specifically, this effort focused on the upper sections of the columns and the shearheads that were either in the process of being adjusted or had been lifted just prior to the collapse. In certain cases the entire upper column stage (stage IV) was found intact and the location of the column could be positively identified by the shop number. In most cases, however, the upper column stage had been flame-cut during the rescue operation. It was therefore necessary to determine the location of the column by measuring the section size, by carefully examining the upper end for the presence of tack welds near the weld plates, and by classifying the types of shearheads whenever they were present. With few

exceptions, the specific location of the upper column stages removed from the debris could be established.

As the investigation progressed, column sections from the west tower assumed the greatest importance. These sections were examined and described in considerable detail. Descriptions of the stage IV columns from the west tower are included in this report as Appendix A. In some cases only segments of the lower column stages could be positively identified. Where these lower segments provide valuable information, such as the remains of the upper-level shearheads, their characteristics are included as a part of the general description. A summary of the tack welds and marks found on the stage IV columns from the west tower is presented in table 4.4.1.

At the time of the collapse, wedges had been placed under the shearheads of slab 9 on column lines G and H and at column E.5. The remaining columns picked up the loads from the package of slabs 9/10/11 through the jacks and, during the collapse, most of these column tops were indented by the jacks. Similarly, the underside of the shearheads at slab 9 were indented by the lifting nuts. A typical imprint caused by the base of a 150-kip (667 kN) jack is shown in figure 4.4.32. Figure 4.4.33 shows a typical indentation in the underside of a shearhead lifting angle. In some cases the lifting nut slid off or "kicked out" from under the lifting angle, leaving a clear track in the bottom face of the angle. This usually was followed by the lifting nut impacting the column web and causing an indentation in the web at approximately 52 in (1.32 m) below the column top.

In general, the columns along line C experienced the most damage in the collapse. Much of this damage was caused by rotation under cantilever action of the shearheads in slabs 9/10/11. Column C4.8, shown in figure 4.4.34, is typical of the observed damage patterns. Most of the columns in this line retained the upper shearheads close to their pre-collapse positions. In at least three cases the top (roof) shearhead slid off the top of the column. Gouges in the column flanges due to interference with the shearheads during the lifting operation were observed on some stage IV column sections. An example of this is column C3 shown in figure 4.4.35.

The columns along line E experienced less damage than did those in line C and the shearheads tended to slide downward to levels 1, 2 or 3. Most or all of the wedges at these three levels had been fully welded at the time of the collapse. With the exception of the columns on line 6 and columns H1 and H2, stage IV of all the columns in lines G and H suffered very little damage. Most remarkable was the condition of the upper weld blocks on these columns. Even though the wedges had been installed under slabs 9 and 12, there were many instances where the wedges were dislodged without any visible damage to the contact surface on the weld blocks.

#### 4.4.7 Summary

The following summarizes the eyewitness accounts of the collapse and NBS observations of the collapsed structure:

1. Wedges were being placed under slabs 9/10/11 in the west tower at the time of the collapse.
2. There was no perceptible displacement or motion of the building immediately prior to the collapse.
3. The collapse was preceded by a loud noise heard as far as 100 yards (91.4 m) from the site.
4. The collapse began in the upper levels of the west tower.
5. The collapse was extremely rapid. The total time involved from initiation to complete collapse was estimated to be from 2 to 10 seconds.
6. Each tower collapsed toward its center; there was no indication of any consistent translation or rotation in which the structure deformed as a unit.
7. The wedges supporting the slabs in the upper levels of the west tower were dislodged and the post-tensioning in the slabs was lost early in the collapse.
8. Many of the shearheads in the upper levels of the structure were undamaged; shearheads in the lower levels were significantly deformed.
9. Displacements of the basement wall on the north side of the building occurred after removal of the collapsed structure.

TABLE 4.4.1

SURVEY OF STAGE IV COLUMNS FROM WEST TOWER

COLUMN NO.	SECTION	COLUMN FOUND	TACK WELD		GOUGES	COL. TOP INDENTED	LIFTING NUT IMPACT
			ROOF/12	11/10/9			
C1	HP10X42	C1	Y	N		Y	Y
C2	HP12X53	C2	Y	N		Y	*
C3	W12X65	C3	Y	N	Y		
C3.8	W12X65	C3.8	Y	N		Y	
C4.8	HP123X53	C4.8	Y	N	Y	Y	
C6	W8X35	MISSING					
C.5	W12X65	C.5	Y	N		Y	
E1	W10X60	E1	Y	N	Y	Y	Y
E2	W12X106	E2	Y	N		Y	Y
E3	W12X120	E3	Y	N			Y
E3.8	W12X120	MISSING					
E4.8	W12X106	E4.8	Y	N		Y	Y
E.5	W12X72	E.5	Y	Y			
G1	W10X60	G1	Y	Y			
G2	W12X106	G2	Y	Y			
G3	W12X136	G3/G4	Y	Y			
G4	W12X136	G3/G4	Y	Y			
G5	W12X106	G5	Y	Y			
G6	HP12X53	G6	Y	Y			
H1	HP10X42	H1	Y	Y			
H2	W12X65	H2	Y	Y			
H3	W12X79	H3	Y	Y			
H4	W12X79	H4	Y	Y			
H5	W12X65	H5	Y	Y			
H6	HP10X42	H6	Y	Y			

\* Some scraping visible but no clear indentation

Note: No entry indicates not observed or not relevant to failure condition



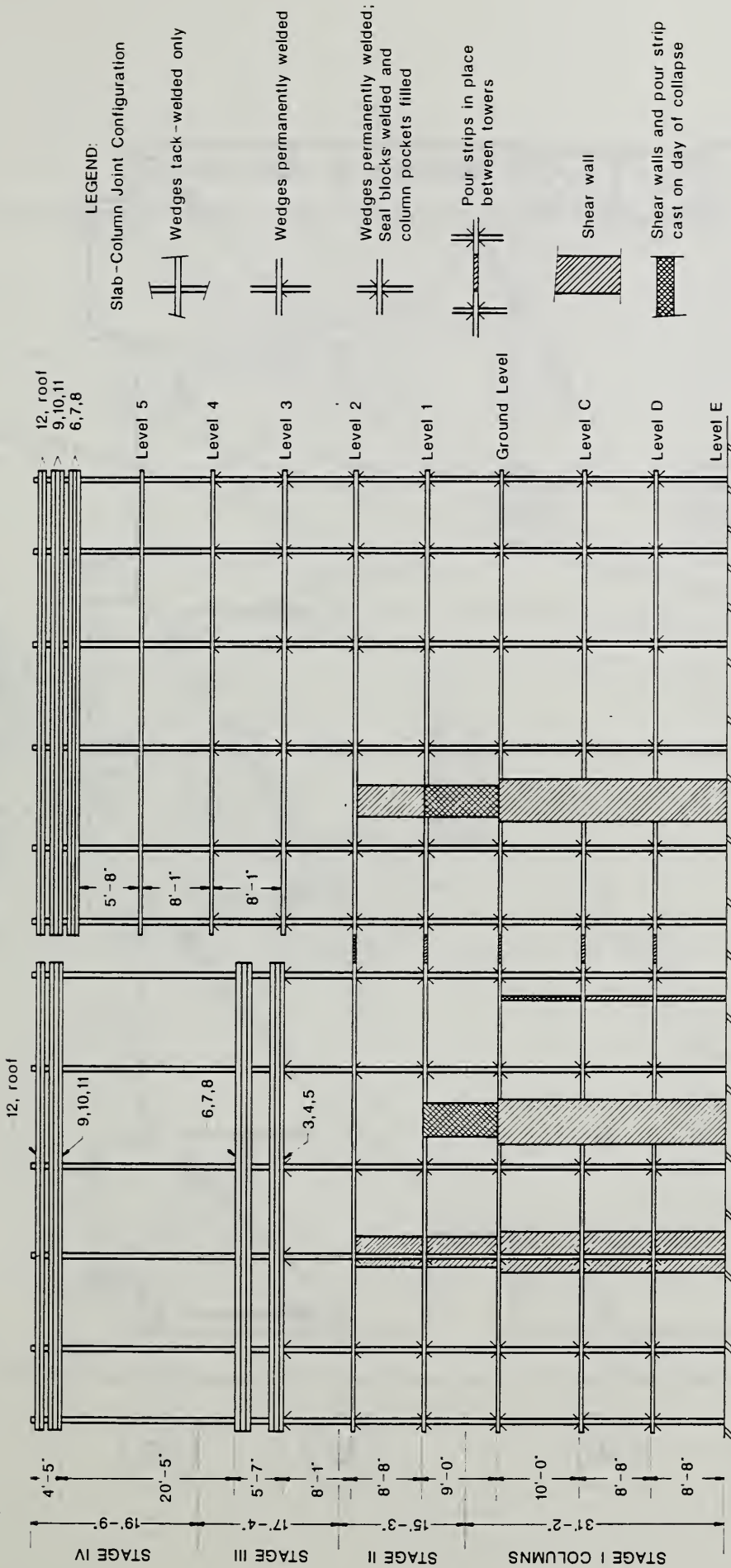
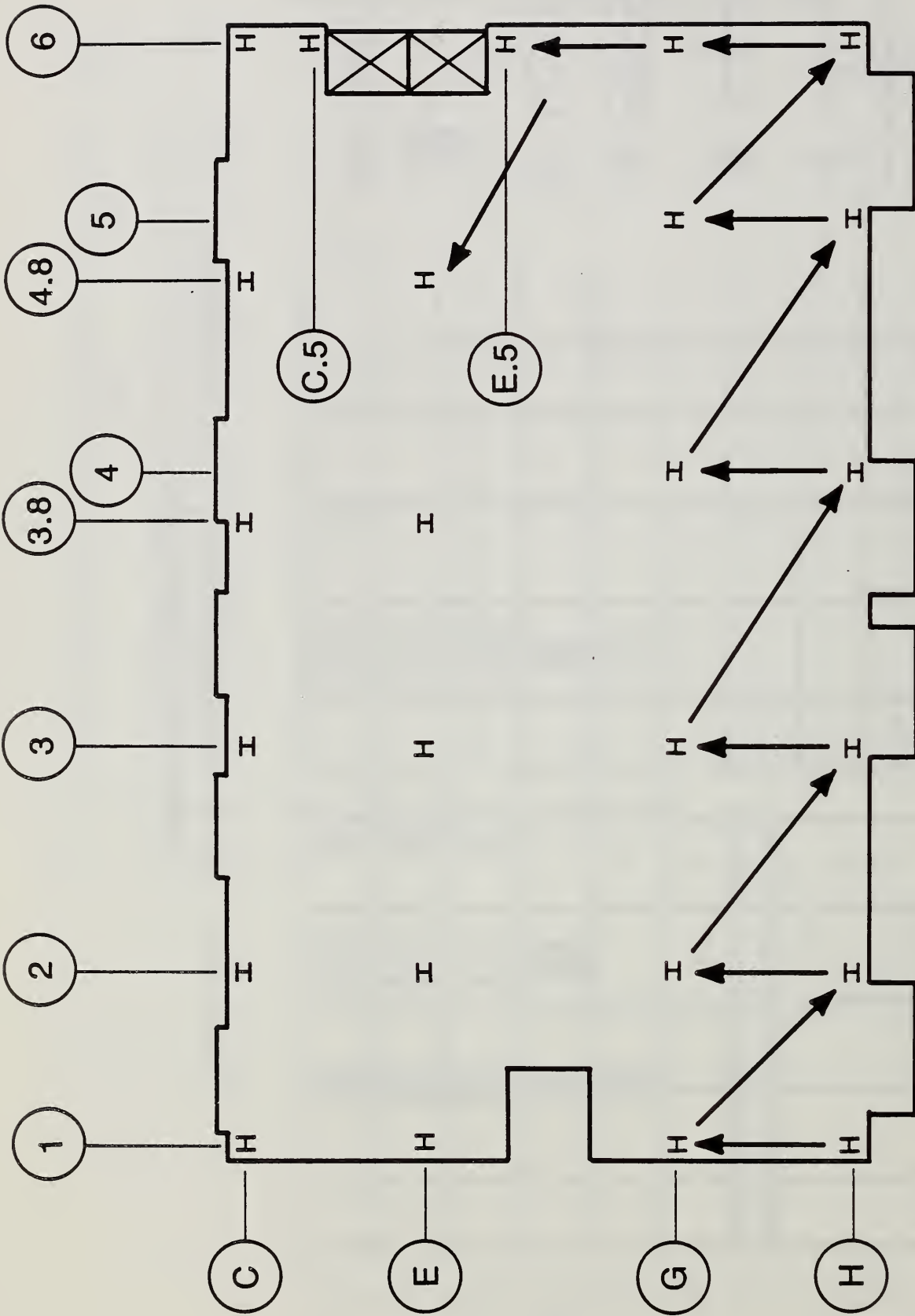


Figure 4.2.1 State of construction at time of collapse  
 - viewed from the South



## Level 9 Slab

Figure 4.2.2 Sequence of placement of wedges immediately prior to collapse  
 - West tower, Levels 9, 10, 11

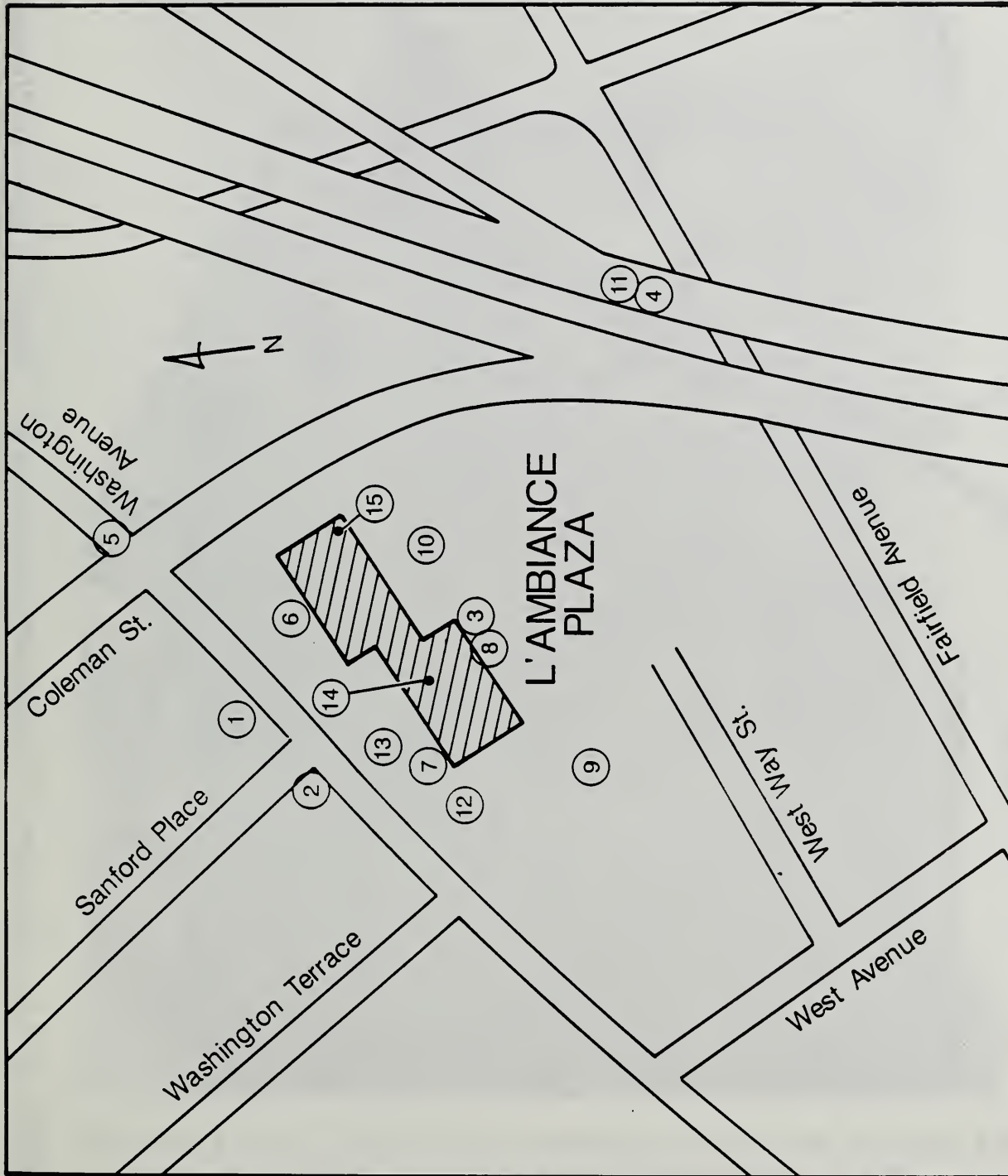


Figure 4.3.1 Location of key eyewitnesses

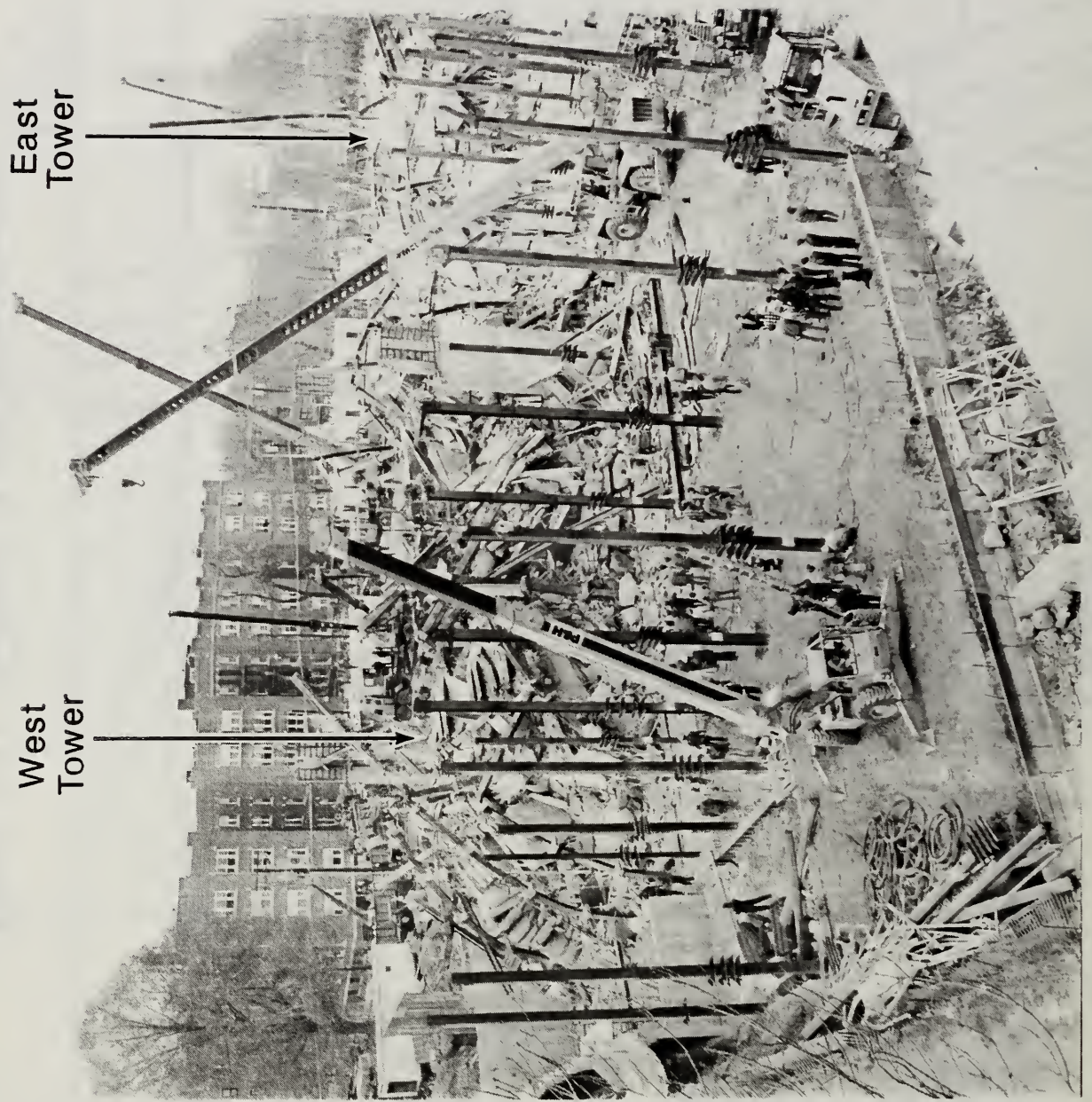


Figure 4.4.1 Overview of collapsed structure – View to the Northeast



Figure 4.4.2 Column C3 bending about the strong axis -  
View to the East, shearwall on left



Figure 4.4.3 Deflected shape of column E1 –  
View to the North



Figure 4.4.4 East perimeter columns at Levels E and D. East tower—  
View to the North; photo taken after rescue  
operations complete



Figure 4.4.5 Diagonal tension crack in East tower shearwall -  
View to the South





Figure 4.4.6 Twisting deformation of column in West tower

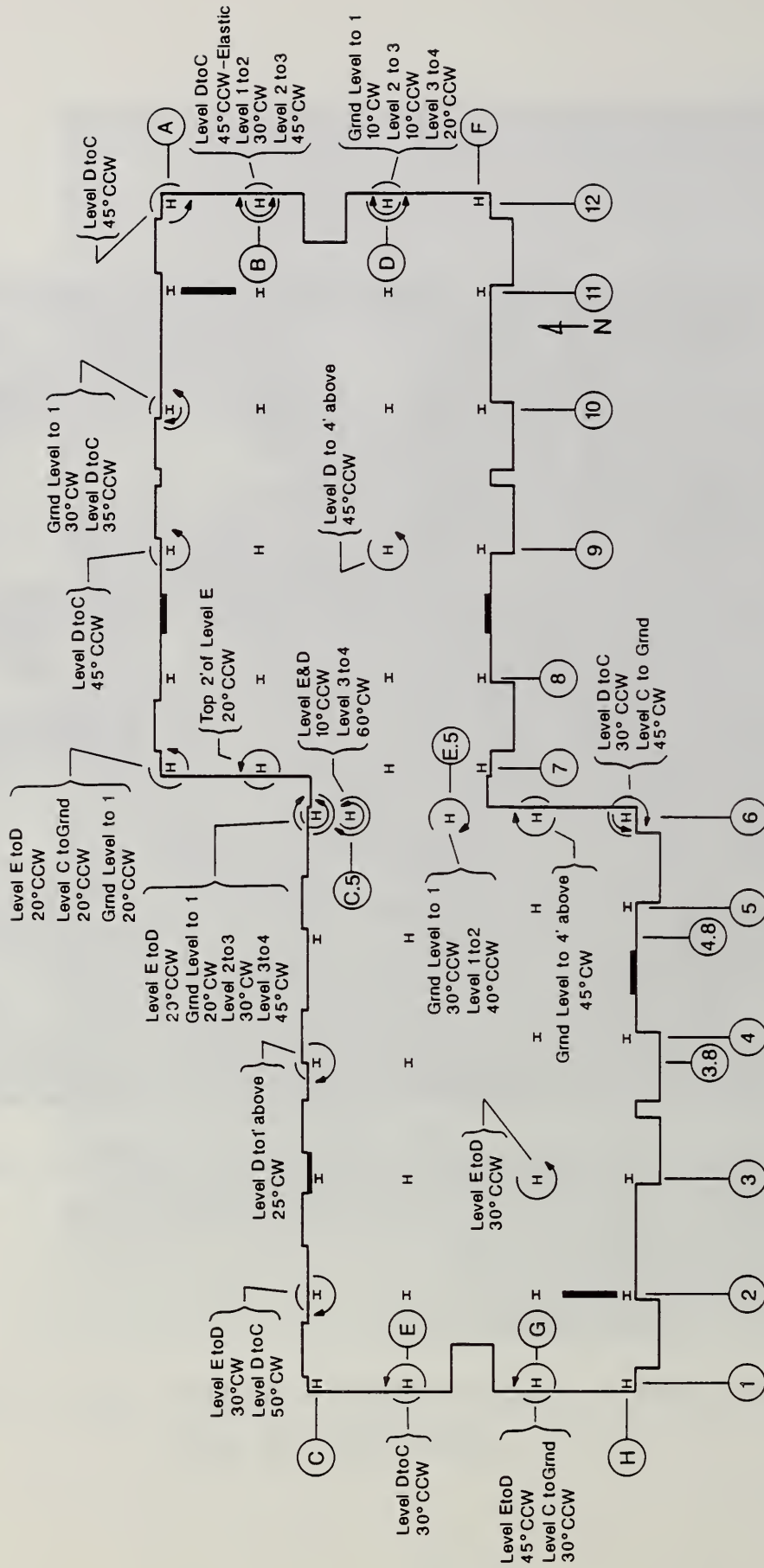


Figure 4.4.7 Pattern of perimeter column twists



Figure 4.4.8 Lower level floor slabs at Northwest corner of West tower – View to the North; column E1



Figure 4.4.9 Upper floor slabs on Northwest corner of West tower - View to the North; column E1



Figure 4.4.10 Lower level floor slabs in center portion of West tower – View to the Northeast



Figure 4.4.11 Floor slabs in the central portion of East tower – View to the Southwest



Figure 4.4.12 Floor slabs in Southeast corner of East tower -  
View to the Northeast

L'Ambiance Plaza  
West Tower Viewed from SE Corner

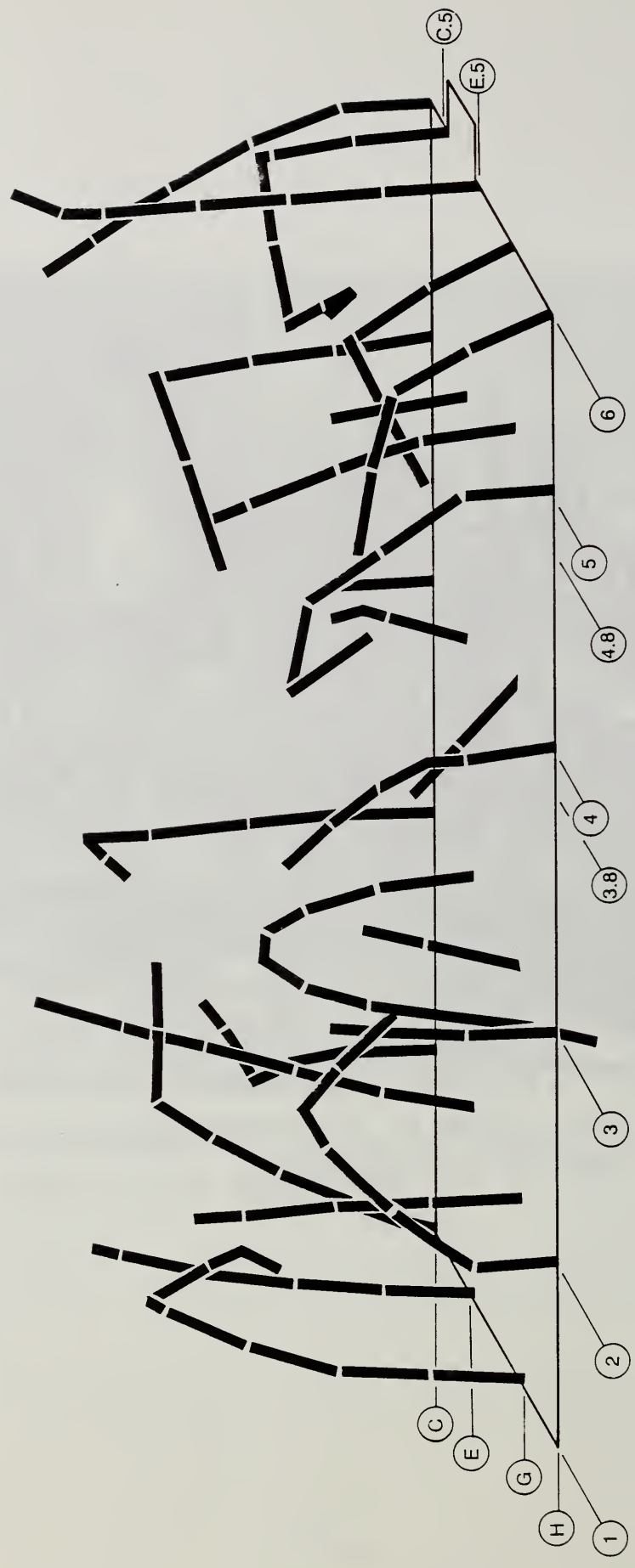


Figure 4.4.13 Pattern of column deformations – West tower



L'Ambiance Plaza  
West Tower - South View

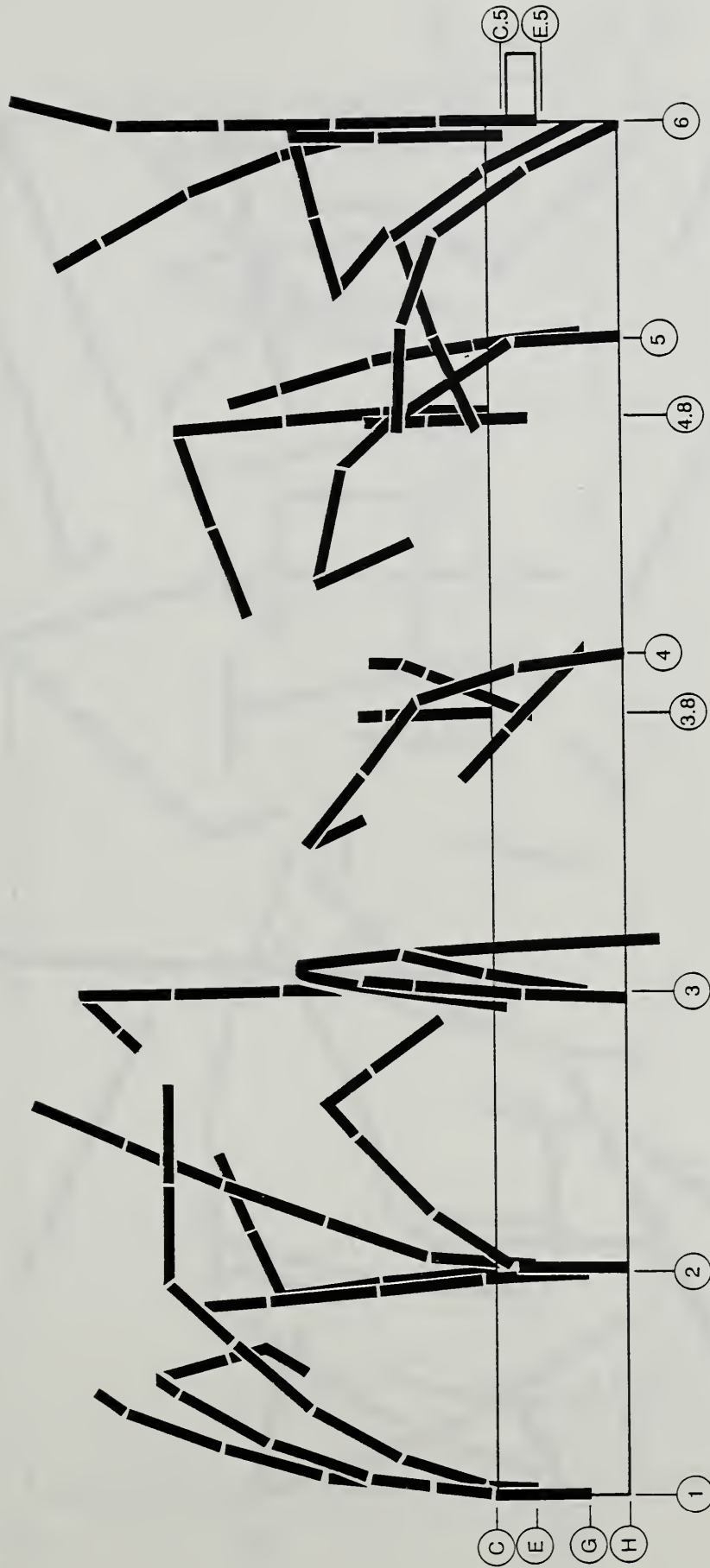


Figure 4.4.13 Continued

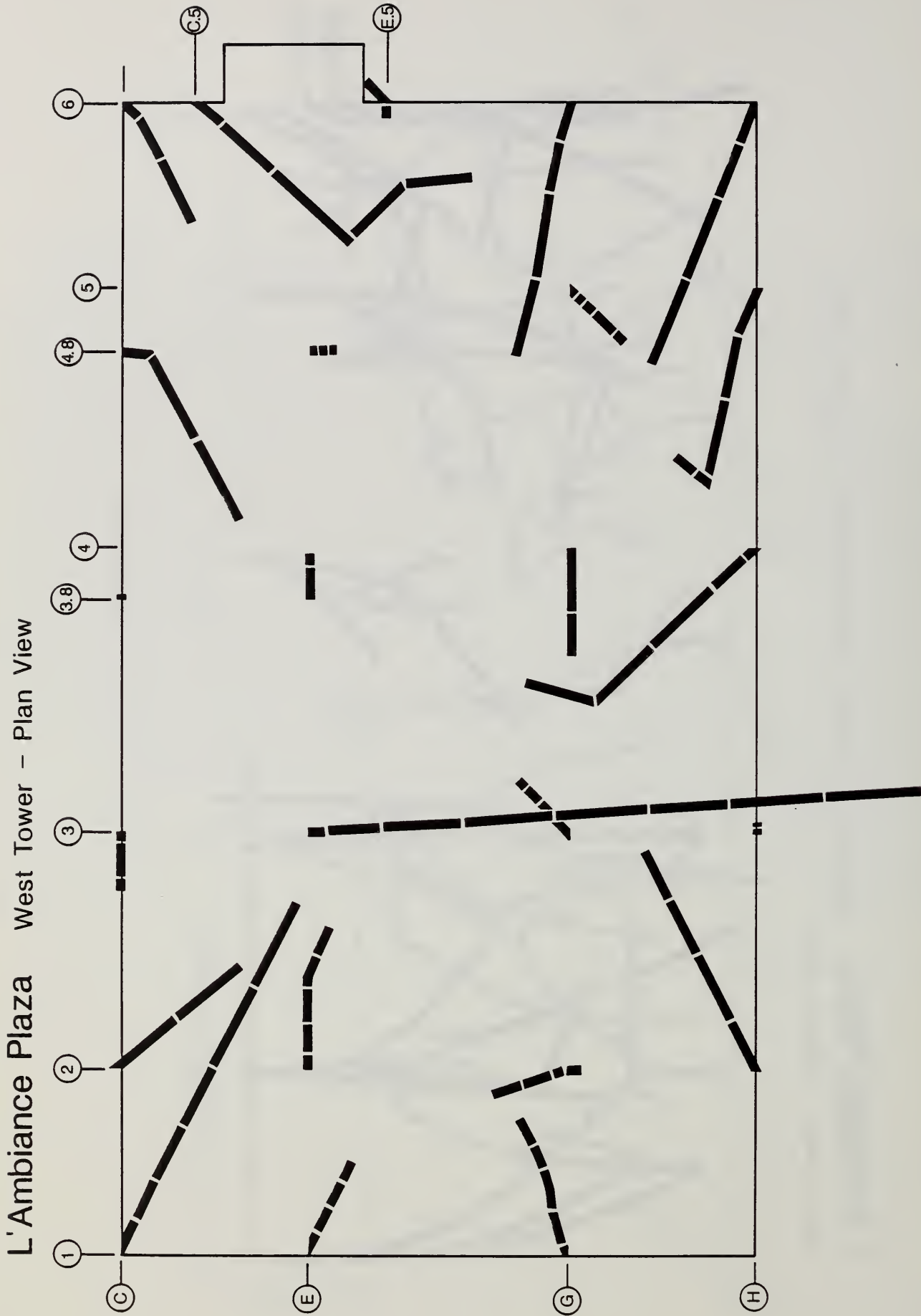


Figure 4.4.13 Continued

L'Ambiance Plaza  
East Tower Viewed from SW Corner

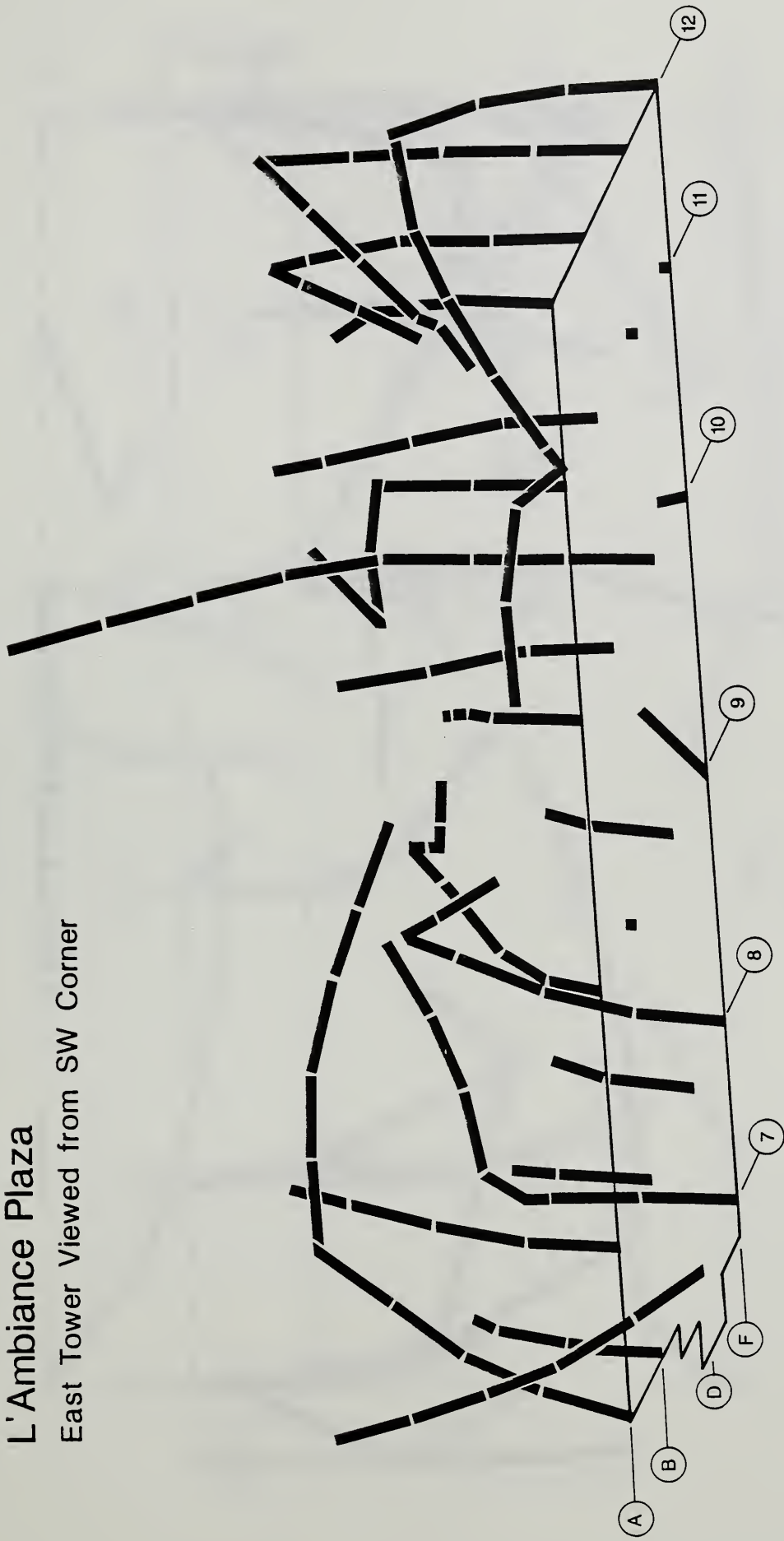


Figure 4.4.14 Pattern of column deformations - East tower

L' Ambiance Plaza  
East Tower - South View

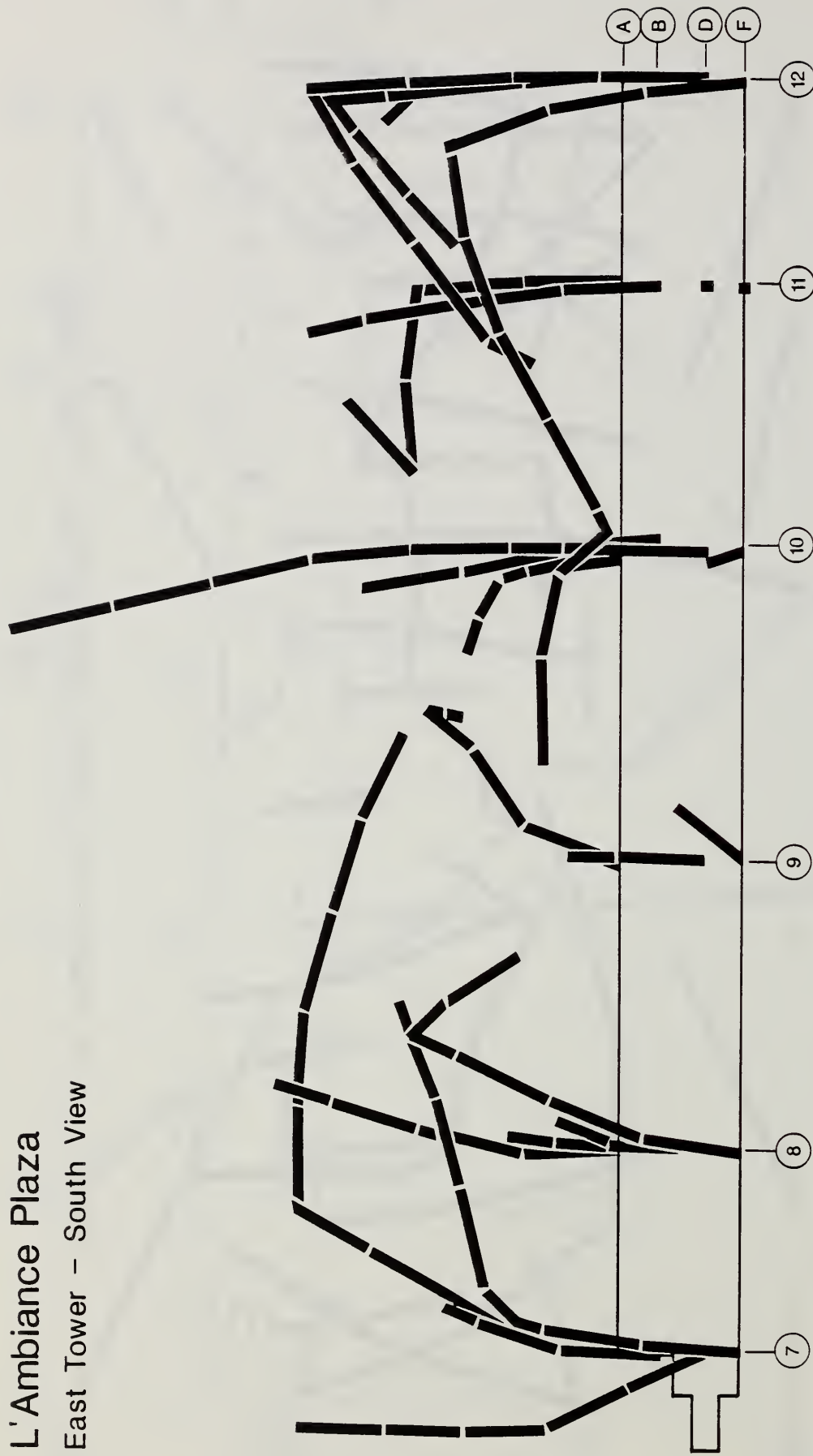


Figure 4.4.14 Continued

L'Ambiance Plaza East Tower - Plan View

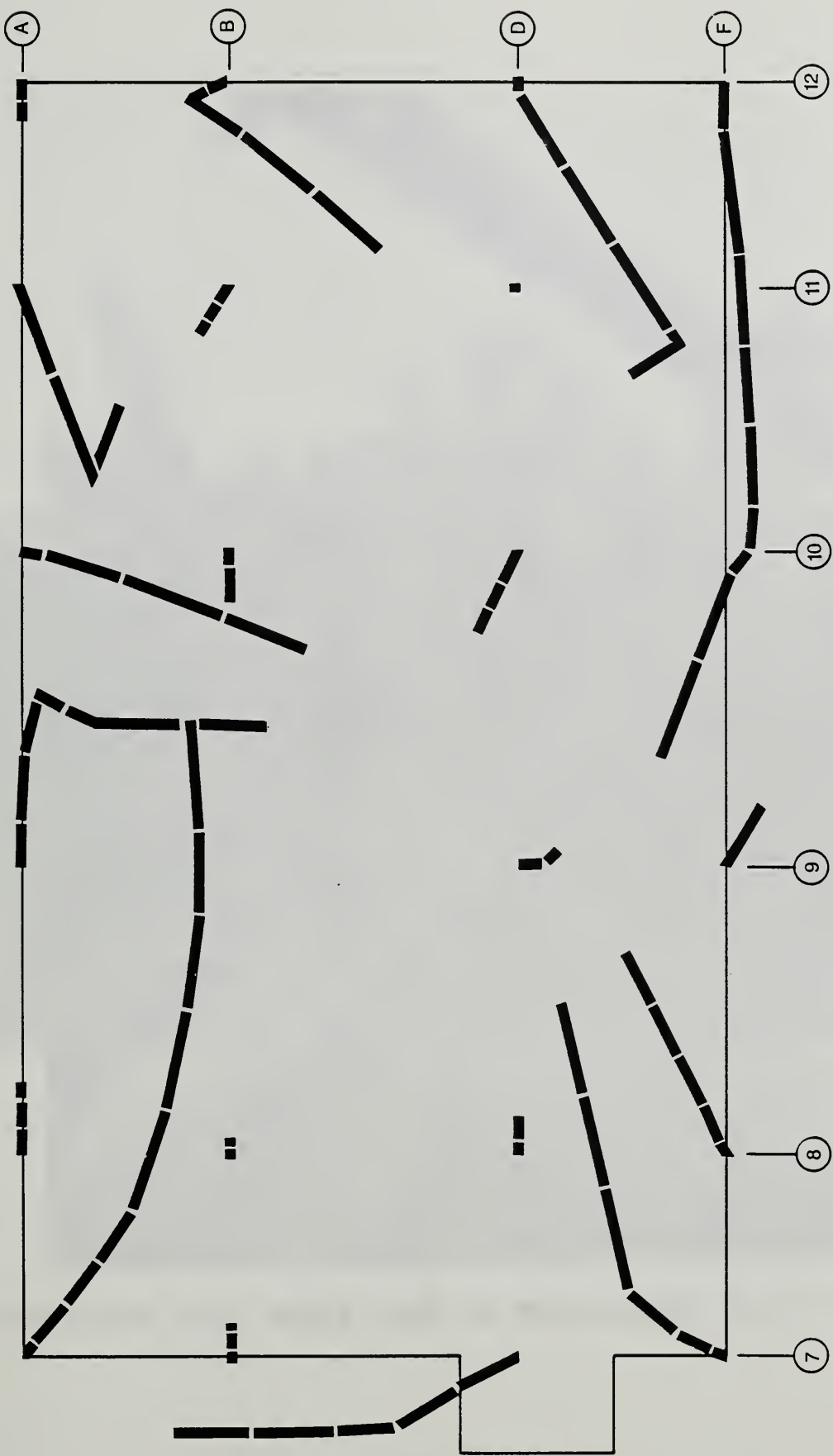


Figure 4.4.14 Continued



Figure 4.4.15 Separation of floor slabs from shearheads



Figure 4.4.16 Floor slab crack pattern



Figure 4.4.17 Broken floor slabs – View to the Southeast; column line H

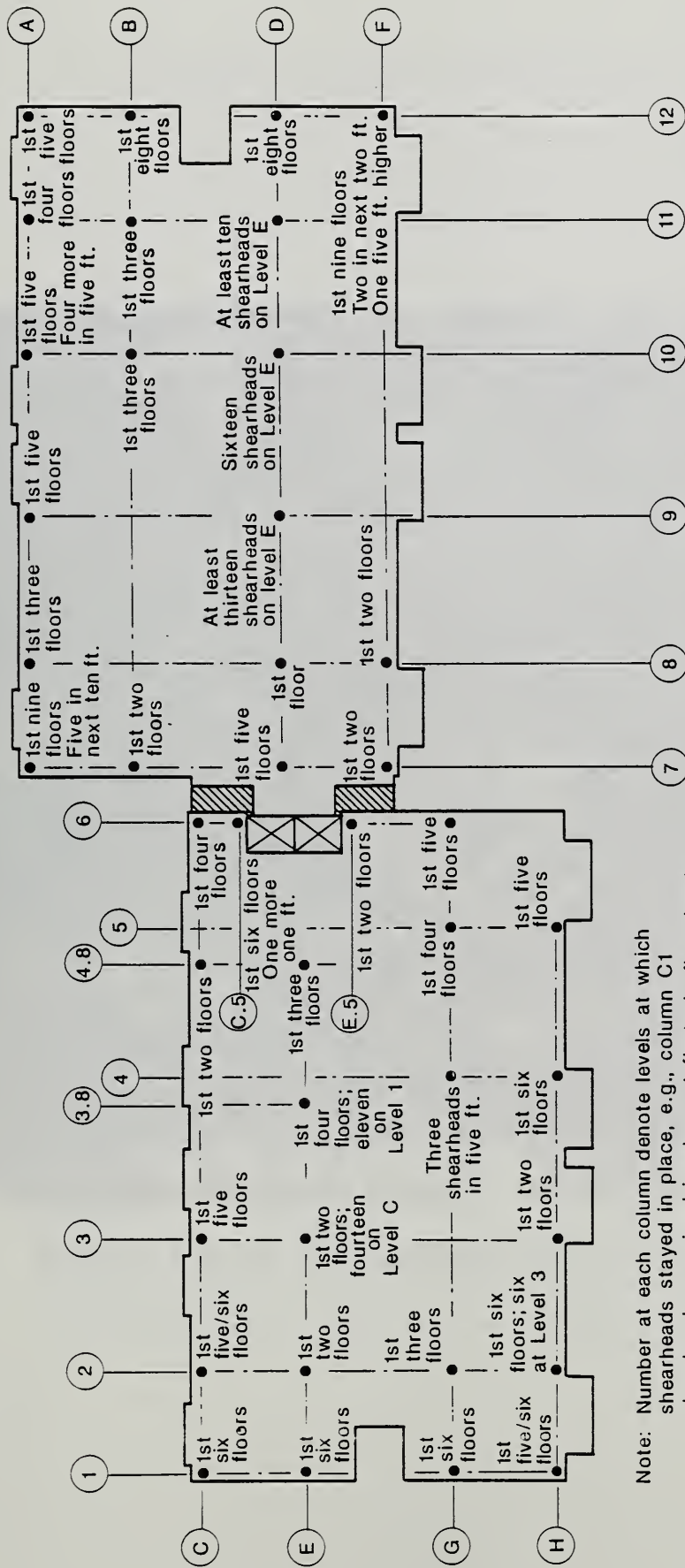




Figure 4.4.18 Deformation pattern of shearheads  
- column D10



Figure 4.4.19 Failed shearheads



Note: Number at each column denote levels at which shearheads stayed in place, e.g., column C1 shearheads remained in place at first six floor levels

Figure 4.4.20 Location of shearheads along column height

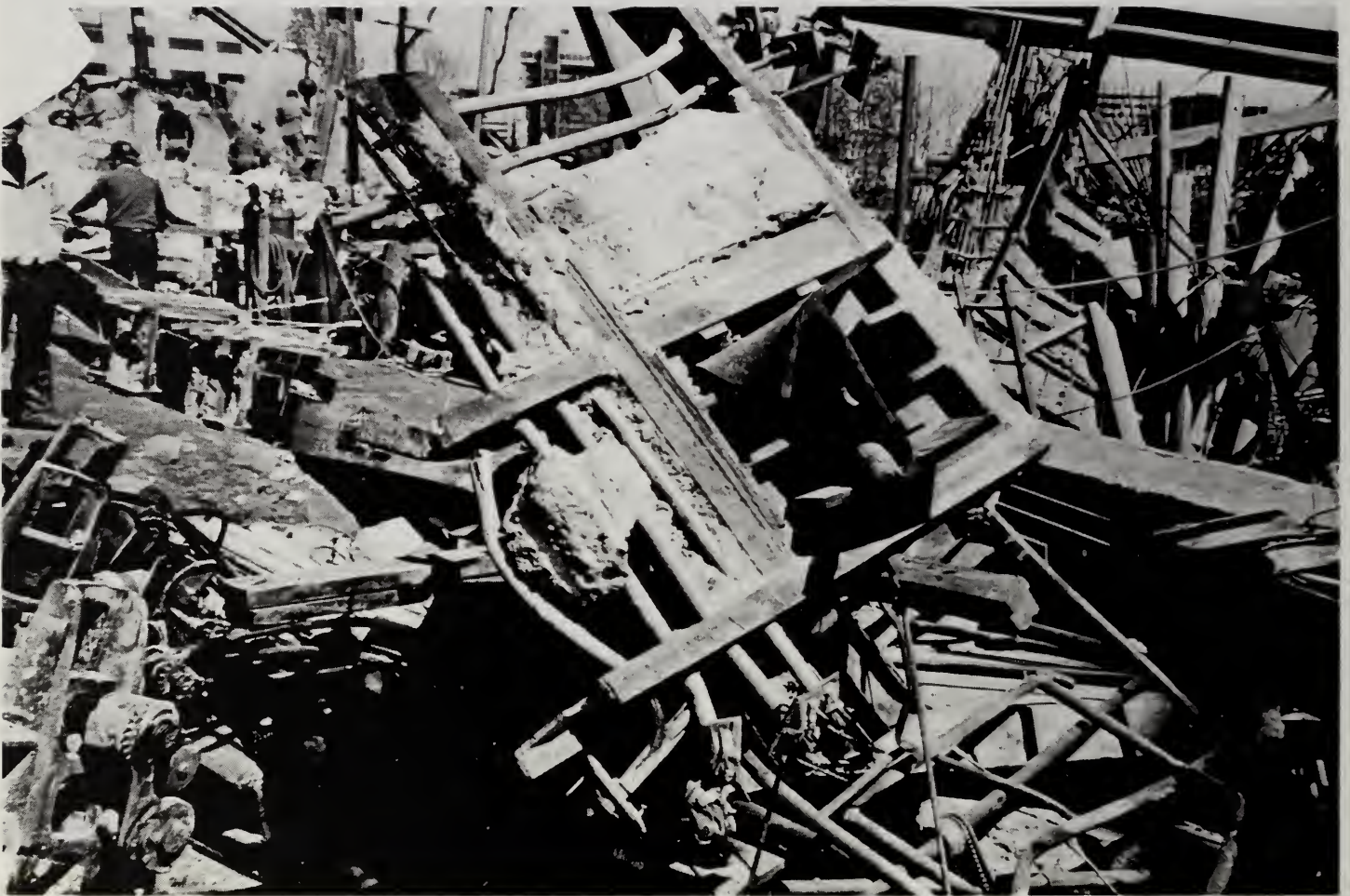


Figure 4.4.21 Corner column shearhead detail



Figure 4.4.22 Deformation at column splice



Figure 4.4.23 Intact shearhead support

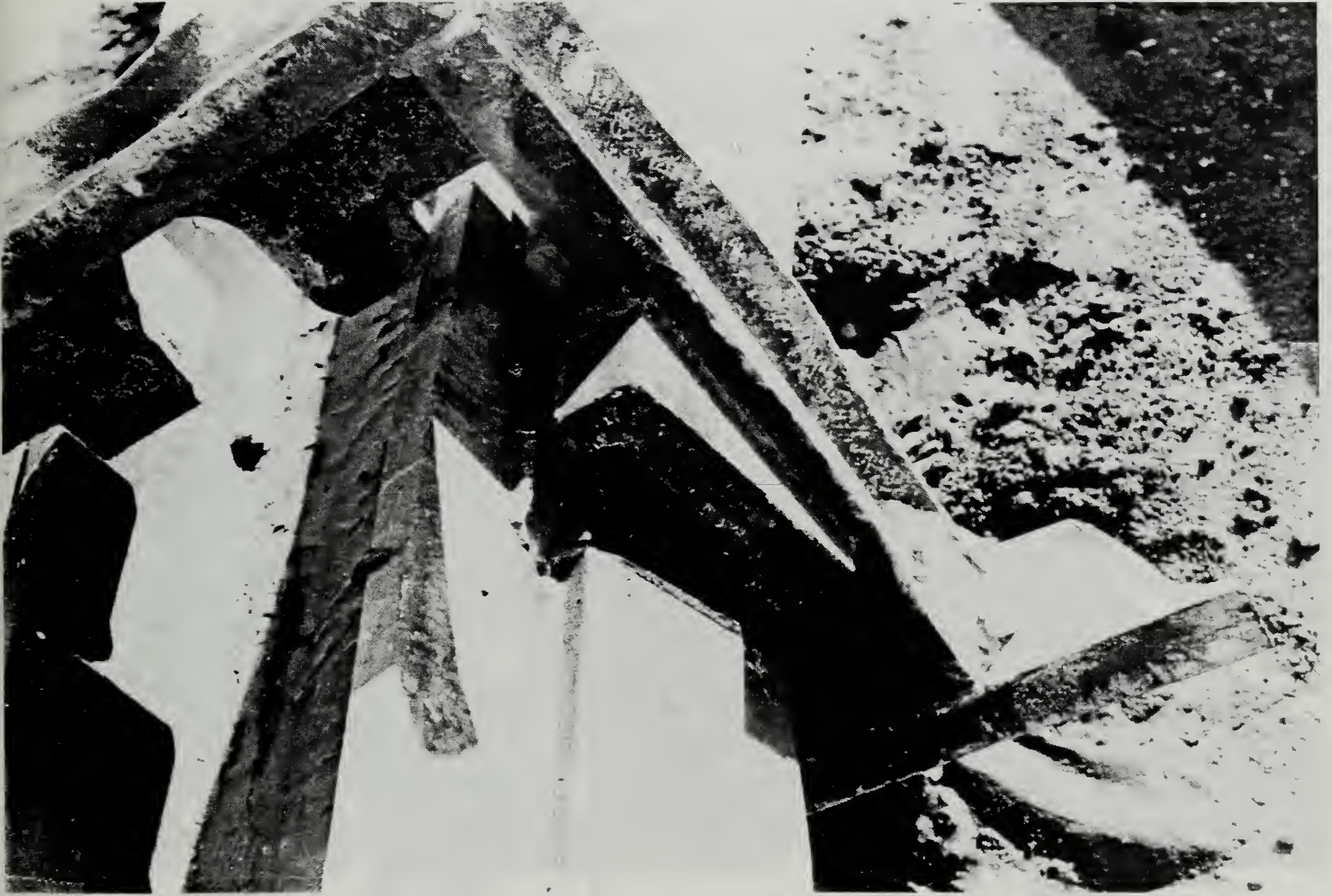


Figure 4.4.24 Weld failure at weld block



Figure 4.4.25 Weld failure at weld block with shim





Figure 4.4.26 Weld failure at weld block

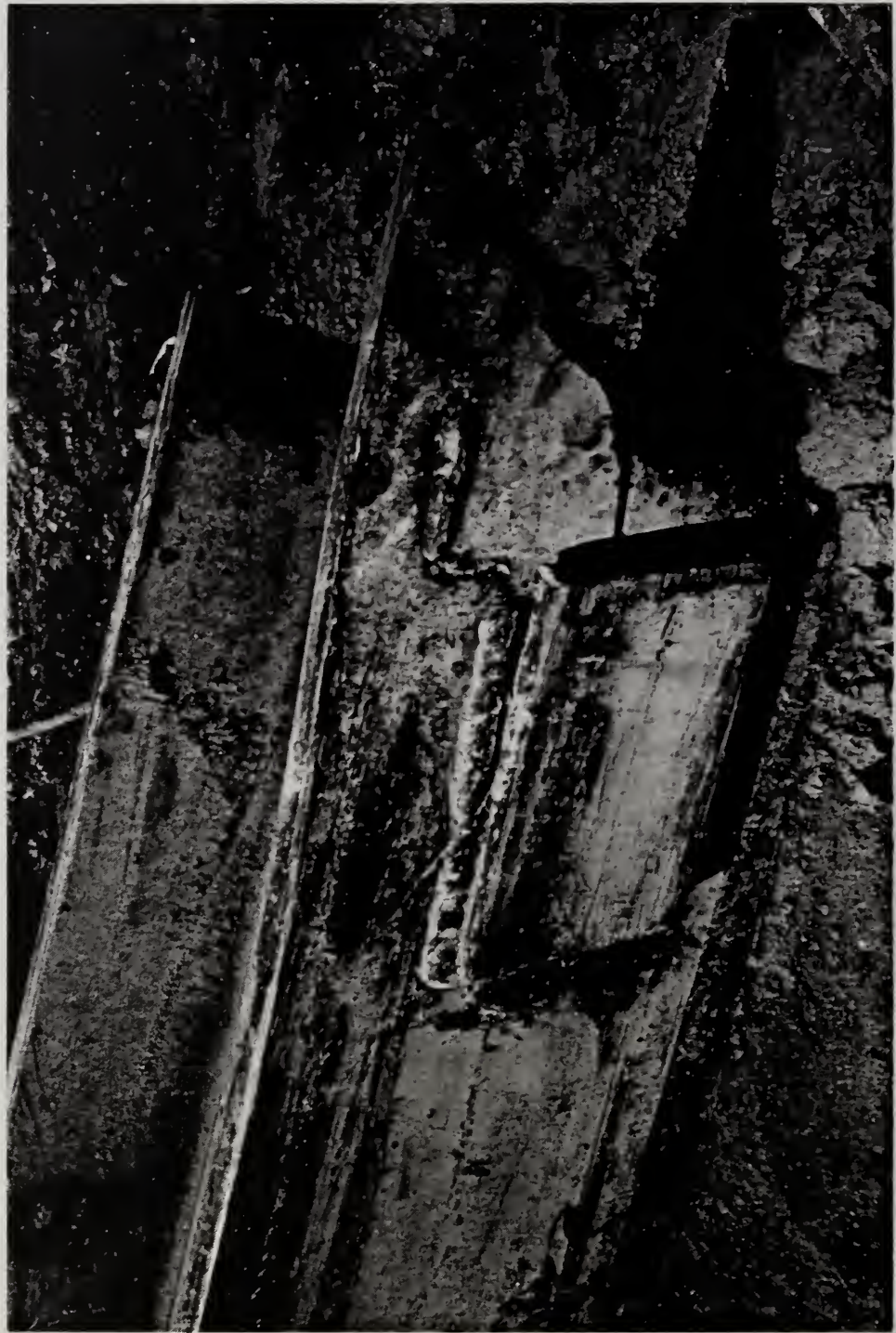


Figure 4.4.27 Weld block weld failure



Figure 4.4.28 Failure of temporary weld at shearhead support



Figure 4.4.29 Basement wall on North side of East Tower – viewed from the East, May 1, 1987



Figure 4.4.30 Basement wall on North side of East Tower – viewed from the West, July 22, 1987



Figure 4.4.31 Tension cracks in backfill behind basement wall - North side of building

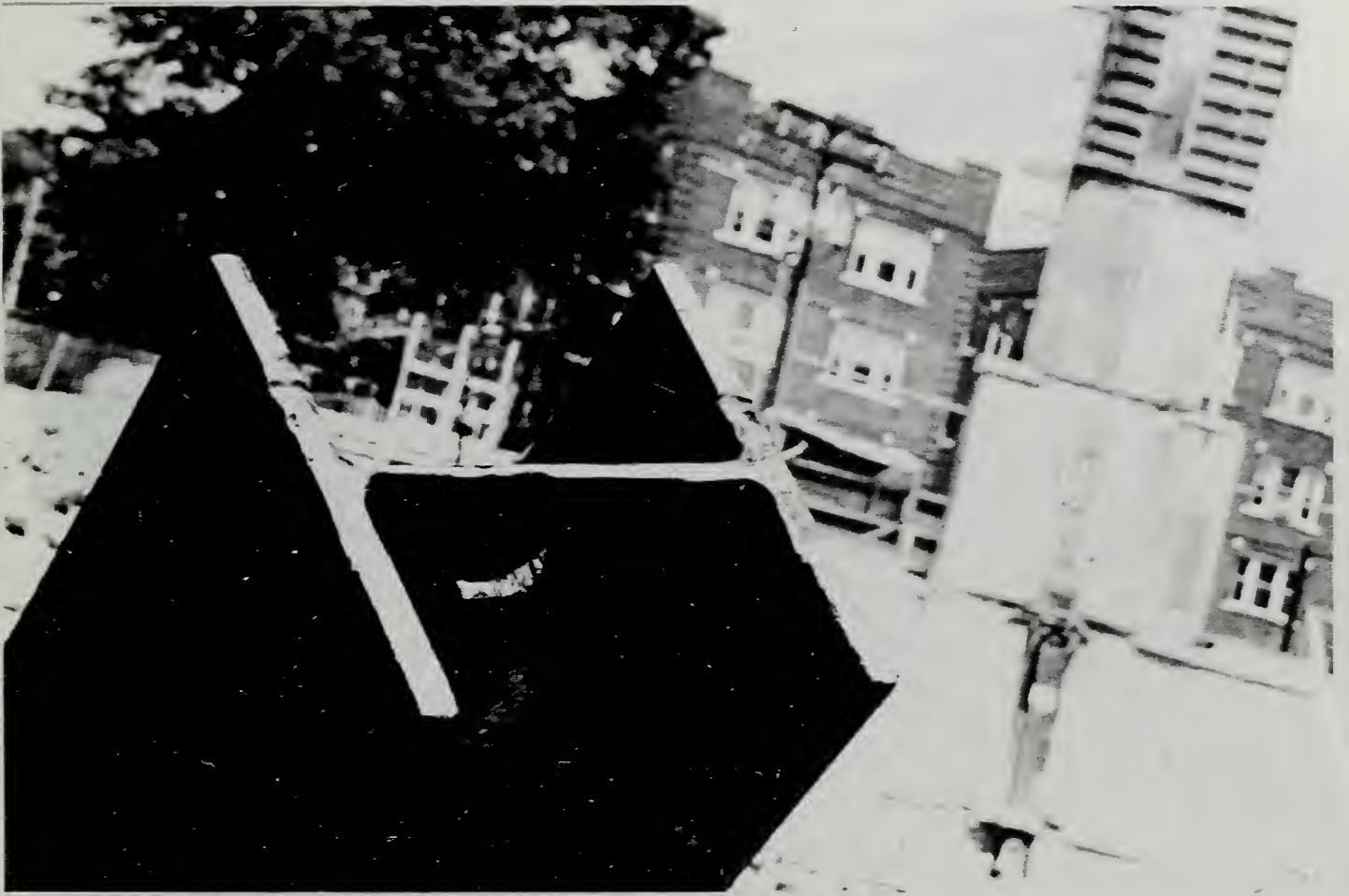


Figure 4.4.32 Typical indentation in top of column due to lifting jack



Figure 4.4.33 Typical indentation in underside of lifting angle



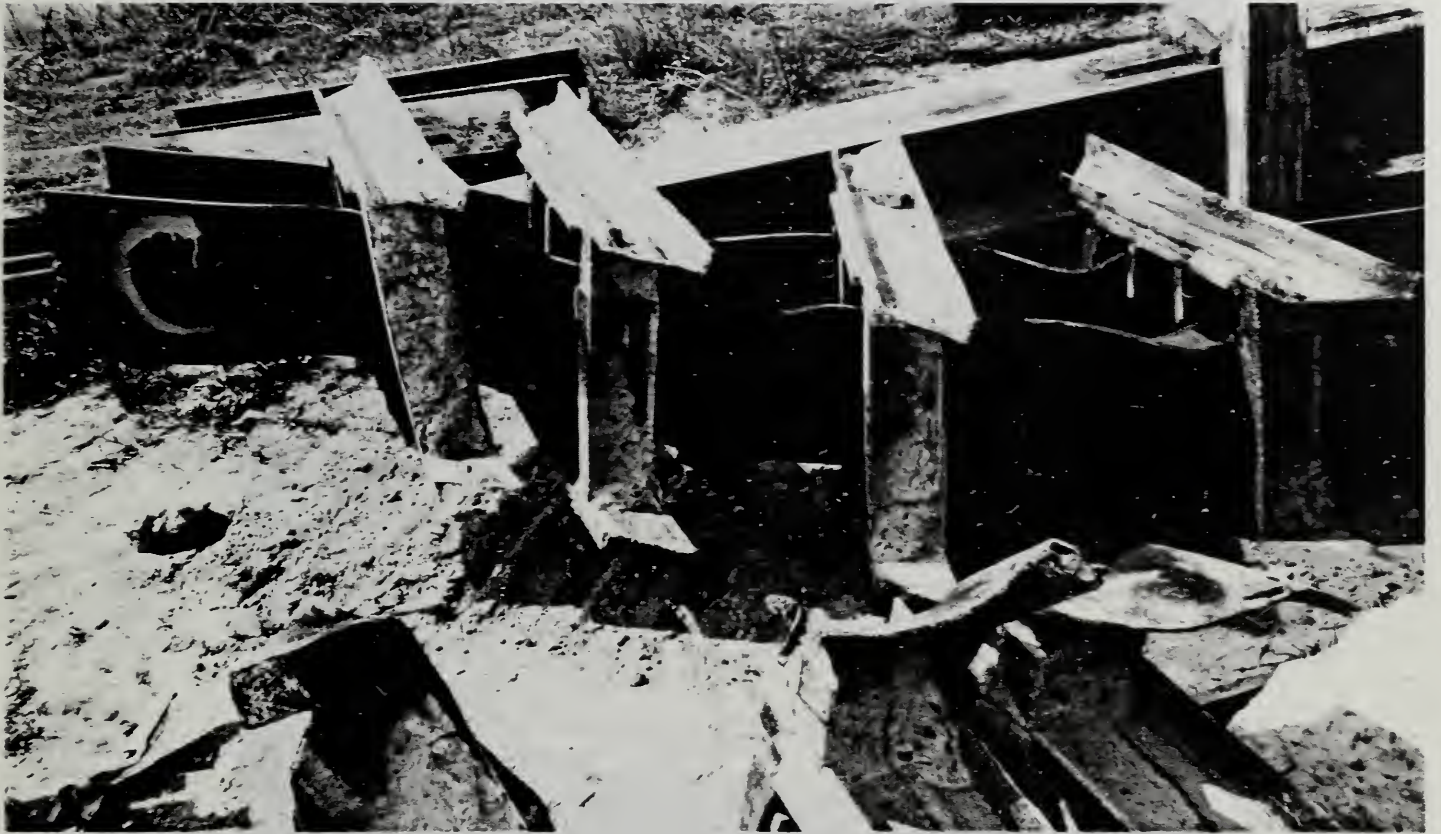


Figure 4.4.34 Deformation of column C4.8 in stage IV

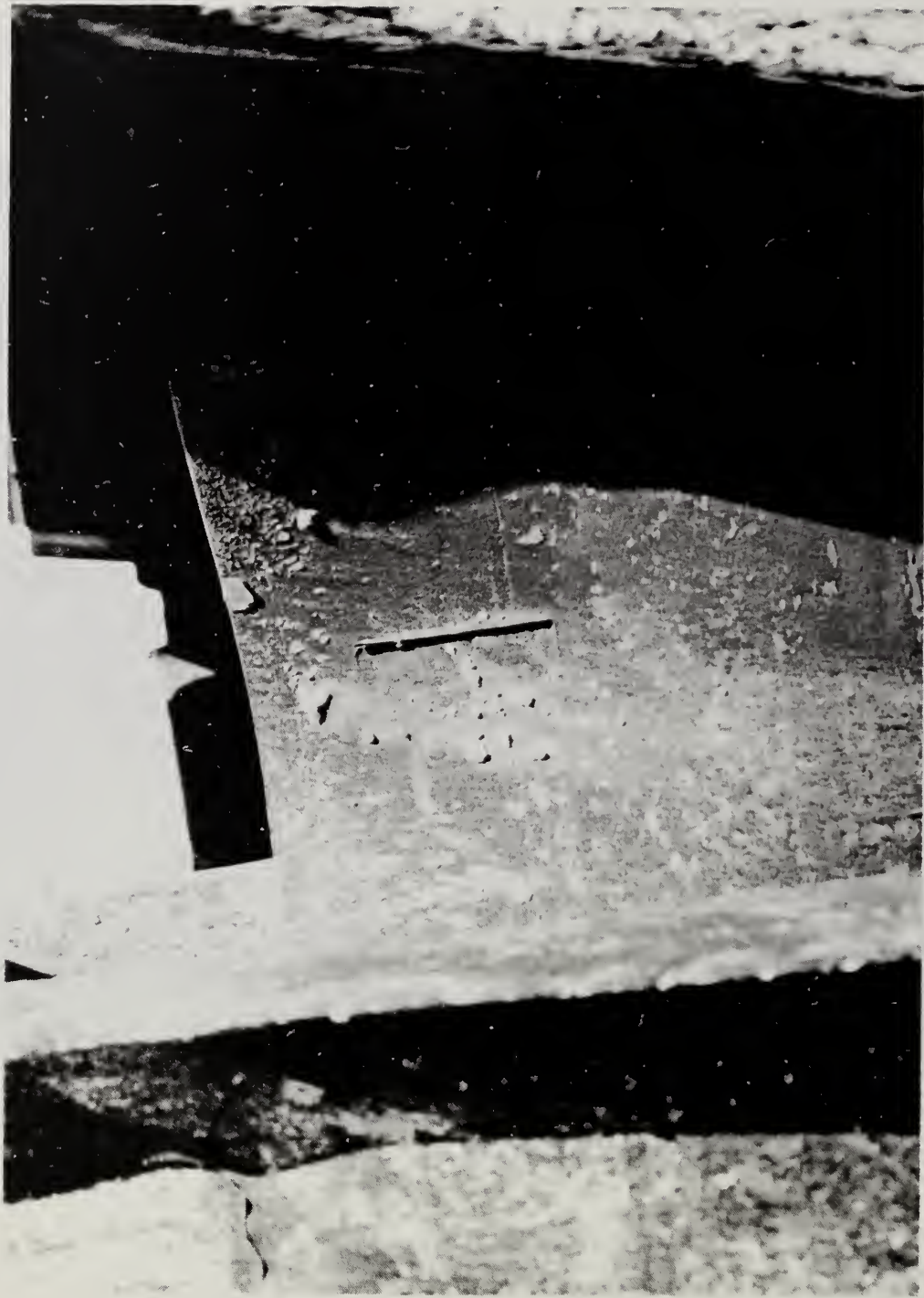


Figure 4.4.35 Gouge caused by shearhead during lifting operation

## 5. LABORATORY TESTS

### 5.1 INTRODUCTION

The material tested during the investigation included cores cut from randomly selected sections of the concrete slabs and shearwalls, coupon specimens cut from flanges and webs of the columns, coupon specimens of the welds used to splice column sections, and coupons cut from the prestressing strand used in construction of the floor slabs. Major structural components tested included shearheads, jack rods, and a shearhead-column connection similar to that used for temporary parking of slabs. The objective of these tests was to determine the strength of the various materials and components and obtain information on the performance of key subassemblies. This information was used in the structural analysis and in determining the most probable cause of the collapse.

Results of the NBS laboratory tests are presented in this chapter. These results are compared with data provided by the material suppliers and results obtained by an independent testing laboratory during construction of the building. Comparisons between the laboratory tests results and values in the project specifications are included in Chapter 8.

### 5.2 TESTS OF CONCRETE SPECIMENS

#### 5.2.1 Sampling and Testing Procedures

The strength of concrete was determined from cores cut from various elements of the structure following the collapse. Cores were cut using a diamond core bit and tested in accordance with ASTM C 42, ("Standard Method of Obtaining and Testing Drilled Cores and Sawed Beams of Concrete"). All cores were 3 3/4 in (95 mm) in diameter. In some instances, cores were cut to a suitable length with a diamond masonry saw prior to testing. Cores were weighed prior to being capped or cut and the length of cores was measured both before and after capping.

Variability of the strength of the concrete throughout the structure was also evaluated approximately using a rebound hammer (ASTM C 805) at the construction site and at the landfill where debris from the collapse was stored. Although the rebound hammer cannot be used to measure concrete strength accurately enough for use in analysis, it can be used to determine if the strength varies widely throughout a structural member. The rebound hammer tests indicated that the quality of the concrete was relatively uniform throughout the structure.

Forty-three core samples were taken from various portions of the slabs and shearwalls. The characteristics and compressive strengths of the cores are listed in tables 5.2.1 and 5.2.2. Field sample numbers designate the locations from which the samples were obtained. S denoted samples taken from a slab. RS denoted samples taken at random and for which the location of the concrete in the structure was not known. SWS denoted samples taken from a shearwall. The floor and column location was used in the designation when the location of the sampled specimen was known. Sample No. 25 in table 5.2.1, for example, came from the level 7 floor slab (FL7) in the vicinity of column G5. Three specimens, indicated by asterisks in tables 5.2.1 and 5.2.2, were determined

to be unacceptable for testing because of damage sustained prior to being tested or because they contained amounts of reinforcing steel which could significantly affect the performance of the sample. Eight randomly-selected specimens were instrumented with a compressometer to measure axial deformations of the cylinders as they were tested. Elastic moduli for these eight specimens were determined in accordance with ASTM C 469, ("Standard Test Method for Static Modulus of Elasticity and Poisson's Ratio of Concrete in Compression").

Five cores were tested under diametric compression in accordance with ASTM C 496, ("Standard Test Method for Splitting Tensile Strength of Cylindrical Concrete Specimens"). Four of the specimens that had been subjected to axial compression were also split diametrically so the interior structure of the concrete could be examined.

### 5.2.2 Results of Tests

The density of the cores given in table 5.2.1 was relatively constant. The mean value was  $144 \text{ lb/ft}^3$  ( $2306 \text{ kg/m}^3$ ), with a standard deviation of  $3 \text{ lb/ft}^3$  ( $48.1 \text{ kg/m}^3$ ).

A summary of the results of the tests of the core samples is given in table 5.2.2. The average compressive strength was 5420 psi (37.4 MPa) for cores taken from slabs and 4570 psi (31.5 MPa) for cores taken from shearwalls. The standard deviation was 544 psi (3.75 MPa) for the cores taken from slabs and 257 psi (1.77 MPa) for cores cut from shearwalls. The compressive strength of the samples obtained from levels 7, 9 and 11 (Sample No. 25, 26, 30) varied by less than five percent. The roof slab core strength (Sample 34) was about twenty percent less than these three samples. The average static modulus of elasticity was  $2.89 \times 10^6$  psi ( $1.99 \times 10^4$  MPa) for cores taken from the slabs and  $3.37 \times 10^6$  psi ( $2.32 \times 10^4$  MPa) for cores taken from shearwalls. The average splitting tensile strength of the cores was 565 psi (3.90 MPa). The splitting tensile strength of these cylinders is in reasonable agreement with values of splitting strength calculated in accordance with ACI recommendations [2] ( $7.5\sqrt{f'_c} = 552$  psi or other proposed procedures  $(1.15 (f'_c)^{0.71} = 515$  psi) for the mean core compressive strength of 5420 psi [2,3].

Failure surfaces for the four axially loaded cores that were split diametrically were examined under 22 power magnification. This examination showed no indication of formation of ice lenses: i.e., all voids seen in the matrix of the paste were essentially spherical.

### 5.2.3 Comparison of Strengths of Core Samples with Quality Control Samples

Concrete was sampled at the jobsite during construction by a commercial testing laboratory. Standard 6 in by 12 in cylinders cast at the time of placement of the concrete were tested in compression at ages of 7 days and 28 days. Field records indicate that approximately four samples were taken for each 50 cubic yards of concrete placed in the floor slabs. The rate varied at which samples were taken from other elements of the structure such as retaining walls and shearwalls.

The 28-day strengths of groups of cylinders for each floor level tested by the testing laboratory are given in table 5.2.4. The average strength of these cylinders was 4650 psi (32.1 MPa) and the standard deviation was 216 psi (1.49 MPa).

The strengths of samples taken from the collapsed structure were higher than the strengths of the standard cylinders tested by the testing laboratory. The standard deviation of strengths was also slightly greater. Both these results are to be expected. The core samples taken following the collapse were much older than the standard cylinders, and the conditions of placement of the concrete in the structure were more variable than those used to cast the standard cylinders.

Two questions have been raised in regard to the concrete present in the structure. The first involves speculation that the concrete used in the floor slabs might have frozen, causing the concrete to be weakened. Although freezing temperatures did exist during some of the days on which the floor slabs were cast, the slab contractor covered the slabs with electric heating blankets to prevent damage to concrete. No indication of damage due to freezing was found in the samples tested by NBS. Furthermore the concrete was apparently not weakened as a result of extremes of temperature. The fact that no concrete was found which had a strength less than that specified on the plans is a good indication that no freezing of concrete occurred, or, if it did occur, that it did not damage the concrete.

A second question has been raised about the use of a set-accelerating admixture in some of the concrete placed in the floor slabs during cold weather. It has been speculated that the admixture weakened the concrete. Records of the commercial testing laboratory indicate that the admixture was used in slabs of both buildings in the second through sixth floors. The average 28-day strength of cylinders cast in conjunction with the placement of these floor slabs was 4830 psi (33.3 MPa). The use of the admixture, therefore, does not appear to have reduced the strength of the concrete. In addition, literature obtained from the manufacturer of the admixture notes that tests by a private materials testing laboratory indicated concrete containing the admixture conformed with required strength provisions of ASTM C 494 ("Standard Specifications for Chemical Admixtures for Concrete") for a Type C admixture.

### 5.3 TESTS OF STEEL SPECIMENS

#### 5.3.1 Sampling and Testing Procedure

Tensile coupon tests were conducted to evaluate the mechanical properties of steel in the columns. The objectives of the tests were: to determine the degree of variability of the mechanical properties within a column sample; to determine the conformance of the test results to the requirements of ASTM A 36 ("Standard Specification for Structural Steel") and ASTM A 572 ("High-Strength Low-Alloy Columbium-Vanadium Steels of Structural Quality"); and to compare the results with those of mill and laboratory tests conducted by the steel manufacturer. Three column segments, two obtained from the landfill and one obtained from the construction site, were the sources of the specimens.

Twelve flat test coupons were machined in accordance with ASTM E 8-85b ("Standard Methods of Tension Testing of Metallic Materials") from three column segments identified as NBS 21-1, 21-2, and 21-3. Four coupons, three cut longitudinal with respect to the rolling direction and one cut transverse to the rolling direction, were machined from each of the column segments. The source of the individual coupons and the pertinent dimensions are presented in table 5.3.1. The six coupons cut from the webs were 8 in (203 mm) long and had a  $2.000 \pm 0.005$  in ( $50.80 \pm 0.13$  mm) gage length. Based on the original thicknesses of the flanges of the column samples, the six coupons cut from the flanges were standard 18-in (457-mm) long except for specimen (21-3A-1). There was insufficient parent material in flange 21-3A from which to extract an 18-in long specimen. Specimen 21-3A-1 was a standard 8-in coupon. All of the flange coupons had a gage length of  $2.000 \pm 0.005$  in ( $50.80 \pm 0.13$  mm).

Specimens were tested to failure in tension according to ASTM procedures in one of two testing machines. A 60,000 lbf (267 kN) capacity Baldwin testing machine, calibrated June 8, 1987, was used for the 8-in long coupons. A 400,000 lbf (1779 kN) capacity Tinius-Olsen testing machine, calibrated June 9, 1987, was used to test the 18-in coupons. Estimated load accuracy was  $\pm 1$  percent. On the Baldwin machine the loading rate was maintained at 5000 lb/min (22 kN/min) up to the yield point. On the Tinius-Olsen machine the crosshead speed was maintained at 0.02 in (0.5 mm) per minute up to the yield point. After reaching the yield strengths of the coupons, the crosshead speeds were adjusted to fall in the range of 0.15 to 0.25 in (3.8 to 6.4 mm) per minute. A static value for the yield stress, a lower bound value, was also obtained by reducing the crosshead speed to zero at several points along the yield plateau.

The elongations of the 8-in and 18-in coupons were measured using a modified Tinius-Olsen LVDT extensometer attached to the reduced section. As a result of the modification, the original AC LVDT was replaced with a DC LVDT, thereby providing for the plotting of load-deformation curves on an X-Y recorder. The extensometer was calibrated on May 21, 1987 and had a gage length of 2.000 in (50.80 mm).

### 5.3.2 Results of Tests

The static yield stress, ultimate tensile strength, elastic modulus, and percent elongation were calculated for each coupon. The individual test results are summarized in table 5.3.2, the specimens being grouped according to the column segment from which they were obtained. Combining the coupons from column segments 21-1 and 21-3, the results are: 1) the average static yield stress was 38.4 ksi (265 MPa); 2) the average ultimate tensile strength was 67.9 ksi (468 MPa); 3) the standard deviation was 1.16 and 0.73 ksi (8.0 and 5.0 MPa) for the static yield stress and ultimate tensile strength respectively; 4) the average percentage elongation in a 2-in gage length was 38.2, 5) the average percentage elongation in an 8-in gage length was 29.4; and 6) the average value for the elastic modulus was 29.8 ksi (205 MPa). The average static yield stress and ultimate tensile strength of column segment 21-2 were 52.9 ksi (365 MPa) and 79.3 ksi (547 MPa). The corresponding standard deviations were 1.29 ksi (8.9 MPa) and 0.91 (6.3 MPa); respectively. The average value for the elastic modulus was 29.2 ksi (201 MPa). The average

percentage elongation in a 2-in gage length was 39.1. The single percentage elongation recorded for an 8-in gage length was 30.6.

As can be confirmed from table 5.3.2, there was no significant difference between the mechanical properties of the coupons obtained from the webs and those obtained from the flanges. Moreover, the longitudinal and transverse web coupons yielded tensile properties that were not significantly different. With the exception of elongation measurements, the tensile property measurements do not indicate any coupon size effects.

### 5.3.3 Comparison of Results with ASTM Standards and Mill Tests

The project specifications [5] stipulated that the column steel conform to the requirements for ASTM A 36 or A 572, Grade 50 structural steel. The pertinent tensile properties for these two ASTM standards are listed in table 5.3.3 and serve as the basis of comparison for the coupon test results. It was concluded that all of the mechanical properties measured satisfied the minimum ASTM requirements for structural steel.

Mechanical properties obtained from the steel supplier are summarized in table 5.3.4. The yield point, ultimate tensile strength, and percentage elongation in an 8-in gage length are listed for some of the structural shapes used at the construction site. The American Institute of Steel Construction (AISC) designation is given in the first column. In the second column are shown the heat numbers obtained from the mill report forms. Adjacent to each heat number, in parenthesis, is shown the applicable ASTM standard. Based on the NBS measurements of the cross-sections of Column Segments 21-1, 21-2, and 21-3, it was concluded that all three specimens were obtained from a W12x72 column. Based on the project column schedule, the column segment conforming to ASTM A 572/50 was probably erected during the stage III operations. The column schedule indicates the use of W12x72 columns conforming to ASTM A 36 in stages IV and V. The tensile properties shown in table 5.3.4 adjacent to the W12x72 entry serve as a second basis of comparison for the NBS test results. The average values for yield stress in the NBS tests are lower than those listed for the mill tests. This is expected because the NBS results indicate the average static yield stress, which tends to be lower than the yield stress reported in the mill test reports. The average value for the ultimate tensile strength in the NBS tests was higher for the A 36 steel and lower for the A 572 steel than the corresponding mill test results. The percentage elongation measured after the NBS tests was higher than that reported in mill tests for both grades of steel.

Results of the NBS analysis of the chemical composition of the column steel are presented in table 5.3.5. These results indicate that the column steel and the weld block attached to the column satisfied ASTM A 36.

## 5.4 TESTS OF WELDMENTS

### 5.4.1 Sampling and Testing Procedure

For the first part of the weldment test series, flat coupons were machined from three column segments containing field splices. On two of the segments,

columns with the same cross-sectional dimensions were joined together. The third segment contained a transition joint from a thick flange section to a thin flange section. Joint preparation was also a variable in that two of the specimens contained column extensions whose lower ends were double-beveled while the third specimen contained a column extension with a single-beveled end. Fifteen flat transverse-weld coupons were machined in accordance with ASTM E 8-85b from three column segments identified as NBS 26, 27, and 28. Column segment 26 was cut from a splice between two W12x136 members. According to the project column schedule, such a splice occurred between stages II and III and between stages III and IV. Column segment 27 includes a W12x120 upper column and a W12x152 lower column. This splice configuration existed only between stages I and II. Column segment 28 consisted of portions of two W12x65 members and was cut from a column marked "12B." This splice configuration existed between stages I and II and between stages II and III. Based on the project column schedule, it is concluded that column segments 26, 27 and 28 consisted of ASTM A 572, Grade 50 steel.

A description of the coupons is given in table 5.4.1. Five coupons were machined from each segment, two from each flange and one from each web. All coupons were centered on the weld lines. The specimens were prepared by first milling the flat surfaces of the rectangular strips to obtain uniform thicknesses and then grinding the surfaces to remove milling marks and to ensure that the faces were parallel. The sketches in figure 5.4.1 illustrate the orientation and relative locations of the flange and web coupons. The bottom sketch in figure 5.4.1 also shows the weld (single bevel) orientation on the coupons obtained from the second flange cut. The bevel joint was across the width of the second-cut coupons in contrast to being across the thickness for the first-cut coupons. The three web coupons and the six first-cut flange coupons were 18 in (457 mm) long, 1.500 in (38.10 mm) wide (except for Specimen 28W1) at the reduced section and had a 2.000 in (50.80 mm) gage length. The second coupons cut from column segments 26 and 27 were 8 in (203 mm) long, 0.500 in (12.70 mm) wide at the reduced section and had a gage length of 2.000 in (50.80 mm). The remaining two coupons, obtained from column segment 28, conformed to the ASTM subsize specimen specifications and measured 4 in (102 mm) long, 0.250 in (6.35 mm) at the reduced section and had a gage length of 1 in (25.40 mm).

For the second part of the weldment test series, one flat coupon was cut from each of column segments 26, 27 and 28. The three coupons were 18 in (457 mm) long and 1.5 in (38.10 mm) wide. In preparing these coupons, only the side surfaces were machined. The face surfaces were left unmachined, thereby giving each coupon the same thickness as the flange of the column segments from which it was cut. None of the weld metal was machined off as in the first part of the weldment test series. The coupons were labeled 26F5, 27F5 and 28F5. The average width in the reduced section and the average thickness of each coupon are presented in table 5.4.1.

Specimens were tested to failure in tension in one of two testing machines. The 60,000 lbf (267 kN) capacity Baldwin testing machine described in section 5.3.1 was used for the 4-in and 8-in long coupons. The 400,000 lbf (1779 kN) capacity Tinius-Olsen testing machine described in section 5.3.1 was used for the 18-in long coupons.



The elongations of the 8-in and 18-in coupons were measured using a modified Tinius-Olsen LVDT extensometer attached to the reduced section. For the 4-in coupons, strain gages were attached to the two flat surfaces. In addition, a dial gage with a least reading of 0.001 in (0.025 mm) was attached to the lower crosshead of the testing machine to measure the elongation.

#### 5.4.2 Results of Strength Tests

The individual test results are summarized in table 5.4.2. Only the ultimate tensile strength is presented in the table because the transverse butt weld tests do not generally provide reliable information regarding yield strength and elongation, particularly when the tests indicate that the weld metal strength is less than that of the base metal. In this instance, most of the strain is localized in the weld region rather than over the entire gage length. The elongation measurements will therefore be lower than if the strain had been uniform over the gage length as is implied in elongation results for uniform base metal. Likewise for yield strength measurements of base metal, implicit in the standard specifications is that the yield strength values assume uniform strain within the specified gage length. Consistent with expected behavior, the load-elongation plots obtained with the X-Y recorder generally did not indicate a yield plateau.

Of the fifteen tests run on machined coupons, only specimen 27W1 failed in the base metal. The other fourteen coupons failed due to fractures in the weld metal.

Observations of the fracture surfaces of specimens 26F1, 26F3 and 27F3 revealed porosity and incomplete joint penetration. All three fracture surfaces showed evidence of incomplete penetration; i.e., the two column sections were not completely fused together over the entire face of the groove. The portions of the joints that were not fused were visible as dark planar regions on the fracture surfaces. The dark planar regions consisted of the original column ends (identifiable by parallel lines with a spacing of about 3 to 4 per mm that appear to be artifacts produced when the columns were cut to length) and weld metal that flowed into the narrow groove but did not have sufficient superheat to fuse to the base metal. These planar regions were darker on the micrographs because they were coated with oxide, while the remainder of the fracture surface was newly fractured metal. These planar (unfused) regions comprise roughly 15 percent of the cross-sectional area of 27F3, 60 percent of 26F1 and 50 percent of 26F3. The amount of unfused region in these three specimens is greater than the value considered acceptable by the workmanship standards of American Welding Society Specification AWS D1.1-83 "Structural Welding Code - Steel" [26], a commonly used guide to the design and construction of welded steel structures in the U.S. Reports of nondestructive evaluation tests of the welds by a commercial testing laboratory did not identify any flaws in the column splices. These unfused regions help explain why the tensile strengths for these welds in table 5.4.2 are less than the values expected for the weld metal (near 75 ksi). The fracture surface of 27F3 contained an amount of porosity comprising as much as 3 percent of the fracture surface area and brittle cleavage fracture comprising about 10 percent of the fracture surface area.

With the exception of the results for Specimen 27F4, the ultimate tensile strength results for coupons cut from column segment 27 compare favorably with the minimum specified ultimate tensile strength for ASTM A 572, Grade 50 steel (refer to table 5.3.3). The ultimate tensile strength for specimen 27W1 (81.1 ksi) compares favorably with the average strength of the column steel in column segment 21-2 (refer to table 5.3.2), which was also concluded to be A 572, Grade 50 steel.

The five ultimate tensile strength results presented in table 5.4.2 for column segment 26 were all considerably lower than the minimum specified ultimate tensile strength of 65 ksi (448 MPa) for A 572, Grade 50 steel.

The results for coupons cut from column segment 28 are also compared to the minimum ultimate tensile strength of 65 ksi (448 MPa) for ASTM A 572, Grade 50 steel. Specimen 28F3 failed at an ultimate tensile strength that exceeded the minimum requirements for A 572, Grade 50 steel, although it failed in the weld joint. The ultimate tensile strength of specimens 28F1, 28F2, 28F4 and 28W1 was lower than the minimal requirements.

The results from testing the three unmachined coupons are presented in the bottom portion of table 5.4.2. Specimen 27F5 failed by fracture in the thinner base metal portion. The specimen exhibited a necking down in the reduced section prior to failure and the fracture was a symmetrical cup-cone one with a fibrous texture. Both specimens 26F5 and 28F5 failed due to fracture in the weld joint. Their failures were less ductile than that of specimen 27F5. The ultimate tensile strength of 27F5 exceeded the minimum required tensile strength of 65 ksi (448 MPa) for ASTM grade 50 steel, and the tensile strength of 26F5 fell below the required minimum. These results are consistent with those obtained from the machined coupons. As was generally the case for the machined coupons, specimen 28F5 had an ultimate tensile strength which exceeded the requirements for A 36 steel, although the fracture occurred in the weld joint.

#### 5.4.3 Metallography Results

Four specimens were obtained from weld block/column sample NBS 21-3A shown in figure 5.4.2. A metallographic examination of the welds confirmed evaluations made on the basis of visual examinations. There was an apparent region of lack of fusion in specimen NBS 21-3A-2 as shown in figure 5.4.3. There were several flaws in the weld of specimen NBS-21-3A-3, including lack of penetration, slag inclusion, and a void. These flaws can be seen in figure 5.4.4. Some lack of penetration was also noted in specimen NBS 21-3A-1.

The results of Knoop microhardness measurements on the 4 specimens from sample NBS-21-3A are given in table 5.4.3. In each case, the hardness of the weld is significantly greater than that of either the column flange or the weld block. What appeared to be the harder regions of the heat affected zones (HAZ's) were either slightly harder than the weld material or were not as hard as the weld material.

Several column butt weld joints were examined. The location of the section from sample NBS 8-T1 is shown in figure 5.4.5. An etched cross section

showing the weld appears in figure 5.4.6. At the upper part of the joint as shown in the figure, the weld is displaced laterally from the joint. The extent of the unwelded part of the joint is shown at higher magnification in figure 5.4.7. The unwelded joint may have extended as a crack into the weld. The microstructure here consists primarily of granular bainite. There was incomplete penetration of the weld in the other column welded joints examined as well. The joint in specimen NBS 6-F1 is shown in figure 5.4.8. There are both voids and lack of penetration in this weld. There may also be some slag inclusions. The weld in sample NBS 6-W1 exhibited a lack of penetration near the center, and a crack in the weld emanated from the region of no penetration. A cross section through this weld is shown in figure 5.4.9. A lack of penetration was also found in sample NBS 4-F1, as shown in figure 5.4.10. The weld in sample NBS 4-W1, shown in figure 5.4.11, exhibits lack of penetration, lack of fusion, and cracking through the weld metal. There was a small region of no penetration in the weld in specimen NBS 8-F1. Sections through specimens 5-W1, 5-F1 and 8-W1 were also examined. No significant lack of penetration, lack of fusion or inclusions/voids were detected in these samples. Some martensite was found in the HAZ associated with the last weld pass in specimen NBS 4-F1.

The chemical composition of the weld and both column components of sample 4-F1 satisfied the requirements of ASTM A 36. The results of the chemical analyses are given in table 5.4.4. Knoop microhardness measurements were made on most of the specimens that were examined metallographically. The results of these measurements are given in table 5.4.5. The hardness measurements indicated a hard spot in the HAZ of specimen 4-F1, where an HK<sub>500</sub> value of 553 was measured.

#### 5.4.4 Fractography Results

Fractography was performed on two specimens, NBS 33B and NBS 33A. Specimen 33B shown in figure 5.4.12 was a wedge found loose in the debris after the collapse. The wedge had been fully welded to the shearhead, weld block, and column flange prior to failure. Specimen 33A, shown in figure 5.4.13, was a wedge found loose in the debris. The specimens were sectioned to facilitate macroscopic inspection and microscopic inspection in a scanning electron microscope (SEM).

Macroscopic examination of the wedge, specimen 33B, revealed substantial deformation. Both the point and heel of the wedge were bent downward (toward the ground when oriented in the structure), indicating that substantial plastic deformation occurred during failure. There were angled gouges on the surface of the wedge where it contacted the weld block. These gouges indicated the wedge slid in both the wedging direction (along the flange surface on the column) and normal to the flange (away from the flange surface) during failure. The ratio of the movement is about 3 times in the wedging direction to that normal to the flange. There were indications that the wedge also rotated about the edge of the weld block as it failed.

The appearance of the welds joining the wedge to the column flange, weld block, and shearhead were all consistent with the use of the shielded metal arc welding process. The compositional analysis in Section 5.4.3 was consistent

with the use of American Welding Society type E7018 electrode, the shielded metal arc (SMA) welding electrode used for field fabrication. These fillet welds were of poor quality, showing evidence of undesirable features such as arc strikes, undercut, overlap, excessive convexity, and general unevenness of the bead profiles. The undercutting of the bead is evident in figures 5.4.14 and 5.4.15, cross sections through the welds at the locations shown in figure 5.4.12.

The project specifications [5] required visual inspection of all shop and field welds. The specifications did not describe the nature of the visual inspection, the specification they were to satisfy, or the way any deficiencies were to be repaired. In view of this, in the NBS investigation the welds were compared to AWS D1.1-83. This specification states that all arc strikes outside the area of permanent welds are to be removed (paragraph 3.10) and the convexity of the weld bead is not to exceed 0.07 inch times the actual face width, plus 0.06 inch (1.52 mm) (paragraph 3.6.1). The arc strikes and convexity observed on the wedge exceeded these levels in several areas.

The welds on the wedge fractured primarily on a 45-degree angle from the root to the center of the face of the welds, the expected failure mode for fillet welds. The fracture surfaces were examined in the SEM and found to consist of fine dimples. The dimples indicate the failure should be classified as a ductile transgranular mode; however, the small depth of the dimples indicates a relatively low fracture energy. A low fracture energy correlates with the smoothness of the fracture surface when examined with the naked eye.

Macroscopic examination of specimen 33A (figure 5.4.13), the wedge joined to the weld block, revealed deformation of the wedge ends similar to that observed in specimen 33B. Both the narrow and wide ends of the wedge were bent downward, but there were no angled gouges on the surface. This is attributed to different failure modes for the two locations. The weld fracture surfaces on specimen 33A have ridges aligned along the column axis indicating the weld block and wedge failed by shearing from the column. In contrast for 33B the gouges are consistent with expulsion of the wedge from between the shearhead and the weld block.

The location of the fracture plane in the fillet welds was also different in specimen 33A. About 60 percent of the fillet weld joining the weld block to the column failed along the 45-degree angle from the root to the center of the face of the welds. The other 40 percent of the weld failed near the interface between the weld and the column. The precise failure location, whether at the weld fusion line or within the weld metal, could not be uniquely identified because the matching surface on the column was not available. Failure along the interface is unusual in fillet welds because the fracture path tends to be shorter at some angle to the interface (usually near 45 degrees). Failure at the interface indicates a lower energy fracture path here. Testimony obtained by the Connecticut Department of Public Safety from the steel fabricator indicated the welds joining the weld block to the column used a different electrode (E70T-4) and process (flux cored arc welding-FCA) than those used to join the wedges to the weld block and shearhead. These differences explain the difference in crack path. A cross section through one of the welds that failed along the weld-column interface is shown in figure 5.4.16. The weld has substantial

convexity and exceeds the limits of AWS D1.1-83 paragraph 3.6.1. Micrographs of the fracture showed a smooth surface which suggested a low-energy fracture. The surface was essentially free of the scratches that would have occurred if the weld block had slid down the column. This indicated that the weld block stayed free of the column surface after the initial shear failure.

The welds that sheared near the weld-column interface had a macroscopic texture similar to that of a weld fractured at the weld fusion line, the interface between the weld and the base metal heat-affected zone. Fracture along a weld fusion surface is unusual and indicates the presence of a low toughness fracture path, which would be consistent with the very smooth fracture surfaces.

The SMA welds in specimen 33A joining the weld block to the wedge had a smoother profile with less undercut and overlap than those on specimen 33B. The better appearance of these welds may explain why the wedge did not separate from the weld block at this location.

In summary, the SMA welds joining the wedge to the weld block and shearhead varied in quality between specimens 33B and 33A. Some of these welds had undesirable features such as arc strikes, undercut, overlap, excessive convexity, and general unevenness of the bead profiles. The FCA welds joining the weld block to the column in specimen 33A exhibited fracture near the weld-column interface. Both the field (SMA) and shop (FCA) welds did not meet some of the requirements of the commonly used welding code AWS D1.1-83. The smoothness of the fracture surfaces indicated a low energy fracture.

## 5.5 TESTS OF COMPONENTS

### 5.5.1 Introduction

Tests were conducted to: 1) determine the tensile strength of the post-tensioning strand, 2) determine the tensile strength of the smaller jack rods and evaluate fractures observed in these rods, and 3) evaluate the performance and strength of the shearhead, wedge, weld block, and seal block assembly.

### 5.5.2 Tests of Post-tensioning Strands

#### 5.5.2.1 Sampling and Testing Procedure

Two series of tension tests, four tests per series, were conducted on specimens of the post-tensioning strands. The first series was run on 50-in (1.27-m) long segments of unused strand obtained from the city landfill. The second series was run on 50-in long segments of strands taken from debris at the construction site. The objective of the tests was to determine the degree of conformance of the specimens to the project specifications for prestressing steel. The specifications called for the use of nominal 1/2-in (12.7-mm), Grade 270, seven-wire, Low-Lax strand satisfying ASTM A 416 ("Standard Specification for Uncoated Seven-Wire Stress-Relieved Steel Strand for Prestressed Concrete"). ASTM A 416 specifies a minimum breaking strength of 41,300 lbf (184 kN) and minimum yield strength of 37,170 lbf (165 kN) (i.e. 90 percent of the specified minimum breaking strength) for such strand.

The tests were conducted in accordance with Supplement VII ("Method of Testing Uncoated Seven-Wire Stress-Relieved Strand for Prestressed Concrete") of ASTM A 370-86 ("Standard Test Methods and Definitions for Mechanical Testing of Steel Products"). Standard V-Grips and special strand holders were used in a 400,000 lbf (1779 kN) Tinius-Olsen testing machine to grip the specimens. Between each set of V-Grips was placed a 5-in (127-mm) long aluminum alloy block, split lengthwise. The block was prepared by drilling a 1/2-in (12.7-mm) diameter hole lengthwise through a 2-in (50.8-mm) square block of aluminum, and then sawing the block in half lengthwise. Thus, a semi-circular trough in the block conformed to the perimeter of the strands. Bearing against the top of the upper block and the bottom of the lower block was a 4-in (101.6-mm) long commercial post-tensioning strand chuck. The chucks served to anchor the strand against the gripping blocks.

The elongations of the strands were measured with two instruments. An extensometer attached to the center of the strand specimen measured elongation up to the yield strength at which point it was removed. A deflectometer was attached to the lower crosshead to measure crosshead separation throughout the test. The DC output of the LVDT extensometer was recorded by a XY recorder. The AC output of the deflectometer was recorded by a drum recorder incorporated in the testing machine console. In addition, the crosshead separation occurring from the time of extensometer removal to the point of fracture of the strand was measured by a steel tape. The LVDT extensometer had a 2.000-in (50.80-mm) gage length and was verified to comply with the requirements of a Class B-1 extensometer as specified in ASTM E 83 ("Standard Practice for Verification and Classification of Extensometers"). The extensometer was attached to the strand specimens after the application of a preload of 4,100 lbf (18.2 kN) as specified in ASTM A 370. After making the specified adjustment in the extensometer reading, the load was increased until the extensometer indicated an extension of 1 percent (i.e. 0.020 in or 0.51 mm). The load concurrent with this specified extension was recorded as the yield strength. After removal of the extensometer, the load was increased until the first wire fractured. The load at first wire fracture is defined as the breaking strength of the strand.

#### 5.5.2.2 Results of Tests

The yield strength, breaking strength, elongation at first wire break and location of the fracture are presented in table 5.5.1 for each of the tensile tests. The first four tests listed in the table constitute Series 1. The average yield strength for Series 1 was 38,200 lbf (170 kN) and the standard deviation was 693 lbf (3 kN). The average breaking strength was 41,075 lbf (183 kN) and the standard deviation was 690 lbf (3 kN). The average elongation at first wire fracture was 2.78 percent with a standard deviation of 0.86 percent. All of the Series 1 strands fractured within the area of one of the aluminum blocks.

The last four tests listed in the table comprised Series 2. The average yield strength and breaking strength of the Series 2 strands were 39,325 lbf (175 kN) and 42,213 lbf (188 kN), respectively. The corresponding standard deviations were 442 lbf (2 kN) and 399 lbf (2 kN). The average elongation at first wire fracture was 5.48 percent with a standard deviation of 1.0 percent. The first

two strands in Series 2 fractured within the chuck area, although with no apparent reduction in the breaking strengths of the specimens and the fractures were sufficiently ductile. After the fracture of specimen 6, it was observed that the surfaces of the aluminum blocks that encased the strands had been indented by the harder strand material, thereby diminishing the gripping ability of the aluminum blocks. To offset the wearing effect of the strands, a mixture of carborundum and oil was pasted on the contact surfaces of the aluminum blocks. This technique was apparently effective in that the remaining two strands had fractures either within the aluminum block area or between the blocks, rather than in the chuck area.

### 5.5.2.3 Comparison of Results with ASTM A416

As shown in table 5.5.1, all eight of the yield strength values exceeded the minimum value of 37170 lbf (165 kN) specified by ASTM A 416. The table also indicates that in Series 1 only one of the strand specimens had a breaking strength above the specified minimum (41,300 lbf-184 kN). The average breaking strength (41,075 lbf-183 kN) is slightly (less than 1 percent) less than the specified minimum. For the Series 2 specimens, all four of the strand specimens had breaking strengths in excess of the specified minimum. ASTM A 416 specifies that the total elongation beginning from the point of application of the preload to the point of failure shall not be less than 3.5 percent measured over a gage length of at least 24 in (610 mm). Establishing the gage length as the crosshead separation at the point of extensometer removal, the test gage lengths ranged from 27 1/16 in (687 mm) to 28 7/8 in (733 mm). Comparing the results in table 5.5.1 with the A 416 minimum requirements, it is observed that two of the elongations measured for the Series 1 strands fell significantly below the specified minimum, while all four of the Series 2 strand specimens exceeded the minimum requirements by at least 25 percent.

### 5.5.3. Tests of Jack Rods

#### 5.5.3.1 Sampling and Testing Procedure

Four 40-in (1.02 m) long segments of the 1 3/4-in (44.5 mm) diameter Acme-threaded jack rods used with the standard jacks were tested to failure in tension. The test specimens were obtained from the debris at the landfill. Although the rated capacity of this proprietary component was not known, the capacity should have satisfied the recommendations given by the National Safety Council of a safety factor of 2.5 [22]. The objective of the tests was to compare the ultimate breaking strength of the rod specimens to this recommended capacity,  $[150,000/2] \times 2.5 = 187,500$  lbf (834 kN) of the rods. The rods were tested in a 400,000 lbf (1779 kN) capacity Tinius-Olsen testing machine. The ends of each specimen were held with the same hardware used during the erection procedure. One end was held by a swing nut, a nut retainer and a bearing block with a spherical seat. The other end was held by an anchorage consisting of a lifting nut, a cylindrical sleeve and a rectangular block. These two end assemblies bore against the upper and lower crossheads of the testing machine. A sketch of the test configuration is presented in figure 5.5.1.

The total elongation of a specimen between the end assemblies was measured by a deflectometer held in contact with the lower crosshead of the testing machine. The deflectometer had a full-scale range of 4 in (101.6 mm). The rod specimens were loaded monotonically to failure. The tensile load and crosshead separation were recorded on the drum recorder attached to the testing machine console.

In addition to testing the full-scale rod specimens, a standard round tensile coupon, machined from a segment of a fractured jack rod recovered from the debris at the landfill was tested in accordance with ASTM E 8-85b ("Standard Methods of Tension Testing of Metallic Materials"). The elongation of the 5-in (127-mm) long coupon was measured with a Tinius-Olsen LVDT extensometer with a gage length of 2.000 in (50.8 mm). Results from metallographic analyses of this fractured rod are presented in Section 5.5.3.3.

#### 5.5.3.2 Results of Tests

The results of the tension tests of the four rod specimens are presented in table 5.5.2. The average failure load was 185,500 lbf (825 kN), which translates to an average ultimate tensile strength of 102.4 ksi (706 MPa). The ultimate tensile strength was computed by dividing the failure load by the net area of the threaded rod [7] (1.811 in<sup>2</sup>-1168 mm<sup>2</sup>). The standard deviation for the failure load is 4,143 lb (18 kN) which yields a coefficient of variation of 2.23 percent. The average failure load exceeded the rated load of 75 kips (334 kN) by a factor of 2.5.

The load-elongation plot for rod specimen 1 is presented in figure 5.5.2. The failure load was 190,000 lbf (845 kN) and the elongation measured over the 40 in gage length was 3.44 in. The percent elongation for each specimen is given in table 5.5.2. The total elongations for specimens 3 and 4 were obtained by matching the fracture surfaces of the two sections and measuring the distance between pre-test gage marks with a metal tape. This procedure was followed because the deflectometer was damaged after the test of specimen 2.

All four of the jack rod specimens fractured outside the holding nuts. Specimens 1, 2 and 4 did not neck down near the fracture surface. Specimen 3 necked down slightly near its center. It is noted that specimen 4 was tested after having been used in one of the lifting assembly tests described in Section 5.5.5. The rod had failed in a ductile manner in combined tension and bending in the lifting assembly test.

The tensile coupon failed at an ultimate tensile strength of 92.5 ksi (638 MPa), which is lower than any of the four values obtained in the full-scale rod tests. The elongation of the coupon in the 2-in gage length was 17.2 percent.

#### 5.5.3.3 Metallography Results

The fracture surface of one of the rods removed from the debris was analyzed in detail. The sample analyzed, designated NBS 11-2, is shown in figure 5.5.3. There was some mechanical damage evident on the surface of the jack rod. The threads appeared to have been rolled rather than machined. A seam from the threading operation was evident at the crest and root of each thread



along the entire length of the sample. The seam was particularly evident on the side of the rod that had been deformed in tension in the vicinity of the fracture. The seam can be seen in figure 5.5.4, which shows part of the rod surface on the tension side.

The jack rod was sectioned transversely adjacent to the fracture so the fracture could be examined with a scanning electron microscope. The fracture surface is shown at low magnification in figure 5.5.5. The apparent fracture origin is at the root of a thread at the darker region in the figure. The fracture in the region adjacent to the apparent origin exhibited primarily dimpled rupture, which indicates ductile fracture. Outside the darker region, the fracture mode is primarily cleavage, indicating a much less ductile fracture. A representative fractograph indicated the fracture appeared to have occurred in overload, probably as a single event rather than as a result of any repeated or fatigue loading.

Two longitudinal sections through the jack rod were examined metallographically. One of these sections was in the deformed region adjacent to the fracture and included the fracture profile. Part of this section is shown in figure 5.5.6. The section was taken through the apparent fracture origin which is at the upper left in the figure. The lap seam at the top and root of the thread adjacent to the fracture is evident in this figure. The lap seam at the root of the first thread removed from the fracture on the tension side of the screw is shown at higher magnification in figure 5.5.7. The etchant solution used to prepare the fracture surfaces was a 2 percent Nital compound. The tip of the seam appears to have a small crack emanating from it. The lap seam at the root of the second thread away from the fracture on the tension side of the rod is shown in figure 5.5.8. A crack appears to have grown from the base of the lap seam at this location. The crack tip is relatively sharp indicating possible recent crack growth. The lap seams on the compression side of the jack rod are not as open as they are on the tension side.

A sample of the jack rod was analyzed for chemical composition. The results are given in table 5.5.3. The material is similar to AISI 4137 grade steel. Knoop microhardness measurements at a load of 500 grams force were also made on a longitudinal section through the jack rod. Two traverses were made, each starting at the thread top and continuing across the diameter of the rod. The results are given in table 5.5.4. The average hardness was 252 HK<sub>500</sub>. There appeared to be no hardness gradient across the jack rod.

#### 5.5.4 Tests of Shearheads

Tests were conducted to develop information on the behavior of the shearhead-wedge assembly under conditions simulating those that existed when the floor slabs were parked in a temporary position. The test setup is shown in figure 5.5.9. The shearhead, column and wedges were samples obtained from the debris at the landfill. The column was from an unused section, the shearhead had been used but there was no visible damage due to the collapse. A plate was welded to the web of each channel under the loading points to prevent web crippling. The shearhead was positioned off the center of the column; i.e., clearance between the shearhead and column was provided on one side only. This

produced the maximum eccentricity of the shearhead on one wedge and simulated the worst case that could occur in the field.

Two tests were conducted. In the first test the wedges were tack welded to the column. A 3/8 in (10 mm) tack weld was placed on the point of the wedge and a 1 in (25 mm) tack weld on the heel. In the second test, no tack welds were used.

Load was applied to the shearhead using a Bliss 12 million pound universal testing machine. Load resolution was 300 pounds (1.3 kN) on the 600 kip (2669 kN) load range used for the tests. A loading rate of approximately 2 kips/min (8.9 kN/min) was used. Load was applied in increments of 10 kips (44 kN). The behavior of the specimen was noted after each load increment.

For the tack welded specimen, the first perceptible deformation occurred at 120 kips (534 kN); a very slight rotation of the wedge with the maximum eccentric load was observed. At 250 kips (1112 kN) the tack welds failed. The maximum load applied to this specimen was 300 kips (1334 kN). There was no apparent distress of the specimen at this load. The test was stopped at this point in order to retest the specimen after grinding the fractured tack welds from the wedges.

The maximum load applied to the assembly without tack welds was also 300 kips (1334 kN). There was also no distress of the specimen at this load. Due to irregularities of flame cut edges of the wedge, the face of the wedge was not in full contact with the column flange at the beginning of the test. The very small clearance between the wedge and the column did not increase, however, up to the maximum load. The tendency for the wedge to "seat" itself in this position was apparently the cause of the tack weld fracture in the previous test. Since the wedge had been clamped flush with the column flange prior to application of the tack weld, the weld had to fracture before the wedge could seat itself.

The lack of distress in the channels of the shearhead, the wedge and the weld block in these tests did not correspond with observations of the debris. Considerable deformations of the wedge and shearhead occurred in the collapse of the structure. It was therefore decided to run an additional test in which no plate was welded to the web of the channel under the loading points. In this third test the shearhead was positioned in the center of the column; i.e., it was loaded symmetrically with each wedge carrying half of the applied load. The wedges were tack welded. Other details of the test set up (figure 5.5.9) and the loading procedure were the same as in the first two tests.

The maximum load in this third test was also 300 kips (1334 kN); however the behavior was considerably different. At a load of approximately 100 kips (445 kN) the tack welds on one wedge broke. As the load increased, the wedge rotated about the outer edge of the weld block; i.e., the wedge separated from the column. This rotation increased and the wedge deformed considerably as the 300 kip (1334 kN) load was applied. The test was stopped at this point because the specimen was not carrying additional load, but the channel and wedge were simply continuing to deform at this relatively constant load.

Deformations of the wedge and weld block are shown in figures 5.5.10 and 5.5.11. Note the substantial rounding of the edge of the weld block. The shearhead channel also deformed substantially. The bottom flange and web rotated and bent outward as the wedge rotated. The deformation of the shearhead channel is shown in figure 5.5.12. These observed deformations of the shearhead wedge and edges of the weld block were similar to those observed in the collapsed structure. The similarity between the shearhead deformations in this test and in the collapsed structure indicates the concrete floor slabs offered little resistance to local deformation of the shearhead channels produced by forces resulting from the tendency for the wedges to rotate on the edge of the weld block.

The three tests indicated the shearhead-wedge assembly subjected to direct shear loads was able to carry a load of 300 kips (1334 kN) with the wedge tack welded or not tack welded.

### 5.5.5 Lifting Assembly

Tests were conducted to evaluate the performance and capacity of the lifting assembly used to raise the floor slabs. The assembly consisted of the lifting jack, jack rods and attachments, and the shearhead. The test setup is shown schematically in figure 5.5.13.

A 150 kip (667 kN) jack recovered from the landfill was used in the test. The shearheads and jack rods used were obtained from the debris at the landfill. Components that exhibited a minimum amount of damage were selected for these tests. The jack rod length of 53 in (1.35 m) from the underside of the hydraulic jack to the bottom of the shearhead in figure 5.5.13 corresponds to the distance from the top of the column to the underside of the floor slab at level 9, as illustrated in figure 4.2.1, i.e., the length of jack rods being used to position the slabs at levels 9/10/11 in the west tower at the time of the collapse.

The lifting jack obtained from the landfill was not used to apply loads during the test, but merely served to support the ends of the jack rods in a manner similar to that present in the structure. Load was applied using two 100 ton (890 kN) capacity hydraulic rams positioned between the base of the lifting jack and a spacer that had been fabricated from structural tubing.

The initial distance between the centerline of the jack rods and the sides of the shearhead was considered to be an important parameter in the tests. Figure 5.5.14 shows the dimensions that were varied for these tests. The gusset plates or stiffeners on the lifting angle are omitted from the figure for clarity. The values of these dimensions used in each of the tests are shown in table 5.5.5.

It was intended that the shearheads in the test assembly be supported uniformly around their top perimeter to simulate the conditions at a shearhead at the bottom of a package of slabs. Bare shearheads (not confined by concrete) were used in three of these tests. Simulated floor loads were transferred to these shearheads through four square steel bars positioned over the flanges of the channel sections of the shearheads. Fiberboard was placed between the

shearheads and the steel bars to improve the bearing between the bars and the arms of the shearheads.

The shearhead used for the third test was specially stiffened in an attempt to determine the sensitivity of the failure mode to lateral restraint of the top flange of the shearhead arm channels. For this specimen, two 2 1/2 in x 1/2 in (63.5 mm x 12.7 mm) steel bars were welded between the tops of the legs of the lifting angles as shown in figure 5.5.15, effectively preventing any lateral movement of the top of the lifting angles and the top flanges of the shearhead arm channels, as shown in figure 5.5.15. This represented an effective upper bound of lateral and torsional restraint.

In tests 4 and 5, shearheads were confined by a concrete slab that was intended to simulate the lateral restraint conditions present in the actual structure. No post-tensioning was used in these specimens. The concrete was confined by steel channel sections that surrounded the specimen and by mild steel bonded reinforcement placed around the shearhead. The configuration of these specimens is shown in figure 5.5.16. Load was transferred to the concrete slab through wooden timbers positioned around the perimeter of the shearhead opening.

Because the overall mode of failure was considered the most important aspect of these tests, little instrumentation was necessary. Small plastic scales were attached magnetically to the specimens so motion of the lifting nuts relative to the bottom surface of the lifting angles could be monitored visually. In four of the five tests, linear variable differential transformers (LVDT's) were attached to the top and bottom flanges of the arm channels of the shearhead to measure the displacement of those flanges. All tests were recorded on videotape.

Load was applied at a rate of approximately 5 kips (22 kN) per minute in 10 kip (44 kN) increments. After each increment of load had been applied, the load was maintained at a constant magnitude so the shearheads and other parts of the specimens could be examined for signs of distress.

Failure of the lifting assembly took place in one of two ways, each of which centered around the connection of the jack rod to the shearhead. In each type of failure, the lifting angle and the arm channel of the shearhead deformed in response to applied loads. This deformation consisted of rotation of the lifting angles and twisting of the arm channels of the shearheads as well as local deformations of the lifting angles near the point at which the lifting nuts applied loads. The first type of failure occurred when the rotation of the lifting angle allowed the lifting nut to slip out from under the lifting angle. In the second type of failure, the rotation of the lifting angle and arm channel of the shearhead caused the jack rod to fracture as a result of combined flexure and axial load.

Deformation of the lifting angles was first observed when the load on the system reached approximately 120 kips (534 kN). At this load, mill scale began to flake off the lifting angles. When load was increased to 130 kips (578 kN), the lifting angles continued to yield and to twist the arm channels of the shearhead. This also caused the web and bottom flange of the shearhead

arm channel to deform inward toward the center of the shearhead as the top flange of the channel deflected outward, or away from the center of the shearhead.

When load was increased to 140 kips (623 kN) and above, further yielding of the lifting angles, stiffeners, and arm channels of the shearheads allowed the end of the jack rods to move away from the side of the shearhead (toward the center of the shearhead). This pattern of lifting angle deformation and accompanying jack rod movement continued until the failure load was reached. Failure occurred when the jack rod and lifting nut slipped off the lifting angle or when the jack rod broke. Both types of failure were very sudden and were accompanied by a loud bang. A summary of failure loads for the lifting assembly tests is given in table 5.5.6. Figure 5.5.17 shows a deformed lifting angle. Deformed lifting angles were observed on several shearheads in the collapsed structure.

Two general observations of behavior of the lifting assembly may be made on the basis of behavior of these specimens. First, because failure of the lifting assembly depended primarily on deformation of the arm channels of the shearhead, confinement of the shearhead significantly affected behavior of the arm channels and the ability of the shearhead to accept loads from the jack rods.

A second observation is that the amount of load a shearhead could accept from a jack rod depended on the distance between the face of the lifting angle and the center of the jack rod, a distance which may be defined as eccentricity of loading of the lifting angle. In each test of the lifting assembly, failure took place in the jack rod having the highest eccentricity of loading. Large eccentricity of loading of a lifting angle produced large twisting moments on the shearhead arm channel and lifting angle. Because failures of the jack rod and slippage of the jack rods was directly related to twist of the lifting angle and arm channels of the shearheads, large eccentricities of loading of the lifting angles gave rise to failure of the entire assembly at lower loads. This result is significant with respect to the configuration of the lifting assemblies used in the L'Ambiance Plaza construction. Because the lifting nuts used with the super jacks were of slightly larger diameter than those used with the small jacks (5 1/2 in vs 4 7/8 in-140 vs 124 mm), it is possible that a lifting assembly employing a large jack could actually have had a somewhat smaller capacity than such an assembly employing a small jack, assuming failure by lifting nuts slipping off in both cases, simply because of the slightly larger eccentricity of loading inherent in the use of large jack rods and large lifting nuts. The arm channel and lifting angles for the shearheads used with the large capacity jacks were the same size as those on the shearheads tested. However, the shearheads designed for use with the super jacks were provided with a reinforcing plate welded to the inside face of the header channel. Typical shearheads used with small jacks and with the super jacks are shown in figure 5.5.21 and 5.5.22.

These two observations are confirmed by the data obtained from LVDT's that measured lateral motions of the flanges of the arm channels of the shearheads. Plots of the relationship of flange motion to load for tests 2 through 5 are shown in figures 5.5.18 and 5.5.19. The effect of very stiff lateral confinement at the top flange of the arm channel can be seen by comparing the plots of top flange motion for tests 2 and 3 in figure 5.5.18. The largest failure load

recorded in any test was that for test 3, in which top flanges of the arm channels were essentially prevented from moving laterally. Even though a large eccentricity of loading was used on one side of the shearhead in test 3 ( $a = 7/8$  in-22 mm) as compared to the small eccentricity of loading used on both sides of the shearhead in test 2 ( $a = 1/8$  in-3 mm), very stiff confinement of the top flange of the arm channel in test 3 reduced rotation of the lifting angle in that test and allowed the jack rod to fail at a higher load than in other tests.

The plots in figure 5.5.18 and 5.5.19, in conjunction with other data from the tests, also illustrate the interaction between eccentricity of loading of jack rods, shearhead confinement, and load capacity of the lifting assembly. Figure 5.5.18 shows that the lateral deflection of the top of the arm channel of the shearhead in test 2 was similar to that observed in tests 4 and 5. Two things must be recalled to put this in perspective. First, minimum eccentricity of loading of the lifting angle was used in test 2. That the side channels of the shearhead in test 2 twisted less than those in tests 3 and 4 is shown by the fact that the deflection of the lower flange of the shearhead in test 2 was very small in comparison to the deflections of the shearheads used in tests 4 and 5. Second, the shearheads in tests 4 and 5 were confined by concrete, whereas the shearhead in test 2 was unconfined. This indicates that the concrete did not provide as much confinement as might be expected.

The support conditions for the shearheads tested here did not duplicate exactly the support conditions that existed for the shearheads in the actual structure. For the first three tests, the square bars used to apply load to the top of the shearhead torsionally restrained the top flanges of the channels of the shearhead. For tests 4 and 5, the 2 x 4 wooden timbers placed between the loading plate and the top of the concrete slab applied shear but could not simulate the moment condition which existed around the shearhead in the real structure. The tests did, however, define the bounds of shearhead strength, within the limits of eccentricity of loading for the lifting angles used in the tests. The shearhead in test 1 represented a lower bound for capacity of the lifting assembly, as the shearhead was essentially unconfined. The capacity of the shearhead in test 3 represented an upper bound of the capacity of the lifting assembly, as the bars welded between the top legs of the lifting angles provided a lateral restraint much larger than could have been provided by confinement by concrete. The tests in which the shearheads were confined by concrete (tests 4 and 5) yielded lifting assembly capacities between these two extremes. In addition, it can be argued that the load capacities of the assembly indicated by these tests were good approximations of the capacities of the lifting assemblies in the actual structure, even though the concrete slab confining the shearheads was small relative to the dimensions of a typical interior panel of the real floor slab and even though the test slabs contained no prestressing tendons. The lateral stresses in the top of the slabs used in tests 4 and 5 were zero. As an analysis of the floor slabs will show in Chapter 7, the lateral stresses in the top of the slabs near column locations E3.8 and E4.8 were also near zero. Therefore, conditions of lateral restraint of the top flanges of the side channels of the shearheads in tests 4 and 5 could be considered approximately equal to the lateral restraint of the comparable sections of the shearheads in the real structure at columns E3.8 and E4.8.

Because they were fabricated by welding rolled shapes, nominally identical shearheads varied slightly from one to another. It is inevitable that some Mark P50 shearheads were somewhat stiffer or more flexible than those used for these tests. Sufficient tests were not conducted to determine statistically the mean stiffness of these shearheads. In addition, the capacity of shearheads other than those of the type tested could have been weaker or stronger. Twenty-five different configurations of shearheads were used in the structure. The sizes of the arm channels and lifting angles were uniform for all but two of these configurations of shearheads. On the basis of the tests conducted at NBS, the flexural and torsional flexibility of the arm channels and lifting angles can be considered to be the primary factor influencing the stiffness and strength of the shearhead and therefore of the lifting assembly, regardless of the size of the jack used to lift the shearhead. This fact made it particularly important that a shearhead of the type used in conjunction with the large jacks (Type 1, Mark X51, Y51, or Z51) used on the project be tested.

A Mark X51 shearhead and P50 shearhead were tested to determine the relative stiffness of the arm channels and lifting angles of the two types of shearheads. In these tests, the shearheads were inverted and supported by steel bars placed between their header channels and the table of a universal testing machine. Load was applied to the lifting angles of the shearheads through a roller placed one inch (25.4 mm) from the inner edge of the lifting angle as illustrated schematically in figure 5.5.20. The objective of these tests was to determine the relative flexibility of the lifting angles under load rather than to duplicate exactly the condition of loading that existed in the structure.

A schematic representation of the test condition and the load vs. deflection relationships determined for these two shearheads is illustrated in figure 5.5.20. As illustrated in this figure, the shearhead used in conjunction with the super jack was slightly stiffer than the P50 shearhead. However, as noted previously, large jack rods applied loads to the lifting angles at a slightly larger eccentricity than did the small jack rods. With this difference in loading taken into consideration, the effective stiffness of the two shearheads is essentially identical. On the basis of these tests, it can be concluded that the effective capacity of a lifting assembly which included large jacks was not significantly greater than that of an assembly in which small jacks were used, even though the large jacks had the ability to apply much larger loads to the jack rods.

A final factor noticed in tests of the shearheads and evident in the plotted data is that the arm channels of the shearheads began to twist plastically when loads larger than 150 kips (667 kN) were applied. The rate at which plastic twist took place was dependent on the amount of load applied. The system of loading of the lifting assembly was designed to maintain load as deformations within the lifting assembly took place, similar to the way load would have been applied in the real structure. However, no attempt was made during the tests to simulate the rate of load application that would have existed in the real structure, in which design loads were applied rapidly and allowed to remain on the shearheads for the time it took to raise the floor slabs as high as necessary to park them at a new location and to install temporary wedges. No test in the laboratory took longer than two hours to complete. The lifting of slabs 9/10/11 to their temporary position in the

fourth stage of lifting of the west building took several hours, and the floor slabs remained supported by the jack rods for approximately an hour on the 23rd of April while the workmen were at lunch. If the capacity of the lifting assembly had been marginal at any column in the west building, any delay in parking the slabs and wedging them in place could certainly have increased the likelihood of a failure.

The actual capacity of the lifting assembly at every column in the structure will never be known exactly. However, the tests performed in the laboratory serve to establish a range of possible capacities. On the basis of these tests, and considering the variability of shearhead construction and loading conditions discussed previously, the minimum capacity of the weakest lifting assembly could have been expected to be approximately 170 kips (756 kN). The largest capacity of any lifting assembly could not have been as large as the load measured in test 3, as the lateral confinement of that shearhead was unrealistically stiff. This would suggest a maximum capacity of approximately 200 kips (934 kN) for the lifting assembly under conditions comparable to those in these tests.

#### 5.6 SUMMARY

The following summarizes the results of the laboratory tests conducted by NBS on the materials, components and subassemblies.

1. The average compressive strength of the concrete in the floor slabs and shearwalls exceeded the value required by the project specifications.
2. There was no evidence that the concrete in the floor slabs or shearwalls had frozen during curing.
3. There was no evidence an admixture had weakened the concrete in the floor slabs or shearwalls.
4. The mechanical properties and chemical composition of the steel used in the columns satisfy the ASTM requirements for the grades of steel in the project specifications.
5. There was evidence of inadequate joint penetration and porosity in the welds. Some of the welds did not meet the workmanship standards of the American Welding Society.
6. The ultimate tensile strength of some of the column splice specimens was less than the strength of the base metal. Failure occurred in the weld metal in most of the column splice specimens.
7. The yield strength of the post-tensioning tendons exceeded the ASTM requirement for the steel in the project specifications.
8. Failure of the lifting assembly (jack rod/shearhead) occurred by fracture of the jack rod or by the lifting nut sliding off the lifting angle. Both types of failure were accompanied by a loud bang.



9. Deformations of the shearhead lifting angles and scrape marks due to the lifting nut sliding off observed in the lifting assembly tests were observed on several shearheads in the collapsed structure.
10. The strength of the lifting assembly is affected by the confinement of the shearhead and the eccentricity of loading of the lifting angle.

TABLE 5.2.1

SUMMARY OF CONCRETE CORE SAMPLE CHARACTERISTICS

NBS Sample No.	Field Sample No.	Length, In.	Weight, Lb.	Density, Lb/Ft <sup>3</sup>	Comments
1	RS-34	6.75	6.40	148.3	
2	RS-30	6.06	6.62	146.6	
3	RS-25	6.88	6.37	145.0	
4	RS-27	6.81	6.28	144.2	rough end
5	RS-23	6.75	6.11	141.6	
6	RS-22	6.75	6.09	141.2	end sloped
7	RS-35	6.56	6.17	147.1	
8	RS-29	7.00	6.68	149.3	contains rebar
9	RS-33	6.75	5.99	138.8	sides chipped
10	RS-31	6.81	6.14	141.0	
11	RS-9	7.00	6.49	145.1	
12	RS-28	6.75	6.35	147.2	
13	RS-1	7.31	6.81	145.7	
14	RS-3	6.94	6.39	144.1	
15	RS-10	7.06	6.35	140.7	
16	RS-2	7.00	6.32	141.3	
*17	RS-4	6.63	6.60	155.9	cracks, tendon, rebar, chair
18	RS-21	6.81	6.25	143.5	
19	RS-15	6.81	6.57	150.9	
20	SWS-8	8.25	7.51	142.4	
*21	SWS-7	8.19	7.50	143.3	cracks, voids
22	SWS-6	8.31	7.73	145.5	
23	RSW-1	8.25	7.65	145.1	
24	S83E	6.69	6.19	144.8	
25	S12G5FL7	6.69	6.13	143.4	
26	S16C2FL9	6.56	6.33	150.9	chipped
*27	S17Y5	6.5	6.00	144.4	cracked, chair
28	S5E	7.06	6.25	138.5	
29	S63E	6.75	5.92	137.2	contains chair
30	S13G5FL11	7.19	6.54	142.4	
31	S73E	6.81	6.40	147.0	contains chair
32	S18Y5	6.56	6.01	143.3	contains chair
33	S19Y5	6.75	6.20	143.7	contains chair
34	S11FL12	6.81	6.20	142.4	light-colored agg.
35	SWS-3	12.31	11.47	146.2	large chip at end
36	SWS-2	12.31	11.60	147.4	
37	SWS-5	12.69	11.72	144.5	
38	SWS-4	12.19	11.41	146.5	

\* Specimens unsuitable for testing due to damage or presence of large amounts of reinforcement

TABLE 5.2.2

SUMMARY OF CONCRETE SAMPLE TESTS RESULTS COMPRESSION TESTS

NBS Sample No.	Field Sample No.	Capped Length, In.	Failure Load, Lb.	Compressive Stress, psi	Ec, psi x 10 <sup>6</sup>
1	RS-34	6.97	64,150	5750	
2	RS-30	7.25	56,800	5140	
3	RS-25	7.12	62,900	5670	3.07
4	RS-27	6.56	64,000	5680	
5	RS-23	6.94	72,000	6460	
6	RS-22	6.88	68,300	6120	
7	RS-35	6.75	65,900	5880	
8	RS-29	7.19	57,250	5170	
9	RS-33	6.75	61,700	5500	
10	RS-31	7.00	56,100	5040	2.69
11	RS-9	7.13	54,600	4920	
12	RS-28	7.03	66,800	6010	
13	RS-1	7.50	64,000	5800	
14	RS-3	7.13	56,600	5100	
15	RS-10	7.31	48,900	4430	
16	RS-2	7.13	59,300	5350	
*17	RS-4	6.81	Specimen damaged		
18	RS-21	7.00	51,400	4620	2.75
19	RS-15	6.94	73,900	6630	
20	SWS-8	7.75	49,700	4500	
*21	SWS-7	7.75	Specimen damaged		
22	SWS-6	7.69	45,100	4080	3.48
23	RSW-1	7.75	49,700	4500	
24	S83E	6.88	58,800	5260	3.11
25	S12G5FL7	6.88	59,000	5280	
26	S16C2FL9	7.00	61,700	5550	
*27	S17Y5	6.75	Specimen damaged		
28	S5E	7.25	52,000	4710	
29	S63E	5.19	59,000	5280	
30	S13G5FL11	7.41	60,800	5500	2.70
31	S73E	7.06	61,300	5520	2.99
32	S18Y5	6.81	60,100	5370	
33	S19Y5	6.88	63,400	5680	
34	S11FL12	7.00	48,700	4380	
35	SWS-3	7.75	51,600	4670	
36	SWS-2	7.75	53,500	4840	
37	SWS-5	7.69	53,200	4820	
38	SWS-4	7.72	50,300	4550	3.26

Where appropriate, strengths have been modified by correction factors given in ASTM C 42 to account for nonstandard length-to-diameter ratios of cores.

\* Specimens unsuitable for testing due to damage or presence of large amounts of reinforcement.

TABLE 5.2.3

SUMMARY OF CONCRETE SAMPLE TEST RESULTS - SPLITTING TESTS

NBS Sample No.	Field Sample No.	Length, In.	Failure Load, Lb.	Tensile Strength, psi
S1	RS-S24	6.81	25,100	626
S2	RS-32	6.75	19,750	497
S3	RS-20	7.06	20,350	489
S4	RS-14	7.00	26,000	631
S5	RS-26	6.94	23,700	580

Average of all cylinders : 565 psi

TABLE 5.2.4

COMPRESSIVE STRENGTH OF CONCRETE MEASURED BY AN INDEPENDENT TESTING LABORATORY

Mean Compressive Strength, psi (Std. Deviation. psi)		
Floor Level	West Building	East Building
Roof	4570 (98.2)	4560 (68.9)
12	4670 (99.5)	4680 (81.9)
11	4670 (84.8)	4600 (72.4)
10	4600 (78.0)	4580 (106)
9	4560 (65.8)	4650 (74.7)
8	4550 (80.1)	4580 (70.0)
7	4590 (99.3)	4680 (105)
6	4950 (203)	4810 (85.1)
5	4980 (82.2)	4560 (87.2)
4	4980 (120)	5290 (86.2)
3	4940 (107)	4720 (133)
2	4450 (88.6)	4650 (84.0)
1	4530 (111)	4420 (83.5)
Ground Level	4540 (75.2)	4670 (116)
C Level	4480 (121)	4380 (81.0)
D Level	4550 (57.7)	4380 (74.0)

Summary - all floors, both buildings: 4650 (216)

Calculated compressive strengths and standard deviations of strength for each floor based on results of nine cylinders.

TABLE 5.3.1

DESCRIPTION OF TENSILE TEST COUPONS

<u>Specimen</u>	<u>Specimen Location</u>	<u>Specimen Orientation</u>	<u>Average Thickness, in</u>	<u>Average Width, in</u>	<u>Area, in<sup>2</sup></u>	<u>Length, in</u>
COLUMN SEGMENT 21-1						
21-1C-1	web	longtd.	0.388	0.501	0.1944	8
21-1C-2	web	transverse	0.388	0.502	0.1948	8
21-1A-1	flange	longtd.	0.578	1.504	0.8693	18
21-1B-1	flange	longtd.	0.578	1.504	0.8693	18
COLUMN SEGMENT 21-2						
21-2C-1	web	longtd.	0.388	0.501	0.1944	8
21-2C-2	web	transverse	0.388	0.500	0.1940	8
21-2A-1	flange	longtd.	0.578	1.503	0.8687	18
21-2B-1	flange	longtd.	0.578	1.503	0.8687	18
COLUMN SEGMENT 21-3						
21-3C-1	web	longtd.	0.388	0.501	0.1944	8
21-3C-2	web	transverse	0.388	0.502	0.1948	8
21-3A-1	flange	longtd.	0.677	0.501	0.3390	8
21-3B-1	flange	longtd.	0.578	1.504	0.8693	18

TABLE 5.3.2

TENSILE TEST RESULTS - COLUMN STEEL

<u>Specimen</u>	<u>Specimen Location</u>	<u>Static Yield Stress,ksi</u>	<u>Ultimate Tensile Strength,ksi</u>	<u>Elastic Modulus,ksi</u>	<u>Percent Elongation</u>
COLUMN SEGMENT 21-1 (ASTM A36)					
21-1C-1	web	37.5	68.5	31.0	36.0(a)
21-1C-2	web	40.0	68.5	29.5	37.6(a)
21-1A-1	flange	37.0	66.5	27.5	29.0(b)
21-1B-1	flange	38.0	67.5	27.5	29.8(b)
COLUMN SEGMENT 21-2 (ASTM A572/50)					
21-2C-1	web	52.5	79.0	29.0	32.8(a)
21-2C-2	web	53.0	79.5	28.5	31.4(a)
21-2A-1	flange	54.5	80.5	29.5	25.4(b)
21-2B-1	flange	51.0	78.0		25.4(b)
COLUMN SEGMENT 21-3 (ASTM A36)					
21-3C-1	web	37.5	68.5	29.5	39.2(a)
21-3C-2	web	40.0	68.0	28.5	37.6(a)
21-3A-1	flange	39.0	68.5		40.6(a)
21-3B-1	flange	38.0	67.5	29.5	30.6(b)

(a) in a 2-inch gage length  
 (b) in an 8-inch gage length

TABLE 5.3.3

ASTM REQUIREMENTS FOR MECHANICAL PROPERTIES

<u>ASTM Standard</u>	<u>Minimum Yield Strength</u>		<u>Ultimate Tensile Strength</u>		<u>Minimum Elongation, %</u>	
	<u>ksi</u>	<u>MPa</u>	<u>ksi</u>	<u>MPa</u>	<u>in 8 in or 200 mm</u>	<u>in 2 in or 50 mm</u>
A 36	36	248	58 - 80	400 - 552	20	23
A 572(50)	50	345	≥ 65	450	18	21

TABLE 5.3.4

MILL TEST RESULTS

Designation	Heat No.	Yield Point, psi	Tensile Strength, psi	Elongation, % <sup>1</sup>
HP 12x53	170J528 (A36)	37100	67000	27.0
	712 (A36)	44300	72500	26.0
	542 (A36)	40600	72000	27.0
	530 (A36)	39600	71500	29.0
	713 (A36)	38800	66500	27.0
W12x72	170J515 (A36)	39200	65500	26.0
	517 (A572)	55500	86500	22.0
W12x79	170J514 (A36)	41400	75500	27.0
	517 (A572)	55500	86500	22.0
W12x87	172H103 (A36)	41200	77500	26.0
	170J513 (A572)	60500	89500	22.0
	514 (A36)	41400	75500	27.0
W12x96	170J514 (A36)	41600	76000	24.0
	513 (A572)	57000	86000	20.0
	513 (A572)	60500	89500	22.0
W12x106	170J125 (A36)	45400	71000	25.0
	180H271 (A36)	44500	77500	26.0
	170J513 (A572)	60500	89500	22.0
	514 (A36)	40900	75500	25.0
	699 (A36)	49200	69000	23.0
W12x120	170J512 (A36)	46100	79000	26.0
	513 (A572)	57000	86000	20.0
	698 (A572)	60000	85000	22.0
	699 (A36)	47300	77500	28.0
W12x136	170J513 (A572)	60500	89500	22.0
	513 (A572)	57000	86000	20.0
	512 (A36)	46600	78000	26.0
	172H111 (A36)	47800	78000	25.0

1/ in 8 inches



TABLE 5.3.5

CHEMICAL ANALYSIS OF COLUMN STEEL

Sample		<u>(Percent)</u>									
		C	P	S	Mn	Si	Ni	Cr	V	Mo	Cu
NBS 3A-4	1	.16	.012	.032	.79	.24	.091	.13	.001	.017	.20
	3	.23	.008	.029	.75	.054	.088	.071	.001	.018	.040

TABLE 5.4.1

DESCRIPTION OF WELDMENT TENSILE TEST COUPONS

<u>Specimen</u>	<u>Specimen Location</u>	<u>Average Thickness, in</u>	<u>Average Width, in</u>	<u>Area, in<sup>2</sup></u>	<u>Length, in</u>
COLUMN SEGMENT 26					
26W1	web	0.565	1.503	0.849	18
26F1	flange	0.956	1.503	1.437	18
26F2	flange	0.956	1.503	1.437	18
26F3	flange	1.443	0.498	0.719	8
26F4	flange	1.446	0.500	0.723	8
COLUMN SEGMENT 27					
27W1	web	0.506	1.503	0.761	18
27F1	flange	0.956	1.509	1.442	18
27F2	flange	0.956	1.507	1.441	18
27F3	flange	1.446	0.500	0.723	8
27F4	flange	1.446	0.500	0.723	8
COLUMN SEGMENT 28					
28W1	web	0.252	1.253 <sup>1/</sup>	0.316	18
28F1	flange	0.412	1.503	0.619	18
28F2	flange	0.412	1.503	0.619	18
28F3	flange	1.462	0.248	0.362	4
28F4	flange	1.463	0.250	0.366	4
UNMACHINED COUPONS					
26F5	flange	1.334 <sup>2/</sup>	1.499	2.000	18
27F5	flange	1.052 <sup>3/</sup>	1.499	1.577	18
28F5	flange	0.722 <sup>2/</sup>	1.499	1.082	18

<sup>1/</sup> The coupon had to be machined to a lesser width than that specified in ASTM E8 due to the presence of a surface flaw within the reduced section.

<sup>2/</sup> Average thickness across weld joint

<sup>3/</sup> Average thickness of thinner flange

TABLE 5.4.2TENSILE TESTS RESULTS - COLUMN SPLICE WELDMENTS

<u>Specimen</u>	<u>Specimen Location</u>	<u>Area, in<sup>2</sup></u>	<u>Ultimate Tensile Load, lbf</u>	<u>Ultimate Tensile Strength, ksi</u>
COLUMN SEGMENT 26				
26F1	flange	1.437	61,500	42.8
26F2	flange	1.437	60,500	42.1
26W1	web	0.849	34,500	40.6
26F3	flange	0.719	12,000	16.7
26F4	flange	0.723	26,250	36.3
COLUMN SEGMENT 27				
27F1	flange	1.442	107,000	74.2
27F2	flange	1.441	91,000	63.2
27W1	web	0.761	61,700	81.1
27F3	flange	0.723	53,050	73.4
27F4	flange	0.723	15,200	21.0
COLUMN SEGMENT 28				
28F1	flange	0.619	33,400	54.8
28F2	flange	0.619	39,500	63.8
28W1	web	0.316	8,800	27.8
28F3	flange	0.362	27,050	74.7
28F4	flange	0.366	23,200	63.4
UNMACHINED COUPONS				
26F5	flange	2.000	117,000	58.5
27F5	flange	1.577	131,000	83.1
28F5	flange	1.082	71,600	66.2

TABLE 5.4.3

KNOOP MICROHARDNESS MEASUREMENTS OF WELD BLOCK/COLUMN SAMPLE  
(NBS - 21-3A)

Location	Specimen					$\bar{X}$
	3A1	3A2	3A3(1)	3A3(2)	3A4	
Plate -	181	168	195	192	185	178
& HAZ -	254	260	230	225	250	244
Hard Spot -	276	333	287	264	262	
Weld -	320	307	300	285	310	304
HAZ -	244	294	244	234	263	256
Block -	202	210	168	160	212	197

TABLE 5.4.4

CHEMICAL ANALYSIS OF COLUMN JOINT WELD METAL

NBS 4-F1  
(Percent)

Sample		C	P	S	Mn	Si	Ni	Cr	V	Mo	Cu
Plate	1	.21	.010	.027	1.19	.034	.058	.071	.057	.011	.20
Weld	2	.097	.010	.012	1.00	.50	.040	.029	.005	<.005	.015
Plate	3	.22	.005	.016	1.25	.026	.124	.038	.058	.022	.060

TABLE 5.4.5

KNOOP MICROHARDNESS MEASUREMENTS OF COLUMN JOINT WELD SPECIMENS  
[HK 500 gm]

NBS 8-F1	HK500			$\bar{X}$	NBS 8-T1	HK500			$\bar{X}$
7/16" Plate -	197	199	198		5/8" Plate -	160	165	163	
& HAZ -	226	280	253		& HAZ -	208	190	199	
Weld Back -	205	202	204		Weld Back -	184	204	194	
Weld V -	280	207	244		Weld V -	180	165	173	
Hard spot -	320	294			Hard Spot -	294	246		
HAZ -	223	226	225		HAZ -	210	206	208	
7/16" Plate -	212	198	205		1/2" Plate -	166	166	166	
NBS 5-W1					NBS 6-F1				
3/8" Plate <sup>2</sup>	188	195	192		1 5/6" Plate -	210	220	215	
& HAZ -	196	203	200		& HAZ -	280	295	288	
Weld Back -	193	212	203		Weld Back -	237	360	299	
Weld V -	208	200	204		Weld V -	237	240	239	
Hard spot -	264	236			Hard Spot -	491	553		
HAZ -	230	216	223		HAZ -	266	329	298	
3/8" Plate -	169	172	170		1 5/6" Plate -	225	254	240	

TABLE 5.5.1

TENSILE TESTS RESULTS - POST-TENSIONING STRANDS

<u>Specimen Number</u>	<u>Yield Strength lbf</u>	<u>Breaking Strength lbf</u>	<u>Elongation @ 1st Wire Fracture %</u>	<u>Location of Fracture</u>
Unused Strand from Landfill Area				
17-1	38,000	40,500	1.9	Alum block area
17-2	39,200	42,000	3.7	Alum block area
17-3	37,600	40,600	2.2	Alum block area
17-4	38,000	41,200	3.3	Alum block area
Strand Obtained from Rubble at Construction Site				
#5	38,900	42,150	6.8	In chuck area
#6	39,600	42,650	5.5	In chuck area
#7 <sup>a</sup>	39,800	42,350	4.4	Alum block area
#8	39,000	41,700	5.2	Between alum blocks

a/ In light of the two immediately previous strands failing in the grip(i.e. chuck) area, a mixture of carborundum powder and oil was pasted along the semi-circular trough of the aluminum blocks prior to testing specimen #7.

TABLE 5.5.2

TENSILE TEST RESULTS - JACK RODS

<u>Specimen Designation</u>	<u>Failure Load, lbf</u>	<u>Ultimate Tensile Strength, ksi</u>	<u>Percent elongation in 40 in.</u>
#1	190,000	104.9	8.6
#2	180,500	99.7	8.2
#4	184,000	101.6	7.7*
#4	187,500	103.5	8.0*

\* Elongation measured by metal tape instead of by deflectometer

TABLE 5.5.3

CHEMICAL ANALYSIS OF JACK ROD  
(Percent)

Sample	C	P	S	Mn	Si	Ni	Cr	V	Mo	Cu
NBS 11-2	.38	.008	.007	.70	.26	.073	.83	.001	.17	.035

TABLE 5.5.4

KNOOP MICHROHARDNESS MEASUREMENTS OF JACKROD (NBS 11-2)  
[TWO HK TRAVERSE'S 500 gm/20x obj]

TRAVERSE	HK <sup>1</sup>	HK <sup>2</sup>
THREAD TIP	260	281
1/10"	302	275
2/10"	253	250
3/10"	280	228
4/10"	248	279
5/10"	269	293
6/10"	245	218
7/10"	228	267
8/10"	201	223
9/10"	201	226
$\bar{X}$	249	254

Table 5.5.5

LOCATION OF JACK RODS IN LIFTING ASSEMBLY TESTS

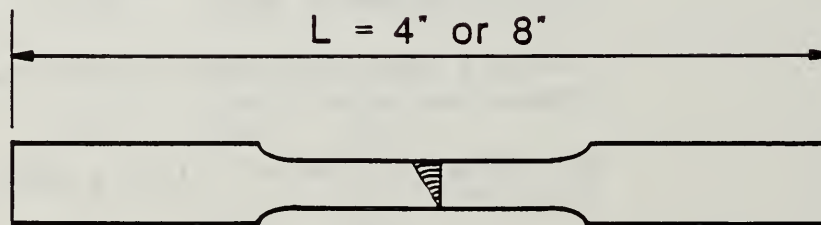
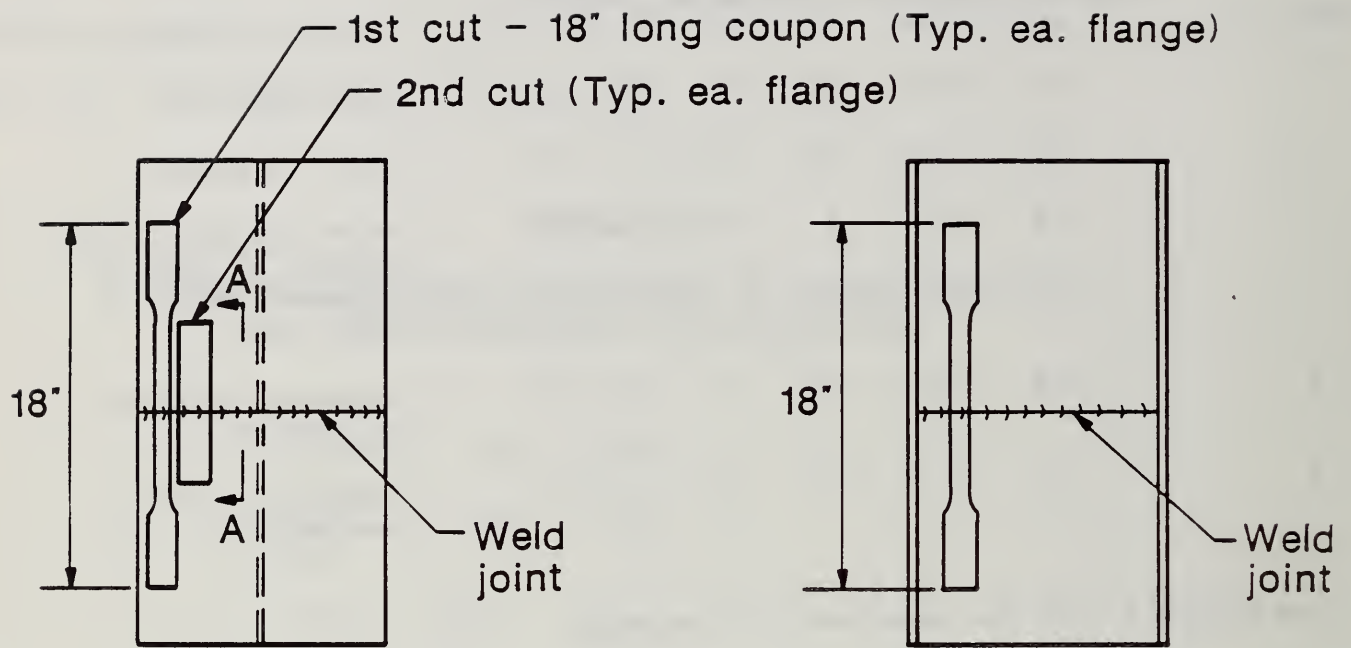
Test No.	<u>Jack rod location dimensions - inches<sup>1</sup></u>					Shearhead details
	a	b	c	d	e	
1	5/8	5/8	3/16	0	13 3/4	bare shearhead
2	1/8	1/8	1/8	1/8	14 1/2	bare shearhead
3	7/8	5/8	0	1/8	14 1/8	bare shearhead - top flanges of lifting angles joined by steel bars
4	5/8	3/4	1/8	0	14 3/8	shearhead confined by concrete
5	3/4	5/8	5/8	5/8	13 5/8	shearhead confined by concrete

1 See Figure 5.5.18 for locations of dimensions

TABLE 5.5.6

SUMMARY OF LIFTING ASSEMBLY TEST RESULTS

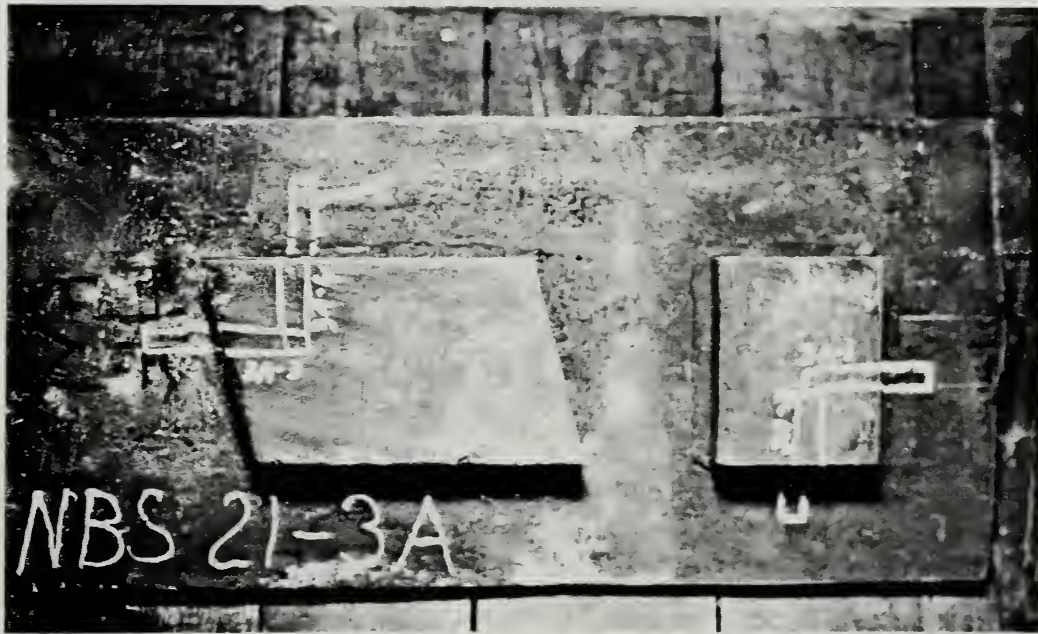
Test No.	Failure Load, Kips	Failure Location and Type
1	165	Bottom nut slipped off lifting angle
2	196	Jack rod broke above lifting nut due to flexure and axial load
3	227	Jack rod broke above lifting nut due to flexure and axial load
4	201	Bottom nut slipped off lifting angle - East side
5	198	Bottom nut slipped off lifting angle - West side



Section A-A. Specimen obtained from 2nd cut

Figure 5.4.1 Orientation and location of Weldment specimens





IC IN AMERICA

Figure 5.4.2 Weld block/column sample NBS 21-3A



Figure 5.4.3 Cross section showing weld in sample NBS 21-3A-2 (x 100)



Figure 5.4.4 Cross section showing weld in sample NBS-3A-3 (x 4)

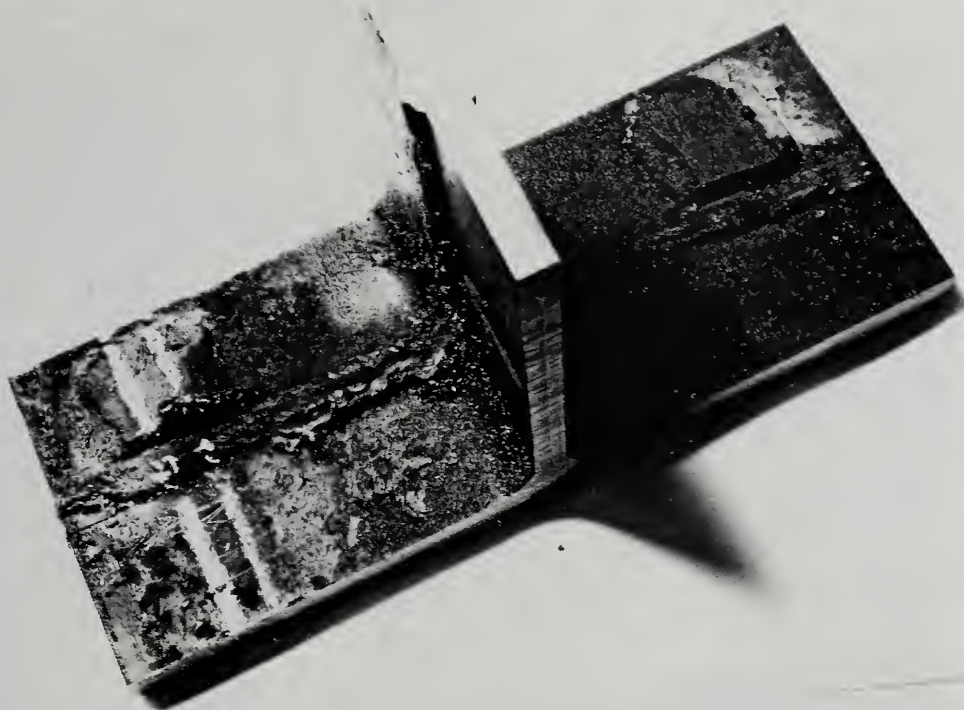


Figure 5.4.5 Location of metallographic specimen from sample NBS 8-T1



Figure 5.4.6 Cross section showing weld in specimen NBS 8-T1 (x 4)

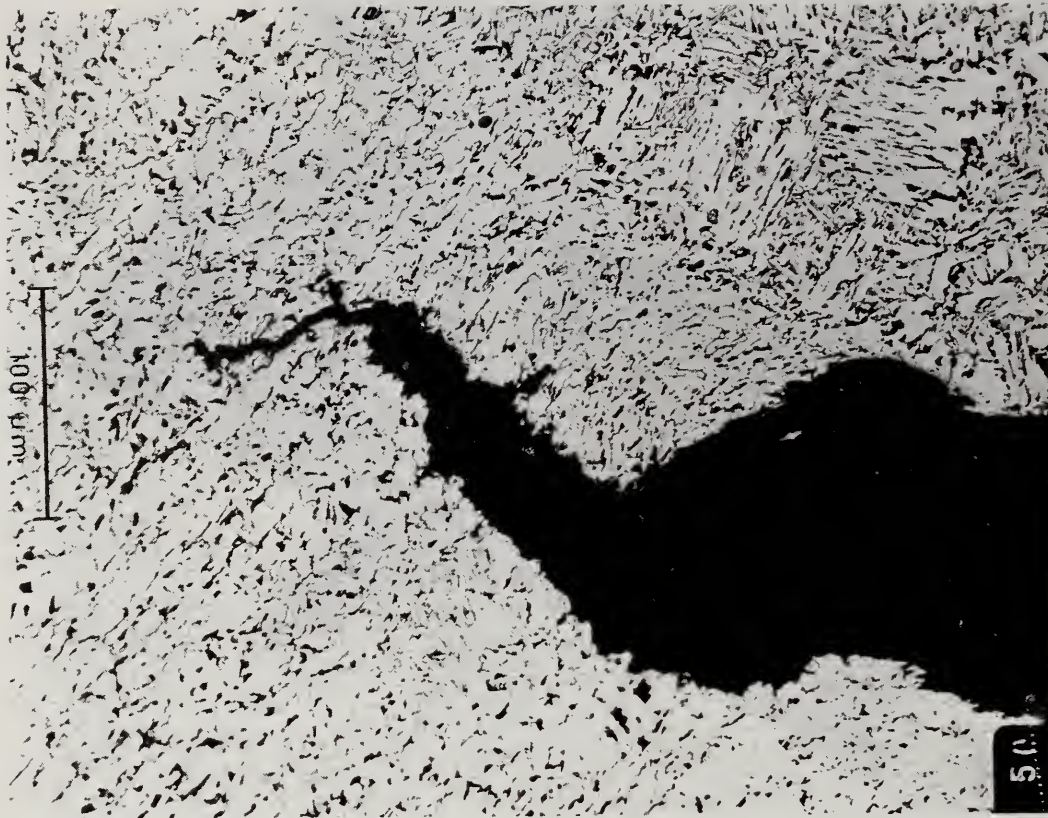


Figure 5.4.7 Cross section showing weld in specimen NBS 8-T1 at higher magnification than in Figure 5.4.6

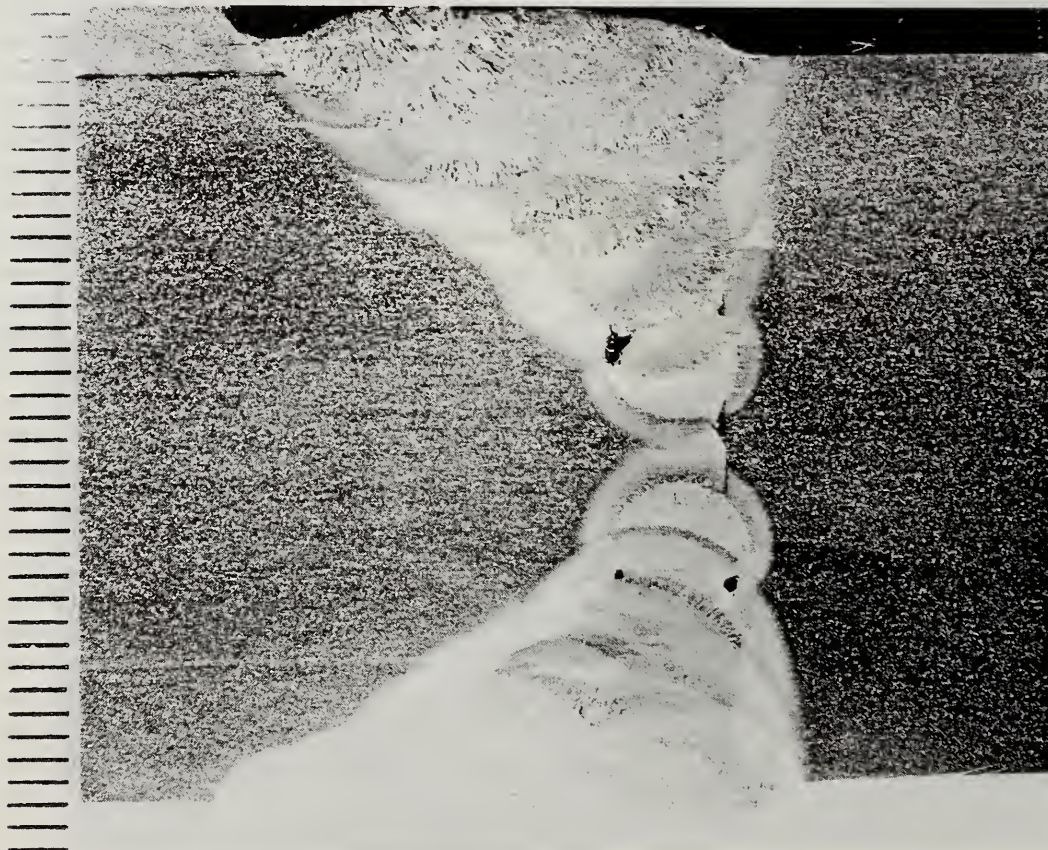


Figure 5.4.8 Cross section showing the weld in specimen NBS 6-F1 (x 4)

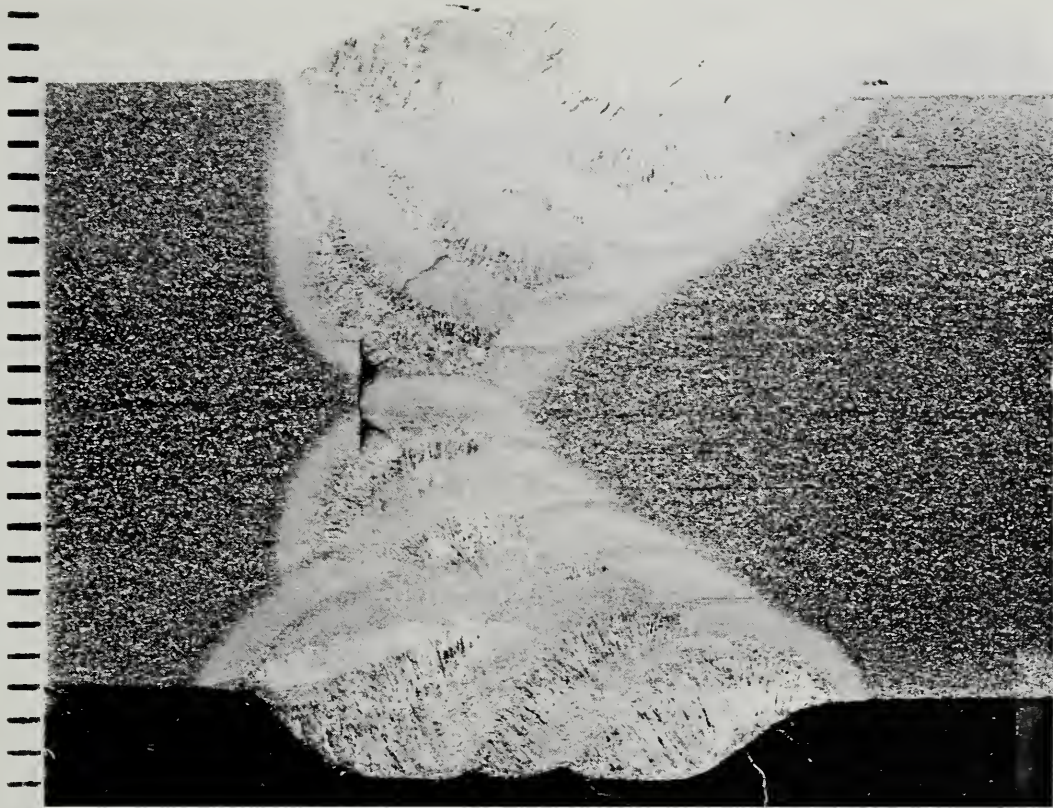


Figure 5.4.9 Cross section showing the weld in specimen NBS 6-W1 (x 4)



Figure 5.4.10 Cross section showing the weld in specimen NBS 4-F1 (x 4)

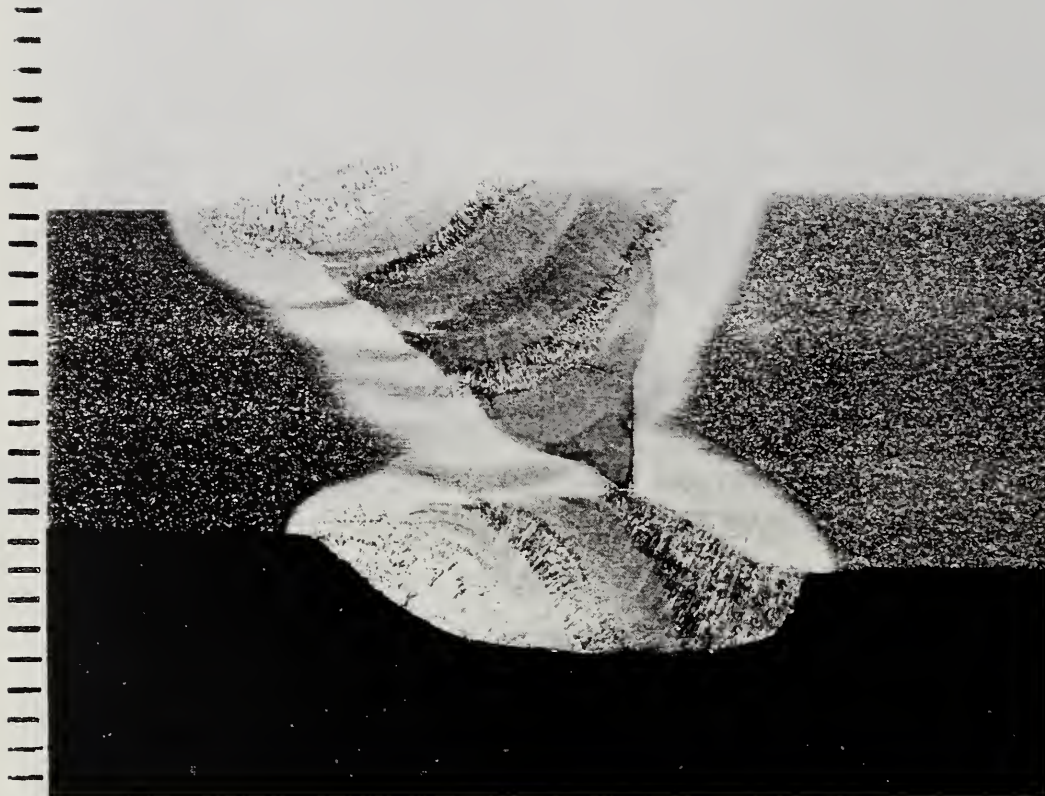
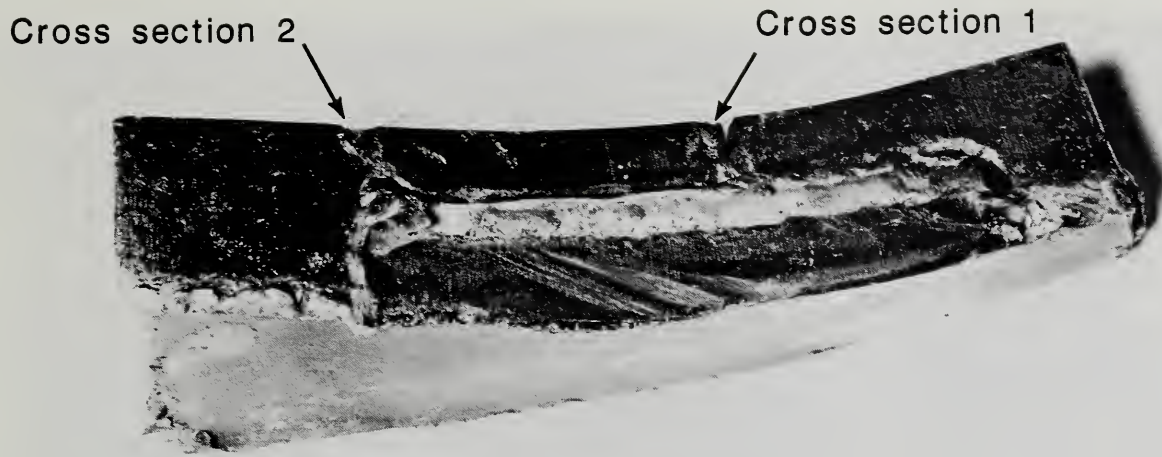


Figure 5.4.11 Cross section showing the weld in specimen NBS 4-W1 (x 4)



NBS 33B

Figure 5.4.12 Fracture of fillet weld on wedge – specimen NBS 33B



Figure 5.4.13 NBS specimen 33A, weld block/wedge sample from debris



Figure 5.4.14 Metallographic cross section #1 -  
specimen NBS 33B



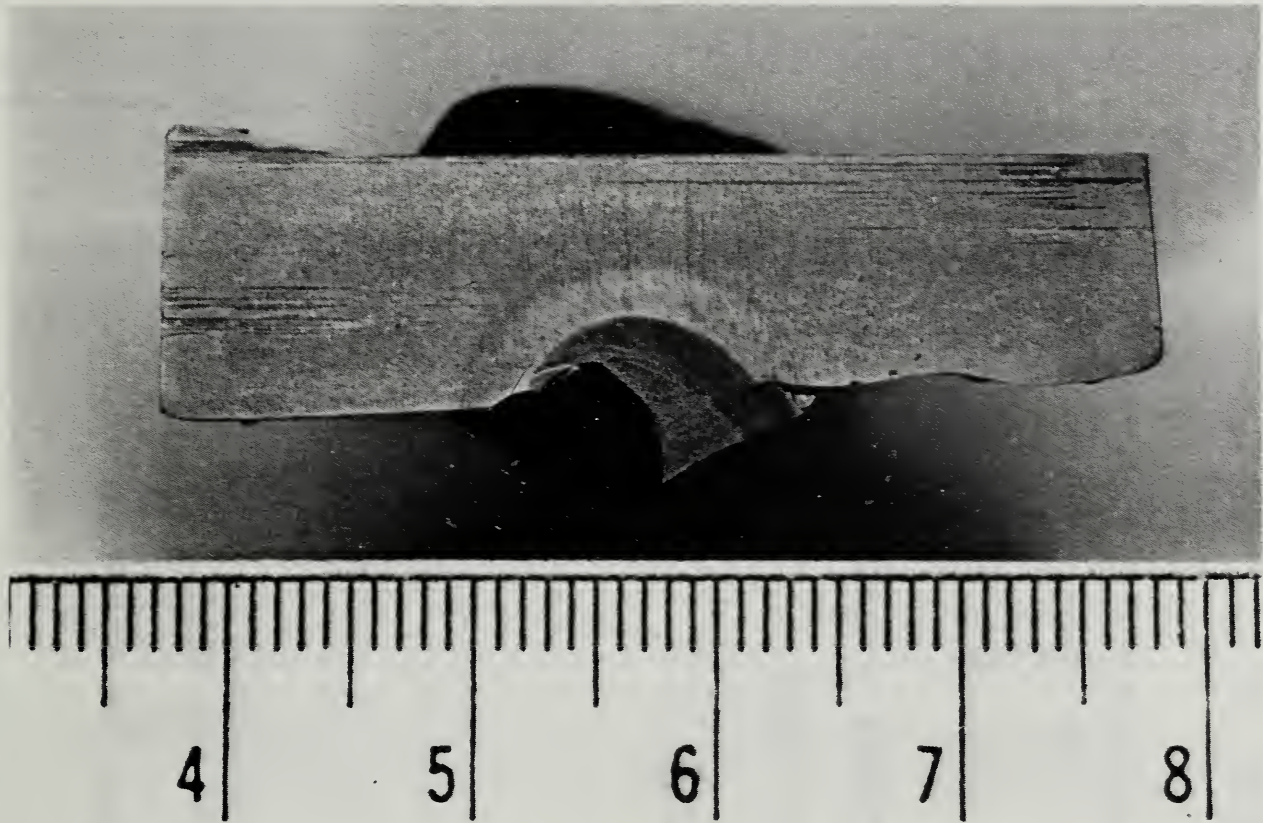


Figure 5.4.15 Metallographic cross section #2 - specimen NBS 33B

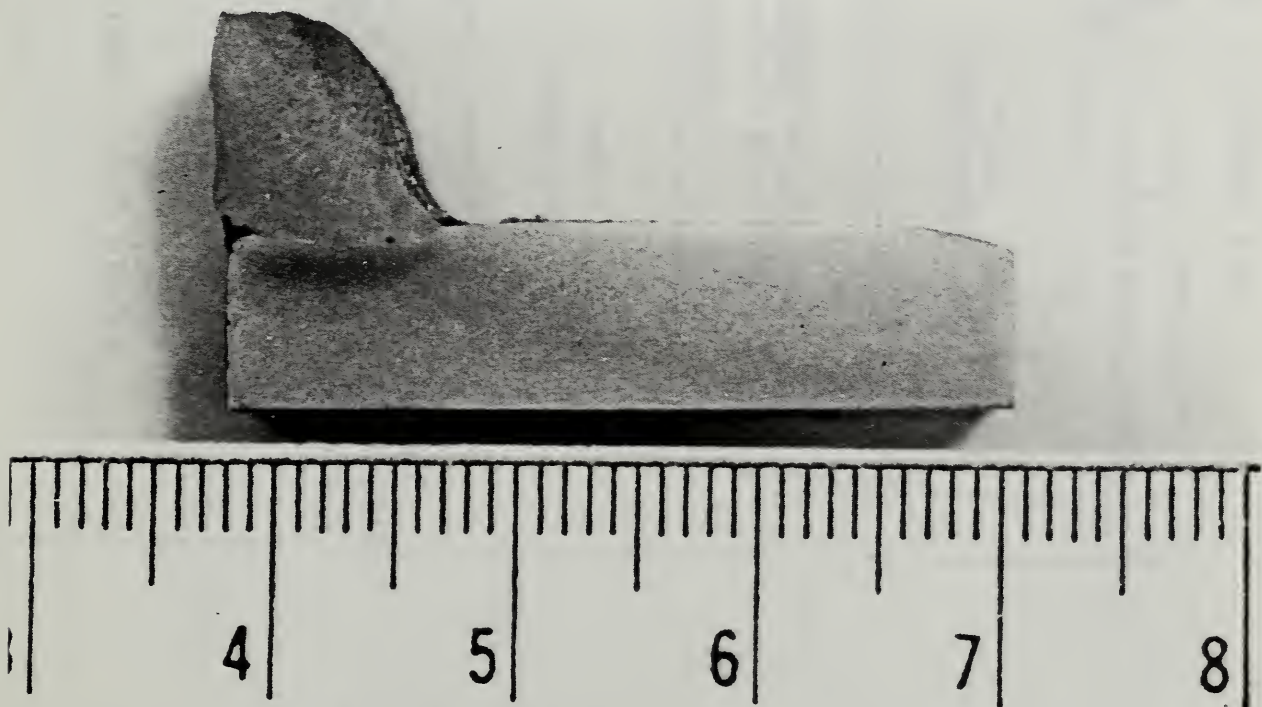


Figure 5.4.16 Metallographic cross section of failed weld along weld/column interface - specimen NBS 33A

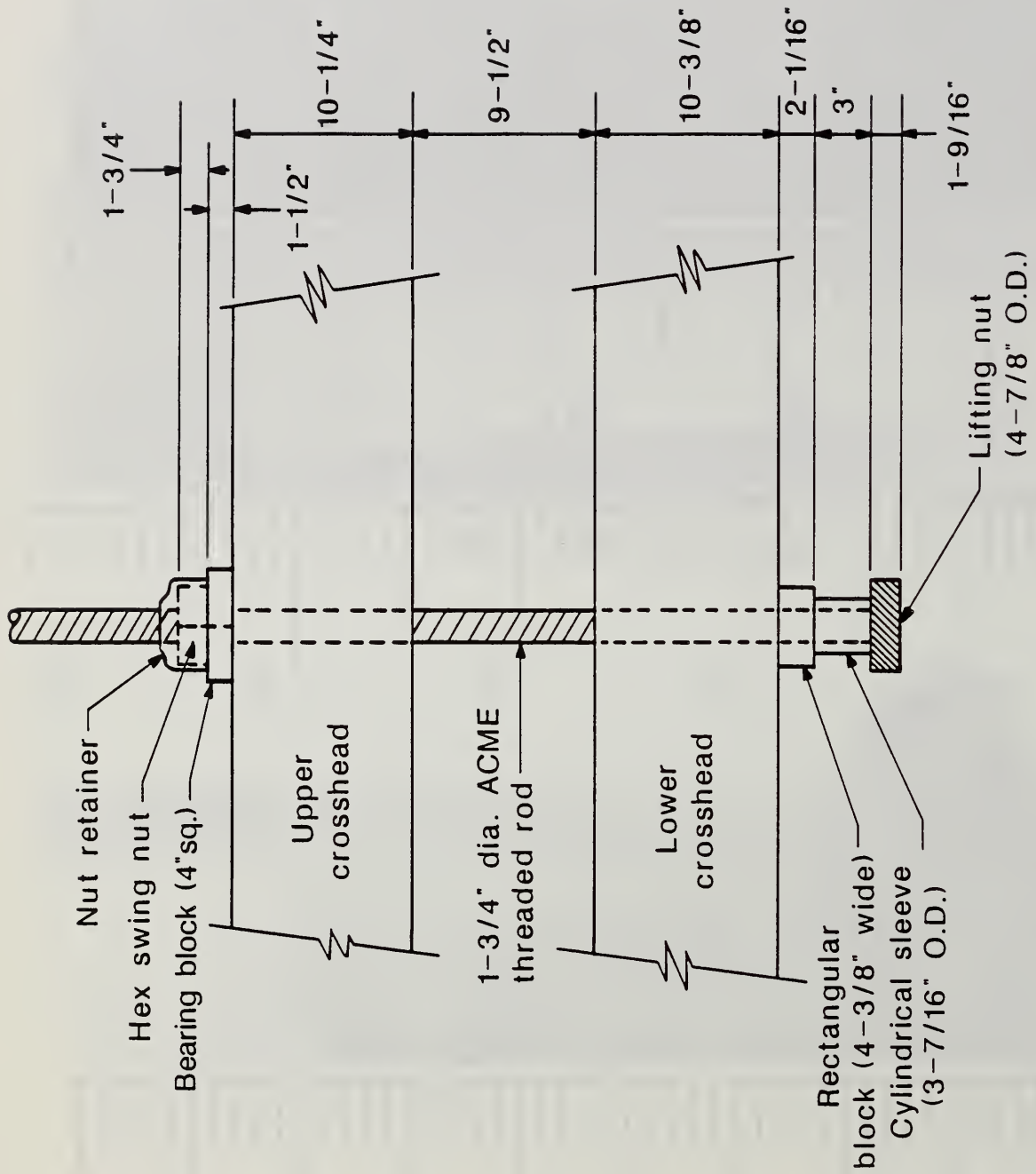
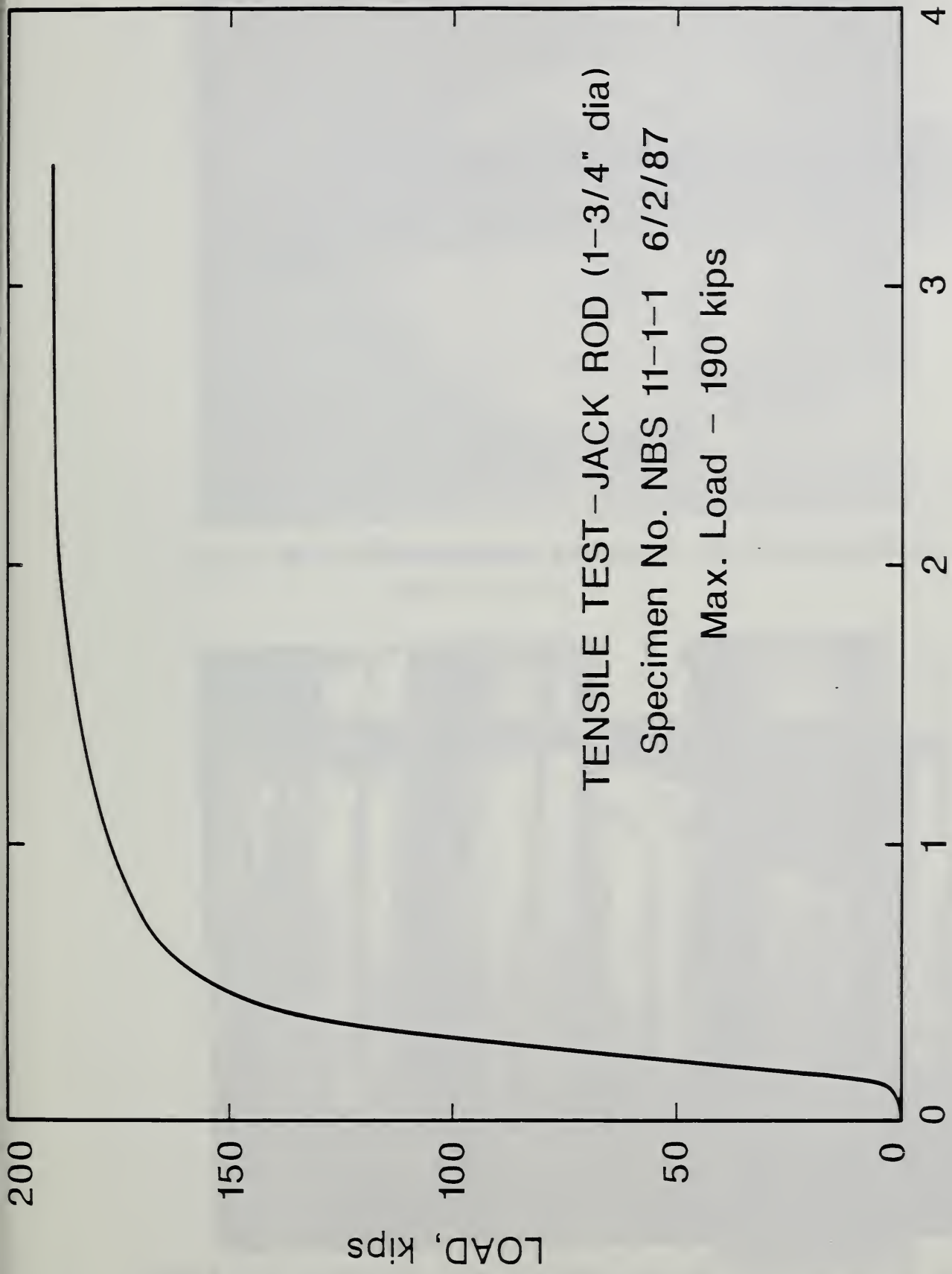
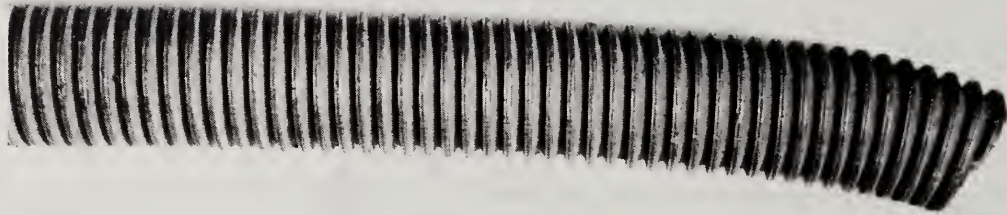


Figure 5.5.1 Test setup for jack rod specimen



ELONGATION, in.

Figure 5.5.2 Load-elongation results for jack rod specimen



17 18 19 20 21 22 23 24 25 26 27 28 29 30 31 32 33 34 35 36 37 38 39 40 41 42 43 44 45 46 47 48 49 50 51 52 53 54 55 56 57 58 59 60 61 62 63 64 65 66 67 68 69 70 71 72 73 74 75 76 77 78 79 80 81 82 83 84 85 86 87 88 89 90 91 92 93 94 95 96 97 98 99 100

Figure 5.5.3 Jack rod sample NBS 11-2



Figure 5.5.4 Jack rod on tension side showing lap seam from thread rolling operation (x 3)



Figure 5.5.5 Fracture surface of jack rod, sample NBS 11-2 (x 1)

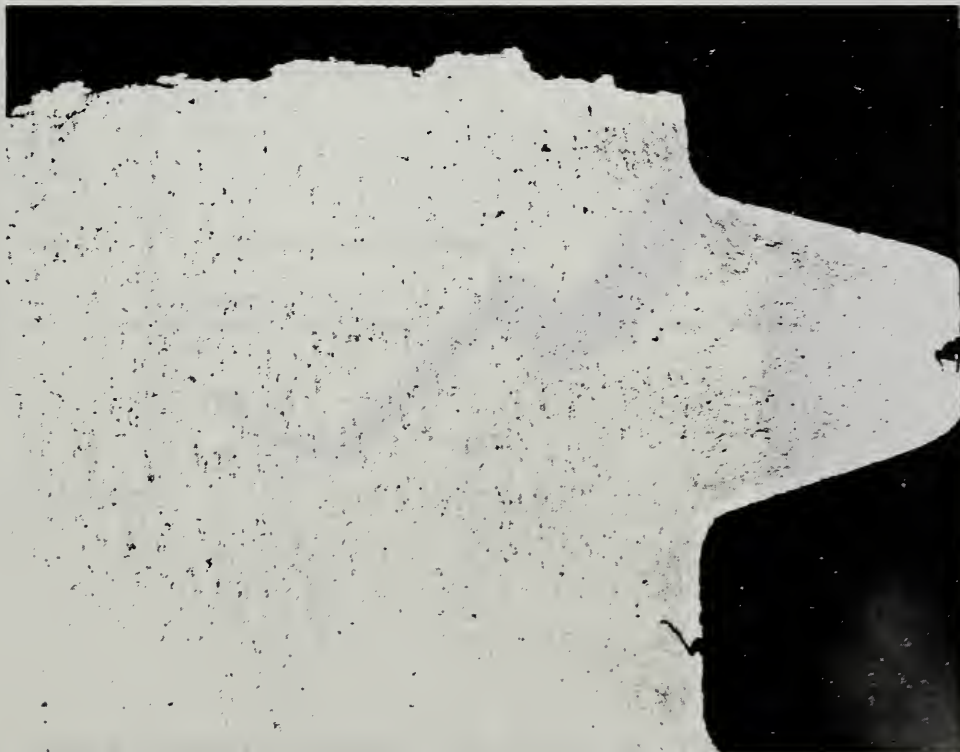


Figure 5.5.6 Fracture profile of jack rod, left, first thread adjacent to fracture (Sample NBS 11-2) (x 9)

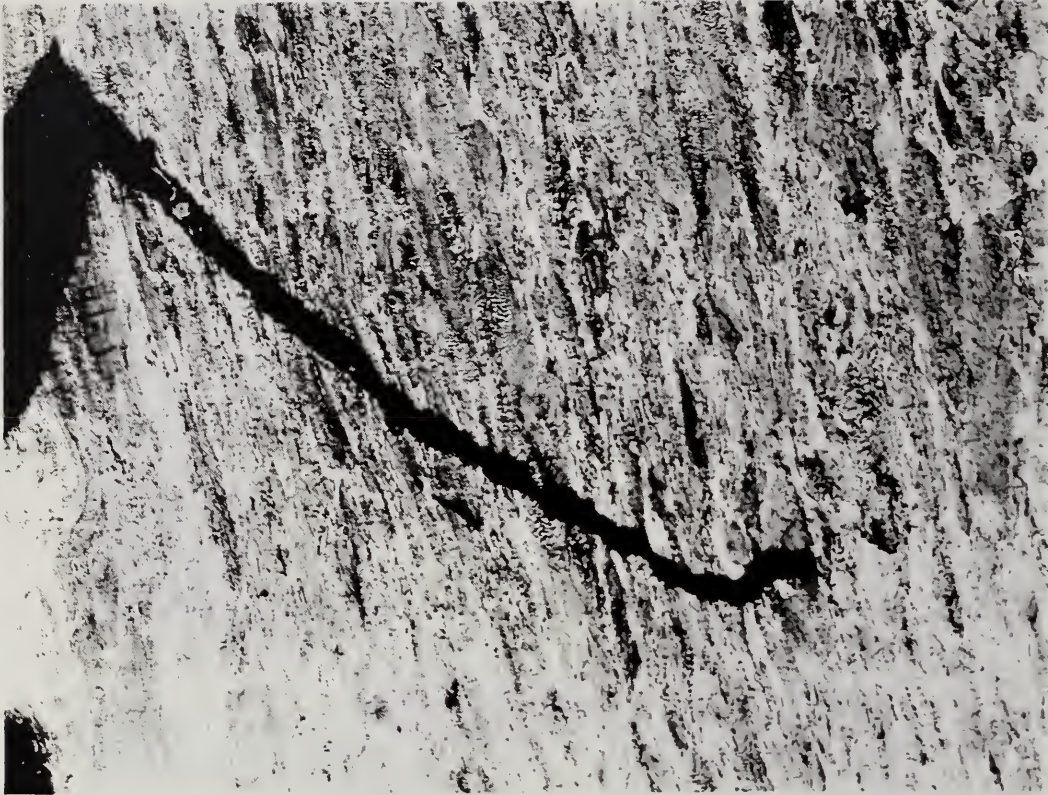


Figure 5.5.7 Lap seam at root of first thread removed from fracture of jack rod (Sample NBS 11-2) (x 500)

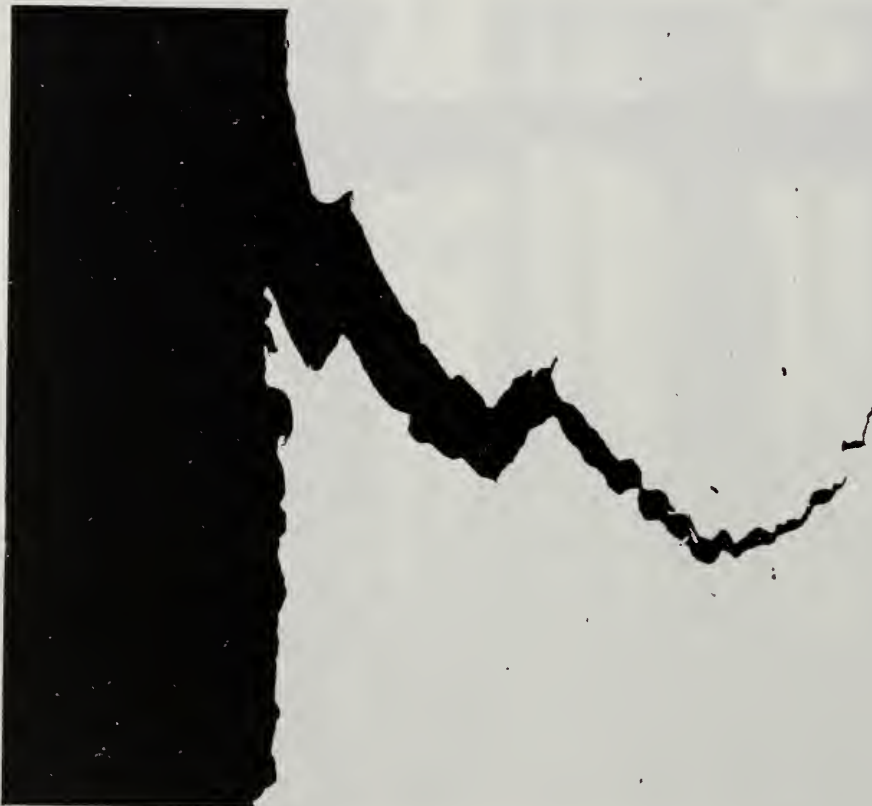


Figure 5.5.8 Lap seam at root of second thread away from fracture of jack rod. As polished (x 40)

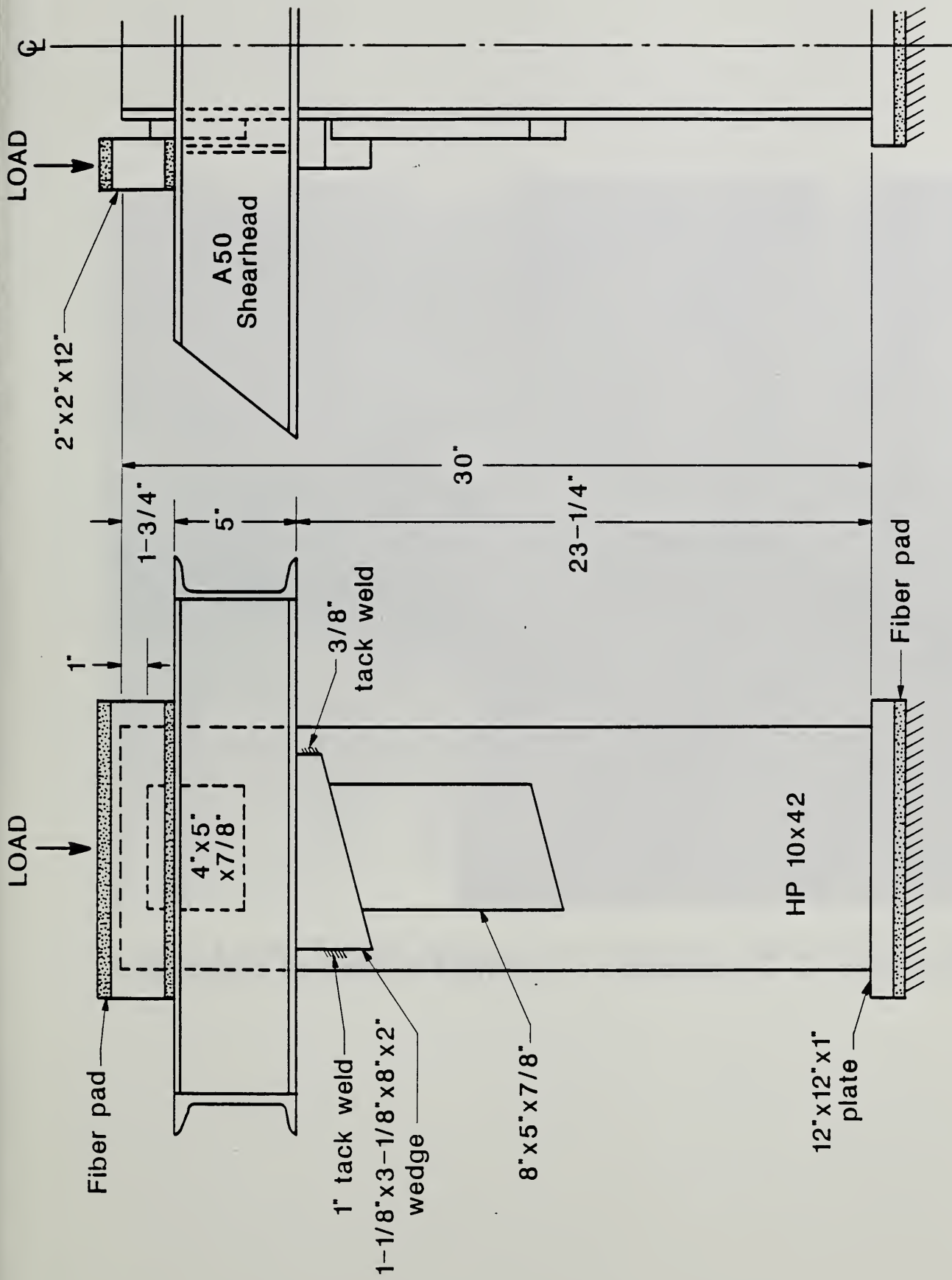


Figure 5.5.9 Shearhead-wedge assembly test setup

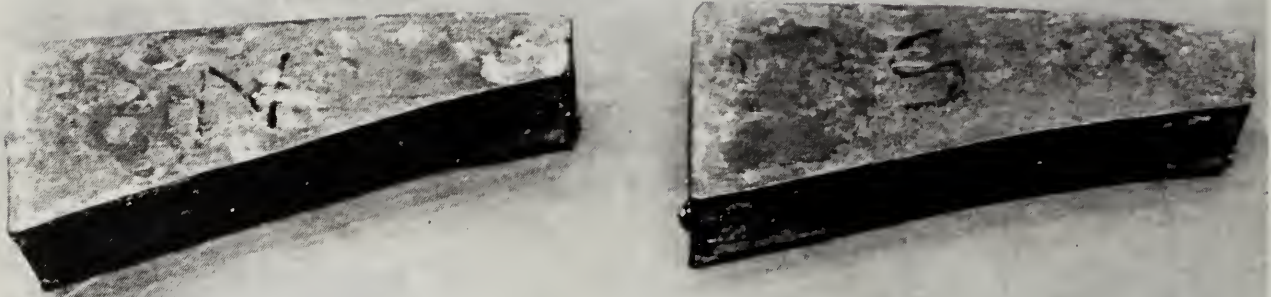


Figure 5.5.10 Deformation of wedges in test of shearhead



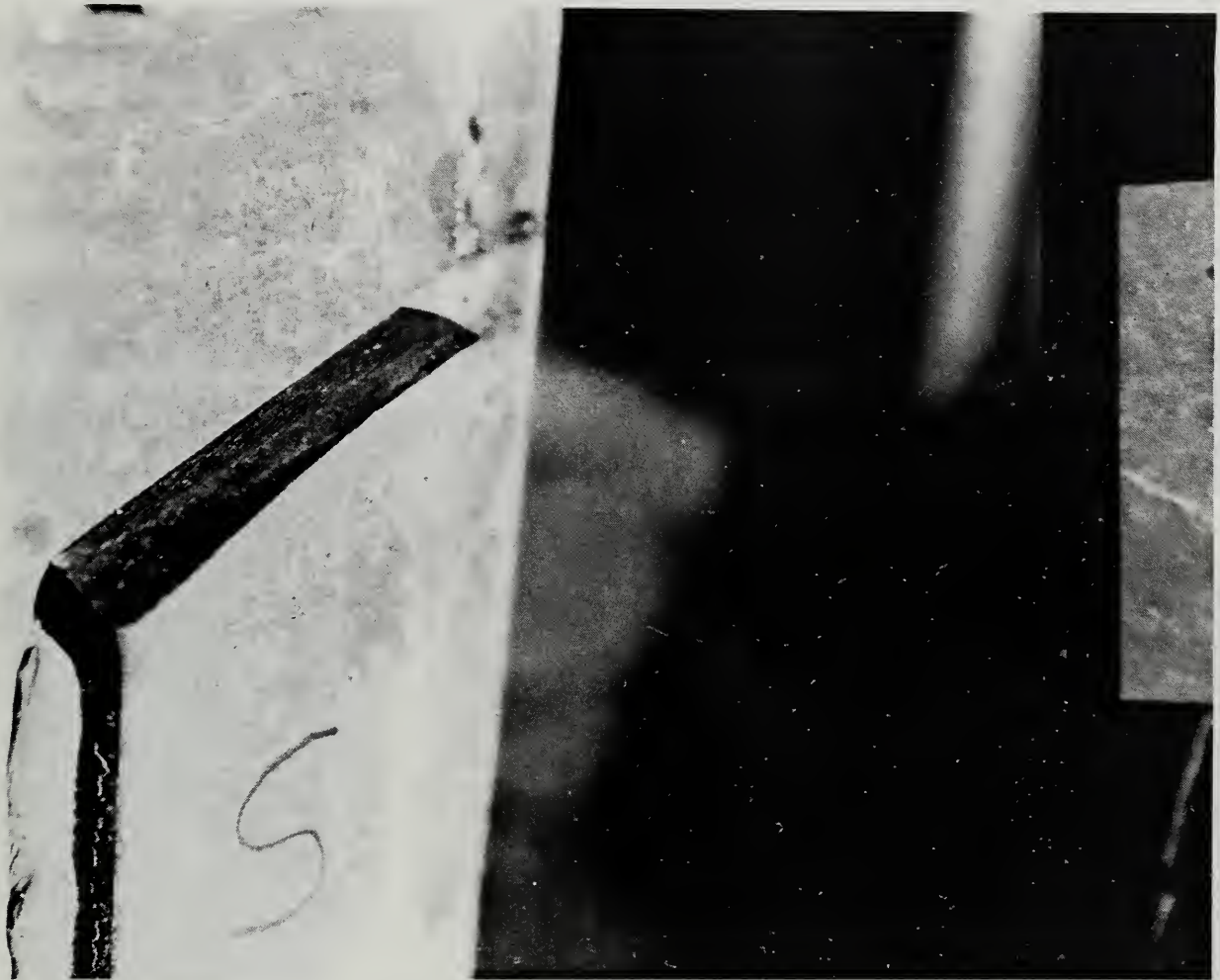


Figure 5.5.11 Weld block deformation in test of shearhead



Figure 5.5.12 Deformation of shearhead channel in test of shearhead

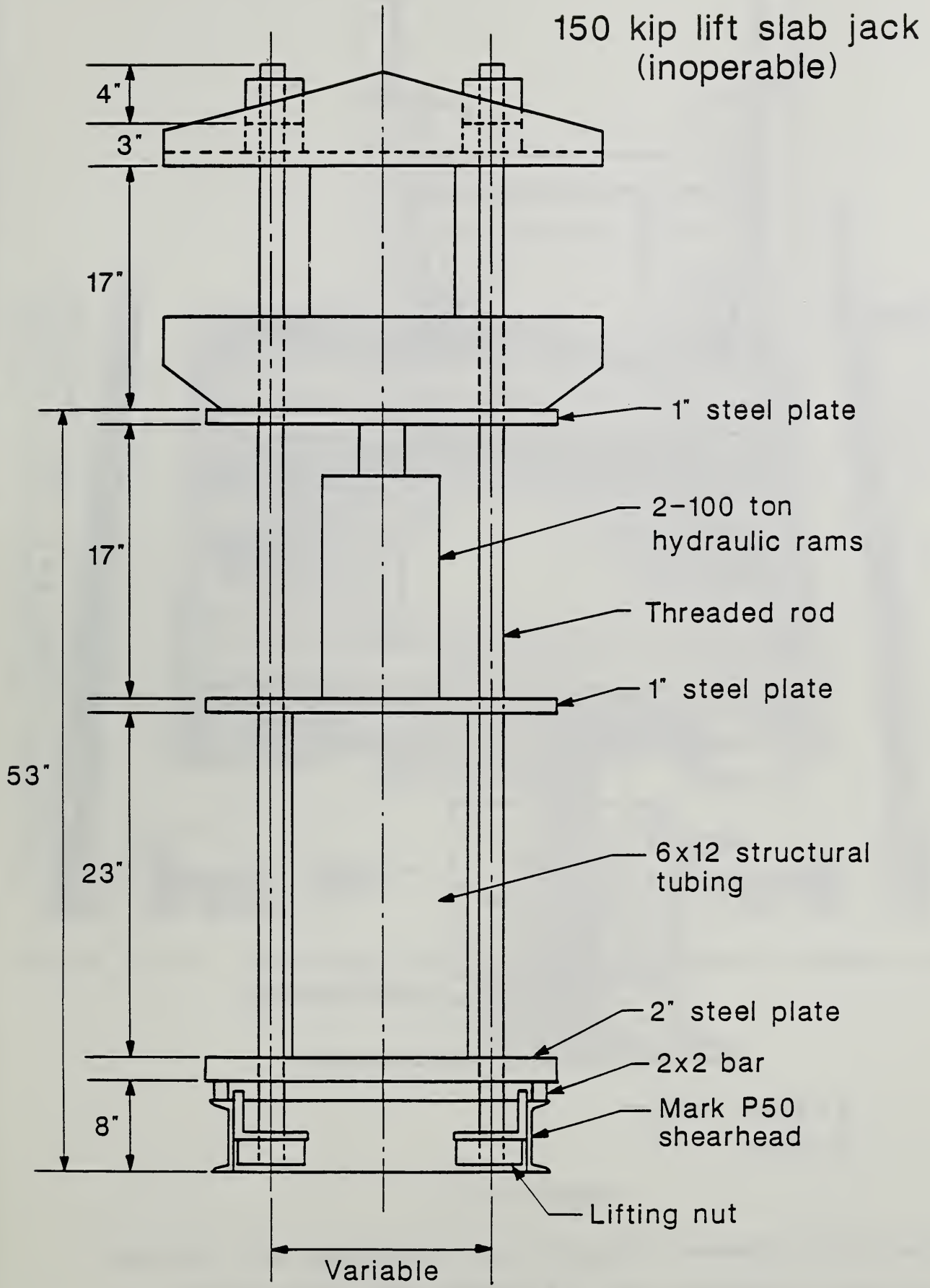
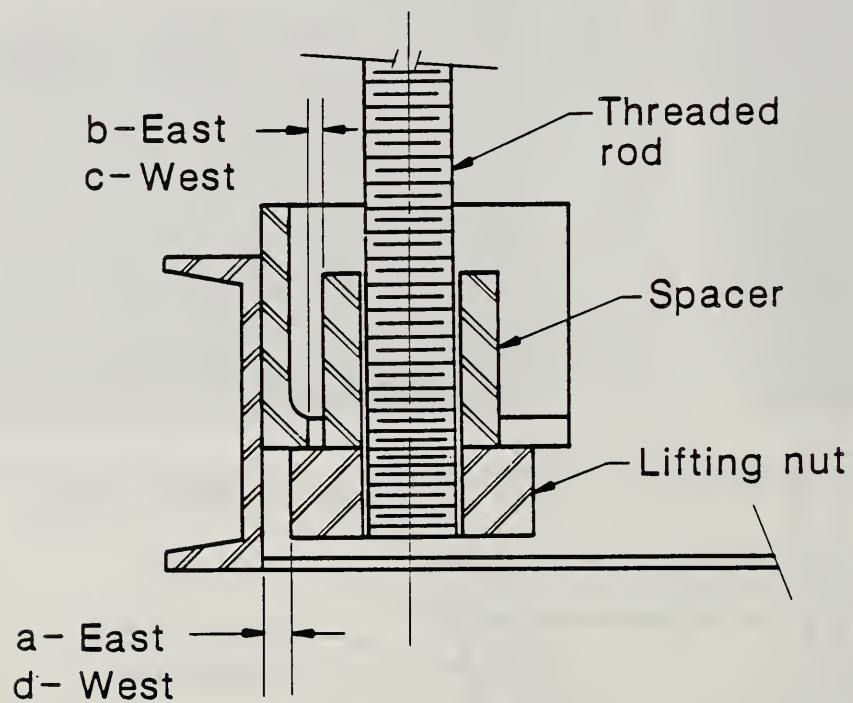
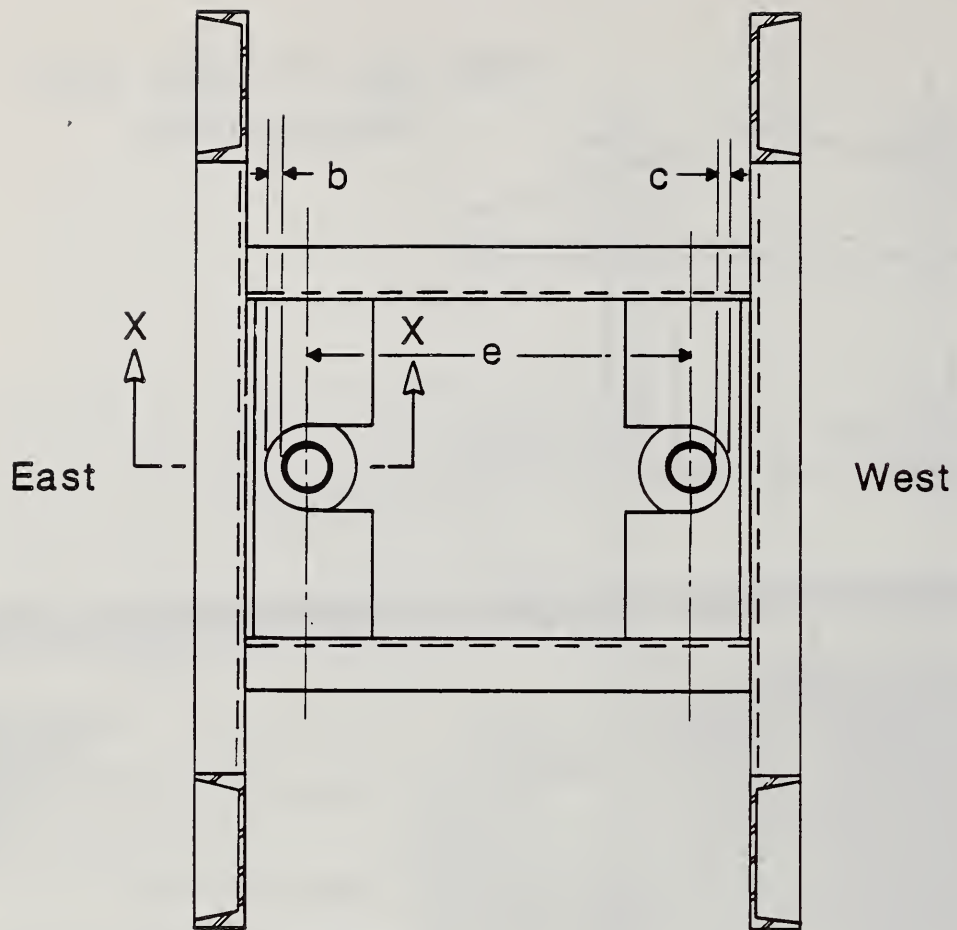


Figure 5.5.13 Lifting assembly test setup



Section X-X

- a,d: Clearance between lifting nut and shearhead arm channel
- b,c: Clearance between jack rod spacer and lifting angle
- e: Center-center spacing of jack rods

Figure 5.5.14 Critical dimensions of shearhead loading



Figure 5.5.15 Shearhead No. 3 stiffened by plates welded between legs of lifting angles

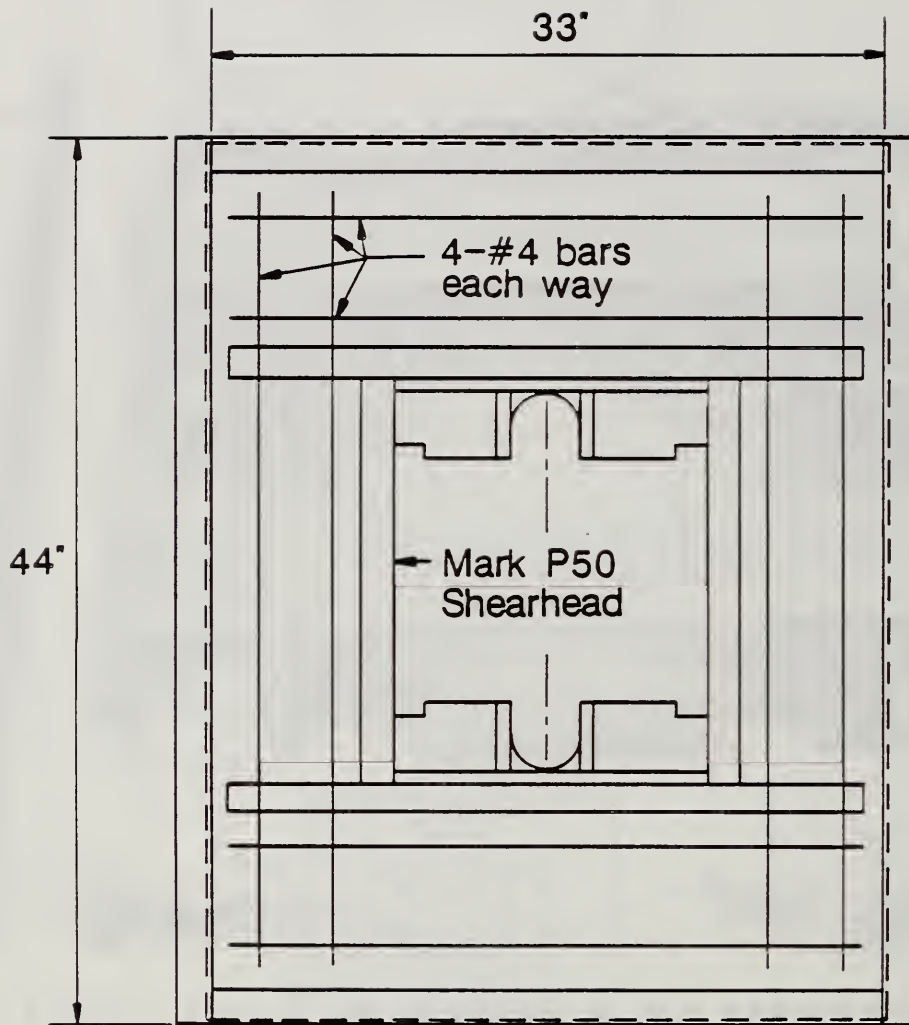


Figure 5.5.16 Shearhead configuration used in lifting assembly tests 4 and 5

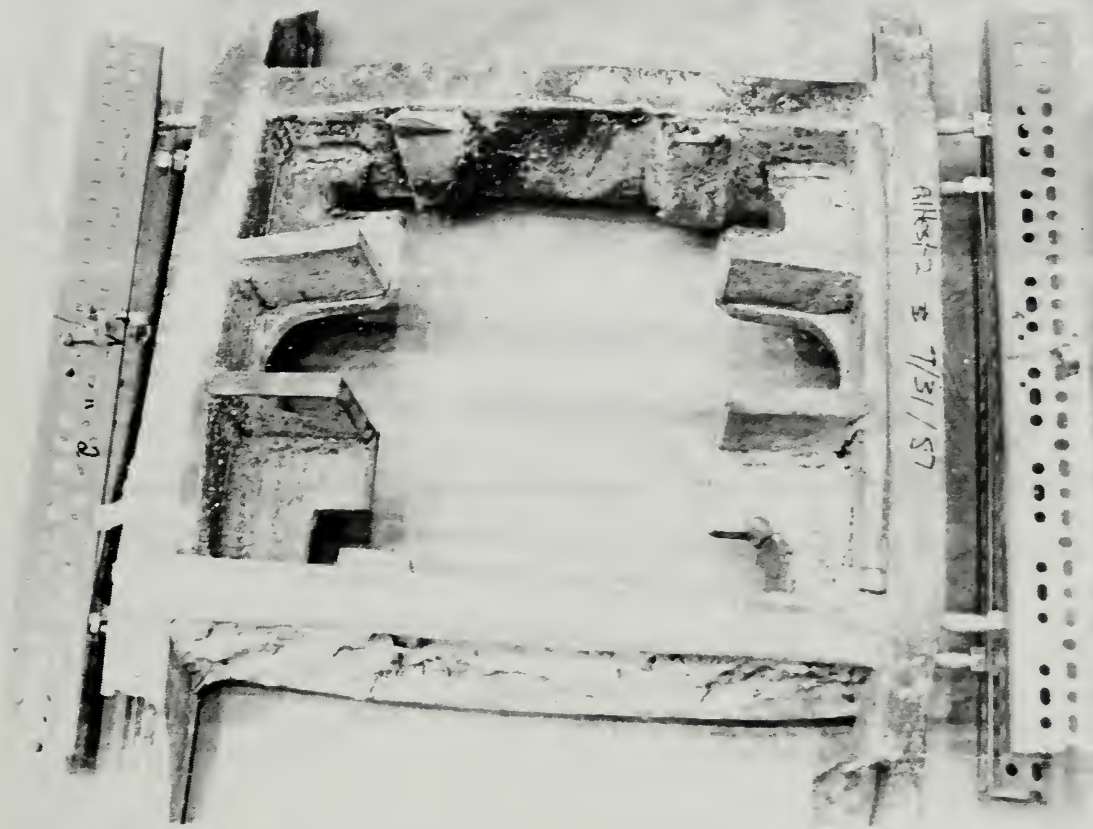
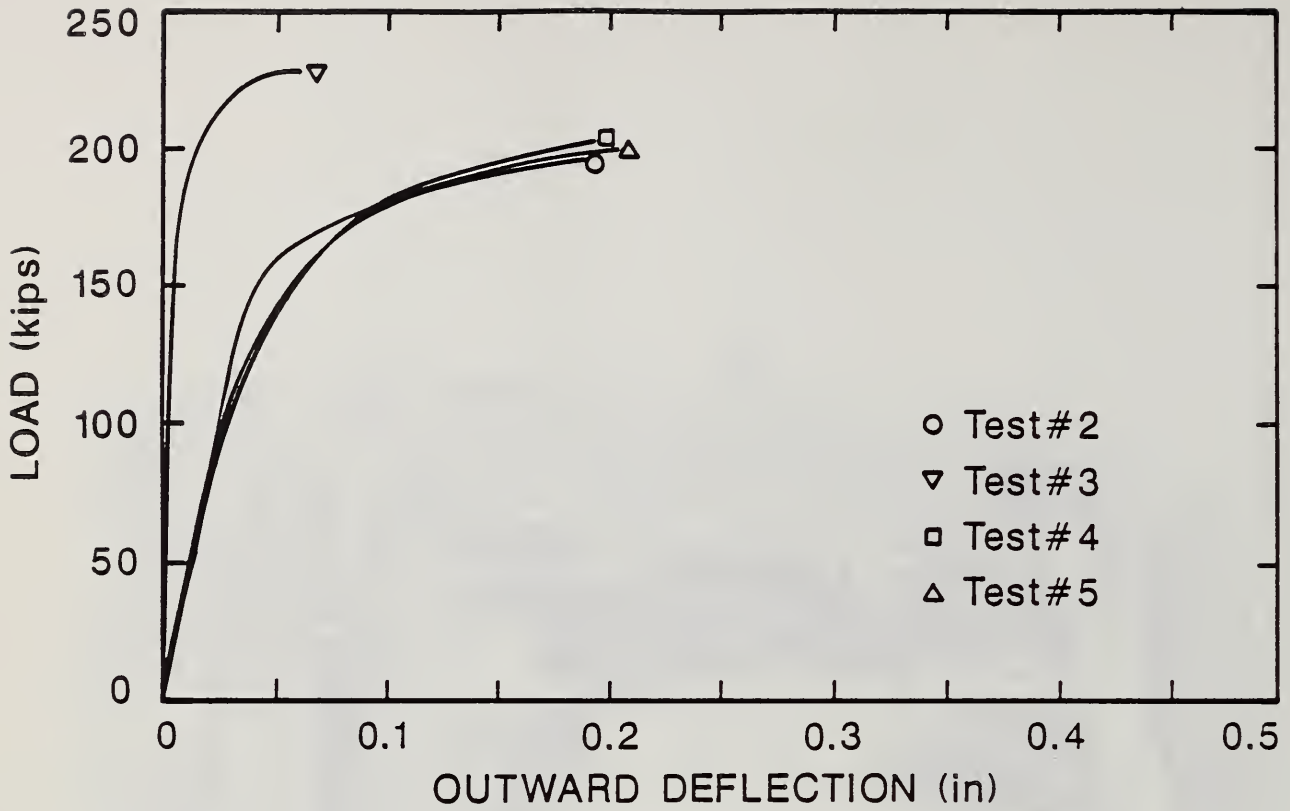
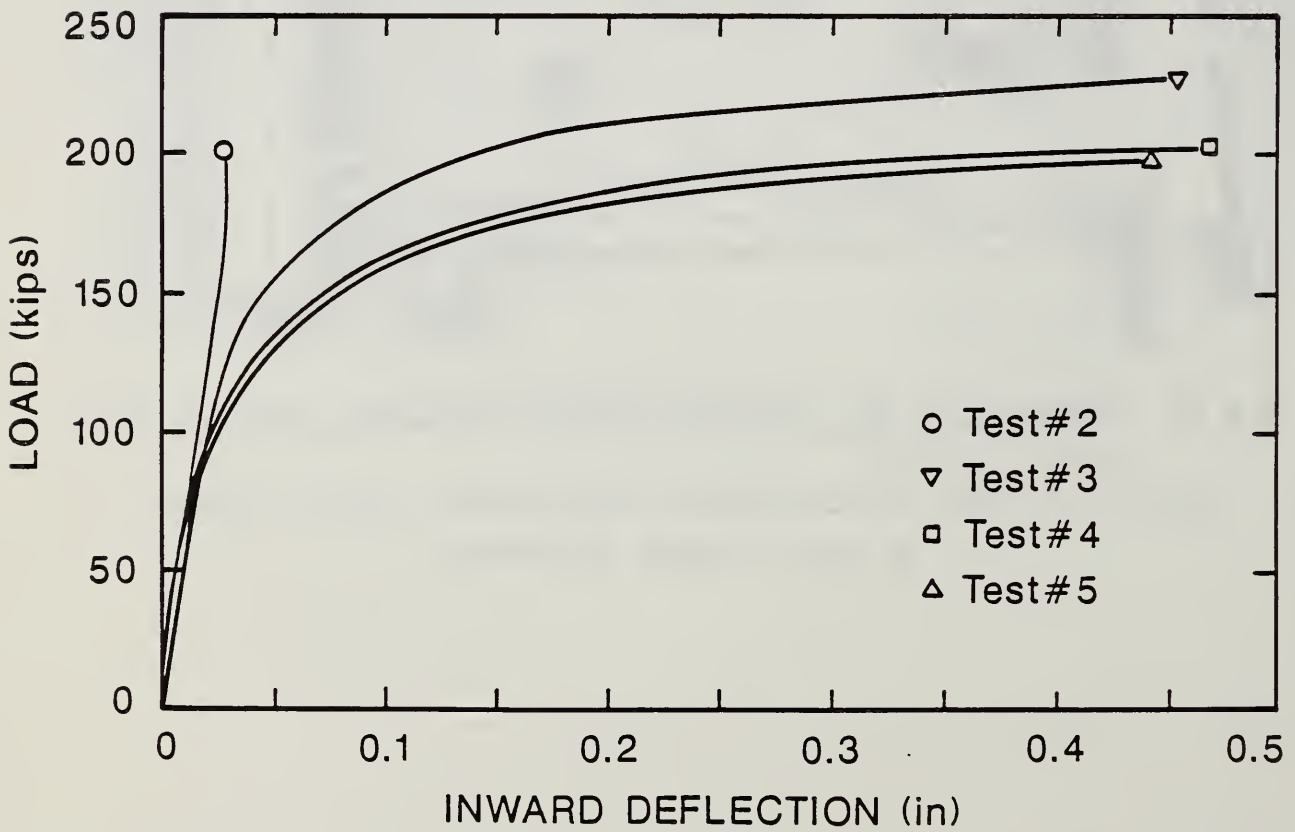


Figure 5.5.17 Shearhead No. 2 after failure showing rotation of lifting angles



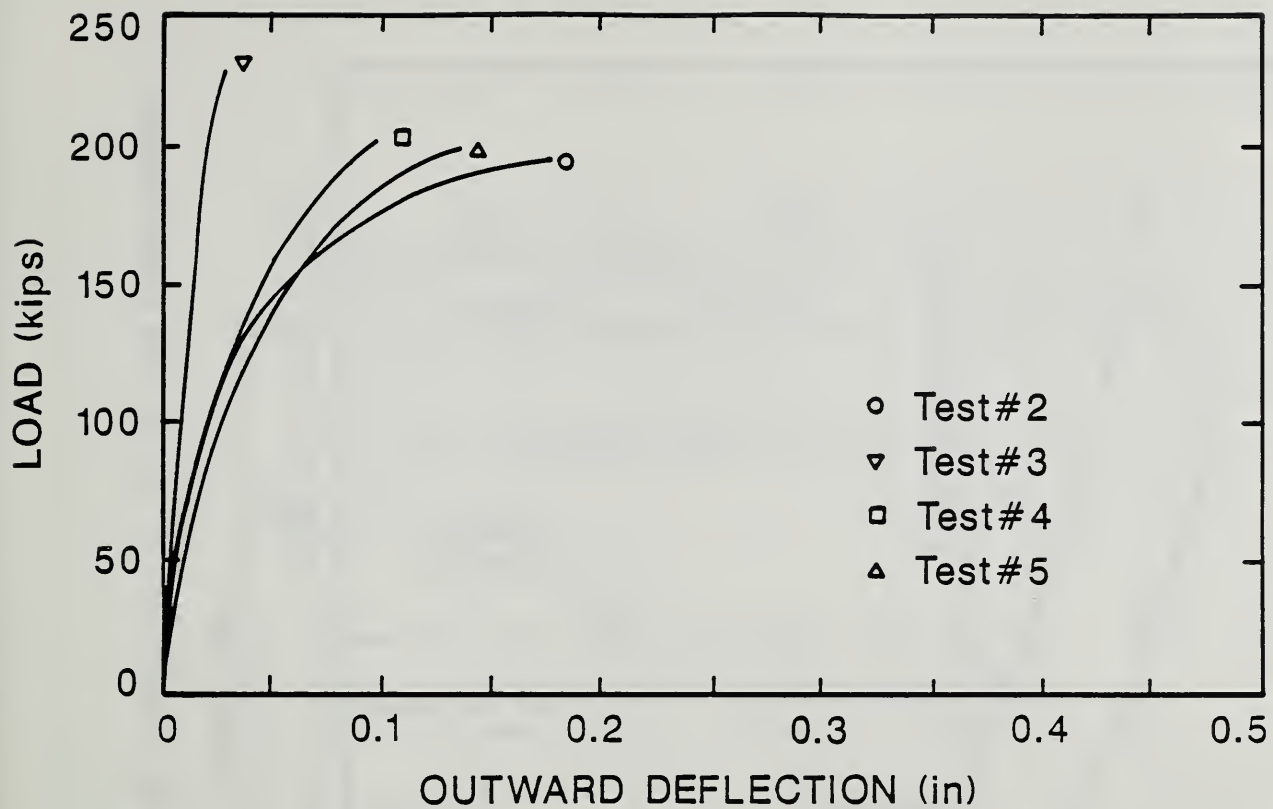
(a) Top flange of channel - failure side



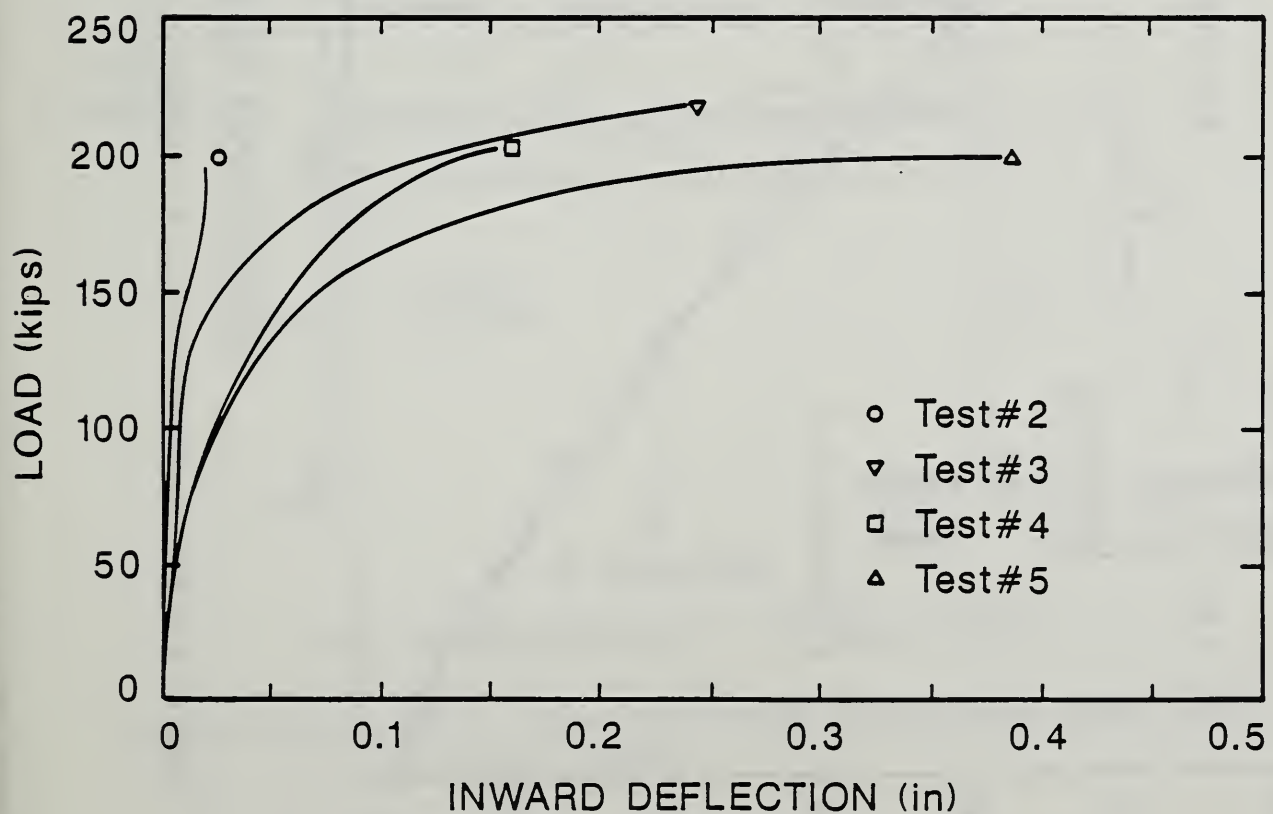
(b) Bottom flange of channel - failure side

Figure 5.5.18 Lateral deformation of shearhead - failure side



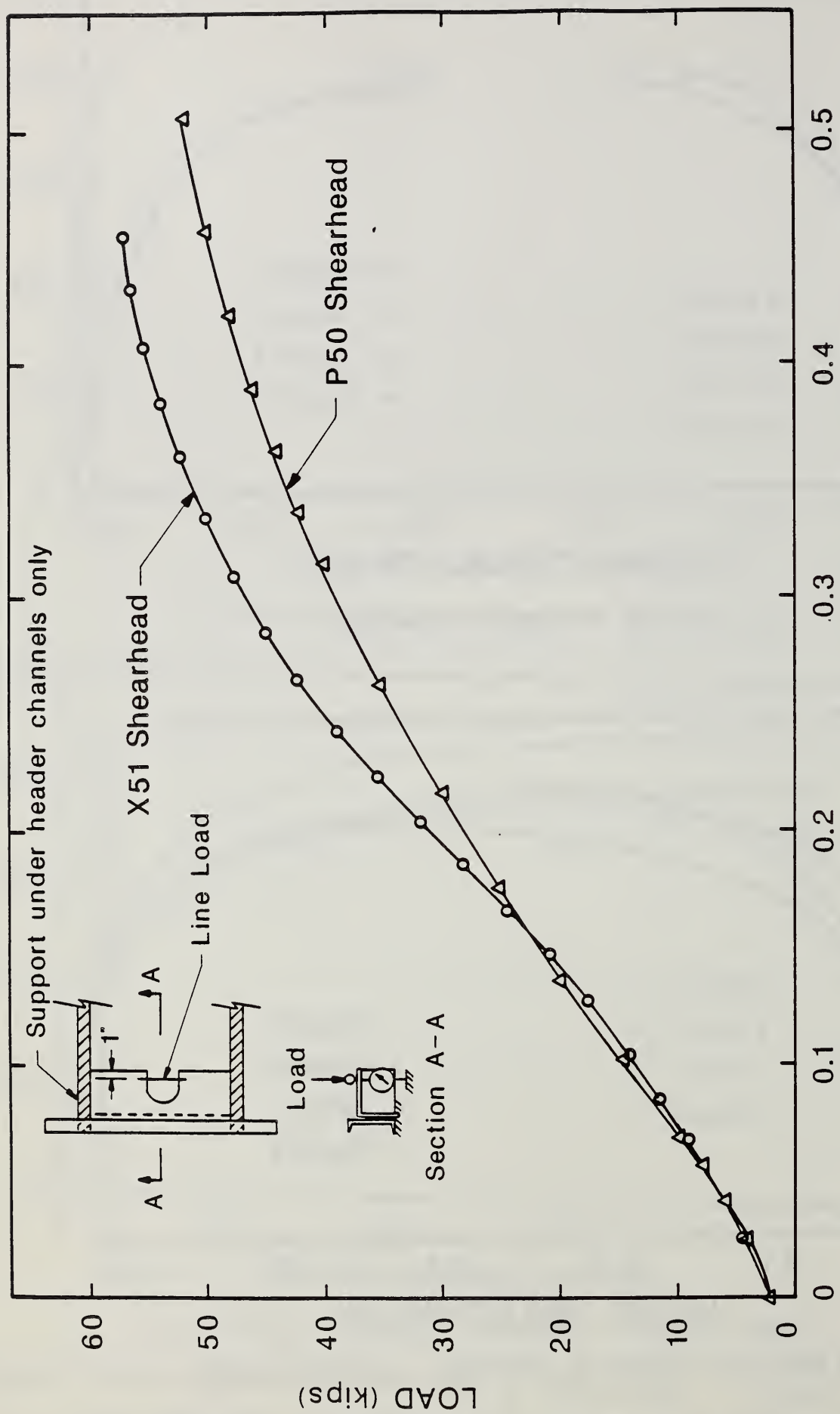


(a) Top flange of channel



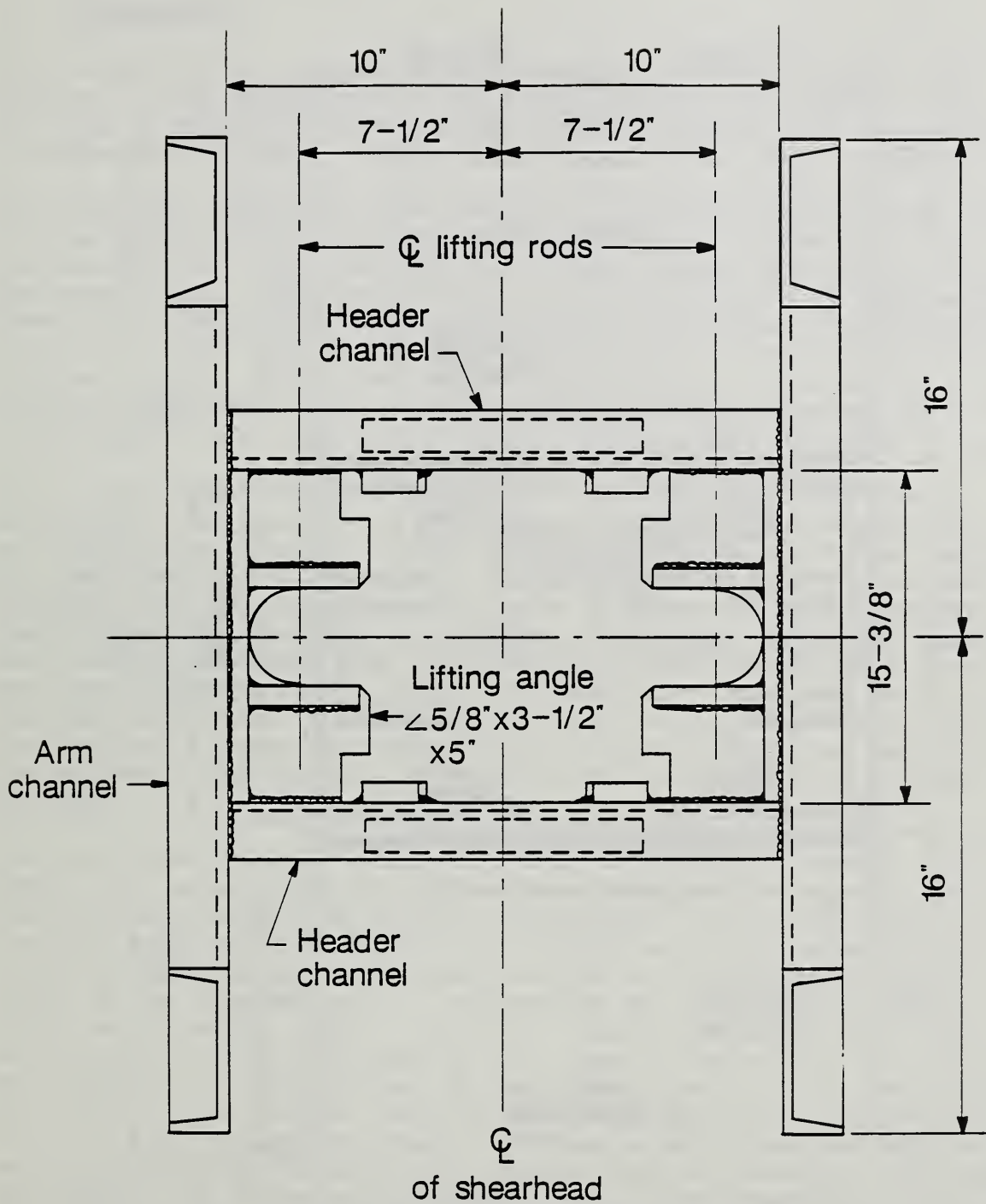
(b) Bottom flange of channel - unfailed side

Figure 5.5.19 Lateral deformation of shearhead - unfailed side



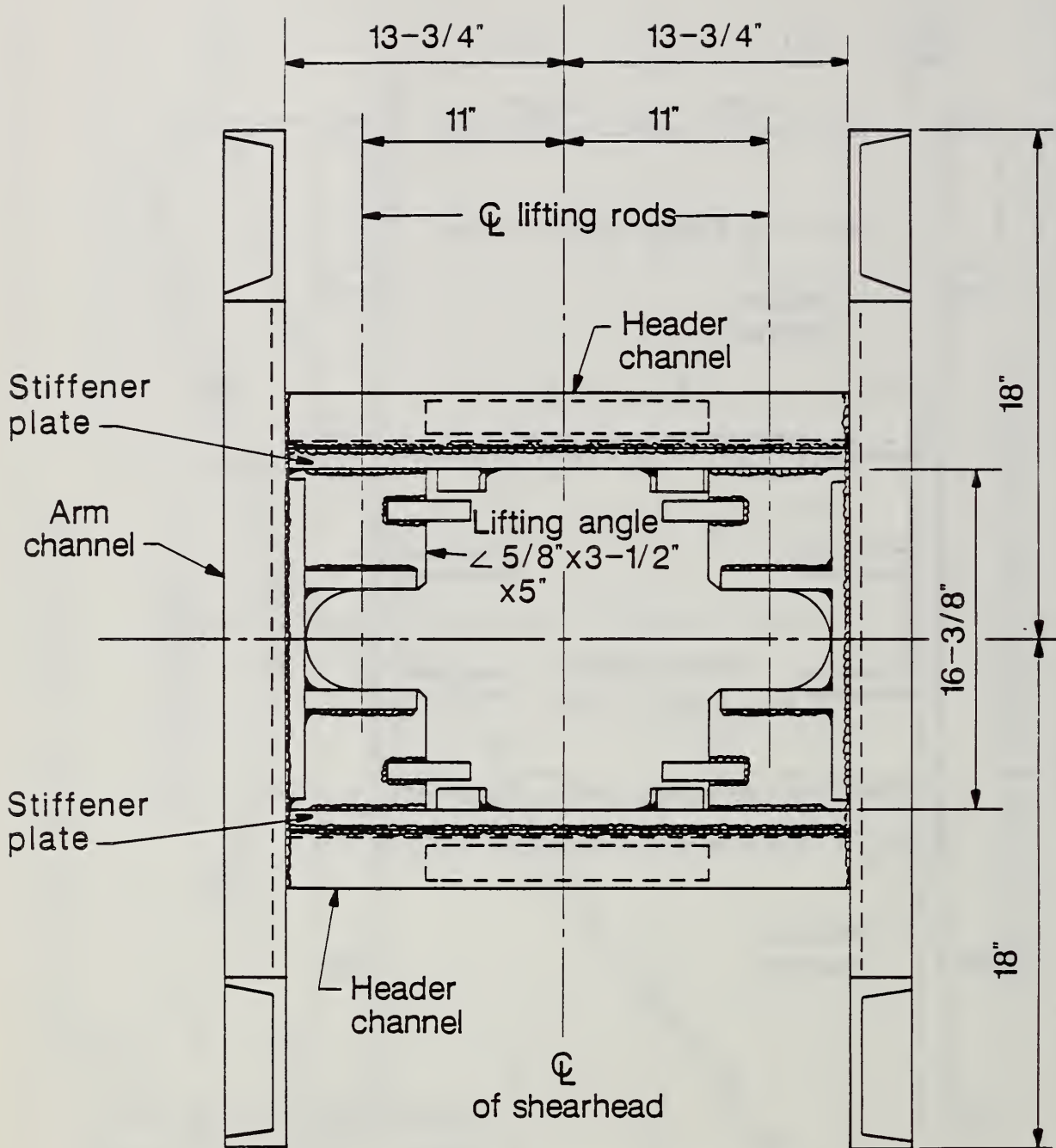
DEFLECTION UNDER LINE LOAD (in)

Figure 5.5.20 Applied load vs. deflection of lifting angle for X-51, P-50 shearheads



P50 SHEARHEAD – PLAN VIEW

Figure 5.5.21 Plan view of typical shearhead used with smaller jacks



X51 SHEARHEAD - PLAN VIEW

Figure 5.5.22 Plan view of shearhead used with super jacks

## 6. SUBSURFACE EXPLORATION

### 6.1 INTRODUCTION

The purpose of the subsurface investigation reported in this chapter was to explore in situ conditions of the footing support and basement wall backfill in order to ascertain whether these conditions could have contributed to the collapse.

The plans for L'Ambiance Plaza specify the following for the tower foundations in the general notes (Drawing S201, Note 2): "All footings shall rest on undisturbed rock. Rock shall have a minimum bearing capacity of 14,000 pounds per square foot." Nineteen reports on the inspection of footing bottoms in the tower area, prepared by a commercial testing laboratory between August 15 and October 1, 1985, contain the following statement: "The material is of broken rock and earth mixed, was placed and compacted with backhoe bucket and vibratory compactor. The basic allowable bearing value for these locations (identified in the report) exceeds the 7 tons job specification."

It is not clear how the commercial testing laboratory reports can be interpreted. The reports indicate that in at least some instances the footings were not placed directly on rock, and that a mixture of broken rock and earth was compacted into place before pouring the concrete. However, neither the thickness, nor the composition or degree of compaction of the material that was placed under the footings is reported. It is also not clear what criteria were used to determine that "the basic allowable bearing value exceeds the 7 tons job specification." Since the possibility that the condition of the footings contributed to the collapse could not be ruled out in advance, and the available information did not clearly indicate what that condition was, it was decided to explore the condition at the base of several randomly selected footings.

Similarly, the general contractor's daily construction reports, starting with Report 211, dated April 8, 1987 and continuing to the date of the collapse, indicate that backfilling behind the basement wall on the north side of the tower was taking place. Figure 6.1.1, which is a reproduction of detail drawing 3/S203 in the plans for L'Ambiance Plaza shows that the lateral earth pressure acting on the basement wall is resisted by the floor slabs at levels D and C, which bear directly against the wall. There was no evidence following the collapse that the keyways shown in the slabs at levels D and C in figure 6.1.1 were present. A field survey of the basement wall of the east tower showed that the wall was cracked, and that the top of the wall displaced as much as 3 in (76.2 mm) toward the tower. Further observations and telltale signs associated with the basement wall rotation and the resulting displacements of the backfill are discussed in Section 4.4.5. It was reasoned that the observed wall displacements resulted from the collapse, which deprived the wall of the support provided by the floor slabs at levels C and D. This in turn was taken as an indication that the slabs on levels C and D and the connected shearwalls were subjected to lateral soil pressures prior to the building collapse. The condition of the backfill behind these walls was therefore explored in order to estimate the magnitude of these pressures and their potential effect on the building during construction.

## 6.2 EXPLORATION PROCEDURES

The locations of the borings and test pits that were used to explore the site are shown in Figure 6.2.1.

The condition below the bottom of the foundations was explored by soil borings, test pits, and in situ tests where feasible. The soil borings were taken through the basement slab (level E), the underlying compacted fill, the footing, the underlying fill or fractured rock and cored into the underlying bedrock formation. In the borings, a HW [4-in (102 mm) I.D.] casing was advanced to within 1 to 2 in (25 to 51 mm) above the bottom of the footing (cutting through the reinforcement). The concrete within the casing was then removed by a 3-in (76 mm) diameter roller bit, and samples of the fill material were taken with a 1 3/8-in (35 mm) I.D. split spoon sampler. The roller bit removed the concrete to the bottom of the footing, and standard penetration testing (SPT) was commenced within 1.5 to 2 minutes, advancing the borehole by continuous sampling through any loose material. The SPT was performed in accordance with ASTM D 1586 "Standard Method for Penetration Test and Split Barrel Sampling of Soils," using a CME 55, 1986 model rig with a 140 lb (63.5 kg) trip hammer dropped from a 30 in (762 mm) fall height. A split spoon sampler [2 in (51 mm) O.D., 1 3/8 in (35 mm) I.D.] without a plastic liner was used. This procedure was designed to minimize the effect of water penetration on the SPT blow count obtained when loose material at the bottom of the footing was penetrated (water had to be circulated during the concrete coring and it was suspected that this water could affect the blow count). Soil samples were saved for visual examination and laboratory classification tests.

NX double tube core barrels were used to take 3 in (76 mm) diameter cores through decomposed or overblasted rock and 3 to 5 ft (0.9 to 1.5 m) into what was judged to be undisturbed rock. The rock cores were saved, and core recovery as well as rock quality designation (RQD) (16) was determined.

The test pits next to the footings were dug by a backhoe along the side of the footing. Excavation continued to a point where no more loose material could be removed. The pits were then pumped out if groundwater accumulated and the condition below the footing was carefully examined. The pits were at least 2 ft (0.6 m) wide at the bottom.

A pressuremeter test was performed under footing F10 using a Rocctest Model G-AM<sup>1</sup> pressuremeter. The specifications for, and interpretation of, the pressuremeter tests are presented in Appendix B.

The conditions of the backfill behind the basement walls were explored by two borings to the north of the wall, one test pit, in situ density tests and direct shear tests in the laboratory.

---

<sup>1</sup> Specification of commercial equipment or products does not imply recommendation or endorsement by the National Bureau of Standards

The borings (B1 and B2) were advanced using a 3 1/4 in (83 mm) I.D. hollow stem auger and SPT sampling. A plug was used during the auger advance to prevent penetration of loose material into the core of the auger. The procedure for SPT testing was the same as that used below the bottom of the footings, except that sampling was performed at 2-ft (0.6 m) intervals.

Two in situ density tests were performed in the test pit at location B2 using the sand cone method (ASTM D 1556 "Standard Test Method for Density of Soils in Place by the Sand Cone Method"), and one pressuremeter test was performed in boring B2.

Laboratory soil classification included visual-manual classification of the samples retrieved and laboratory soil classification in accordance with ASTM D 2487 "Standard Test Method for Classification of Soils for Engineering Purposes" (unified soil classification).

Direct shear tests were performed on samples retrieved from the pit at B2 which were re-constituted to the in situ density. The tests were performed in accordance with ASTM D 3080 "Direct Shear Test of Soils Under Consolidated Drained Conditions."

### 6.3 EXPLORATION RESULTS

The results of the soil exploration are presented in detail in Appendix B and summarized and interpreted in this section.

#### 1. Footings

In the following discussion settlements are estimated in accordance with references 17 and 18, which utilize empirical data that were developed for soil and rock deposits similar to those encountered on the site. The following findings and estimates are derived from the available subsurface exploration data:

- (1) The rock cores taken below the footings indicate that, except in the case of footing D10, the rock underlying the footings was competent to safely support the 7 ton/ft<sup>2</sup> (670 kPa) design pressure. In the case of footing D10, the poor RQD recorded is attributed to the coring procedure (a single tube core barrel) rather than the rock quality. Estimated total and differential settlements of the footings due to bedrock compression during construction were probably very small (17), and therefore could not have contributed to the collapse.
- (2) In all borings a layer of disintegrated rock, approximately 1 ft (0.3 m) thick, was encountered on top of the rock that was cored. It was difficult to confirm the presence of this layer by visual examination of the pits which were on the perimeter of the footings, but it is assumed it was present. Using an estimated compression modulus ranging from 250 ton/ft<sup>2</sup> to 1000 ton/ft<sup>2</sup> (24-96 MPa) (18) footing settlements during construction, attributable to a 1 ft (0.3 m) thick layer of disintegrated rock under a 10x10 ft (3x3 m) footing subjected to a 4.5 ton/ft<sup>2</sup> (431 kPa) load would have ranged from 0.02 to 0.1 in (0.5 to 2.5 mm). The condition described corresponds to that at

footing E4.8, which was the most heavily loaded during construction. Some of these settlements could have shown up as differential settlements if one footing rested on disintegrated rock, and the adjacent footing on solid rock.

- (3) In Boring B-3E there was a 1-ft + (305 mm) thick layer of fill, followed by a 11.5 in (292 mm) thick layer of disintegrated rock. Using an estimated compression modulus of 70 ton/ft<sup>2</sup> (6.7 MPa), derived from the SPT blow count (18, 19), the resulting settlement under construction loads is estimated to have been on the order of 0.3 in (8 mm). This settlement could have shown up as a differential settlement with respect to adjacent footings. Similarly, Footing F10, where the compression modulus of the fill is estimated to be on the order of 80 ton/ft<sup>2</sup> (7.7 MPa), based on SPT and pressuremeter tests (Appendix B and 19), could have settled an average of 0.35 in (9 mm) and rotated 1/300 th of a radian (causing a differential settlement of 1/300 th of its width) as a result of the backfill which varied in thickness.

In summary, it is estimated that differential settlements not exceeding 3/8 in (10 mm) could have occurred between some footings after the full construction load was applied. However, in most instances, the differential settlements between footings were probably on the order of 0.1 in (3 mm) or less. Footing F10 probably rotated, as well as settled under the applied load.

When creep criteria from reference (18) and a two months time span between the fixing of the first slab in its permanent position and the collapse are assumed, it is estimated that about 95 percent of the settlement occurred before the first slab was fixed in its permanent position and the remaining 5 percent were creep settlements which gradually increased until the time of the collapse.

Residual footing settlements after the debris was removed from the site are difficult to determine from available data which are confined to single points. The only reference point encountered was the top of the footings which probably originally deviated from their specified elevation by more than the anticipated residual settlements. The data indicate that residual differential settlements are small and do not exceed 1/2 in (13 mm) between adjacent footings.

## 2. Basement Wall

The backfill behind the basement wall was explored by two borings with SPT samples, one test pit, a pressuremeter test, two in-place density tests, several density tests taken from two tube samples and three laboratory direct shear tests, one considered drained and one undrained. The material consisted of silty sand fill with rock fragments and some construction debris and was classified as silty sand (SM). The material in boring B-1 had a natural moisture content of 9.4 percent and 17 percent of fines (passing No. 200 sieve). The material in boring B-2 had a natural moisture content of 10.7 percent and 25.6 percent of fines. The in-place dry densities of the two sand



cone test samples taken were 90 lb/ft<sup>3</sup> (1.44 ton/m<sup>3</sup>) and 110 lb/ft<sup>3</sup> (1.76 ton/m<sup>3</sup>), and their moisture contents 24 percent and 9 percent, respectively. Dry densities determined from two "undisturbed" tube samples varied from 84 to 102 lb/ft<sup>3</sup> (1.35 to 1.63 ton/m<sup>3</sup>) and corresponded to 70 to 80 percent of maximum dry density per ASTM D 1557 "Test Method for Moisture-Density Relations of Soils and Soil-Aggregate Mixtures Using 10-lb Rammer and 18-in Drop." No ground water was encountered. Angles of internal friction determined by direct shear tests of samples re-constituted to the densities of 90 and 110 lb/ft<sup>3</sup> were of the order of 37 degrees. These results seem high when compared with the low blow counts and densities in borings B-1 and B-2 (20, 21) and probably resulted from particle interlocking associated with this constant volume test. At small shear displacements (0.2 in (5 mm) or less), the shear stress obtained corresponded to an angle of internal friction of 33 degrees or less. On the basis of all the available data, including interpretation of blow counts using references [20, 21] it is estimated that, on the average, representative values for lateral soil pressures should be based on a moist unit weight of 110 lb/ft<sup>3</sup> (1.76 ton/m<sup>3</sup>) and an angle of internal friction between 28 and 30 degrees. Since there was no significant precipitation between April 19 and April 23, it is assumed that no hydrostatic pressures acted on the basement wall.

Differential foundation settlements and lateral soil pressure on the basement wall based on the subsurface exploration data will be presented in Chapter 7.

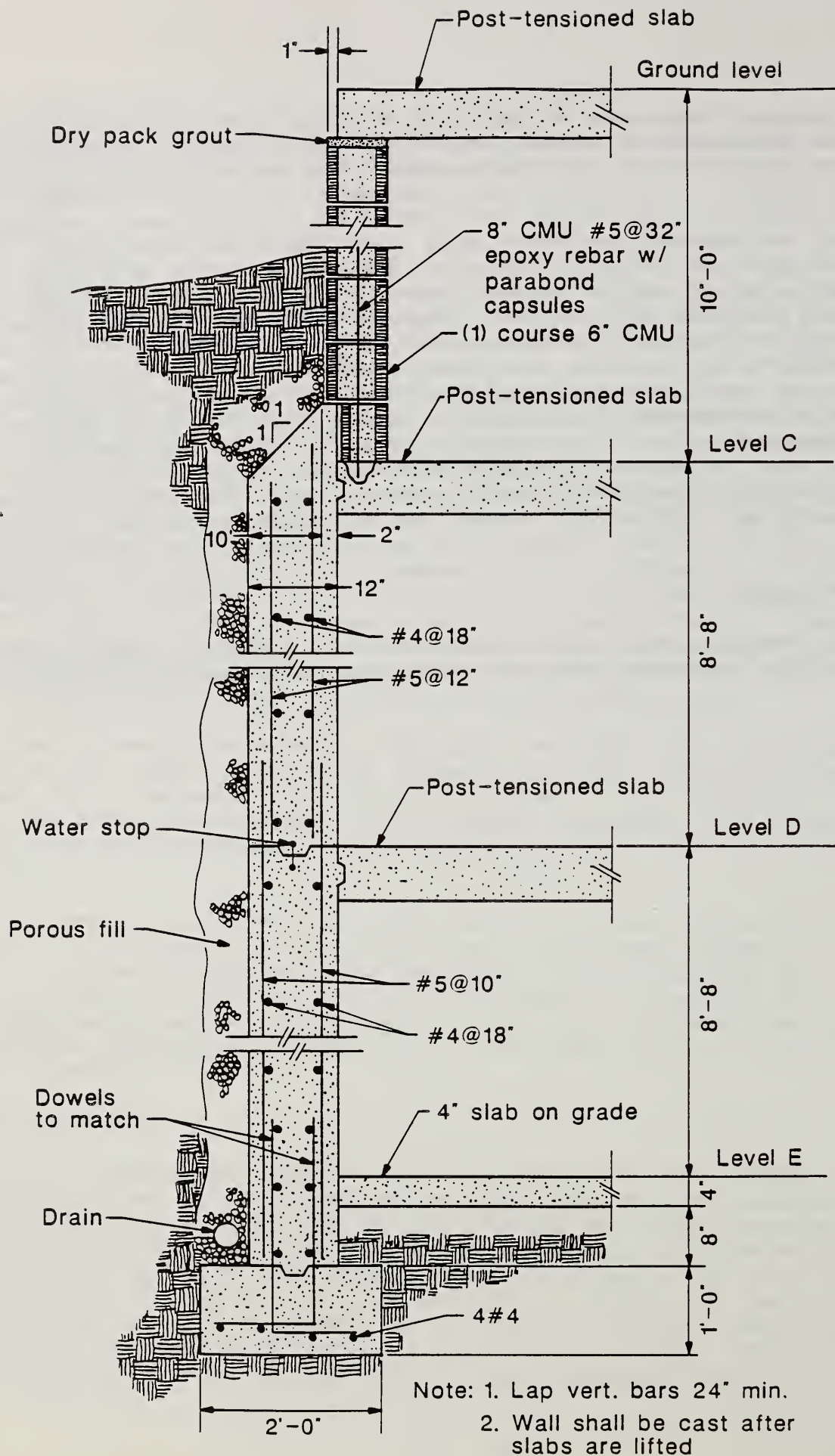


Figure 6.1.1 Typical cross section of basement wall – North side

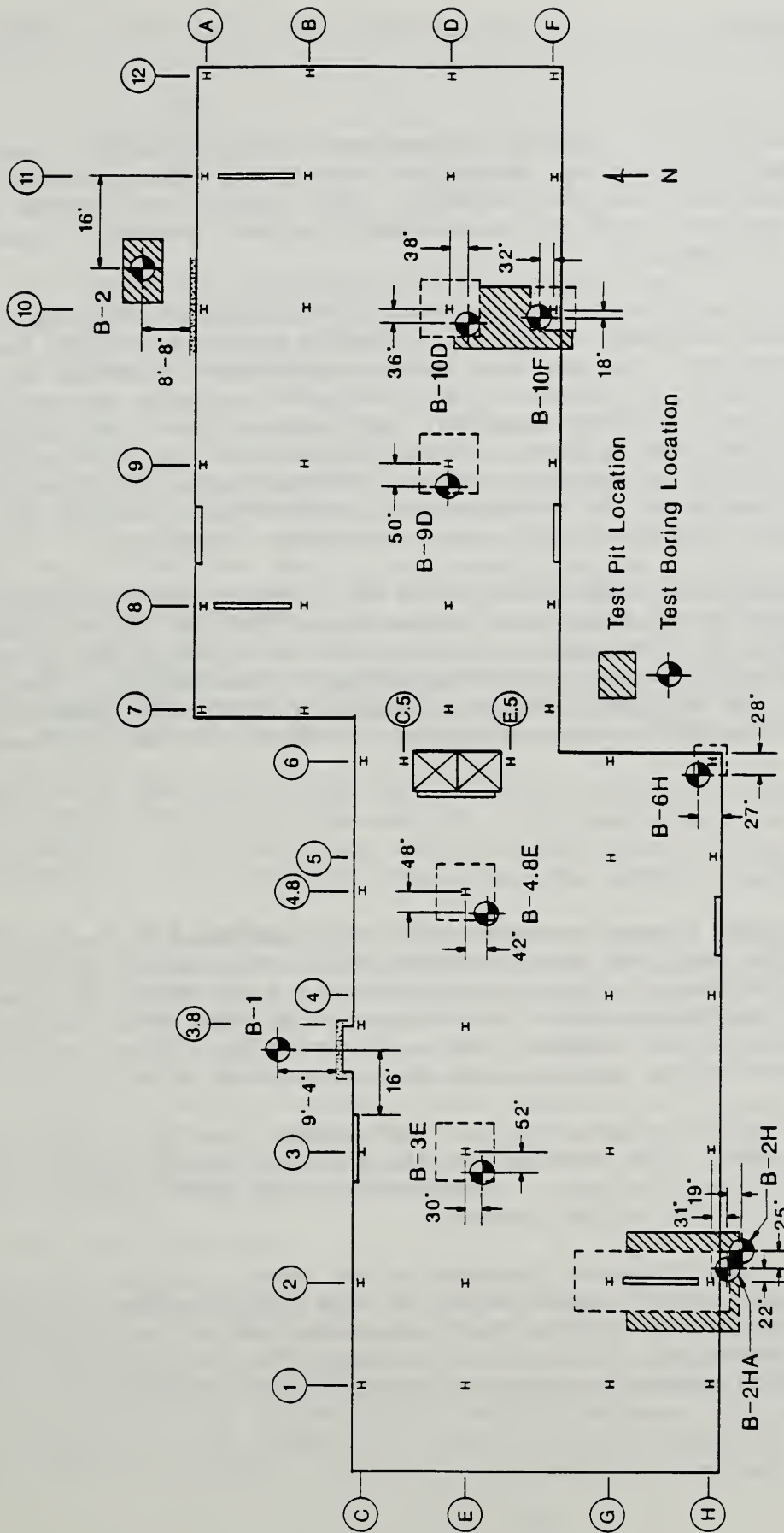


Figure 6.2.1 Location of soil borings and test pits for subsurface exploration

## 7. STRUCTURAL ANALYSIS

### 7.1 INTRODUCTION

The structure was analyzed for loadings encountered during erection. Loadings induced by a number of possible conditions that could have precipitated collapse of the structure were also studied. This latter case served as a sensitivity study and was used in determining the most probable cause of collapse discussed in Chapter 9.

Two types of analysis were performed. The first considered only the floor slabs. The floor slab was modeled with plate bending elements with the columns treated as pinned supports. Deformations and stresses in the slab and support reactions were calculated. The second type of analysis considered the structural frame. A two-dimensional nonlinear analysis was performed for the structural framing system. Internal member forces and deformations of the structure were calculated in the elastic and inelastic range. The resistance of the structure to lateral earth pressure on the basement wall at the lower levels and the effect of differential foundation settlements were also considered.

Results of the analyses and comparisons with the strength of the structural components determined using resistance values specified in current design standards are included in this chapter. Resistance values which are compared with estimated construction loads are not multiplied by the capacity reduction factors specified in the applicable design standards. Evaluation of these results to determine the most probable cause of collapse of the structure are presented in Chapter 9.

### 7.2 FLOOR SLABS

#### 7.2.1 Computer Model

A two-dimensional finite element computer model was developed to analyze the floor slabs [9]. The model was based on small deflection theory and linear elastic behavior. Isotropic, homogeneous four-node plate bending elements with six degrees of freedom per node (three translations and three rotations) were used. A total of 768 elements was used to model a slab to ensure accurate representation of the loading conditions and stress distribution.

Openings in the slab at the column locations (shearheads) and pipe chases were not included in the model. The opening for the shearwall along column line 2 between lines G and H was included. Reactions at the lifting points were considered point loads at the column centers.

The effects of post-tensioning were included in the model. Normal stress due to the post-tensioning force in the plane of the slab was calculated. Secondary moments induced by the drape of the post-tensioning cables were evaluated using the procedure developed by Lin [10]. Assuming the drape of the cable could be approximated by parabolic segments, the uniformly distributed line

load normal to the plane of the slab required to produce drupe-induced moments would be:

$$w = \frac{8hF}{L^2}$$

where:

- w = equivalent uniformly distributed line load
- h = total drupe of cable for parabolic segment
- F = force in post-tensioning cable
- L = span of parabolic segment

The location of the post-tensioning tendons in each slab was shown schematically in figure 3.2.3. A line load along the centerline of the columns was used to represent the load for the banded tendons oriented in the east-west direction. This was done for computational convenience. It should be noted that the centroids of the banded tendons do not necessarily coincide with the column centerlines. Any effects due to this simplification would be more significant along exterior column lines. The displacement of the tendons from the column centerline in the vicinity of column E4.8 was modeled. In view of the uniform spacing of the tendons in the north-south direction, the loads for these tendons were treated as uniformly distributed over the entire element. Material properties (unit weight of concrete, elastic modulus) used in the analysis were based on the test results presented in Chapter 5.

The models were generated using the interactive graphics computer facility at the NBS Center for Building Technology. The models were solved using a VAX 11/750 computer. Pre-processing and post-processing of the data were done using PATRAN [11]. The analysis program was the ANSYS stress module.

The majority of the analyses deal with the west tower. Results for the east tower would be similar except for the effects of displacing the post-tensioning tendons around column E4.8 and the variable column spacing around the service core. Several load cases were considered. Support reactions and rotations at each column location and stresses and displacements throughout the slab were determined for the slab subjected to its own dead weight. The influence of loss of support at various columns on the reactions and stresses was determined. Support reactions due to jacking the slab at one location and due to differences in elevations of the slab supports were also determined. Support reactions in the east and west towers were determined.

#### 7.2.2 Results of Analyses

The results of the analysis for a single floor slab in the west tower are shown in figures 7.2.1 through 7.2.4. The loading case considered represents a slab subjected to its own dead weight and simply supported at each column location. The columns and the jack rods are approximately ten times stiffer than the slab and the assumption of simple supports is reasonable. The results obtained for a single slab may be extrapolated to the case where multiple slabs are lifted. Since a bond breaking agent was applied to the

slabs during casting, it is reasonable to assume there is no significant horizontal shear transfer at the interface between slabs when multiple slabs were lifted. In this case, the series of slabs behaves as a laminated plate with each plate bending independently. The stresses and deformations of each slab, therefore, are the same. The support reaction at a column equals the sum of the reactions for the slabs at that column. The column extensions for stages V, VI, and VII were stored on the roof slab. The total weight of the column extensions for the three stages was 81.5 kips (362 kN) or 14 percent of the weight of one floor slab. They were positioned at the various column locations and this total weight was essentially uniformly distributed over the roof slab. Support reactions for the package consisting of the roof and level 12, therefore, can be obtained by multiplying the results for one slab by 2.14.

The support reactions for one slab are shown in figure 7.2.1a. The reactions in the center of the slab (columns E3, E3.8, G3 and G4) are higher than the reactions around the perimeter. Larger jacks or super jacks were used in these locations to lift the slabs. Note, however, that the reactions at columns E2, G2, E4.8 and G5 are about the same magnitude with the reaction at E4.8 being the largest in the west building. If the reactions in figure 7.2.1 are multiplied by three for the case where three slabs are lifted, the loads for columns E3, E3.8, G3 and G4 are well below the 300 kip (1334 kN) capacity of the super jacks at these column locations. For most of the other columns the loads are below the 150 kip (667 kN) capacity of the regular jacks. For column E4.8, however, this three-slab load is equal to the nominal 150 kip (667 kN) capacity of the jack.

The ratio of the load required to cause a punching shear failure of the slab to the support reactions is given in figure 7.2.1b and is denoted as "reserve capacity." The punching shear failure loads were computed according to the ACI values [2] given in Appendix C. These values are given in table 7.2.1; they are a function of the shear area (perimeter of shearhead) and post-tensioning stress at each column. The reserve capacity values range from 4.0 to 23.1. A large reserve capacity is to be expected since the reactions are due only to the dead weight of the slab. When a package of three slabs is lifted, it is possible there may be lack of intimate contact of the slabs at some points. In this case, the shearhead at the bottom of the package could be subjected to the shear force for three slabs. Even for this extreme case, the reserve capacities obtained by dividing the reserve capacities in figure 7.2.1 b by three range from 1.3 to 7.7.

The distribution of normal stress at the top surface of the slab is shown in figure 7.2.2. Compressive stress is denoted as minus, tensile stress as plus. The large dots represent the column locations. Stresses in the longitudinal (east-west direction) are shown in figure 7.2.2a and in the transverse direction (north-south) in figure 7.2.2b. At some locations in this figure and subsequent stress contour plots, e.g., at the shearwall opening, the stress on the free boundary is obviously zero. The stress gradient at these locations is very steep. Because of the size of the finite element mesh and the contouring algorithm used to generate the figures, the gradient, i.e., the reduction to zero stress, is not shown. The compressive stresses are relatively low since the moments induced by the post-tensioning effectively balance the dead load moments. In most areas these stresses are 400 psi (2.76 MPa) or

less. These stresses are well within those allowed by ACI [2] for service load conditions for post-tensioned structures. Localized stresses as high as 800 psi (5.52 MPa) occur in the vicinity of the service core and around column H2 and the adjacent shear wall opening. These higher stresses result from the positioning of the post-tensioning cables (see Figure 3.2.3). In several locations, most notably near columns H2, E5, H4, H5, F8, and F9, either the majority or all of the east-west banded tendons are placed on one side of the column.

The transverse stresses in figure 7.2.2b are similar in magnitude to the longitudinal stresses although the distribution is different.

The distribution of the normal stresses at the bottom surface of the slab is shown in figure 7.2.3. The magnitude of the compressive stresses is similar to that at the top surface. Again the post-tensioning effectively balances the dead load moments. Note that tensile stresses do occur in the vicinity of the service core.

Rotations of the slab about its longitudinal and transverse axes in its plane at each column location are given in figure 7.2.4. Rotations about the longitudinal axis (east-west) are similar in magnitude along all the column lines. An unusual combination of rotations occurs in the northeast corner at column C6. Large rotations occur at H1 and H6. The largest rotations occur at columns C1 and C6 about the transverse axis (north-south). These rotations would likely have a negligible effect on the behavior of the structure.

The computer model was used to investigate the sensitivity of the floor slab to loading conditions associated with loss of support. Such loss of support could be due to a jack rod failure, failure of a shearhead, failure of a weld block or loss of a wedge. Two illustrative examples will be discussed in this section, loss of support at a perimeter column (column C1) and at an interior column (column E4.8).

Stresses and deflections for the case of loss of support at column C1 are shown in figure 7.2.5 and 7.2.6. The deflections are referenced to the "as cast" condition. The normal stresses at the top surface of the slab in figure 7.2.5 are essentially the same as those in figure 7.2.2. The situation was similar for the stresses at the bottom surface. Loss of column C1 apparently has a minor effect on the slab stresses. This is not surprising in view of the small load (6.3 kips - 28 kN) in column C1.

Deflections due to loss of support at column C1 shown in figure 7.2.6 are also small (approximately 0.6 in - 15 mm) at the column.

Stresses and deflections for loss of support at column E4.8 are shown in figures 7.2.7, 7.2.8 and 7.2.9. The stress distribution throughout the slab is affected. There is a significant change in the stresses in the vicinity of column E4.8. This is as expected in view of the large load the column was carrying. Compressive stresses over a large area of the top surface of the slab around the column reach 800 psi (5.52 MPa). Tensile stresses at the bottom surface in this vicinity reach 1000 psi (6.90 MPa). These tensile stresses exceed the tensile strength of the concrete ( $7.5 \sqrt{f'_c}$  reference 2).

Deflections due to the loss of support at column E4.8 are shown in figure 7.2.9. The deflection at the column location is 1.8 in (46 mm). Deflections in excess of 1 in (25 mm) occur over a large area.

Loss of support at column E4.8 causes a redistribution of forces to the other supports. The magnitude of this redistribution is shown in figure 7.2.10. The support reactions due to a package of three slabs with all supports in place are given in figure 7.2.10a. Reactions due to loss of support at column E4.8 are given in figure 7.2.10b. Note the considerable increase in reactions at the surrounding columns, C4.8, E3.8, G5 and E.5. With the loss of column E4.8, column E3.8 becomes the most heavily loaded column, experiencing a forty-eight percent increase in load.

The influence on the support reactions of jacking the slab at one column location was also studied. This loading condition corresponds to the situation encountered during the placement of the wedges at a column. In this case the slab is raised to its approximate final position (for parking or permanent placement) by operating all the jacks. The wedges are then positioned at each column by raising or lowering the slab at that column as necessary. The amount of the displacement required at each column varies. To evaluate the magnitude of this effect on the support reactions, localized jacking of the slab at column E4.8 was considered. Results are shown in figure 7.2.11. Support reactions for a three slab package are given in figure 7.2.11a. The reactions due to raising the slab 1/2 in (12.7 mm) are given in figure 7.2.11b. One-half in (12.7 mm) corresponds to one full stroke of the jack. The load on the jack at column E4.8 must be increased from 151.8 kips (675 kN) to 201.1 kips (894 kN), an increase of thirty-three percent. Reactions at the surrounding jacks change, in general, to a lesser degree. A forty-four percent decrease occurs in the reaction at column C.5. Roughness of the surface of the slabs could cause some interaction between the slabs. In this case the force required to raise the slabs at one point would be greater than the value given.

The preceding results are based on the assumption that the supports are all at the same elevation; i.e., the slab is level. During lifting, the slab will not remain perfectly level since the jacks are not perfectly synchronized. There will be some differences in elevation between the various support points prior to placing the slab at its final position on the columns. The lifting specifications permit a tolerance of 1/2 in (12.7 mm) difference in elevation between adjacent supports. This will affect the reactions on the jacks. Results for two conditions are presented in figure 7.2.12 to illustrate this effect.

Figure 7.2.12a gives the reactions on the jacks for a package of three slabs in which the support at location E3.8 is 1/2 in (12.7 mm) high. This could have occurred since there was a super jack on this column and it would have reached its upper limit earlier than the small jacks. Figure 7.2.12b gives the reactions for the case in which the support at location C4.8 is low by 1/2 in (12.7 mm). This could have occurred if there were any binding between the column and slab during lifting. Comparing the results in figure 7.2.12 with those in figure 7.2.11a illustrates the influence of difference in elevation at the supports. The effects are somewhat localized. The magnitude of the



effect is a function of the load in the jack at the point at which the slab is high or low. A 1/2 in (12.7 mm) increase in elevation at E3.8 affects primarily the reactions at E3.8, C3.8, and E4.8. The reaction at E4.8, for example, is reduced by 13 percent. Similarly, if the slab is low by 1/2 in (12.7 mm) at C4.8 the reactions at C3.8, C4.8, C6 and E4.8 are primarily affected. An increase of 12.5 percent in the reaction at E4.8 occurs in this case.

It is of interest to compare the support reactions or loads on the lifting jacks in the east and west towers. A comparison for the case of a single slab is given in figure 7.2.13. Support reactions for the west tower are given in figure 7.2.13a and for the east tower in figure 7.2.13b. Note that the east tower slab has a different configuration than the west tower slab and is slightly heavier (622 kips vs. 601 kips, 2767 kN vs. 2673 kN). For the east tower, the largest reactions occur at columns B9, B10, D9, and D10. These were the locations of the super jacks.

### 7.3 COLUMN INSTABILITY

Instability of the columns in stage IV of the west tower was investigated to determine whether this mode of failure could have caused collapse of the building. Critical loads were calculated for each column in accordance with the AISC LRFD procedure [8]. The unbraced length of each column was assumed to be 30 ft-5 in (9.3 m). Referring to figure 4.2.1, this corresponds to the length of column from level 3 to the top of stage IV, or the location of the jacks. Level 3 was selected as one end since the wedges had been welded in place at this level. Level 12 rather than the top of stage IV could have been selected as the other end since wedges had been tack welded at this level. Using the top of stage IV as one end point for the effective column length increased the unbraced length slightly and provided conservative results. The slabs at level 3 up to and including the roof were assumed to offer no lateral restraint in view of the clearance between the columns and the shearheads at the floor levels. Pinned end conditions were assumed. Rotational restraint provided by the column below level 3 was neglected and an effective length factor of  $K = 1$  was used.

Results of the analysis are given in table 7.3.1. Critical loads according to LRFD are listed in the fourth column of the table. A value of 1.0 was used for the reduction factor for compression in calculating these loads. The calculated critical loads therefore represent upper bounds. The reserve capacity or the ratio of the calculated critical loads to the loads on the columns due to the weight of the roof slab and levels 12 through 9 is also given for each column. This reserve capacity ranges from 2.15 for column E4.8 to 7.77 for column C.5. Clearly, the columns in this case have considerable reserve capacity and stability of individual columns was not a problem.

During the initial stages of collapse of the building, it is possible the intermediate floor slabs could have collapsed while the upper level slabs remained temporarily in place. In this case the unbraced lengths of the columns would have increased considerably and column buckling could have occurred after the initial failure but during collapse of the building. The unbraced lengths required for this to occur were calculated for two conditions: condition 1 with the roof and levels 12 through 9 in place, and condition 2 with

only the roof and level 12 in place. These unbraced lengths are also given in table 7.3.1. Note the values are quite large, in some cases exceeding the total length of the column. Buckling could have occurred in those cases where the critical length is less than 79 ft 1 in (24 m), the distance between level E and level 9 in figure 4.2.1. This was possible for many of the columns under condition 1 in table 7.3.1. This will be discussed further in Chapter 9 in considering the sequence of the collapse.

The possibility of frame instability or sidesway buckling will be considered in Section 7.4.

## 7.4 LATERAL LOAD ANALYSIS

### 7.4.1 Introduction

Three cases of lateral loading were considered in this investigation. The first case involved loads applied by a hydraulic jack placed between the west and east towers at the upper levels in order to plumb the building. The second involved lateral soil pressure on the basement wall on the north side of the building at levels D and C. The third involved wind loads. Frame stability or sidesway buckling was also analyzed. These are considered in this section.

### 7.4.2 Frame Stability

The possibility of sidesway buckling of the west tower is considered in this section. It is necessary to check this mode of failure since there was no evidence that the west tower, at the time of collapse, had effective lateral bracing above the shear wall at level 2 as indicated in figure 4.2.1.

To check the capacity of the partially complete structure against sidesway buckling, several analyses were conducted. First, inelastic stability in the east-west direction was determined by a two-dimensional, linear, inelastic analysis of each column line. A schematic of column line C of the west tower and diagram of the model used for the stability analyses are shown in figure 7.4.1. The steel columns in the structure were modeled as line elements, 83 ft 6 in (26.4 m) in length (measured from level E to the top of stage IV) and were fixed at the base (level E). The shear wall was assumed to provide restraint against lateral movement. The columns were, therefore, restrained against lateral displacement at level D through level 2 (top of shear wall). The concrete slabs were assumed to be infinitely rigid in their plane and the attachment between the floor slabs and columns was assumed to be incapable of transmitting a moment. Consequently, the floor slabs were modeled as rigid links pinned at the columns.

Geometric properties of the steel sections were obtained from the AISC Manual of Steel Construction [7]. Material properties used in the computer model for the 36 ksi and 50 ksi steel were based on the test results reported in Section 5.3.

The loads on the west tower at the time of collapse were the gravity loads of the slabs supported by the columns. The magnitude of these loads was determined from the linear analysis of a single slab supported at each column at the same

elevation and loaded with self weight. The column reactions found from this analysis are shown in figure 7.2.1.

At the time of collapse, wedges were being placed beneath slabs 9/10/11. At those columns where the wedges had not yet been installed, the slabs were supported by the jacks and the slab loads, therefore, were applied at the top of the column. For the purpose of this analysis, this was neglected and the loads were assumed to be applied through the wedges in all cases.

The computer program used for this study [12] is capable of analyzing elasto-plastic steel frames subjected to non-proportional static loads. It uses an incremental, nonlinear analysis procedure and includes post-collapse behavior. Both large displacement and member stability effects are included. The beam-column element consists of an elastic component and an elastic-perfectly plastic component in parallel. The element may yield through the formation of localized plastic hinges. The member yield criterion is defined by a two-dimensional yield surface which accounts for the interaction between axial force and bending moment. The effects of strain hardening may be accounted for in an approximate way by assigning a non-zero elastic component. Geometrical nonlinearities are accounted for by including the frame member geometric stiffness matrix and formulating the equilibrium equations on the basis of the displaced structure.

Results of the inelastic stability analysis for each column line are given in table 7.4.1. The results are reported as the ratio of column line capacity to total load on the column line. A value less than 1.0 indicates that the column line by itself is not capable of carrying the gravity load of the slabs. Similarly, a value greater than 1.0 indicates that the column line can not only carry its share of the slab loads, but that it has some reserve capacity for bracing the other column lines.

Since the floor slabs are effectively rigid in their plane, no single column line can fail in a sidesway mode without all column lines failing in this manner. Consequently, one needs to consider the capacity of the entire west tower (all four column lines). The capacity of the building may be determined from the individual column line capacities by noting that the building will not fail until the sum of the capacities is exceeded by the total applied load. The capacity of an individual column line is determined by multiplying the load on the column line by the ratio reported in the first column of table 7.4.1. The column line loads and the resulting capacities are given in the second and third columns of table 7.4.2, respectively. The sum of the four column line capacities is computed to be 10265 kips (45659 kN) while the sum of the loads on all column lines is 9621 kips (42794 kN). The ratio of capacity-to-load is, then,  $10265/9621 = 1.07$  which can be interpreted as a seven percent reserve capacity against inelastic sidesway buckling.

From the above analyses it was found that inelastic behavior (yielding of the steel columns) did not occur until the elastic buckling capacity was just about reached. This was determined by observing the load vs. top of frame displacement curves and noting that the slope was almost flat at the time of first yielding. This means that, for practical purposes, an elastic stability analysis for sidesway is adequate. The four column lines were analyzed again ignoring inelastic behavior. The results of these analyses are presented in table 7.4.2. It can be seen that the capacities obtained are only slightly greater than those found from an inelastic analysis. Using the procedure described above for determining the stability of the entire building, one obtains a capacity-to-load ratio of 1.08, or an eight percent reserve capacity against elastic sidesway buckling.

Since an elastic stability analysis was shown to give good results for this structure and loading, a single column model was used for determining the sidesway buckling capacity in the north-south direction. The geometry was the same as that used for the column line analyses except that there was only a single column. The moments of inertia and cross sectional areas were computed by summing the contributions from all columns at each level. Similarly, the gravity loads were found by adding all the loads at a given elevation. An elastic stability analysis in the east-west direction was first performed using this model to compare with the calculations made above. The results indicated a capacity-to-load ratio of 1.08 which agrees with the results considering the four column lines individually. Next, an analysis in the north-south direction was conducted and a capacity-to-load ratio of 1.16 was obtained. From these analyses, it can be concluded that the west tower is more susceptible to sidesway buckling in the east-west direction than in the north-south direction.

Whether the computed reserve capacity is eight percent or even 16 percent, such a low value is cause for concern. The assumptions under which the stability analyses were performed should be challenged. First, the slab-to-column connections where the wedges and seal blocks were fully welded and the cavities around the columns filled (level D through level 1) provide a rotational restraint which was ignored in the above analysis. Omitting this restraint should not affect the results significantly since very little rotation of the columns occurs below level 2. However, it would tend to increase the stiffness of the structure and thereby increase the lateral buckling capacity. To verify this, the model was laterally restrained at level 2 and completely restrained at level 1 to simulate the condition of infinite slab rigidity below level 2. Results indicated a capacity-to-load ratio of 1.10, only slightly greater than the value of 1.08 obtained assuming the slabs do not provide any rotational restraint.

Next, the assumption of full lateral restraint at level 2, the top of the freshly cast shear wall, could be questioned. To test the extreme case, the single column model was analyzed again with no lateral restraint at level 2. Results showed a capacity-to-load ratio of 0.65. This analysis serves to point out that the capacity-to-load ratio of 1.08 should be regarded as an upper bound and that the true capacity for the idealized structure analyzed is somewhat lower than this value.

Construction of the east tower was slightly ahead of the west tower at the time of collapse (see figure 4.2.1). In the east tower, slabs 6/7/8 had been parked at elevation 76 ft 8 in (23.4 m) and slabs 3, 4 and 5 had been lifted to their final positions. Rather than analyze the east tower, the west tower was analyzed for the configuration of slabs in the east tower under the assumption that the behavior of the two towers is essentially the same. For this analysis, no rotational restraint was assumed for any of the slabs, but level 2 was laterally restrained as assumed in previous analyses. Results indicated a capacity-to-load ratio of 0.72. A more severe condition existed in the east tower during lifting of slabs 4 and 5 since the weight of these two slabs would have been supported by the jacks on top of the columns. This case was analyzed also and a capacity-to-load ratio of 0.59 was obtained. It remains, however, that the east tower survived the lift to the configuration shown in figure 4.2.1. There was obviously some stabilizing effect which has not been considered in the analyses so far. A discussion of this effect follows.

In the above analyses, no rotational restraint was assumed for those levels where the seal blocks were not welded nor the cavities around the columns filled. This condition existed from level 2 to the top of Stage IV in the west tower as indicated in figure 4.2.1. While the building remains undeflected, the slab load,  $W$  at each column is shared by the two wedges with each carrying approximately the same load as shown in figure 7.4.2 (a). However, if the building were to sway, the load in those columns oriented with their web in the plane of sway would transfer to one wedge. Because the wedges are separated by a distance approximately equal to the column depth, this shift in load would produce a moment which acts to resist the sway deflection as indicated in figure 7.4.2 (b). When the slab load is completely transferred to one wedge, the slab would lift off the other wedge as shown in figure 7.4.2 (c) and the moment due to the eccentricity of the load would remain constant. The rotational restraint produced by this restoring moment was not considered in the above analyses and is felt to be important.

Prior to lift off, the slab and column rotate together (compatible deformations) and behave as if they are rigidly connected. The slab resists rotation since it is continuous at the column support and has a stiffness,  $k$  greater than zero. After lift off, however, the moment due to the eccentricity of the slab load remains constant with increasing rotation. Thus, the slab offers no rotational restraint, or  $k=0$ . The slab may be considered as providing linear elastic rotational restraint up to the point of lift off and no rotational restraint from that point on. This is analogous to the elastic-plastic behavior depicted in figure 7.4.3. The limiting moment (moment at lift off) is  $M_L = Wx(d+t)/2$  in which  $W$  is the slab load,  $d$  is the column depth, and  $t$  is the thickness of a wedge.

The influence of this rotational restraint on sidesway buckling capacity is illustrated in the following simple example. Consider an axially loaded column of length  $L$  which is fixed at the base as shown in figure 7.4.4. If this column is rotationally unrestrained at the top, the theoretical  $K$ -value is 2. If, on the other hand, the column is fully rotationally restrained at the top, the theoretical  $K$ -value is 1 which increases the buckling capacity to four times that of the unrestrained case. If there is a rotational restraint at the top of the column with a stiffness greater than zero and less than

infinity, then the buckling capacity will be greater than that of the unrestrained case and less than that of the fully rotationally restrained case, i.e.,  $1 \leq K \leq 2$ . However, if sufficient rotation occurs to cause lift off ( $\phi > \phi_L$  in figure 7.4.3), then the rotational spring stiffness becomes zero and the buckling capacity becomes that of the unrestrained column. This means that a load greater than the sidesway buckling load can be carried by a column with such a rotational spring until such time that the rotation is sufficient to cause the spring stiffness to go to zero (lift off) at which time the buckling capacity drops and the column buckles.

To understand the effect of this restraining force on the capacity of the west tower, an analysis was performed using the computer program cited above. A single column model of the entire building was used as shown in figure 7.4.5. The base elevation was chosen to be level 1 where full fixity was assumed and lateral restraint was provided at level 2. The slabs were assumed to be one half the average bay spacing or approximately 10 ft (3.05 m). The effective width of the slabs on either side of a column line was taken to be  $8 \cdot h$  where  $h$  is the slab thickness. The ends of the slabs (centerline of a bay) were not fixed against rotation but were constrained to move vertically with the slab to-column joint to eliminate slab bending due to axial shortening of the column.

It was assumed that 30 slab panels act to resist moment where each panel has an effective width of 56 in (1.42 m). This was determined by noting that the slab resists rotation only at those columns which are oriented with the plane of their web in the east-west direction. Since 45 percent of the slab self weight was carried by columns oriented with their webs in the east-west direction, the lift off moments were computed on that basis. Additionally, the weight of the column sections for stages V through VII, which were stockpiled on the roof, and the weight of the lifting jacks were included.

Results indicated that the sidesway buckling capacity-to-load ratio was increased to 5.6. Therefore, this effect explains the apparent stability of the structure and how slabs in the east tower were lifted into position despite a capacity-to-load ratio of 0.59 computed earlier. The lateral deflection at which instability occurred, however, was computed to be only 0.56 in (14.2 mm). This indicates that the structure was extremely vulnerable to lateral displacements and that a displacement at the top of the structure of only about one half inch was capable of causing lift off and subsequent instability.

#### 7.4.3 Horizontal Jacking Load

A 12 ton (107 kN) hydraulic jack was used on the day of the collapse to plumb the building during erection of the floor slabs in the west tower. The location of this jack is shown in figure 7.4.6. The foreman for the firm responsible for constructing the floor slabs indicated the west tower was plumbed by moving the slabs approximately  $5/8$  in (16 mm) laterally. Representatives from the lifting subcontractor confirmed this in interviews on July 9 and 10, 1987. The magnitude of the load applied was not known. This jack was in-place and under load at the time of the collapse.

To determine the influence of this jacking force, the single column computer model, including the restoring moment and lift off mechanism, was used. Two load cases were applied. First the gravity loads were applied and then a lateral load was applied at the top of the structure to simulate the jacking force. Results showed that a lateral load of 41 kips (182 kN) was required to obtain first lift off which occurred at a lateral displacement of 0.54 in (13.7 mm). All slabs had lifted off under a lateral load of 47 kips with a displacement of 1.54 in (39.1 mm). Since the structure was just barely stable under the boundary conditions of no rotational restraint provided by the slabs, sideways buckling did not occur. The lateral stiffness, however, was found to be 0.76 kips per inch. Since a lateral load of 41 kips (182 kN) is required for lift off and the capacity of the jack was approximately 24 kips (107 kN), it is not likely that the use of this jack to plumb the building initiated the collapse of the west tower.

#### 7.4.4 Earth Pressure

##### Introduction

It is deduced from available evidence that the lateral pressures exerted by the backfill placed behind the basement wall to the north of the building prior to the building collapse were in part resisted by the floor slabs at levels C and D. The evidence includes the observed basement wall deflections after the collapse and the construction logs. The reaction forces acting on the slabs were in turn transmitted by the slabs to the columns and shearwalls, which carried the forces to the foundations. This section presents an estimate of the effect of these forces on the building under construction.

##### Loads

Data on the backfill behind the basement walls are presented in Chapter 6 and Appendix B. It is estimated on the basis of these data that the average unit weight of the backfill at the time of the collapse was approximately 110 lb/ft<sup>3</sup> (1.76 ton/m<sup>3</sup>), that the material was cohesionless, and that the average angle of internal friction was between 28 and 30 degrees. No significant precipitation was recorded during the five-day period preceding the collapse and it is thus assumed that no hydrostatic pressure acted on the wall. Since the slabs restrained the wall from rotating over its base it is assumed that a reasonable upper limit for the soil pressure acting on the wall was the at-rest pressure, which is estimated to have been approximately 55 to 58 times the depth of the backfill, where the depth of the backfill is in ft and the pressure is in psf. Actually, as the backfilling behind the wall proceeded, some wall movement had to occur, somewhat relaxing the pressure against the wall. A lower limit for the backpressure would be the active pressure, which is estimated to be approximately 37 to 40 times the depth of the backfill in psf. The pressure would drop to the active pressure only after a rigid body rotation producing displacement on the order of 1/4 to 1/2 in (6-13 mm) at the top of the wall, which is more than the displacement that is estimated to have occurred during construction. In the following calculation a lateral soil pressure of 50 times the depth of the backfill is used.

Figure 7.4.7 shows the assumed soil pressure diagram together with the calculated reaction forces. It was conservatively assumed that the wall was hinged at the top of the foundation. Even though the dowels to the footing provided moment resistance, the footing itself was narrow. Calculated forces per linear foot of wall are 251 lb (3.66 kN/m) at level C and 5610 lb (25.0 kN) at level D.

### Resistance Mechanism

The lateral forces are resisted by the shearwalls and the columns. If it is assumed that the in-plane stiffness of the slabs is large, an assumption which reasonably represents actual conditions, then the portion of the lateral load acting on each load resisting element will be approximately proportional to its stiffness. The following element stiffnesses were calculated for the west tower in the north-south direction (those for the east tower do not differ significantly):

$$\begin{aligned} \text{N-S shearwalls: } \Sigma \quad I &= 7.593 \times 10^6 \text{ in}^4 \quad (3.16 \text{ m}^4) \\ \Sigma \quad EI &= 2.580 \times 10^{13} \text{ lb-in}^2 \quad (7.404 \times 10^4 \text{ MN-m}^2) \end{aligned}$$

$$\begin{aligned} \text{columns: } \Sigma \quad I &= 1.515 \times 10^4 \text{ in}^4 \quad (6.306 \times 10^9 \text{ mm}^4) \\ \Sigma \quad EI &= 4.395 \times 10^{11} \text{ lb-in}^2 \quad (1.261 \times 10^3 \text{ MN-m}^2) \end{aligned}$$

$$\begin{aligned} \text{E-W shearwalls: } \Sigma \quad I &= 2.070 \times 10^4 \text{ in}^4 \quad (8.616 \times 10^9 \text{ mm}^4) \\ \Sigma \quad EI &= 7.050 \times 10^{10} \text{ lb-in}^2 \quad (2.02 \times 10^2 \text{ MN-m}^2) \end{aligned}$$

where  $I$  = moment of inertia, in the north-south direction,  $E$  = Young's modulus, and  $\Sigma$  stands for the algebraic sum of the quantities indicated for the west tower building.

These stiffnesses show that, unless a shearwall displacement by structural failure, slippage, or tilting occurs, only approximately 2 percent of the load resulting from lateral soil pressures is transferred to the columns and east-west shearwalls, and the remaining 98 percent of the load is resisted by the shearwalls in the north-south direction. A similar situation occurs in the east-west direction, even though the longitudinal shearwalls in that direction are somewhat shorter. Thus it is reasonable to assume that the lateral loads attributable to the soil pressures against the basement walls are resisted by the shearwalls in the north-south direction, and torsional effects are resisted by the shearwalls in the north-south direction and the shearwalls in the east-west direction.

### Resistance to Shear Forces

The following material properties are used in the assessment (the properties were derived from the NBS laboratory test results and the project specifications):

$$\begin{aligned} \text{Concrete cylinder strength (} f'_c \text{):} & \quad 4,570 \text{ psi (31.2 MPa)} \\ \text{Concrete modulus (} E \text{):} & \quad 3,400,000 \text{ psi (23443 MPa)} \\ \text{Re-bar strength (} f_y \text{):} & \quad 60 \text{ ksi (414 MPa)} \end{aligned}$$



If it is conservatively assumed that the shear forces shown in figure 7.4.3 acted on the slabs over the entire 112 ft (34.14 m) length of the building (the resistance provided by the cross wall to the east end of the west tower basement wall is disregarded), then the total shear force acting on the two north-south shear walls between levels D and E was 656 kips (2918 kN). The shear force acted with an eccentricity of 5.2 ft (1.59 m) with respect to the center of rigidity of the building. The resulting torsional moment was resisted by the shearwalls in both directions, inducing a shear force of 27 kips (120 kN) in each wall in the north south direction and a force of 18 kips (80 kN) in each wall in the east-west direction. The resulting shear forces are 355 kips (1579 kN) for wall H-G2 and 301 kips (1339 kN) for wall E.5-C.5 between lines 5 and 6. The forces induced in the shearwalls in the east-west direction had a negligible effect.

The shear capacity of the 13-ft (3.96 m) long and 1-ft (305 mm) wide shearwalls is calculated as follows (2):

$$V_u = V_{uc} + V_{us} = [3.3 (f'_c)^{1/2}hd + A_v f_y d/s] = 499 \text{ kips (2220 kN).}$$

where: h = wall thickness = 12 in (305 mm)

d = effective wall depth =  $0.8 \times 13 \times 12 = 124.8$  in (3.17 m)

$A_v$  = reinforcement area for 2 #4 horizontal reinforcing bars  
=  $0.4 \text{ in}^2$  (258  $\text{mm}^2$ )

s = vertical spacing between horizontal reinforcing bars  
= 18 in (457 mm).

Thus the ultimate shear resistance of the most critical shearwalls is 40 percent greater than a conservative estimate of the horizontal soil pressure.

A failure could also occur between the slab at level D and the shearwalls to which it transmits the lateral load. Details of the slab connection to the shearwall are shown in structural drawings S302, S303 and S304. The slab is connected to the shearwalls by #4 dowels spaced at 12 in (305 mm) on center. In accordance with the plans, the slab surface was roughened to improve frictional resistance. The load capacity of the connection for wall H-G2, where the slab to wall connection is subjected to double shear, is calculated in accordance with reference [2], using the shear-friction method as follows:

$$V_n = A_{vf} f_y = 2(13 \times 0.2 \times 60) = 312 \text{ kips (1388 kN) (with a friction coefficient of 1 for roughened concrete)}$$

where:  $A_{vf}$  is the area of the shear friction reinforcement.

Thus the ties were not quite adequate to transmit the entire shear force of 340 kips (1512 kN) transmitted by the level D slab. However, for a shear failure to occur, the slab bearing against the north side of the shearwall would also have to fail. Assuming that the contact area of the slab with the 12 in (305 mm) wall face was  $84 \text{ in}^2$  and the concrete strength 4,500 psi (31.0 MPa), it would take a force of approximately 320 kips (1423 kN) to crush the slab. It is conceivable that the slab could have deflected excessively or buckled before reaching its crushing strength. Such a failure mode is resisted by the transverse post tensioning. Since the difference between the shear load and the capacity of the ties was only 28 kips (125 kN), this type of failure is

considered unlikely. The reserve capacity against failure of the connection between the slab and shearwall is therefore 1.9  $[(312 + 320)/340]$ .

For wall E.5-C.5 the shear force transmitted by the slab at level D is 287 kips (1277 kN). For this wall which is adjacent to the elevator shaft this force is transmitted in single shear. Thus the load capacity of the connections is  $1/2 \times 312 = 156$  kips (694 kN) and the difference between the capacity of the ties and the shear load is 131 kips (583 kN). The reserve capacity of this latter connection is estimated to be 1.65  $[(156 + 320)/287]$ . Since the shearwall was cast after the slab was in place there was probably a tight fit between the vertical face of the slab and the shearwall. It is therefore unlikely that the simultaneous mobilization of the shear-friction mechanism and the bearing of the slab against the wall resulted in any horizontal displacements.

The question also arises whether sliding or overturning of the shearwalls could have occurred. Sliding resistance at the foundation level is examined for the two north-south shearwalls in the west tower building.

Footing H-G2 rests on a 1 ft thick layer of disintegrated rock underlain by undisturbed bedrock. No soil fill material was found under the footing. The plans do not call for a shear key into the rock, and the test pits indicate that the footing was poured against a form by overexcavating the rock in front of the footing. Thus no lateral resistance is provided by the rock itself, except for the frictional resistance at the bottom of the footing. In addition to this frictional resistance, sliding resistance can be provided by the 4-in (102 mm) thick slab on level E which bears against the shearwall and by the backfill below the slab on level E.

In addition to the shearwall, footing H-G2 supported columns H2 and G2, which in turn supported the dead weight of the lifted slabs. The shear wall itself did not support any dead weight of slabs, because the slab-shearwall connection was poured after the slabs were in place. Because of the shrinkage of the cast in place concrete, the shearwall may even have pulled down on the slabs. However, this effect was probably negligible. Thus the total dead weight is estimated as the two column reactions plus the dead weight of the footing and the shearwall. Assuming that five levels of shearwall were in place, the total weight of the shearwall, the footings, and the two columns is estimated to have been 1270 kips (5649 kN). To resist the 355 kips (1579 kN) lateral force, a friction coefficient of 28 percent is required. The friction coefficient at the base of the footing was controlled by the material under the footing. The borings and test pits indicate that in general there was either fill material or disintegrated rock; however, the field data indicate that this particular footing rested primarily on disintegrated rock. The fill material encountered under footings in the field exploration is estimated to have an angle of shearing resistance between 31 degrees and 34 degrees. The disintegrated rock would have a much larger resistance; however, construction records indicate that the footings were leveled using at least a thin layer of soil. Using the worst case of a 31 degrees angle, the coefficient of friction would be on the order of 60 percent. Thus sliding of this footing was unlikely. The other potential mechanisms providing sliding resistance would require some lateral displacement and therefore were probably not mobilized. The reserve

capacity against failure, relying on sliding resistance alone, was on the order of 2.7 or more.

An analysis for overturning at shearwall footing H-G2 indicates that the resulting force acted within the middle third of the footing. Thus the footing was stable.

Footing E.5-C.5 between lines 5 and 6 was not explored by borings or test pits. It is assumed that conditions were no worse than those encountered at footings resting on soil fill. In addition to its own weight and the weight of the supported shearwall, the footing supported columns C.5 and E.5 on line 6. The total weight of the wall, the footing and the supported columns is estimated to have been 723 kips (3216 kN). To resist the 300 kips (1334 kN) lateral force by friction alone, a friction coefficient of 42 percent is required. It is estimated that the actual friction coefficient between the bottom of the footing and the fractured rock was at least 53 percent. The reserve capacity attributable to frictional resistance alone was therefore at least 1.26 and probably more.

An analysis for overturning indicates that the resulting force acted at a distance of 6.6 ft. (2.0 m) to the south of the centerline of the footing, which is 1.93 ft (0.59 m) outside the middle third of the footing. Thus there was contact pressure over only part of the footing area. However, the footing was stable, even though it could have rotated slightly if there was fill below the footing, causing an increase in lateral deflections. Boring B-4.8E, which is the closest to this wall, shows a foundation resting on disintegrated rock with no fill. If similar conditions prevailed at the shear wall the effect of tilting was negligible.

Thus it is concluded that it is unlikely that the lateral soil pressures acting on the north basement wall caused the shearwalls to fail either by sliding or overturning over their base or by a structural failure of the concrete, or by a failure of the connection between the shearwalls and the lift slabs.

#### Lateral Displacements

Lateral displacements were conservatively calculated assuming that the floor slabs have an infinite in-plane stiffness and no out of plane stiffness. Lateral displacements caused by flexural and shear deformations of the shearwall were calculated to be on the order of 1/8 in (3 mm) or less at level C and 3/100 in (0.08 mm) or less at level D. Rotation due to foundation settlements could have increased these displacements.

#### Conclusion

It is concluded that it is unlikely that shearwall failure or excessive displacements caused by lateral soil pressure against the basement wall to the north of the tower structure contributed to the building collapse.

#### 7.4.5 Wind Loading

The maximum wind loads likely to have been acting on the structure at the time of collapse were calculated using the procedure described in ANSI A58.1 [14] and the wind speed data described in Section 4.3.

From the maximum recorded 10-minute mean speed of 16 knots (8.24 m/s) at the anemometer site, the corresponding hourly mean speed at a height of 10 meters in open terrain (Exposure Category C) was 18.7 mph (8.36 m/s). The corresponding wind direction was approximately 120 degrees. Conversion of this speed to the equivalent fastest-mile speed yields 21.1 mph (9.43 m/s) which is the basic wind speed defined in ANSI A58.1 for the calculation of wind loads.

The terrain surrounding the construction site is considered to be best described as Exposure Category B for which the exposure factor and the gust response factor at the tops of the stage IV columns are 0.79 and 1.34, respectively. Depending on the reference data used, drag coefficients for the floor slabs and columns can range from 1.5 to 2.0. Making a conservative choice of 2.0 for the drag coefficient and assuming that the local variation in wind direction is sufficient to bring the wind normal to the E-W column lines, the computed unit drag load at the top of the structure is 2.4 psf (115 Pa).

If it is assumed that the unused column extensions lying on the roof slab formed a barrier with an effective height of 3 ft (0.91 m) and the three packages of floor slabs in the east building acted aerodynamically as a single obstacle, the effective blockage height for drag load calculations at the top of the building is 9 ft (2.74 m). The corresponding drag load per unit width is  $(9) \cdot (2.4) = 21.6$  lbs/ft (315 N/m). The nominal load on an interior N-S column line due to wind acting on the parked slabs and column extensions is  $(21.6) \cdot (27 + 24.5) / 2 = 556$  lb (2.47 kN). A similar calculation yields 454 lbs (2.02 kN) for the nominal load on an interior E-W column line assuming the wind direction is parallel to the column line.

Because the "project north" does not coincide with the true north, the wind direction at the site could have ranged from 130 to 160 degrees, referenced to "project north." As a result, the above calculations could overestimate the wind loads by 30 percent or more. However, this analysis does not include the drag load contribution of the vertical columns or the permanently positioned floor slabs, nor does it account for the actual terrain features at the site. In Section 7.4.3 the lateral load in the east-west direction required to obtain first lift off from a supporting wedge was shown to be 41 kips (182 kN). Since this is an order of magnitude greater than the combined drag force on the column lines, it is concluded that wind effects did not play any significant role in the collapse.

#### 7.5 DIFFERENTIAL FOUNDATION SETTLEMENTS

As pointed out in Chapter 6, it is estimated from available subsurface data that differential foundation settlements not exceeding 3/8 in (10 mm) could have occurred during construction with approximately 90 percent of these settlements occurring before any slab was fixed in its permanent position. In

the lift-slab method of construction, all the slabs are lifted at the beginning of the process. Once the slabs are lifted, most of the foundation loads are applied and subsequent load increases during construction are much smaller. Another feature of this construction method is that slabs are leveled after they are lifted close to their final position.

In the case of the L'Ambiance Plaza project this means that, to the extent that differential settlements occurred, a major portion of these settlements probably occurred during the initial stages of the project, a considerable time before the collapse. The subsequent leveling of the slabs compensated for these initial differential settlement effects and it was well within the tolerances of the system to compensate for the estimated differential settlements.

Since foundation settlements occurring after slabs are leveled and in a fixed position could result in a downward displacement at column supports, and since the post-tensioned slabs are sensitive to a downward displacement occurring at a location where the post tensioning strands are near the upper surface of the slabs, it is of interest to quantify possible settlements that could have occurred after the slabs were fixed. Such settlements would be the sum of creep settlements and settlements occurring from additional construction load.

The maximum creep settlements are estimated to have been five percent of the maximum  $3/8$  in (10 mm) settlement or 0.02 in (0.5 mm). The maximum construction load, resulting when a package of three slabs is lifted up  $1/2$  in (13 mm) was calculated by a finite element analysis to be on the order of 60 kips (267 kN). Under the worst foundation condition encountered in the subsurface exploration, it is estimated that such an overload could have caused a settlement on the order of 0.025 in (0.64 mm). Thus the maximum settlement after initial lifting of the slab is estimated to have been on the order of 0.05 in (1.3 mm) or less. It is considered unlikely that a settlement of that order of magnitude could have caused a structural failure of a slab.

Another characteristic of the L'Ambiance Plaza footings is that, even though there was evidence of fill in some locations which could have in some cases permitted settlements and footing rotations, the depth of the fill layers and underlying disintegrated rock layers was limited and there was a base of competent bedrock usually 1 ft (305 mm), and probably not more than 3 ft (0.9 m) below the base of the footing. Thus the possibility of major settlements or stability failures is considered unlikely. This point is addressed in more detail in Appendix B.

It is therefore concluded that it is unlikely that the building failure was triggered by differential foundation settlements.

This conclusion is based on available data, which are confined to borings and test pits taken by NBS at several randomly-selected footings, and borings taken by Heynen Engineering prior to the construction. Actual physical data are only available where actual borings were taken and test pits were dug.

TABLE 7.2.1

SHEAR CAPACITY OF FLOOR SLAB

<u>Column Location</u>	<u>Shearhead Type</u>	<u>Shear capacity <math>V_c</math> (Kips)</u>
C1	Mark A50	54.2
C2	Mark C50	106
C3	Mark W50	101
C3.8	Mark G50	116
C4.8	Mark C50	106
C6	Mark J50	53.8
C.5	Mark L50	54.4
E1	Mark B50	106
E2	Mark P50	182
E3	Mark X51	223
E3.8	Mark X51	220
E4.8	Mark P50	202
E.5	Mark U51	54.4
G1	Mark B50	76.7
G2	Mark P50	184
G3	Mark Y51	219
G4	Mark Y51	218
G5	Mark P50	198
G6	Mark C50	77
H1	Mark A50	54.2
H2	Mark D50	112
H3	Mark N50	130
H4	Mark N50	130
H5	Mark D50	130
H6	Mark A50	54.2

TABLE 7.3.1

## COLUMN STABILITY DATA

Column No.	Section (Stage IV)	Axial* Load (kips) (1)	Critical** Load (kips) (2)	Reserve Capacity (2)/(1)	Critical Length (ft)	
					Condition 1	Condition 2
C1	HP 10x42	31.5	135.7	4.3	63.1	99.8
C2	HP 12x53	79.5	236.5	3.0	52.7	83.4
C3	W 12x65	81.5	318.4	3.9	61.0	96.6
C3.8	W 12x65	79.5	318.4	4.0	61.8	97.8
C4.8	HP 12x53	96.5	236.5	2.5	47.9	75.7
C6	W 8x35	11.5	80.0	7.0	80.2	127
C.5	W 12x65	41.0	318.4	7.8	86.6	136
E1	W 10x60	68.5	219.0	3.2	54.4	86.0
E2	W 12x106	213	543.4	2.6	49.7	78.6
E3	W 12x120	223	620.5	2.8	52.0	82.2
E3.8	W 12x120	222	620.5	2.8	52.1	82.4
E4.8	W 12x106	253	543.4	2.2	45.6	72.1
E.5	W 12x72	61.0	355.3	5.8	74.6	118.0
G1	W 10x60	67	219.0	3.3	55.0	87.0
G2	W 12x106	199.5	543.4	2.7	51.4	81.2
G3	W 12x136	242	711	2.9	53.6	84.7
G4	W 12x136	248.5	711	2.9	52.9	83.6
G5	W 12x106	221.5	543.4	2.5	48.7	77.1
G6	HP 12x53	60.5	236.5	3.9	60.4	95.6
H1	HP 10x42	42.5	135.7	3.2	54.4	86.0
H2	W 12x65	85.5	318.4	3.7	59.6	94.2
H3	W 12x72	119	392.6	3.3	65.2	88.9
H4	W 12x79	124	392.6	3.2	55.1	87.1
H5	W 12x65	92	318.4	3.5	57.5	90.9
H6	HP 10x42	41.5	135.7	3.3	55.0	87.1

Roof, Levels 12,11,10,9

K=1, unsupported length = 30 ft 5 in

Condition 1 - Load due to Roof and Levels 12,11,10,9

Condition 2 - Load due to Roof and Level 12

Note: capacity reduction factor  $\phi_c = 1$

Table 7.4.1

COLUMN LINE CAPACITIES FOR INELASTIC SIDESWAY BUCKLING IN THE EAST-WEST DIRECTION

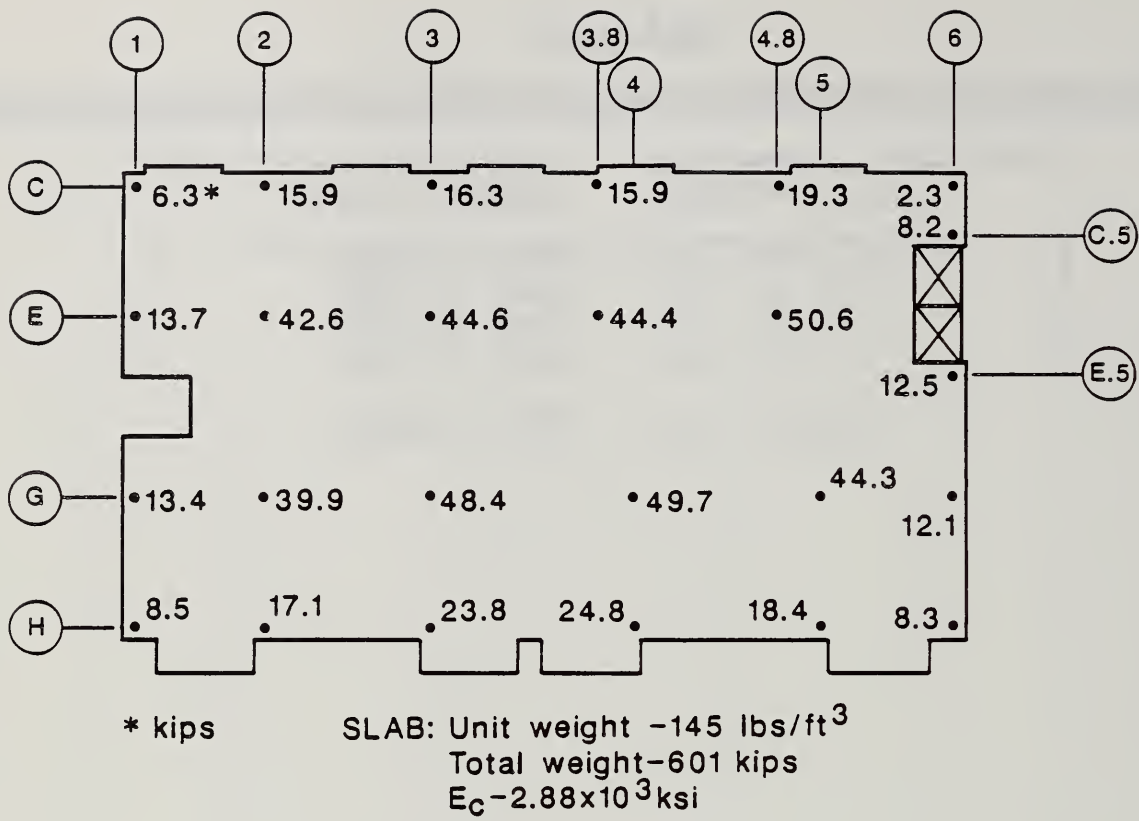
Column Line	Capacity-to-Load Ratio	Load (kips)	Capacity (kips)
C	0.87	1216	1058
E	1.20	3466	4159
G	1.13	3325	3757
H	0.80	1614	1291
	Total	9621	10265



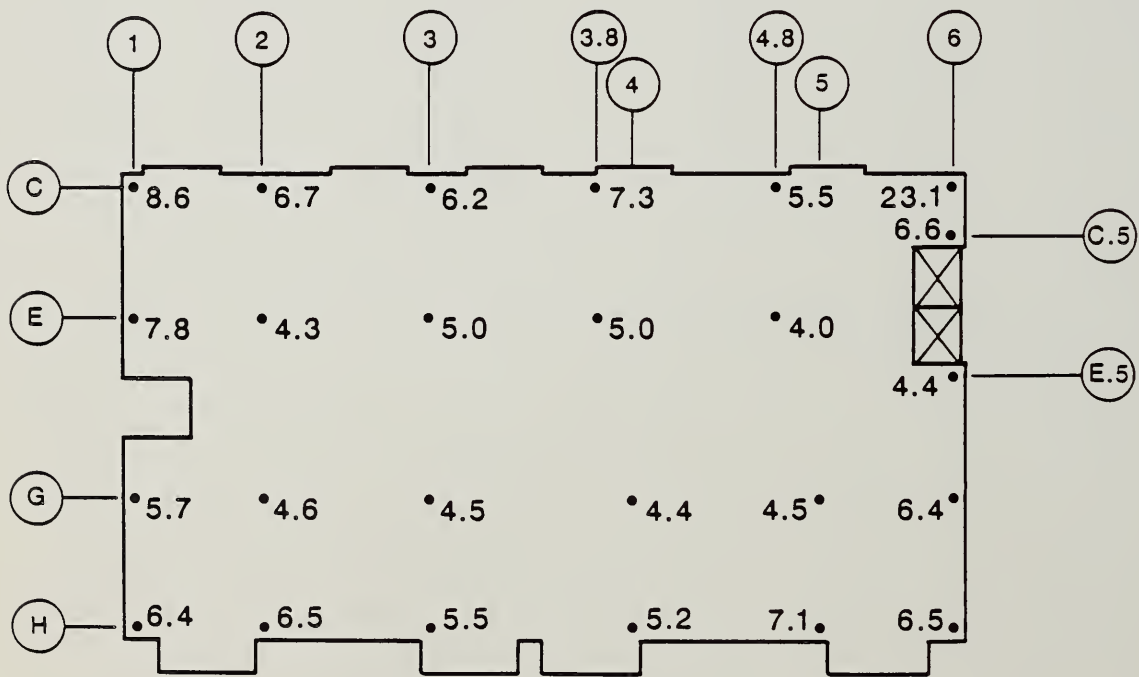
TABLE 7.4.2

COLUMN LINE CAPACITIES FOR ELASTIC SIDESWAY BUCKLING IN THE EAST-WEST DIRECTION

Column Line	Capacity-to-Load Ratio	Load (kips)	Capacity (kips)
C	0.89	1216	1082
E	1.21	3466	4194
G	1.14	3325	3791
H	0.82	1614	1323
	Total	<u>9621</u>	<u>10390</u>



(a) Support Reactions



(b) Reserve Capacity - Punching Shear

Figure 7.2.1 Support reactions and shear capacity of floor slab

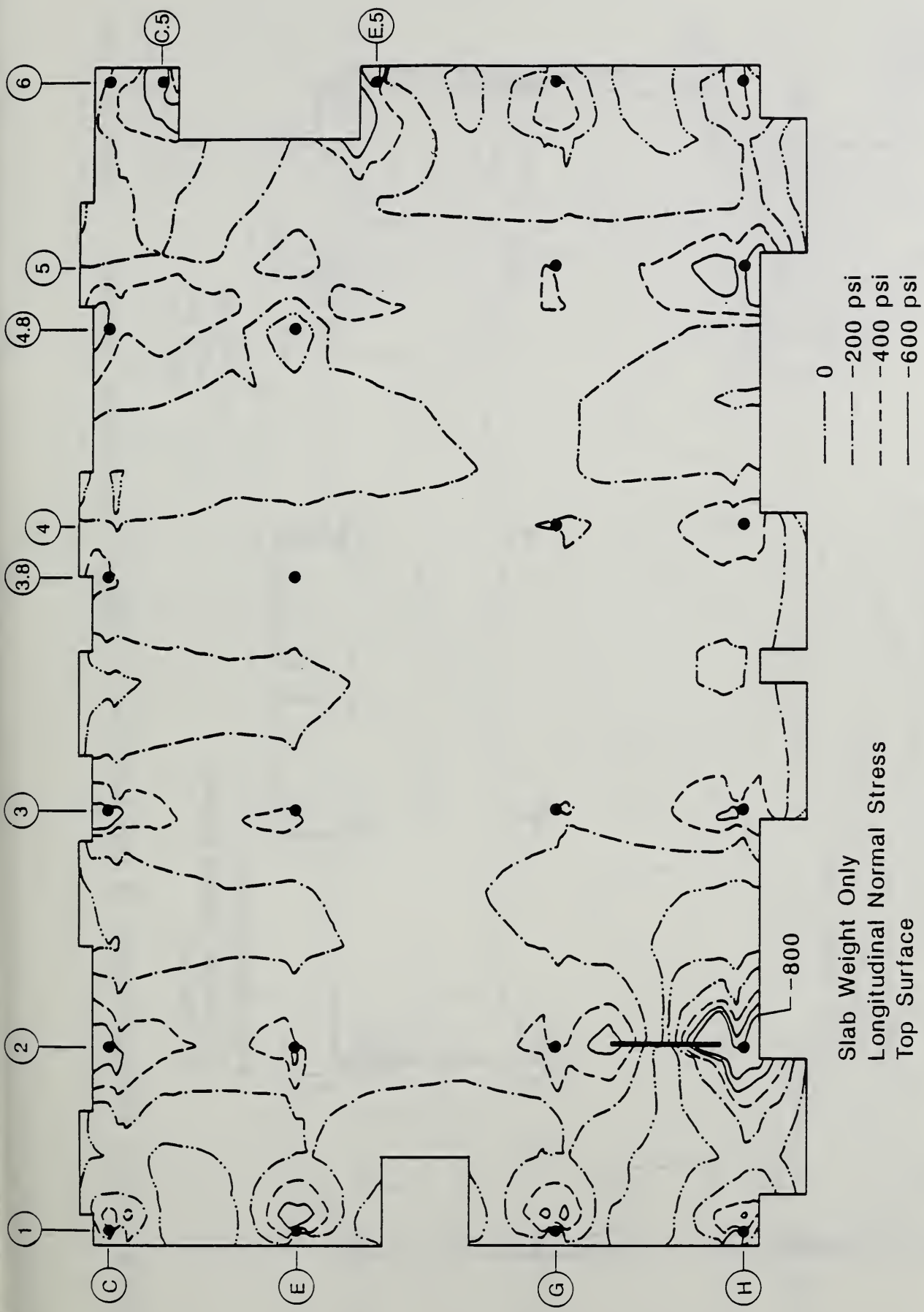


Figure 7.2.2a Normal stress at top surface of slab in longitudinal direction - dead weight

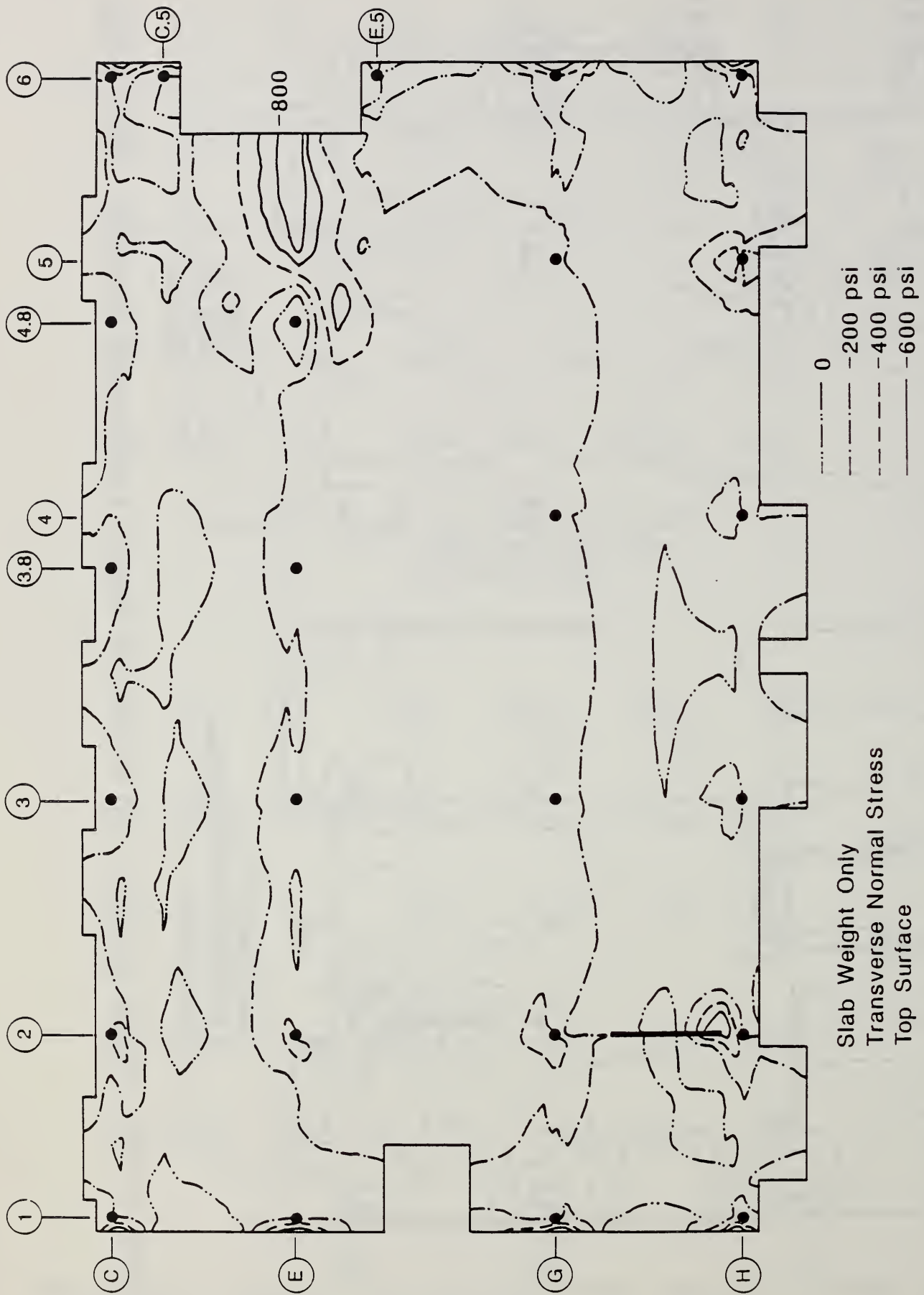
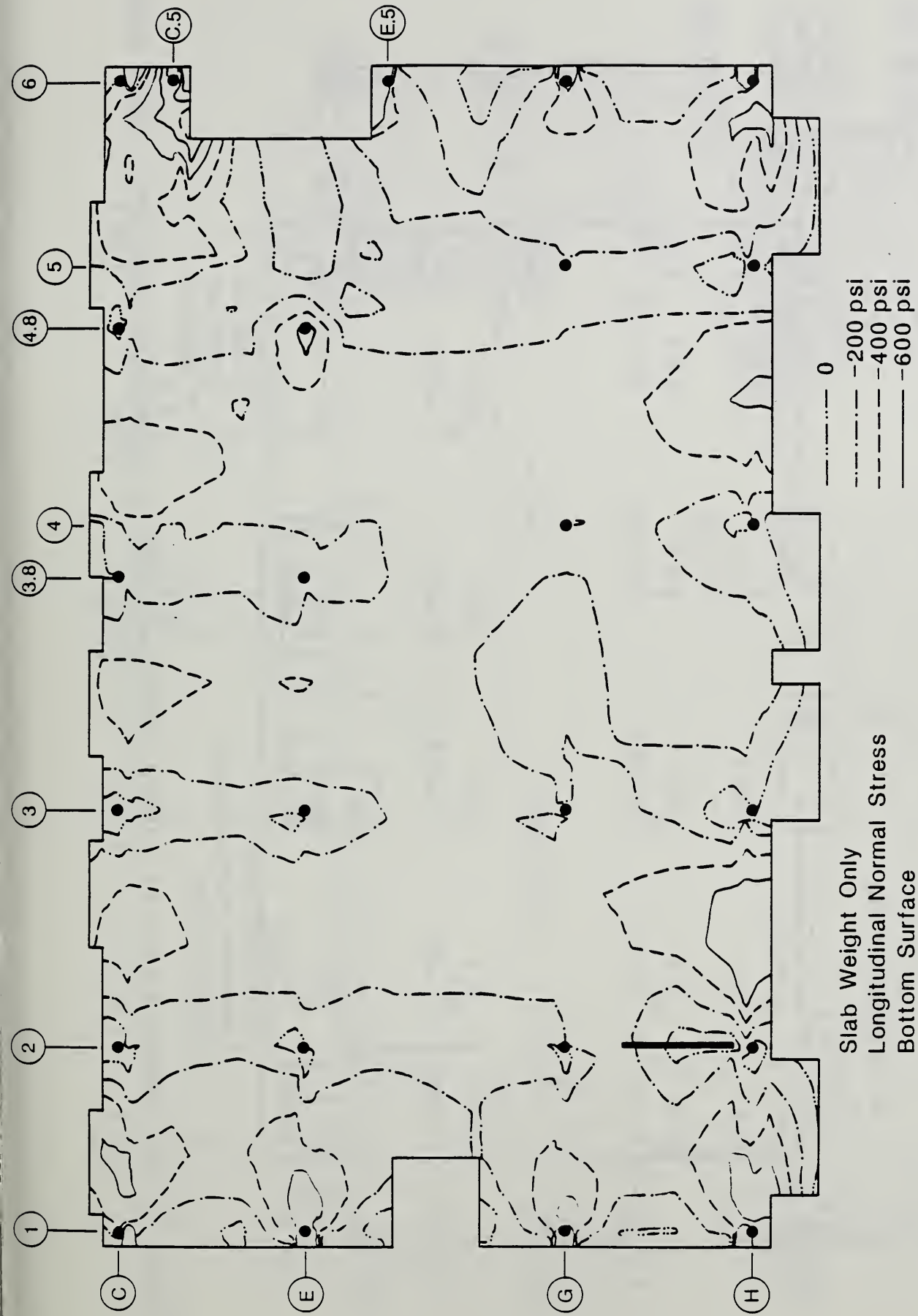


Figure 7.2.2b Normal stress at top surface of slab in transverse direction - dead weight



Slab Weight Only  
 Longitudinal Normal Stress  
 Bottom Surface

Figure 7.2.3a Normal stress at bottom surface of slab in longitudinal direction - dead weight

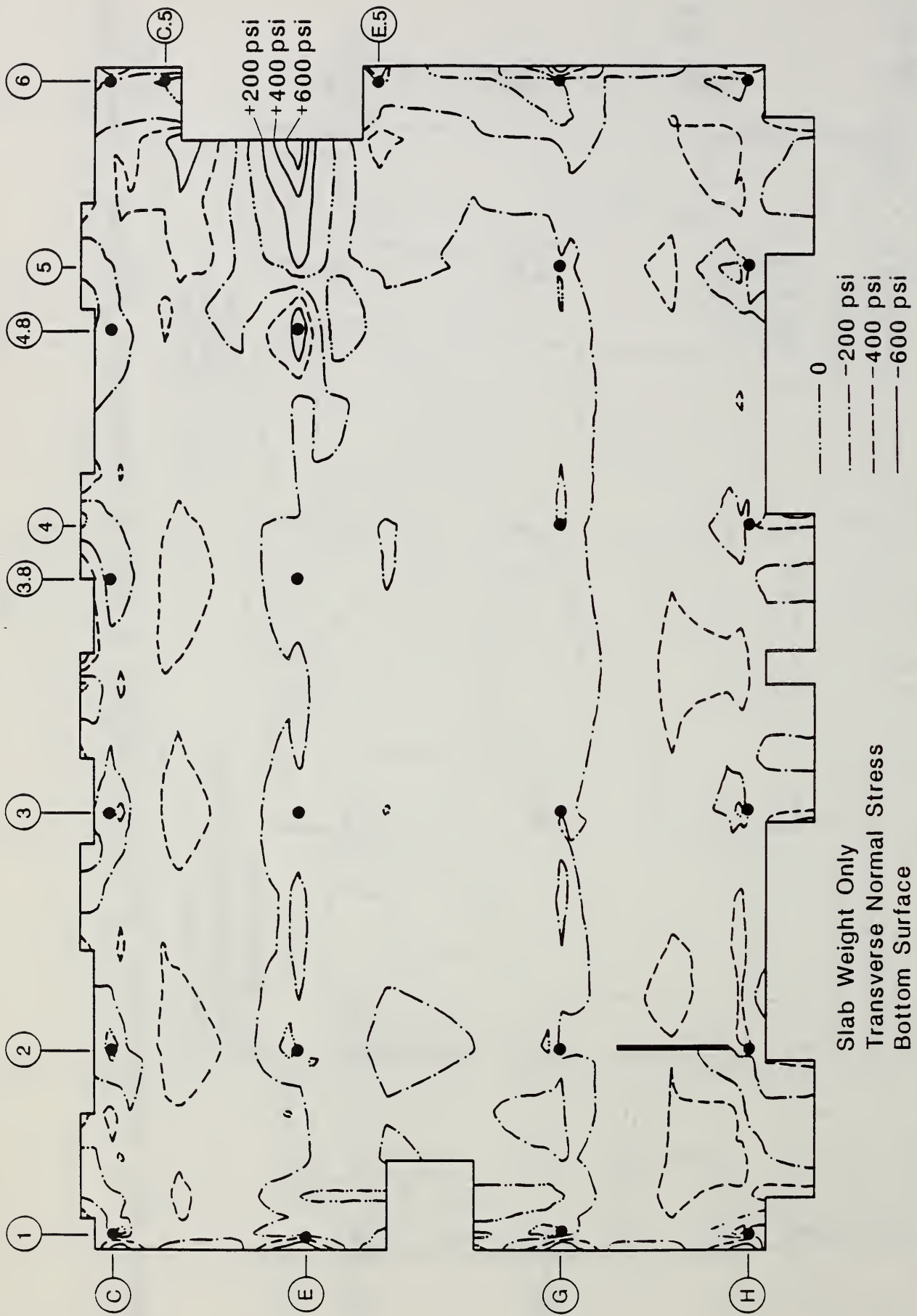


Figure 7.2.3b Normal stress at bottom surface of slab in transverse direction - dead weight

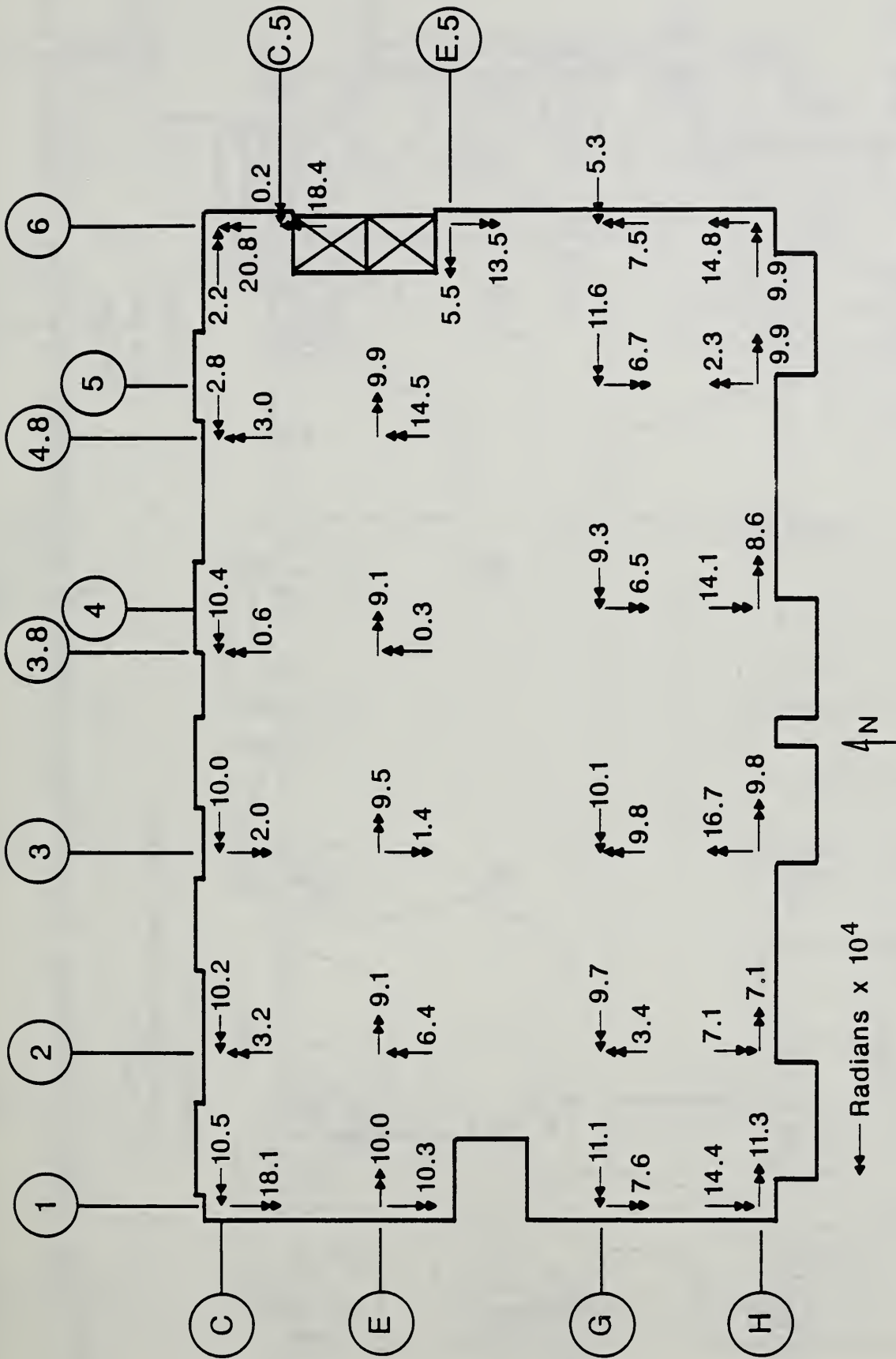


Figure 7.2.4 Slab rotations at column locations

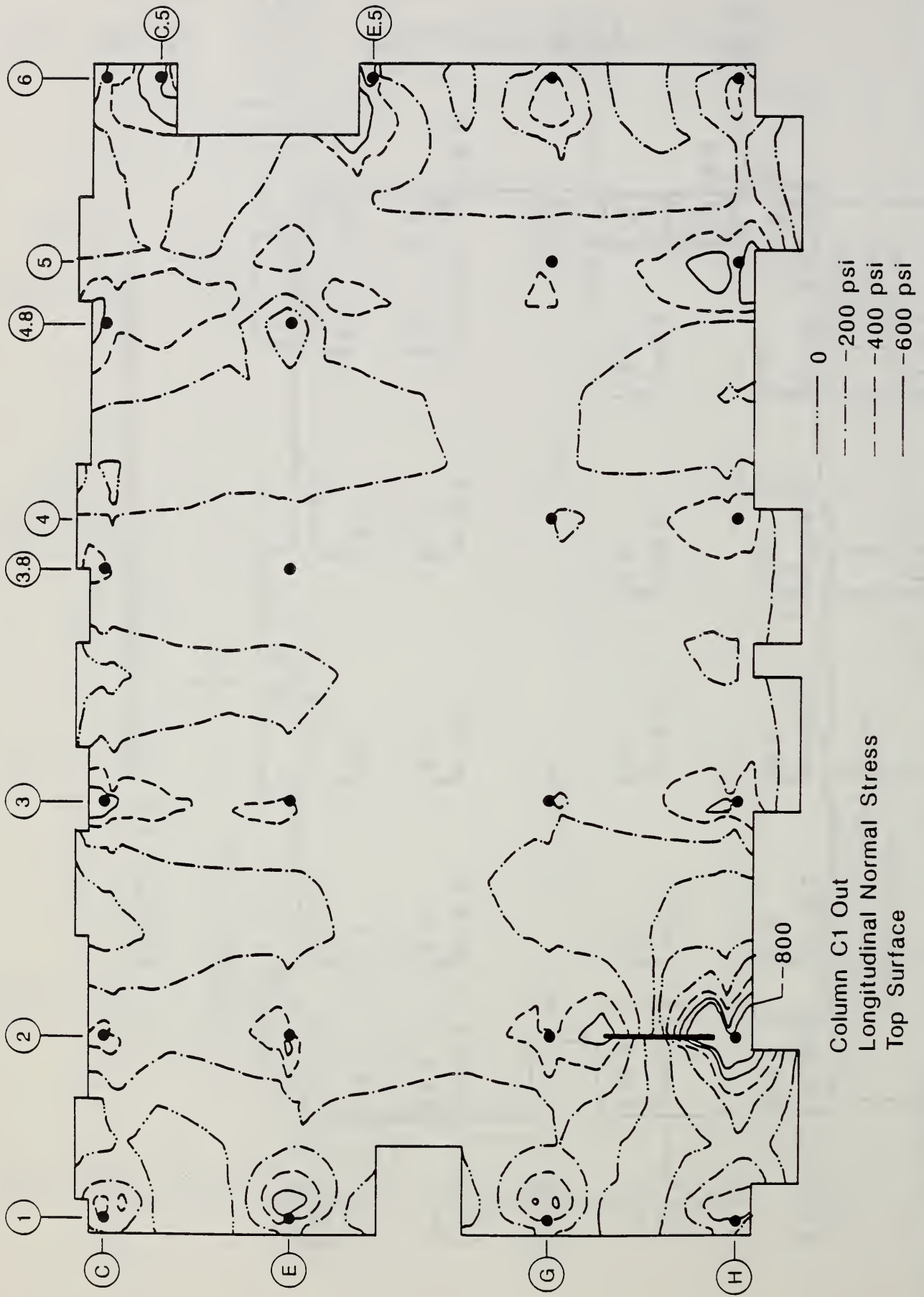


Figure 7.2.5a Normal stress at top surface of slab in longitudinal direction - column C1 out



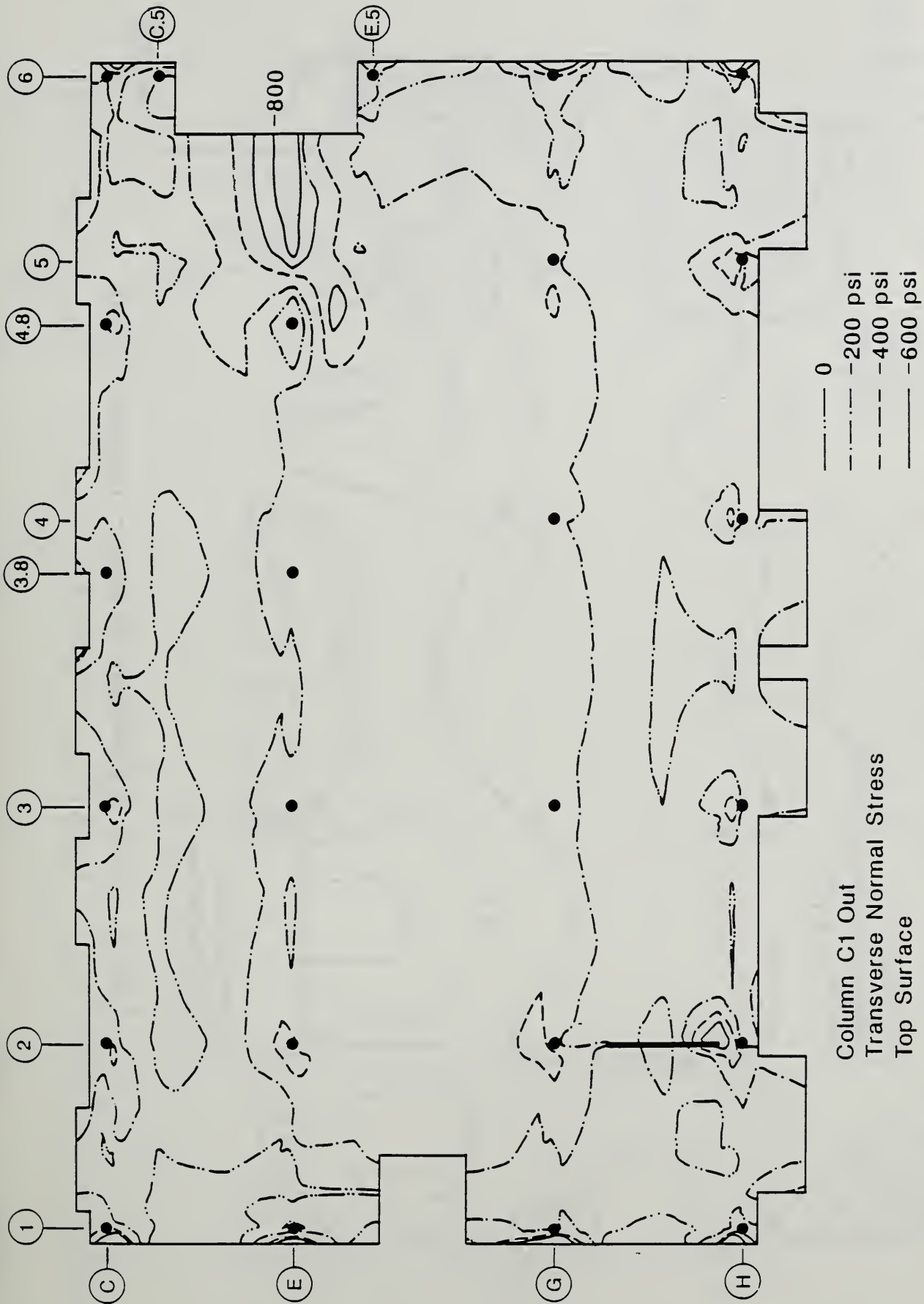


Figure 7.2.5b Normal stress at top surface of slab in transverse direction – Column C1 out

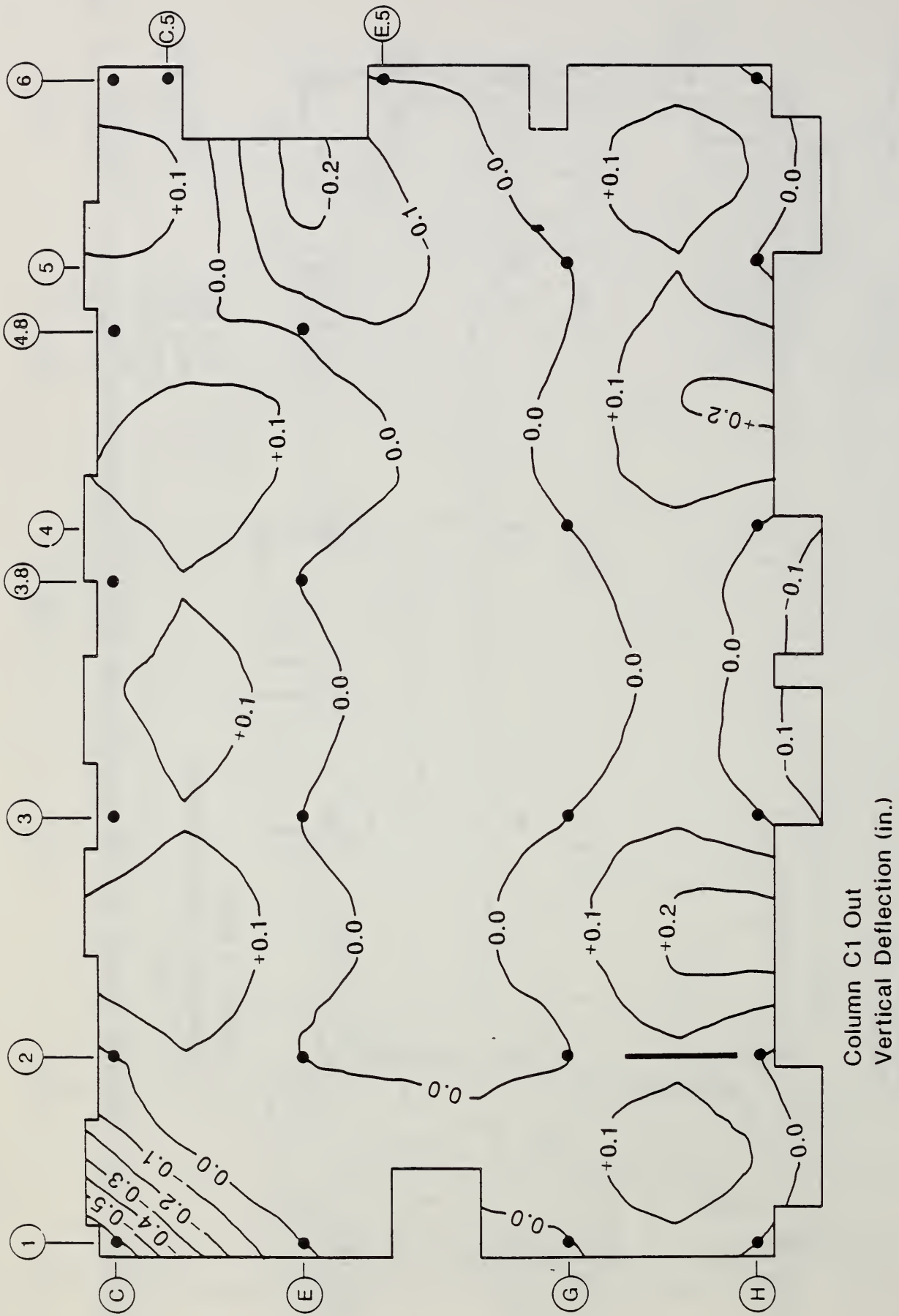


Figure 7.2.6 Deflection of slab - column C1 out

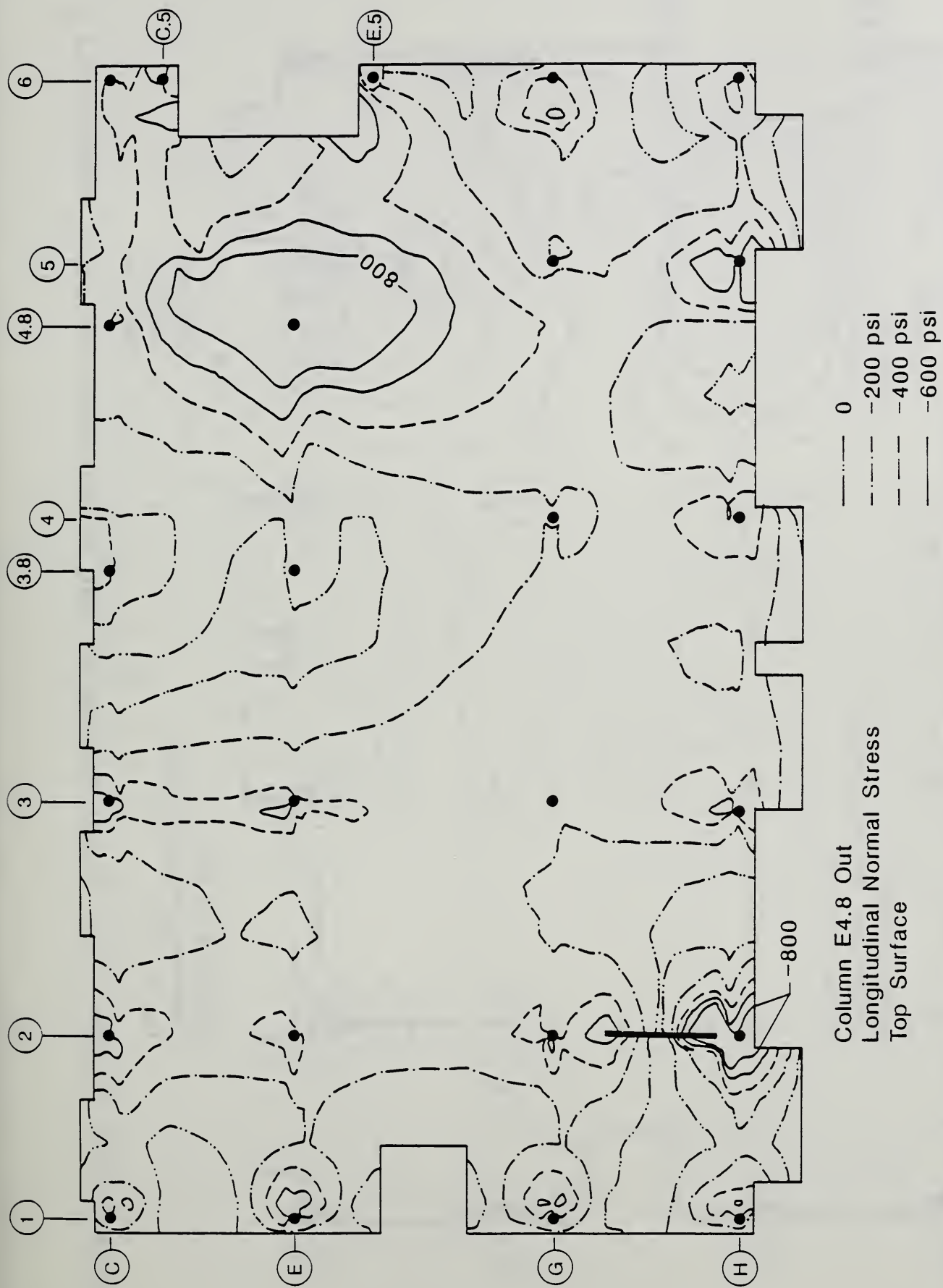


Figure 7.2.7a Normal stress at top surface of slab in longitudinal direction - column E4.8 out

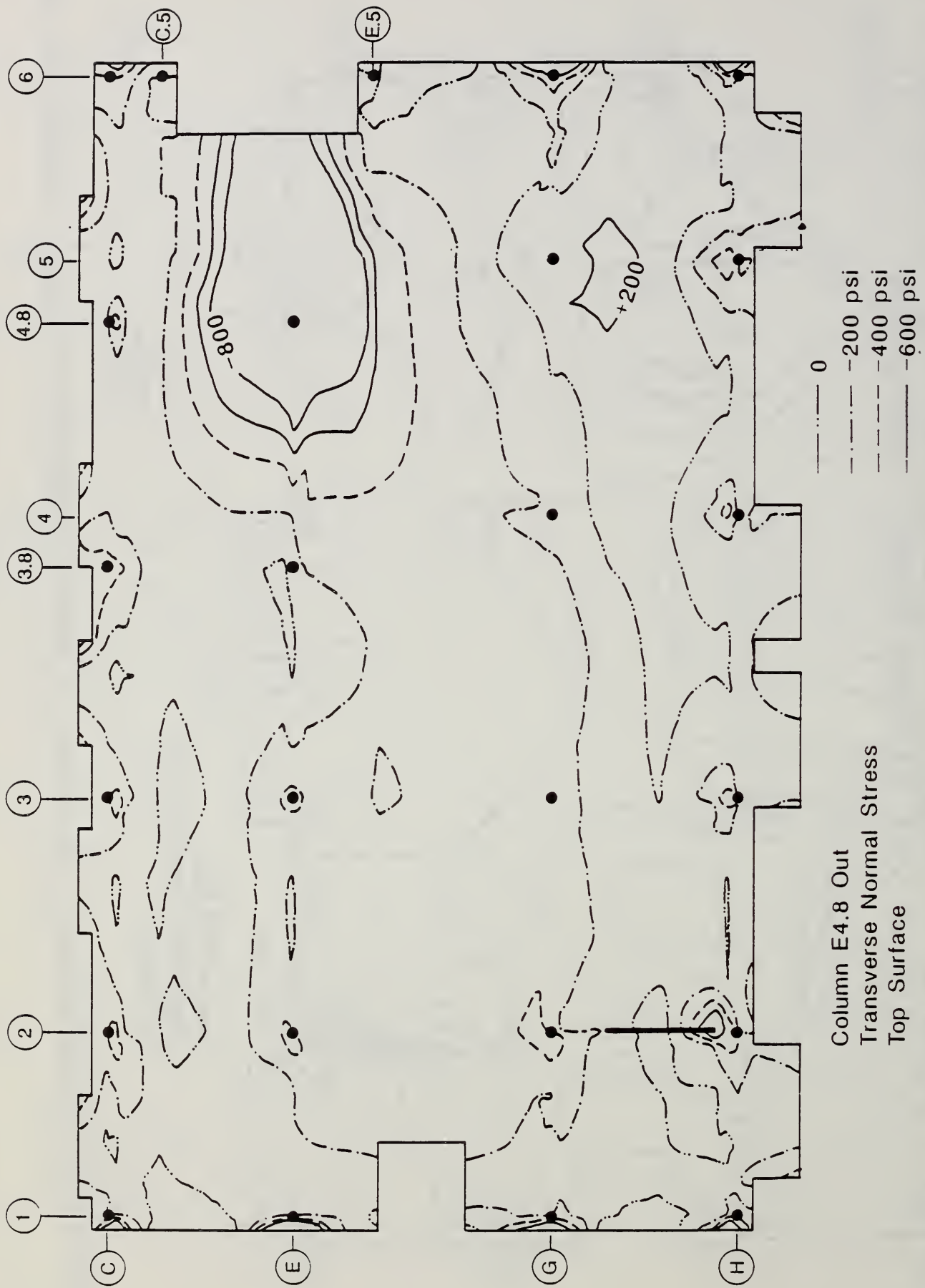


Figure 7.2.7b Normal stress at top surface of slab in transverse direction, - column E4.8 out

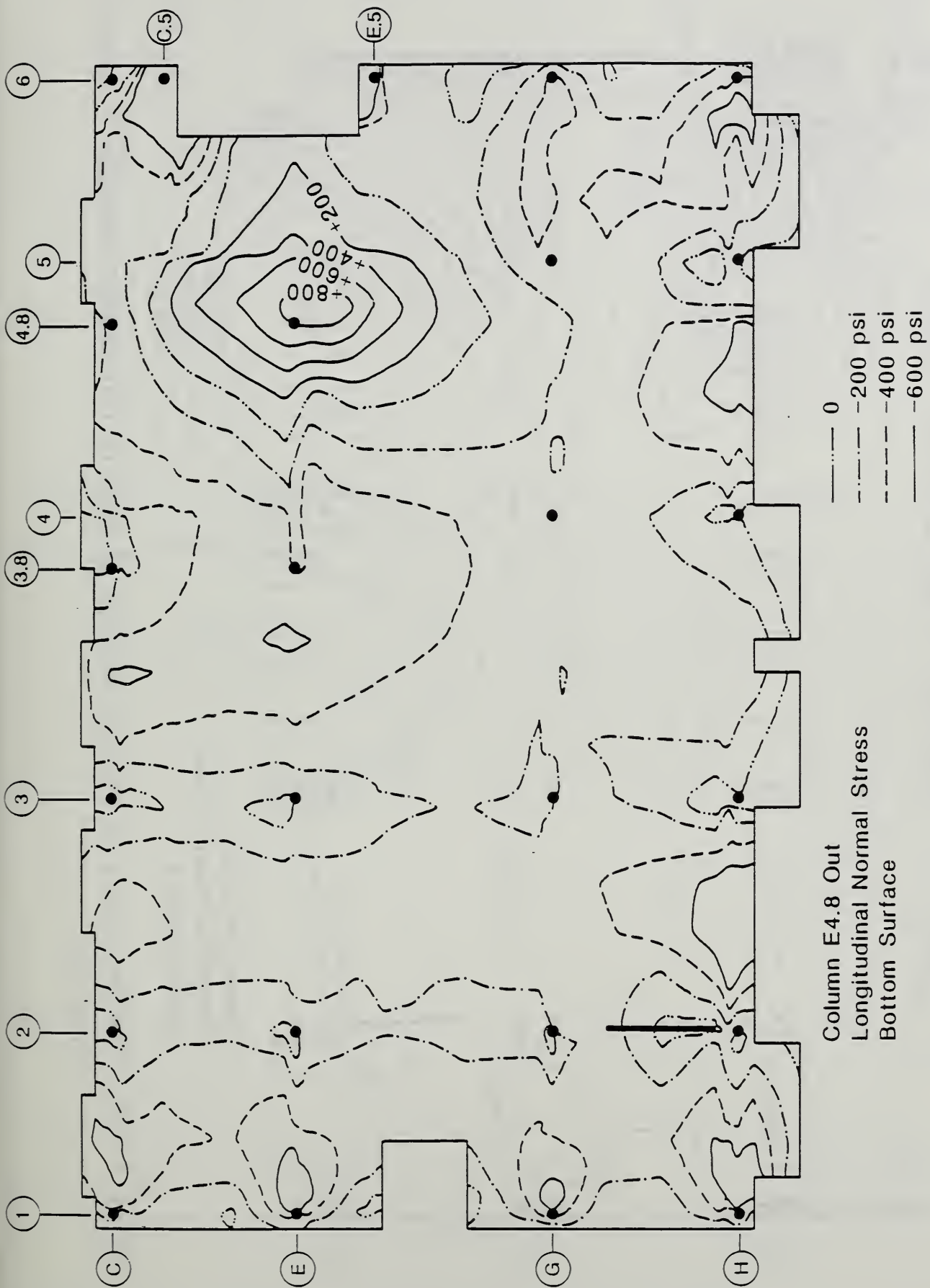


Figure 7.2.8a Normal stress at bottom surface of slab in longitudinal direction - column E4.8 out

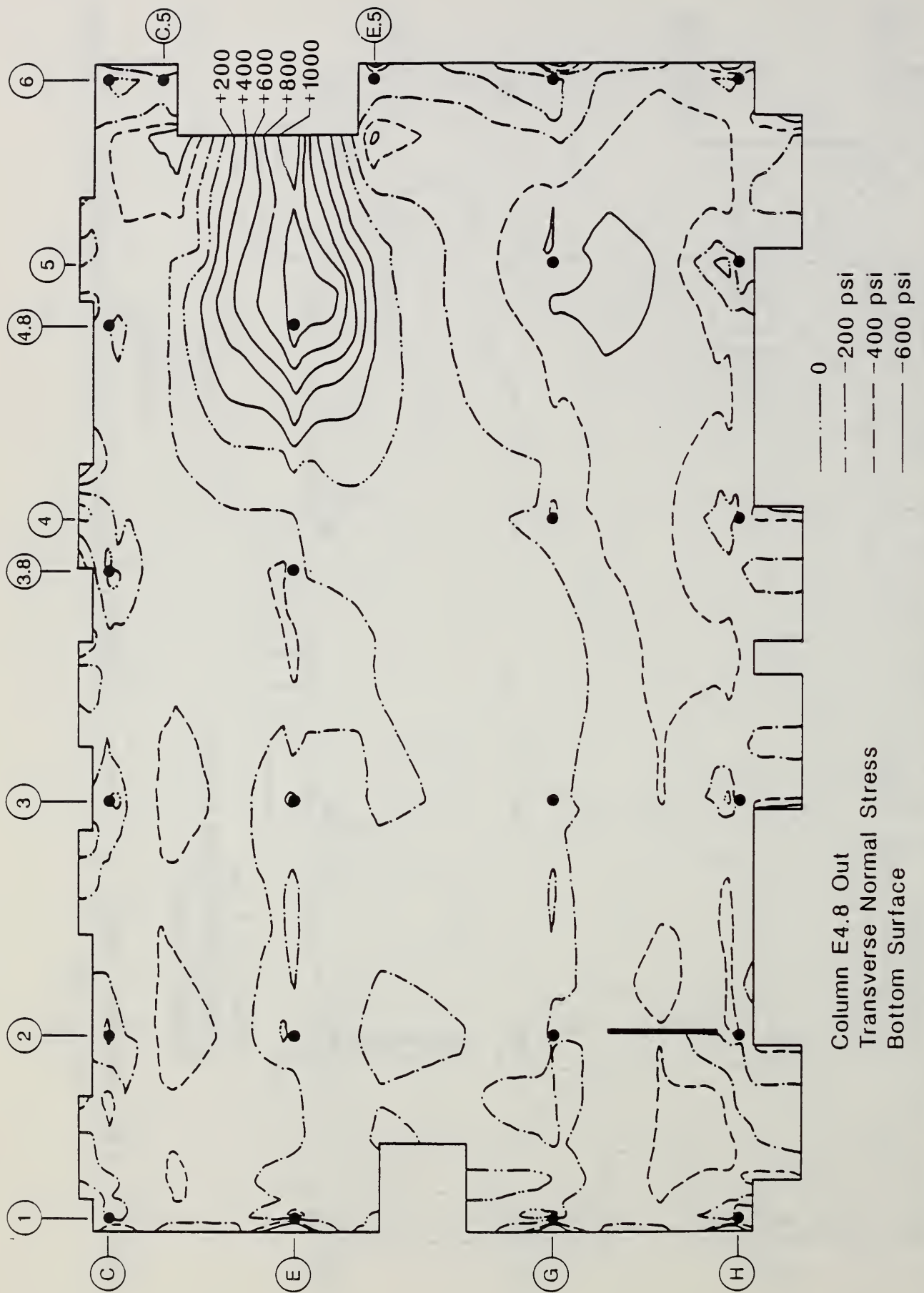
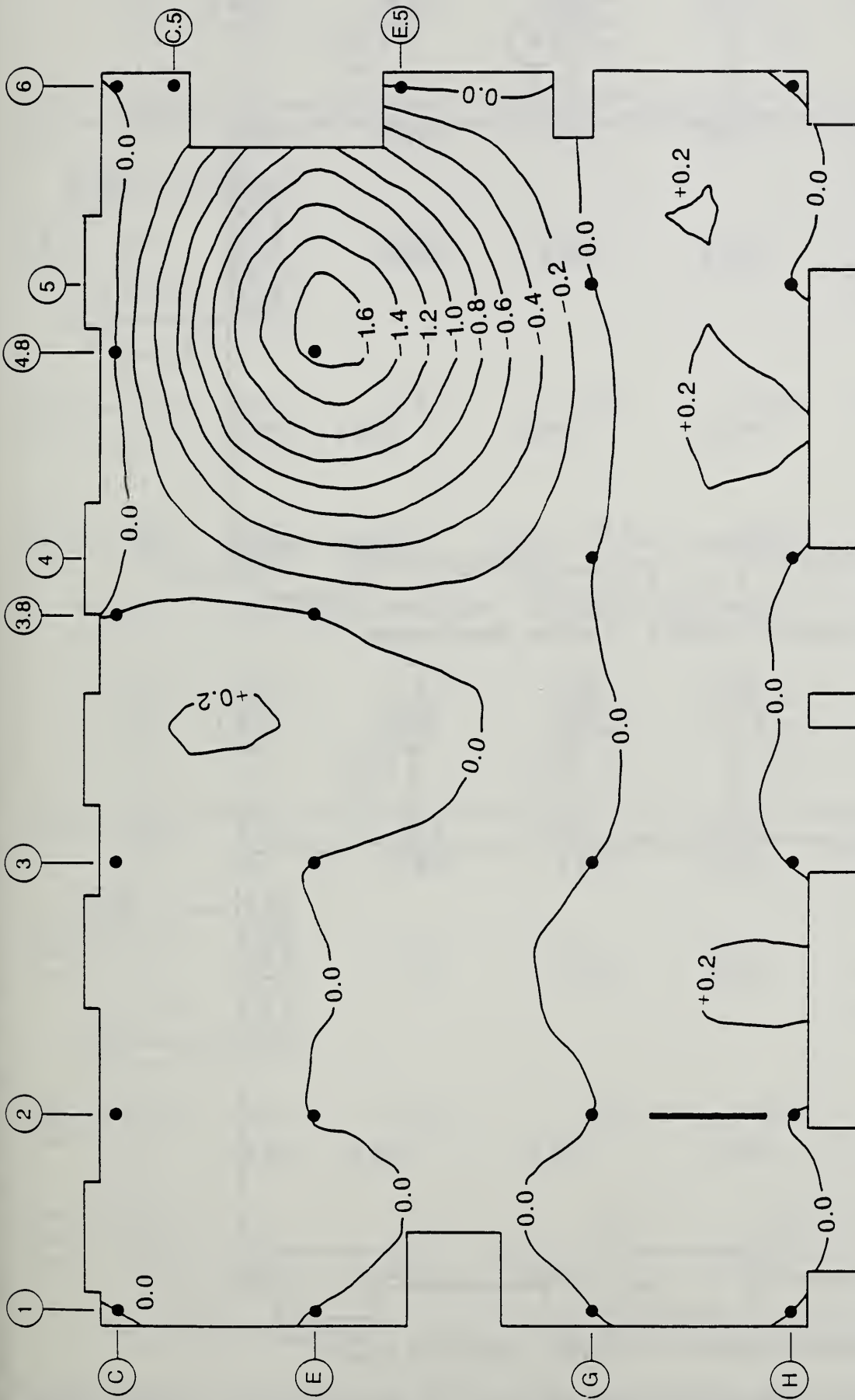
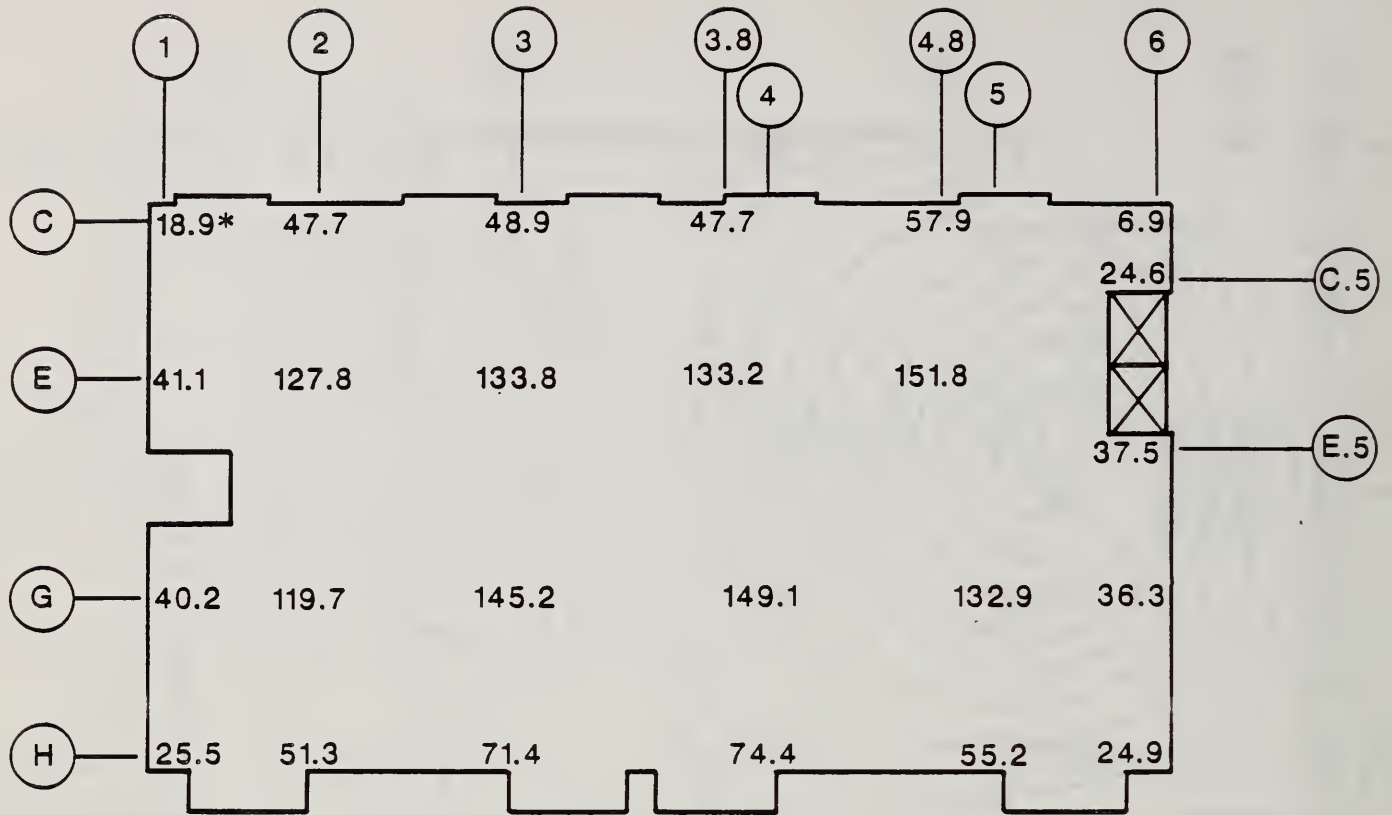


Figure 7.2.8b Normal stress at bottom surface of slab in transverse direction - column E4.8 out



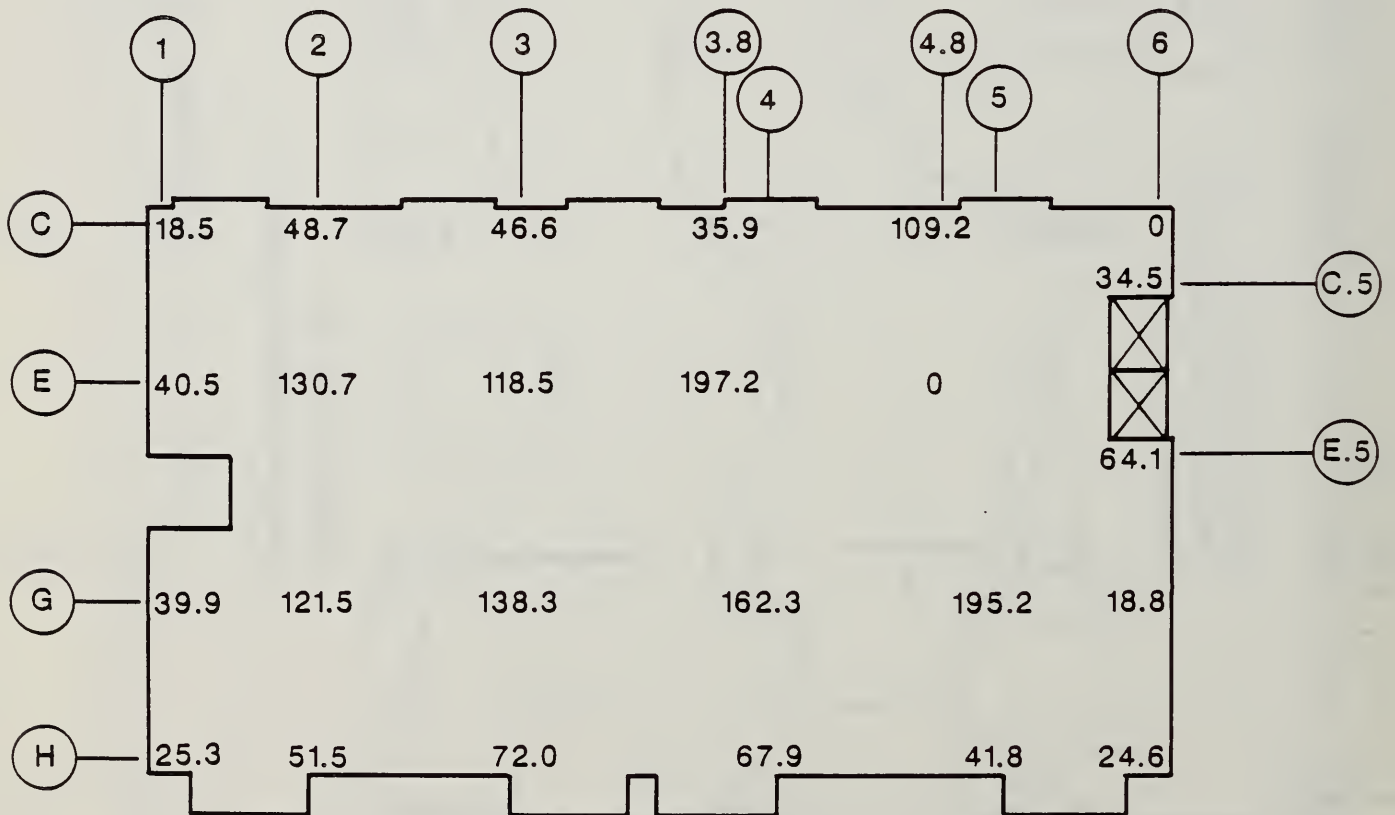
Column E4.8 Out  
Vertical Deflection (in.)

Figure 7.2.9 Deflection of slab – column E4.8 out



\*kips

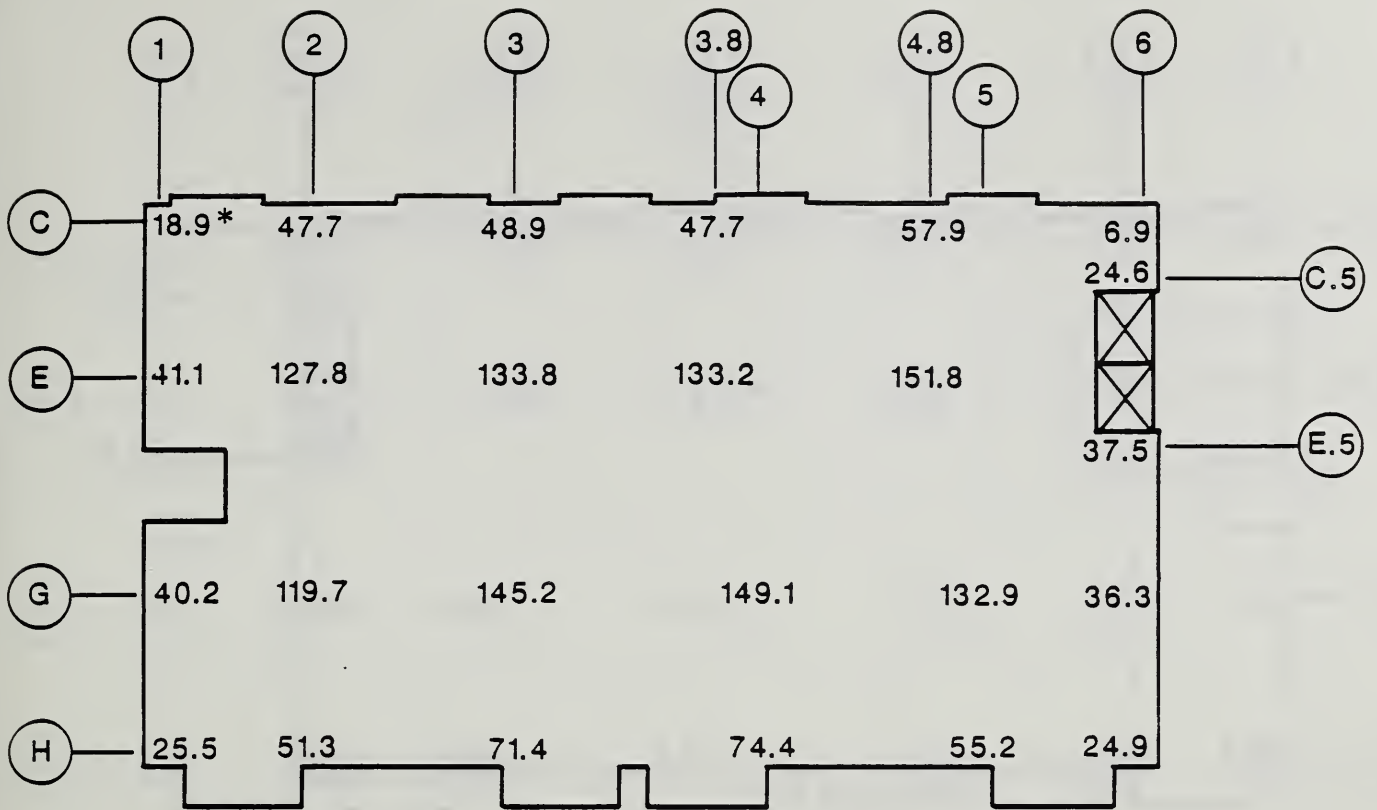
(a) Support reactions - 3 slabs, dead weight



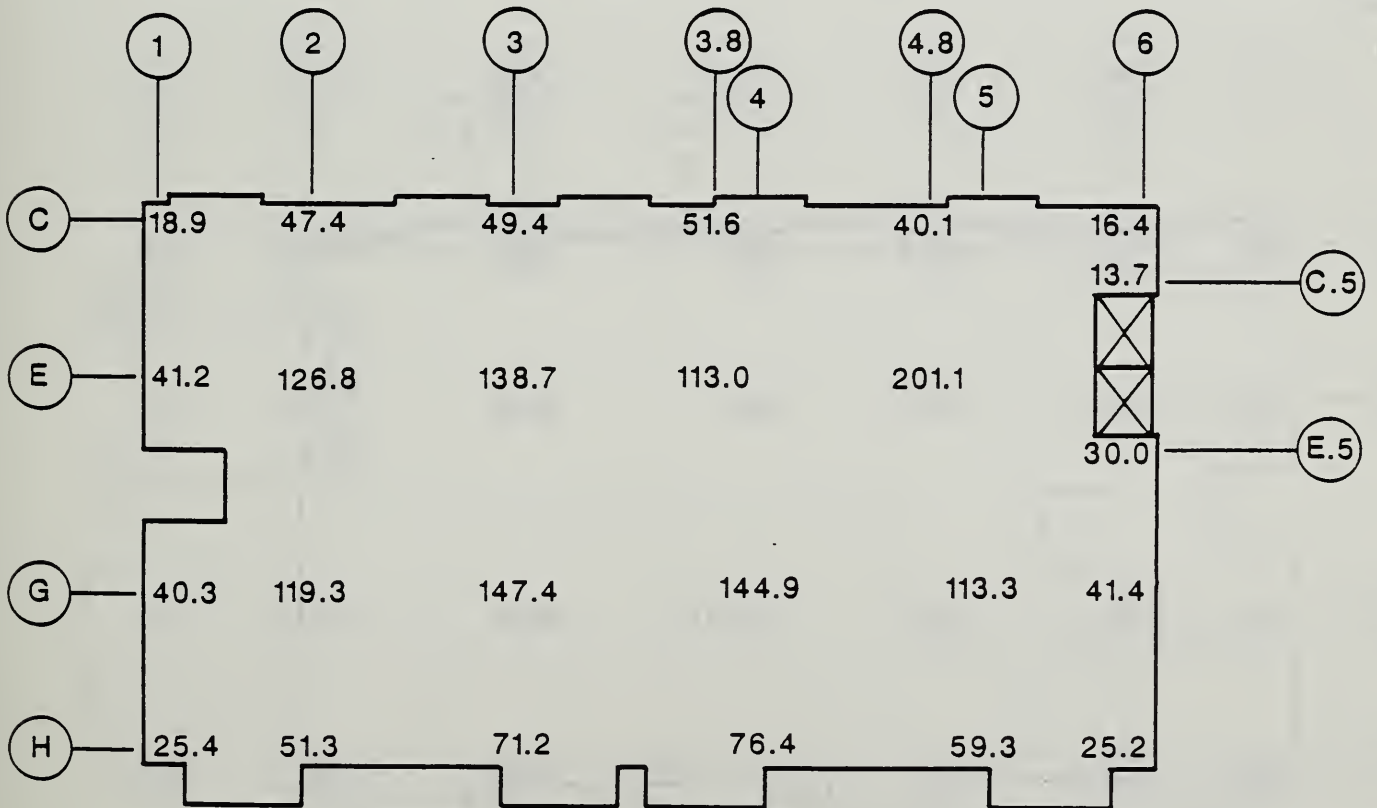
(b) Support reactions - 3 slabs, column E4.8 out

Figure 7.2.10 Support reactions due to loss of support at column E4.8



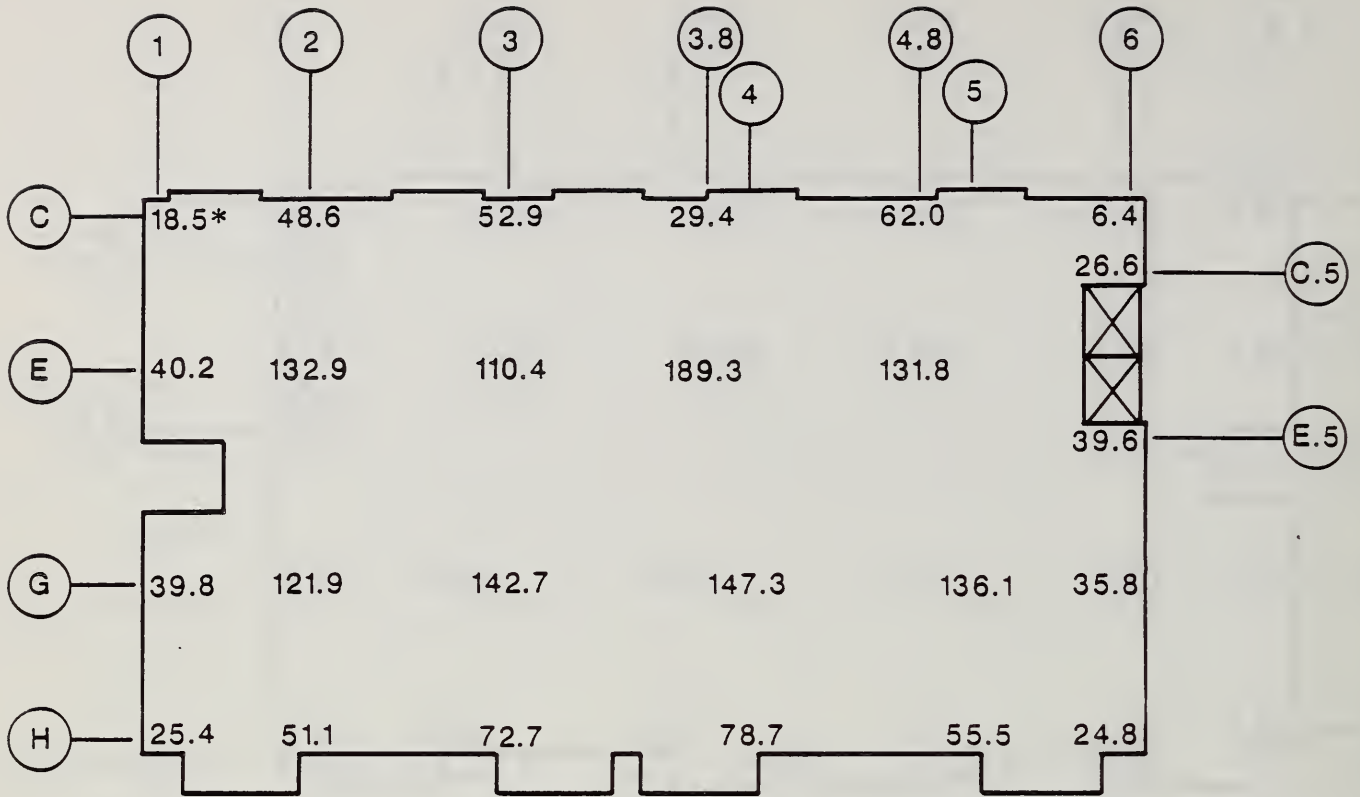


\* kips (a) Support reactions - 3 slabs, dead weight



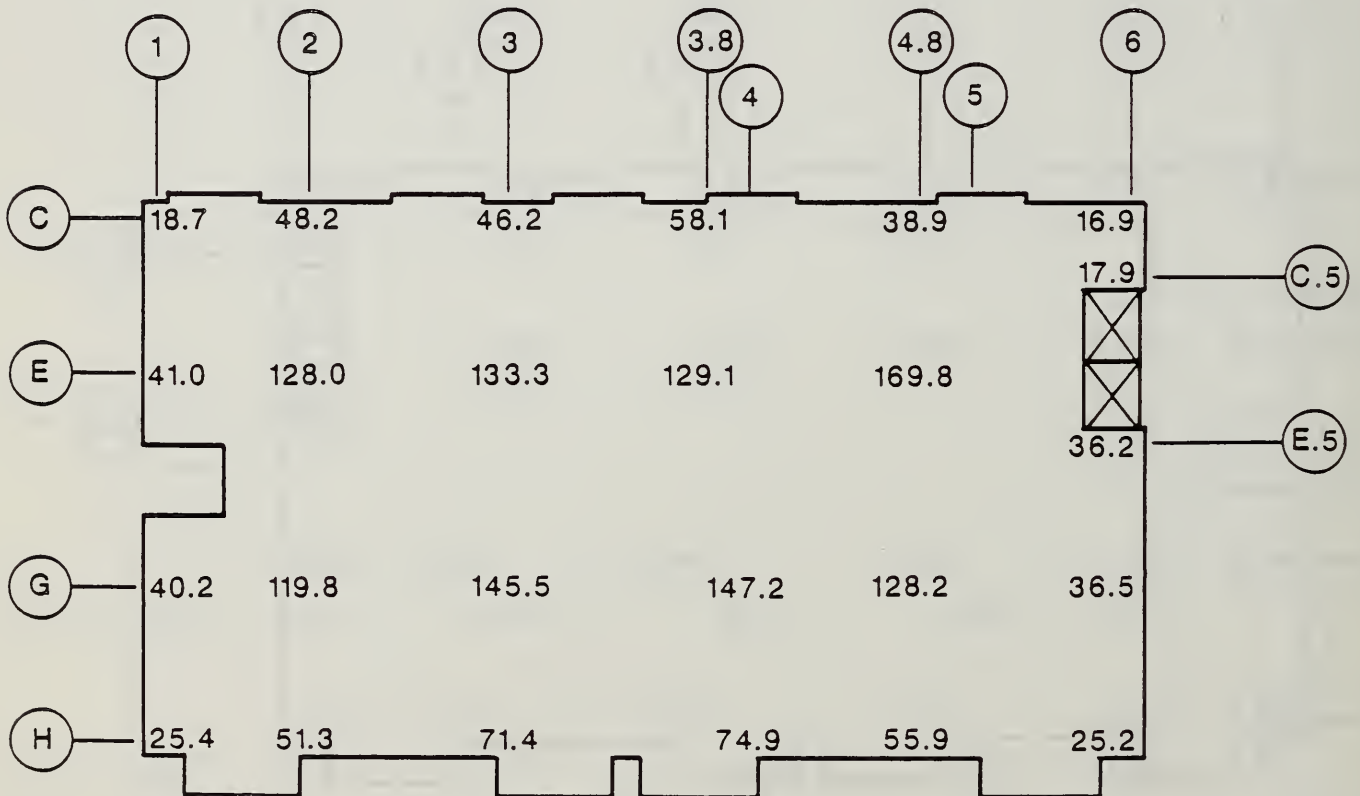
(b) Support reactions - 3 slabs, raise slabs 1/2" at column E4.8

Figure 7.2.11 Support reactions due to jacking slab at column E4.8



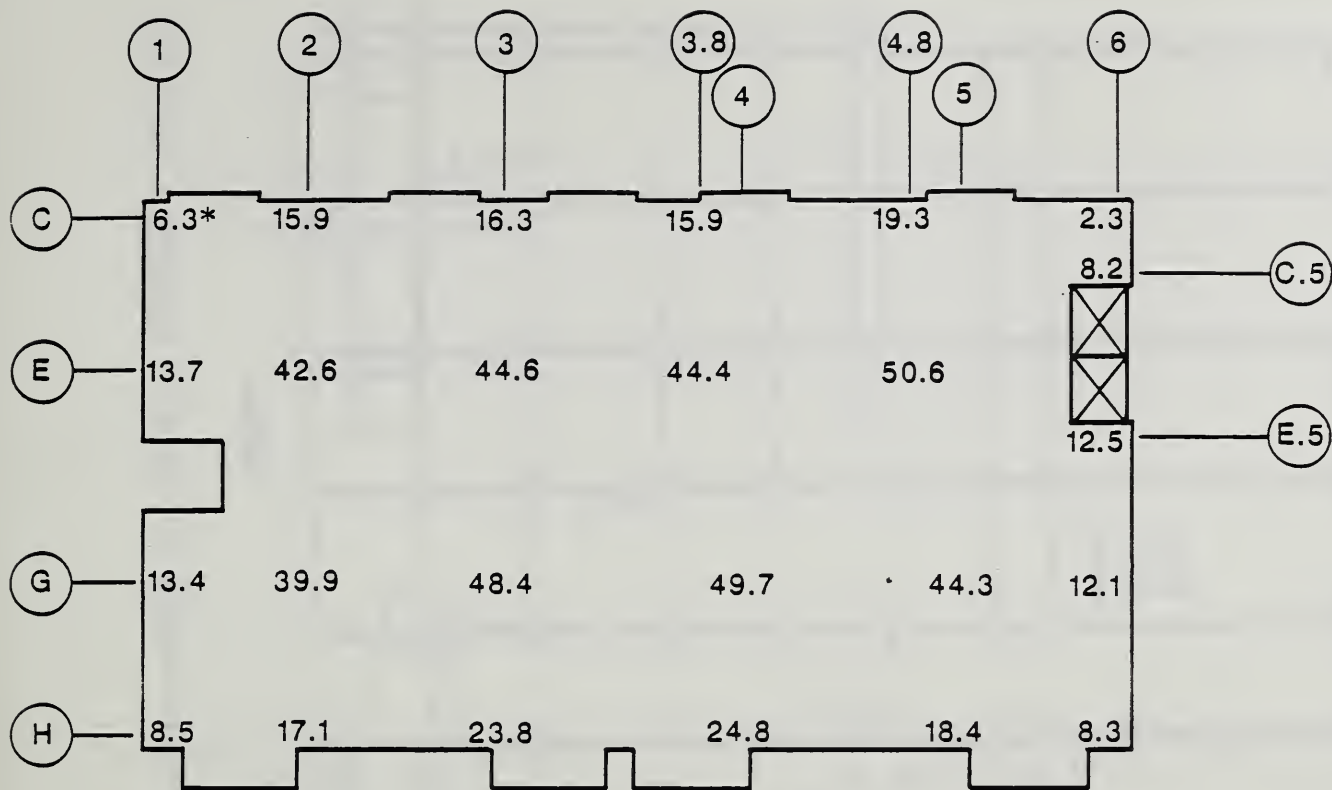
(a) Support reactions - 3 slabs, dead weight, support E3.8 1/2' high

\*kips



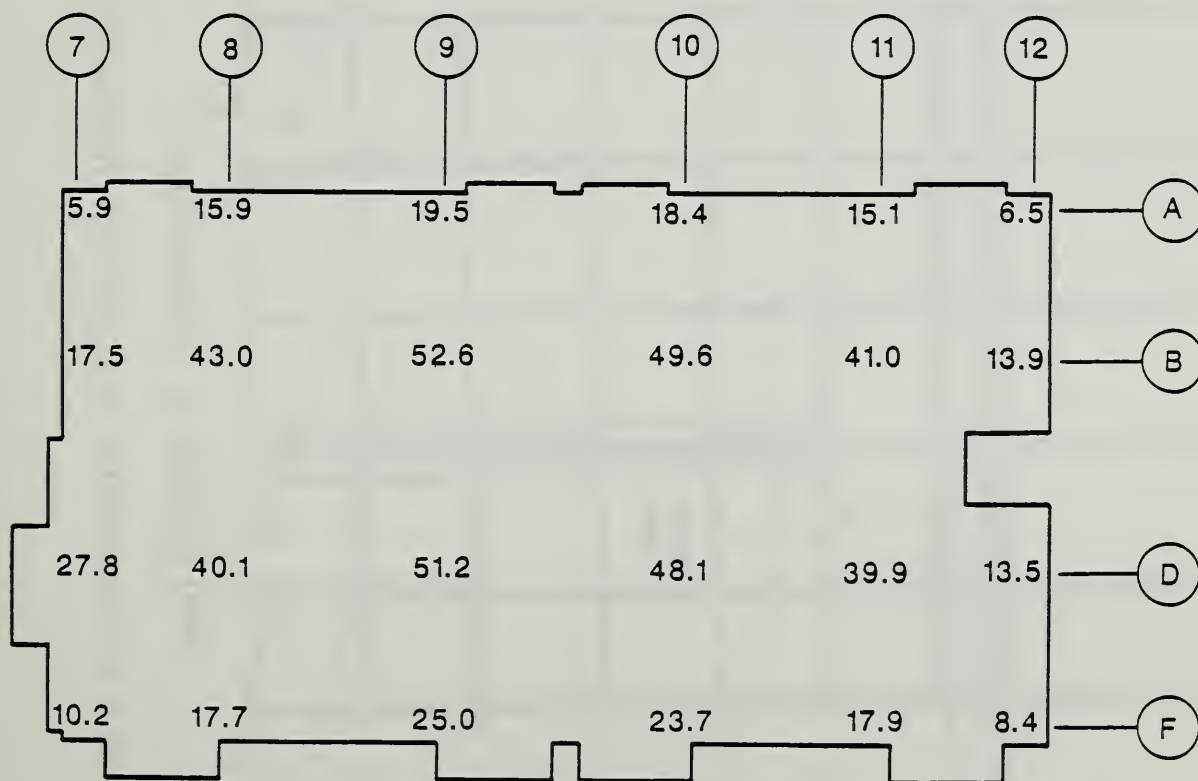
(b) Support reactions - 3 slabs, dead weight, support C4.8 1/2' low

Figure 7.2.12 Support reactions due to difference in support elevations



\*kips

(a) West Tower



(b) East Tower

Figure 7.2.13 Comparison between single slab reactions in East and West towers

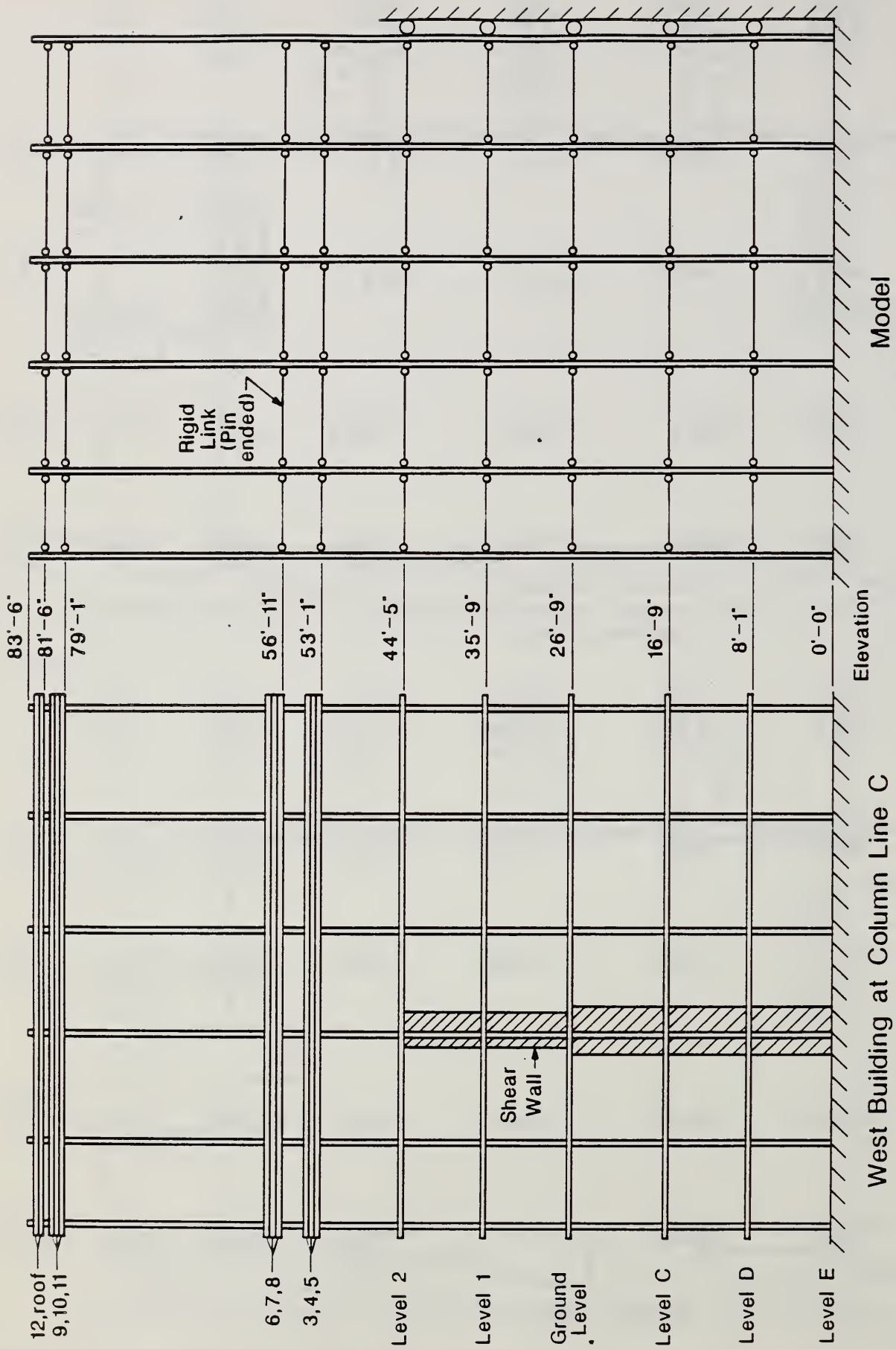
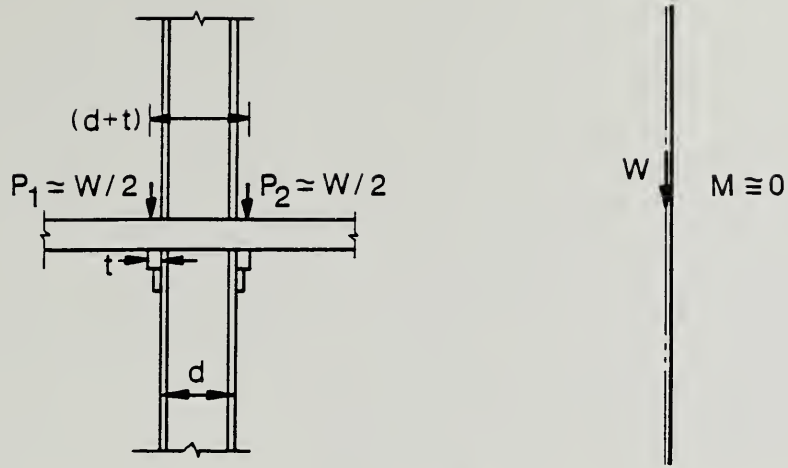
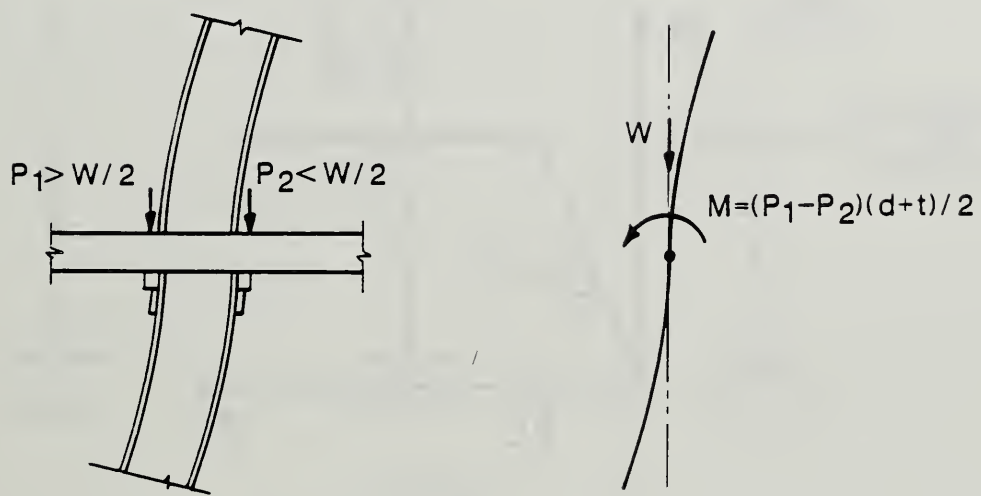


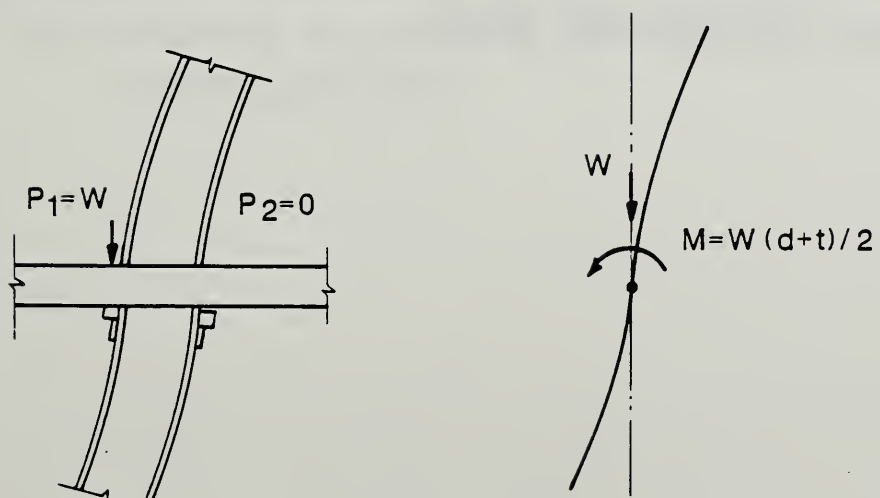
Figure 7.4.1 Schematic diagram of frame line and model used for lateral stability analysis



(a)



(b)



(c)

Figure 7.4.2 Restoring moment mechanism

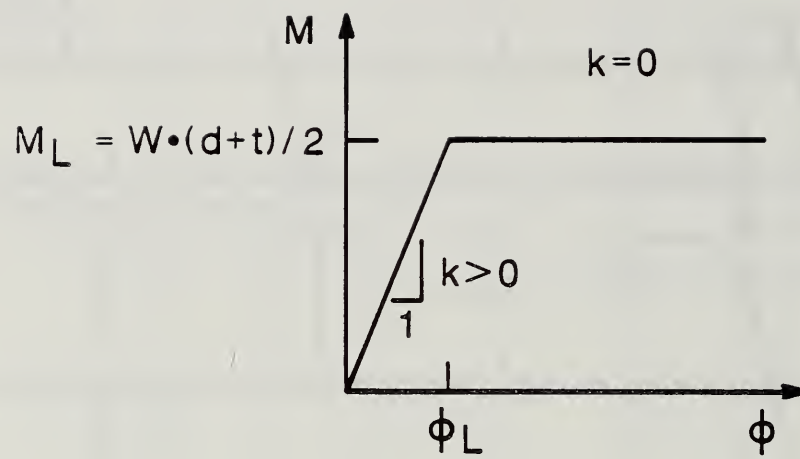


Figure 7.4.3 Moment-rotation relationship for restoring moment with liftoff

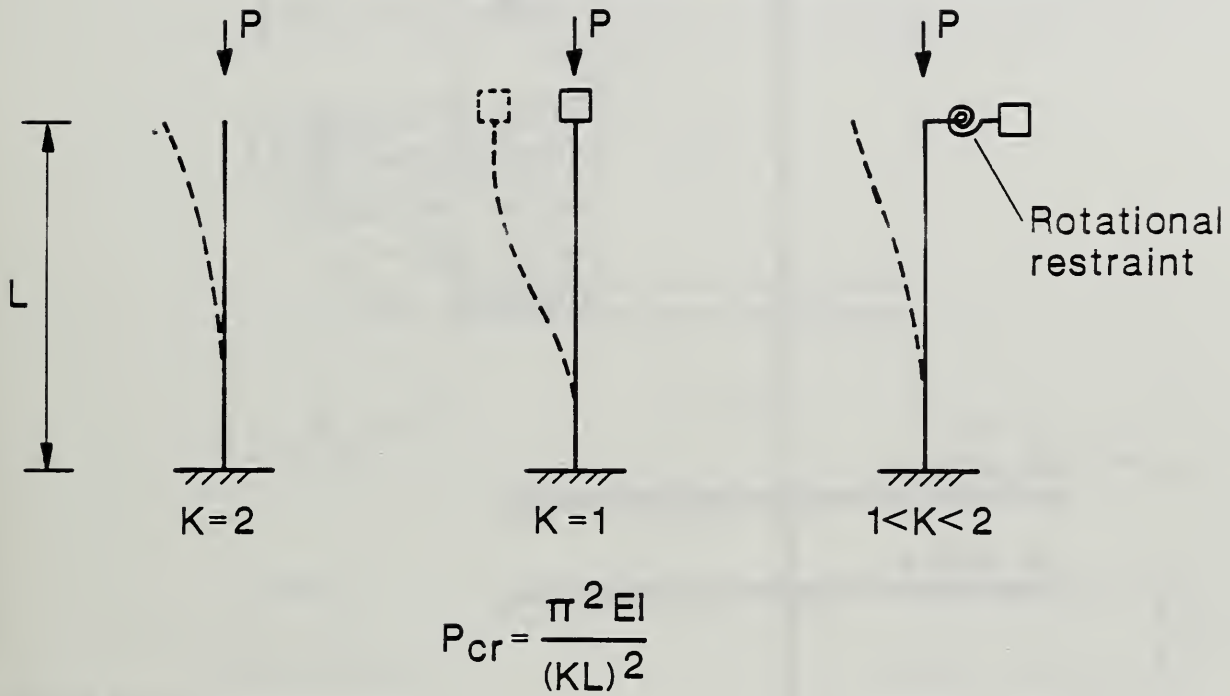


Figure 7.4.4 Influence of rotational restraint on sidesway buckling capacity

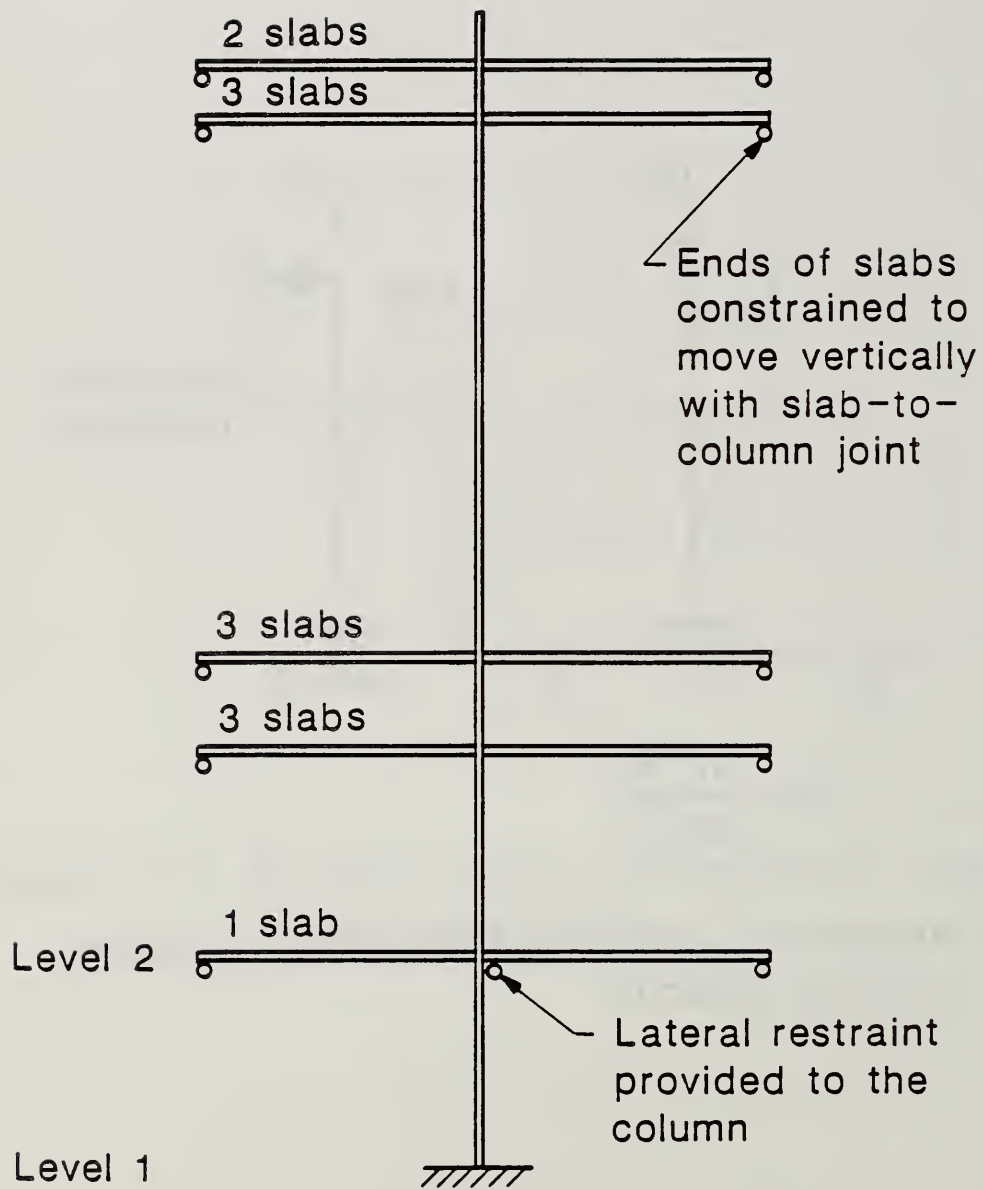


Figure 7.4.5 Single column computer model of West tower with slab restraining effects



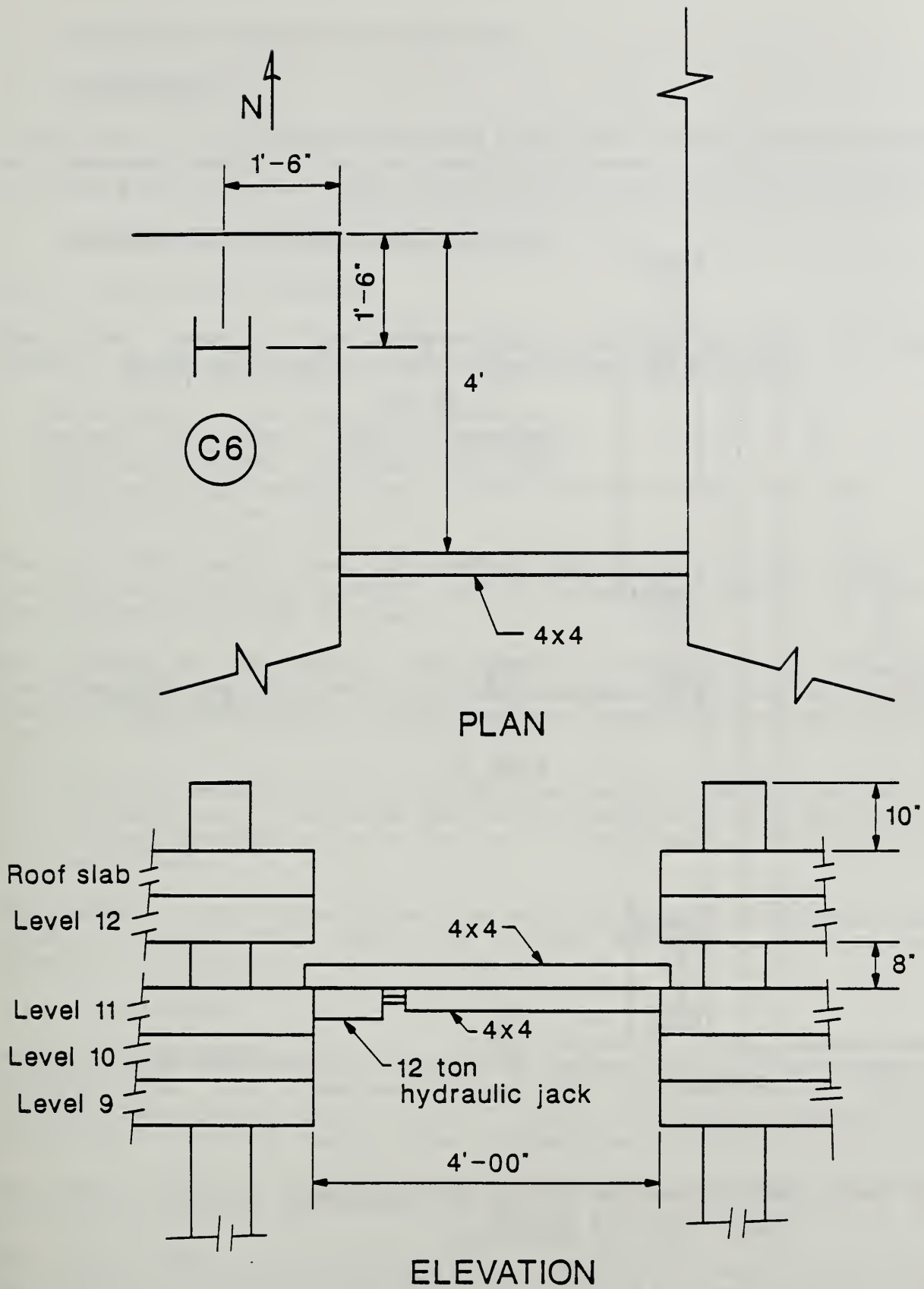


Figure 7.4.6 Location of horizontal jack used to plumb the building

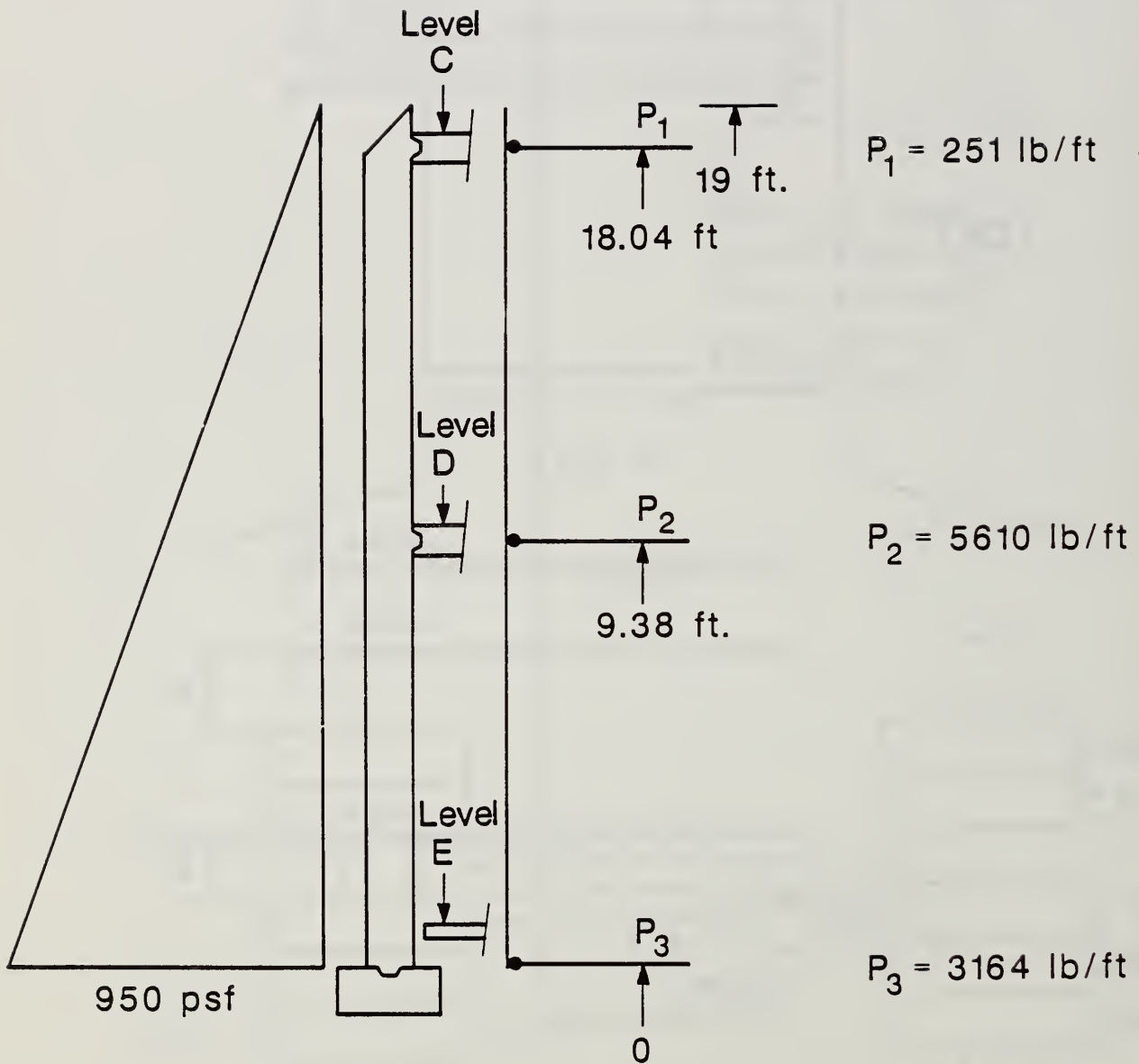


Figure 7.4.7 Soil pressure acting on basement wall - North side of building

## 8. EVALUATION OF CONSTRUCTION PRACTICES

### 8.1 INTRODUCTION

Comparisons of the laboratory tests and field tests with the project specifications are important considerations in identifying factors that may have contributed to causing the collapse. These comparisons are included in this Chapter.

### 8.2 COMPARISON WITH PROJECT SPECIFICATIONS

#### 8.2.1 Construction Materials

The project manual [5] and the structural drawings specified the following material properties for the various components of the structure:

- Column Steel - A 36 and A 572, Grade 50
- Concrete Floor Slabs - 4000 psi (27.6 MPa)
- Shear Wall Concrete - 4000 psi (27.6 MPa)
- Post-Tensioning Strand - 7 wire strand, 270 ksi Low-lax (1862 MPa)
- Welding Electrodes - E70 Series

The mill test reports and the chemical analyses and tensile coupon tests reported in Section 5.3.2 verify that the column steel used in the structure was A 36 and A 572 Grade 50 steel.

The strength of the concrete core samples in Section 5.2.2 exceeded the specified 4000 psi (27.6 MPa) for both the floor slabs and the shearwalls. There was some variation in concrete strength between the various floor levels tested.

The breaking strength of the 7 wire post-tensioning strand reported in Section 5.5.2 exceeded the 270 ksi (1862 MPa) value specified in only half the tests. All the yield strength values in Section 5.5.2 exceeded the 37,170 lbf (165 kN) value specified.

Observations of the debris at the site indicated that E7018 welding rods were being used for the field welds. The chemical analysis of the weld material reported in Section 5.4.3 also confirms this.

#### 8.2.2 Foundations

Pertinent specifications for foundation construction are contained in the Project Manual for L'Ambiance Plaza, [5] Sections 02010, "Subsurface Investigation," 02210, "Site Grading," 02220, "Excavating, Backfilling and Compacting," and in the General Notes: Foundations on structural drawing S201.

The general notes in structural drawing S201 address footing support in the following notes:

The general notes in Drawing S201 require that all footings in the east and west tower rest on undisturbed rock with a minimum bearing capacity of 14,000 psf (670 kPa). The notes also make provision for the case where the material

below the bottom of the footing can not support the design load. Three options are provided: replacement of the unsuitable material with approved engineered fill; increase in the footing size; and lowering of the footing to soil of suitable bearing capacity. These requirements, taken together with those in the project manual, stipulate that the footings have to be poured on rock of suitable quality, and if this cannot be accomplished at the elevation shown in the plans, the footings either have to be lowered, or the gap between the footings and the rock surface has to be filled with lean concrete. No other "approved engineering fill" could be chosen by the soils engineer without written approval from the architect. As an alternative solution, footing sizes could be increased.

The borings and test pits indicated that most footings rested on a layer of disintegrated rock, about 1 ft (0.3 m) thick. In addition, a layer up to 2 ft (0.6 m) of local material was placed under some footings. Even though the fill material at the bottom of the footings has been certified by the independent testing laboratory to be capable of supporting 14,000 psf (670 kPa), no record is available to indicate whether written permission had been obtained from the architect to deviate from the specifications, or whether the independent testing laboratory ascertained the thickness of the disintegrated rock layer, or otherwise performed tests or analyses to ascertain that the bearing capacity of the footings was adequate.

Thus it is concluded on the basis of available information that support conditions below the footings, as encountered in a number of soil borings and test pits, do not comply with those stipulated in the specifications. This conclusion applies to locations where boring and test pit information is available. It does not necessarily apply to other locations. The conclusion does not imply that the support condition of the footings in any way contributed to the collapse, or that the footings would have settled excessively under the conditions for which they were designed.

### 8.2.3 Column Sections

In studying the debris at the site and the landfill, measurements were made of the cross sectional dimensions of a number of the column sections.

The columns measured were those from stage I (levels E, D, C and ground) and stage IV (levels 5 and 6) where it was possible to identify their positions in the structure. Fourteen columns from stage I in each tower were located. In each case the measured dimensions corresponded to the specified dimensions [7] for the sections in the column schedule in the structural drawings.

### 8.2.4 Lateral Bracing

A drawing by the lifting subcontractor provided to NBS by the Department of Public Safety of the State of Connecticut (obtained from the construction site) described lateral bracing to be used in the construction. The drawing entitled "Concrete Deadman Layout and Details" was approved on 12/5/85. The drawing shows the placement of deadmen in the vicinity of the exterior corners of each tower. The stated purpose of the deadmen is:

"Deadmen for attaching guy cables to grade shall be provided by the General Contractor prior to the arrival of the lifting subcontractor. Guy cables are used to maintain plumbness on the building frame during the lifting phase of erection."

It was further stated:

"Guy cable attachments to be provided in following slabs:  
Tower: Roof, 10th flr., 8th flr., 5th flr., 3rd flr., 1st flr., C Lvl; Parking: 4 Lvl., B Lvl"

There was no evidence of these deadmen or guy cables at the site. One witness interviewed following the collapse said this type of lateral bracing was not used on this job. A review of the project manual and project correspondence did not indicate any approval for elimination of this lateral bracing.

Shearwalls constructed as the slabs are lifted provide lateral support after the concrete achieves a certain strength. The structural drawings note that the shearwalls shall be 4000 psi (27.6 MPa) concrete and

"shear walls shall be cast so that no more than three equivalent floors of height of lift slab structure shall be advanced above cast top of shear wall"; also "Structure may advance when shear walls have attained 75% of design strength"

This was not the case at the time of the collapse of the structure. On April 23, 1987 the shearwalls between the ground level and level 1 on the south side of the building were being poured. The shearwalls on the north side of the building were up to level 2 (figure 4.2.1). The lift slab erection for stage IV had proceeded to five equivalent floors of height (level 1 to level 6) above the cast top of the shearwall at level 1.

#### 8.2.5 Welding

The project specifications include requirements for inspection and testing of the shop welds and field welds under the section entitled "Structural Steel Inspecting and Testing." Requirements for the shop welds include using certified welders and conducting inspections and tests as required. Types and locations of defects and work required and performed to correct deficiencies were to be recorded. All welds were to be visually inspected. Tests for fillet welds included liquid penetrant inspection and magnetic particle inspection. For complete penetration welds, tests included radiographic inspection and ultrasonic inspection. These tests were to be used at the testing agency's option. Inspection requirements for field welds were the same as those for shop welds.

In an interview provided to the State of Connecticut Department of Public Safety on June 24, 1987 the vice president of the steel fabricator indicated that no testing was done on the shop welds; he noted the welders were certified, that visual inspection was used as an ongoing process and that no ultrasonic or other type of non-destructive tests were called for in the specifications. It should be noted that the vice president of the structural engineering firm

of record for L'Ambiance Plaza waived the requirements for inspection of shop welded steel under the following conditions:

- Welders must have current certification for types and position of weld they are installing.
- Complete penetration welds must be shop inspected in accordance with the specifications.
- Fillet welds made in the shop shall be inspected when steel arrives in the field in accordance with the specifications.

This waiver was transmitted to the general contractor by the structural engineer of record on March 3, 1987 [13].

Information obtained by the State of Connecticut Department of Public Safety from the independent testing laboratory providing inspection of the welds on the job site, indicated the shop welds were visually inspected and the complete penetration field welds were ultrasonically inspected.

The General Steel Notes listed on Drawing S301 contain the following provisions that are relevant to the evaluation of the field-welded column splices:

4. All steel details and connections shall be in accordance with the requirement of the AISC Specifications (latest edition), including all supplements and revisions.
6. Field splices shall be designed to develop the full capacity of member at the point of splice in bending, shear and axial load (compression and tension) unless otherwise noted.

Column splice details are shown on Drawing TCC-2. As drawn, these details do not meet the requirements of the AISC Specification or of the AWS Structural Welding Code for prequalified complete-penetration groove-welds.

The results from the tensile coupon tests described in Section 5.4.2 and the fractographic analysis described in Section 5.4.4 raise questions about the quality of some of the welds in the structure. In some cases the strength of the welds was less than one would expect and definitely less than the strength implied by Note 6 in the General Steel Notes (Drawing S301). Visual inspections conducted in the course of this investigation indicated some of these welds did not meet the requirements of the AWS D1.1-83. It is not possible to determine the frequency with which this occurred throughout the structure based on the limited amount of weldment testing included in this investigation.

#### 8.2.6 Post-Tensioning Tendon Detail

In the vicinity of column E4.8, east-west tendons are splayed in such a way they are separated from the column by over 5 ft. The American Concrete Institute building code [2] appears to prohibit such a detail when it states in section 18.12.4 that:

"A minimum of two tendons shall be provided in each direction through the critical shear section over columns."

The report of ACI-ASCE Committee 423 [25], also suggests such a detail should be avoided. The committee states:

"Within the limits of tendon distribution that have been tested, research indicates that the moment and shear strength of two-way prestressed slabs is controlled by total tendon strength and by the amount and location of nonprestressed reinforcement, rather than by tendon distribution. While it is important that some tendons pass within the shear perimeter over columns, distribution elsewhere is not critical ..."

It may be inferred from this statement that a tendon layout such as that used near column E4.8 does not satisfy the assumption that banded tendons pass within the shear perimeter of the support.

The horizontal curvature of cables near column E4.8 is also questionable. Committee 423 specifically discourages the use of horizontally curved, banded monostrand tendons unless special reinforcement transverse to the axis of the banded tendons is provided.

## 9. ANALYSIS OF COLLAPSE

### 9.1 INTRODUCTION

A number of possible failure mechanisms were considered prior to determining the most probable cause of the collapse. These mechanisms are discussed and the basis for considering them unlikely causes for triggering the collapse is noted. The most probable cause of the collapse and the sequence of failure events are then presented.

### 9.2 REVIEW OF POTENTIAL FAILURE MECHANISMS

The following failure mechanisms leading to collapse of the building were considered: (1) lateral instability, (2) column instability, (3) floor slab failure, (4) weld failure, (5) foundation failure (6) failure due to lateral soil pressure and (7) loss of support of floor slab. Each of these mechanisms are discussed in turn.

The potential contributions of problems that occurred with respect to the floor slabs during construction and lifting as causes of the collapse were also considered. The problems included: exposure of a post-tensioning tendon during casting of a slab, accidental lifting of an extra slab and misplacement of a lifting nut while lifting a slab. Information obtained from representatives of the lifting contractor indicated that concrete was placed over the exposed post-tensioning tendon, damaged concrete in the floor slab due to accidental lifting of an extra slab was repaired using pressure injected epoxy and the damage to the shearhead caused by misplacement of a lifting nut was not serious. It was therefore considered unlikely any of these problems were the cause of the collapse.

#### Lateral Instability

The lack of external lateral bracing and the fact that construction of the shearwalls was behind the schedule called for on the erection drawings raises the question of stability of the structure under lateral loads. The analysis in Section 7.4.2 indicates that, by classical theory, the west tower had essentially no reserve capacity against sidesway buckling. When finite member size was accounted for in an approximate way, the reserve buckling capacity increased to around 6. Lateral bracing provided by the shearwalls constructed in accordance with the plans and specifications or other lateral supports (guy wires, etc) would have been consistent with good practice. It was not likely, therefore, that lateral instability was the main cause of the collapse. Evidence supports this conclusion. Eyewitnesses did not report seeing the building move laterally but rather collapse vertically toward the center of each tower. They also did not report any perceptible lateral movement at the time of collapse. Observations of the debris reported in Section 4.4 also did not indicate any evidence of significant lateral displacement of the structure.

The displacements produced by the horizontal jack used to plumb the building were small. The analysis in Section 7.4.3 indicated that the lateral load required to reduce the effect of the restoring moment associated with load transfer between the wedges exceeded the capacity of the horizontal jack. It is, therefore, not likely that the use of this jack to plumb the building initiated the collapse of the west tower.



## Column Instability

The results in Section 7.3 indicate that instability of the individual columns was not a problem. For the conditions prevailing at the time of collapse in the west tower (figure 4.3.2), the reserve capacity or ratio of the buckling loads for columns in stage IV (unsupported length = 30 ft 5 in) to the dead weight of the roof and level 12 and level 9/10/11 ranged from 2.2 to 7.8. Using the capacity reduction factor of 0.85 in the LRFD design procedure [8] reduces these to a range of 1.9 to 6.6. The unsupported length required for column buckling under these dead loads ranged from 45.6 ft (13.9 m) to 86.6 ft (26.4 m). As the failure progressed and the slabs began falling, column buckling could have occurred as the floor slabs moved down the columns or separated from the columns, thus increasing the unsupported length. As this occurs however, the slab dead load is removed, thereby reducing the probability of column buckling.

## Floor Slab Failure

The test results in Sections 5.2 and 5.5 indicate the concrete and post-tensioning strand in the floor slabs conformed to the project specifications. Also there was no indication that any freezing of the concrete had occurred in the floor slabs during curing. It is unlikely, therefore, that failure of a floor slab due to inadequate material strength caused the collapse.

The post-tensioning tendon detail in the vicinity of column E4.8 was discussed in Section 8.2.6. There are no indications that this detail led specifically to collapse of the structure, or to propagation of the collapse after it had begun. Nevertheless, in light of the recommendations discussed previously, a tendon detail such as that employed near column E4.8 should be avoided until its behavior and capacity can be established through research.

The floor slab at level C in the east tower in the vicinity of columns 9B, 9D 10B, and 10D had been damaged during lifting as noted in Section 3.4. This damage had been repaired. It was discounted as the cause of the collapse since eyewitness accounts clearly point out initiation of the failure in the upper levels of the west tower. Note that one eyewitness, the concrete pump operator (#3 in figure 4.3.3), was in the vicinity of the level C floor slab near the center of the building and did not report noticing anything relating to this slab at the initiation of failure of the building.

## Weld Failure

The laboratory tests and metallographic examination presented in Section 5.4 raise questions regarding the quality of some of the welds in the structure, both shop welds and field welds. A detailed inspection was made at the landfill of the shop welds on the weld blocks and the tack welds on the wedges supporting the roof and level 12 slabs on the west tower. Very few failures were observed of any of the welds on the weld blocks. Those that were found were located in the lower levels and were caused by extreme loads. The tack welds on the wedges obviously had failed since the roof and level 12 slabs failed as the building collapsed. The failure of these tack welds was considered a consequence of the overall failure of the building rather than the initial

cause of the collapse. Failure of a tack weld alone also would not cause the wedge to fall out. The noise one would expect to be associated with failure of a tack weld is much less than that reported by the eyewitness as occurring at the initiation of the collapse. Other weld failures including failure of the column splice at the ground level in column E4.8 were considered a result of the collapse and not the cause.

### Foundation Failure

The results in Chapter 6 indicate there was no significant settlement or rotation of the footings supporting the columns. Representatives of the lifting subcontractor also indicated there was no column for which the weld blocks were consistently low when the wedges were placed under the slabs. This would not have been the case had there been differential foundation settlement. Foundation settlement was therefore discounted as a cause of the collapse.

### Lateral Earth Pressure

The behavior of the basement wall on the north side of the building discussed in Section 4.4.5 raises the question of the effects of lateral earth pressure. The analysis in Section 7.4.4 indicates the structural elements, the connections and structure as a whole were capable of resisting these loads.

As noted previously, there was no indication of overall lateral displacement of the structure during collapse. Also, the displacement of the basement wall probably did not occur until after removal of the debris. Examination of the connection between the floor slab and the shearwall in the east tower near the center of the building did not indicate any relative movement. Lateral earth pressure was also discounted as the cause of the collapse.

### Loss of Support of Floor Slab

Tests of the lifting assembly reported in Section 5.5.5 indicated the floor slabs could lose support due to combined bending and tension failure of the jack rod or due to the lifting nut slipping off the lifting angle of the shearhead. The likely location for such a failure would be the most heavily loaded jack. As shown in figure 7.2.10a, for a level slab the jack on column E4.8 had the largest load (152 kips - 676 kN). The failure load for the lifting assembly was estimated to range from 170 kips (756 kN) to 200 kips (873 kN). Based on the 152 kip (676 kN) load on column E4.8, the reserve capacity against loss of support of the slab ranges from 1.1 to 1.3. Note that the 200 kip (873 kN) load exceeds the capacity (180 kips - 801 kN) of the lifting jack discussed in Section 7.2.2. This possibility of loss of support of the floor slab causing collapse of the building will be discussed further in Section 9.3.

### Summary

The reserve capacity or the ratio of ultimate load to the applied load provides a basis for comparison of the various failure mechanisms. A summary of these reserve capacities is given in table 9.2.1. The reserve capacities for a

punching shear failure of the slab are the highest and this failure mechanism was not considered to be a likely cause of the collapse. The reserve capacities for loss of support of the floor slab and lateral instability of the frame are the lowest. As discussed previously for each of the failure mechanisms, these reserve capacities need to be considered together with other factors (eyewitness accounts, orientation of debris) in determining the most probable cause of the collapse.

### 9.3 PROBABLE CAUSE OF COLLAPSE

Based on the review of possible failure mechanisms described in Section 9.2, the most probable cause of the collapse of the L'Ambiance Plaza building was loss of support of the package of floor slabs 9/10/11 along column line E in the west tower. More specifically, it is considered likely that this loss of support originated at either column E3.8 or E4.8.

At the time of the collapse temporary wedges were being installed under floor slab 9 (Elev. 51 ft 9 in-17 m) at column E4.8, and it is probable that the installation of these wedges required some adjustment of the elevation of the slab package at that column. Although their sections were heavier than that of column E4.8 and they were equipped with 300-kip (1334 kN) jacks, each of columns E3, E3.8, G3 and G4 carried less load than did E4.8. The nominal reaction at E4.8 due to slabs 9/10/11 was 152 kips (676 kN) which, for the erection stage, made it the most heavily loaded column in the west tower.

Using the computer model described in Section 7.2.1, it was determined that increasing the elevation of the slab package at column E4.8 by one full jack stroke of 0.50 in (12.7 mm) from its "as cast" position would involve a jack load of 201 kips (894 kN). Employees of the lifting subcontractor testified that the line pressure normally supplied by the system console ranged from 2300 to 2500 psi (15.9 to 17.2 MPa) while lifting a package of 3 slabs and that the maximum line pressure attainable was approximately 3000 psi (20.7 MPa). Allowing for a friction loss of 5 percent, the corresponding jack forces at column E4.8 normally would be 137 to 149 kips (609 to 663 kN) and the maximum force would be 179 kips (796 kN). Thus the jack at column E4.8 would have had slightly less than the required lifting capacity when operating at the upper end of the normal pressure range. It would not have developed the force required for an upward adjustment of 0.50 in (12.7 mm) from the "as cast" position, even when operating at the maximum possible line pressure. Note that the limiting jack load of 179 kips (796 kN) falls within the range of failure loads of 170 to 200 kips (756 to 889 kN) for Type P50 shearheads as discussed in Section 7.2.

The top of column E4.8 is shown in figure 9.3.1. The form of the indentations suggests that one of the jack rods lost its load, allowing the jack to roll off the column top and chamfering the edge of the web. An examination of the column showed the existence of lifting nut impact marks on each side of the web at approximately 52 in (1.32 m) below the top of the column. These impact marks are an indication that each of the lifting nuts "kicked out" from under the lifting angles on the shearhead at slab 9. The bottom surfaces of the lifting angles are shown in figure 9.3.2. The bearing surface on the left clearly shows the lifting nut contact area. The contact area on the right is

not so sharply defined, but there is evidence that the lifting nut kicked out from under the lifting angle.

Whether loss of the jack at column E4.8 was the cause of the collapse or simply one of its effects cannot be established with certainty, but there is at least one other sequence of events that could have produced the same result. If an upward adjustment exceeding the capability of the jack at column E4.8 was required, it is possible that the 300-kip (1334 kN) jack at column E3.8 was used to effect this adjustment. Again assuming an operating line pressure of 2500 psi (17.2 MPa), the jack at column E3.8 could have developed a lifting force of approximately  $2 \times 149 = 298$  kips (1.33 MN). A full-stroke upward displacement of 0.50 in (12.7 mm) at column E3.8 would have developed a reaction of about 190 kips (845 kN) and, therefore, the jack could easily have produced this force within the limit of its stroke.

As has been noted in the discussion of test results in Section 5.5.5, a jack load of 190 kips (845 kN) acting on the type X51 shearheads of column E3.8 would produce very significant rotations of the lifting angles, possibly leading to kick out of one or both of the lifting nuts. The bottom surfaces of the lifting angles of the shearhead at slab 9, column E3.8, are shown in figure 9.3.3. The marks on these surfaces show that kick out did indeed occur. This sudden release of energy would be expected to raise dust from the surfaces of the concrete slabs and the noise associated with the kick out experienced in the lifting assembly tests described in Section 5.5.5 could readily be described as steel breaking under stress. This is consistent with the eyewitness accounts (#3 and #4 - figure 4.3.1). The surviving witness working at column E4.8 at the time of the collapse (#14 - figure 4.3.1) noted that the first indication of a problem was a loud noise either right above his head (E4.8) or more towards the center of the slab (E3.8). Due to load redistribution, loss of a jack at either E3.8 or E4.8 would lead to failure of the other jack. As floor slabs 9/10/11 moved downward, the shears and moments in the slabs adjusted to the new support conditions. Because the post-tensioning tendons now were located in the compression side of the slabs, the tendons adjacent to columns E3.8 and/or E4.8 became ineffective and flexural cracks developed in the bottom face of the slabs. This explains the sudden appearance of cracks in the slab directly above the workmen who were installing wedges at column E4.8. The underside of shearhead 10, column E3.8, is shown in figure 9.3.4 and that of shearhead 11 is shown in figure 9.3.5. It appears that one of the lifting nuts glanced off of the web and became partially lodged under shearhead 10. As the slabs moved downward due to loss of support at column E3.8, the lifting nut was again kicked out from under a lifting angle. The imprint on the underside of shearhead 11 suggests that this process was repeated for a third time. It was not possible to confirm this sequence of events with lifting nut impact points on the web because the top section of column E3.8 could not be positively identified. The likely progression of the collapse through the upper levels of the west tower is described in the following paragraphs.

In order for load redistribution to have taken place, the slab would have had to redistribute forces after the loss of support at a single column. To determine if the slab capacity was sufficient to allow redistribution to take place following loss of support at a single column, yield line analyses were

performed considering loss of support at either column E3.8 or E4.8. For each analysis, it was conservatively assumed that force in all post-tensioning tendons would be ten percent less than the tendon force used for design of slabs. Positive moment capacity of the slabs was neglected for each analysis. Simple yield mechanisms and a virtual work solution method were used to determine distributed load capacity of the slabs. These analyses showed clearly that the floor slabs would be able to distribute loads much larger than the dead weights of the slabs, regardless of whether support was lost initially either at column E3.8 or column E4.8.

#### 9.4 PROBABLE SEQUENCE OF COLLAPSE

It is difficult to accurately predict how the initial failure propagated through the structure because of the unknown dynamic loads and load redistribution that occurred during the collapse. The failure sequence postulated is a best estimate based on eyewitness accounts and observations of the debris.

The probable sequence of collapse is indicated in figure 9.4.1. With the loss of support of slabs 9/10/11 at column E3.8 and/or E4.8, it is likely that the remaining jacks on this line shed their load by kick out of one or both lifting nuts as the loads were redistributed. Calculations of the ultimate strength of the floor slab with the loss of support at either column E4.8 or E3.8 using a yield line approach indicated the slab could support its own weight if only one of these supports were lost. For the initial failure to progress, therefore, it was necessary for additional supports to be lost. This loss of support along the E line is in agreement with observed marks on the stage IV column extensions and on the shearhead lifting angles (See Appendix A, columns E1, E2 and E3). It is also likely that some loss of prestress in the tendons along and normal to E line accompanied this load redistribution. Calculations indicate, for example, that loss of the drape in the tendons in the east-west direction would decrease the post-tensioning by 10 to 15 percent. At approximately this same time a negative moment crack would have developed along the length of the west tower just to the north of G line due to the clear span between lines C and G. With loss of support along the E line, the span of the slab in the north-south direction increases by 140 percent (C-E-G-H to C-G-H). The negative moment at the G line about an axis parallel to the G line in the east-west direction increases by a factor of approximately 3.6. Analysis of a unit width of slab indicates this negative moment exceeds the ultimate moment capacity of the slab (14.6 kip-ft/ft vs 9.6 kip-ft/ft) (64.9 vs 42.7 kN-m/m). On the north side of E line, slabs 9/10/11 caused bending in the C-line columns with portions of the floor slabs being held in place by the conventional reinforcing around the columns. This is clearly illustrated by the distortion of shearheads 9/10/11 at column C4.8 as shown in figure 4.4.34. Also, it is apparent from figure 4.4.34 that during the progression of failure of slabs 9/10/11 along column lines C and E, the two slabs at the top of the building (12/roof) remained intact. This is the reason for the reverse curvature at the very top of column C4.8. Along column line E the falling debris from floor slabs 9/10/11 caused the progressive failure of floor slabs at the lower levels with the result that shearheads on the interior columns along this line ended up closely stacked above level 1.

A different mechanism is believed to have been involved with the progression of the failure along G line and south to column line H. Neither column lines G or H involved the failure of jacks as slabs 9/10/11 had been temporarily wedged and the lifting nuts had been removed from the jack rods in preparation for the next lift. An inspection of the column tops (stage IV) from these two lines revealed that very little scraping or gouging occurred during the collapse and, with the exception of the columns in lines 1 and 6, the shearheads released cleanly and slid straight down. At columns G6, H1 and H6 the shearheads at the upper levels did not release cleanly and some local bending of columns resulted. To a lesser degree, this also happened at column H2. The bending moment about G line, and eventually about H line, would have led to progressive loss of the wedges under floor slab 9. This action would have been augmented by the racking forces produced by the transverse (north-south) tendons with the effect that wedges also were lost under floor slab 12 along column lines G and H. The analysis in Section 7.4.2 also indicated that the slab would lift off one wedge at each column at small lateral displacements. This lift off could be followed by the wedges being lost.

Laboratory tests conducted on a column segment with a pair of weld blocks as described in Section 5.5.4 showed that the tack welds fail at small increases in load and that a wedge can be "rolled out" from under a shearhead at a load on the wedge of from 100 to 150 kips (445 to 667 kN) with very little distortion of the weld block. This is consistent with the marks on the stage IV columns recovered for column lines G and H between lines 2 and 5. It is also consistent with the orientation of the floor slabs in this same region as can be seen from photographs taken shortly after the collapse and prior to any substantial removal of debris (Section 4.4.1). The absence of scrapes and gouges on the stage IV column extensions along these two lines and the extensive damage to the stage IV extensions along C line strongly suggest that failure of the upper two floor slabs (12/roof) initiated in the south sector of the west tower.

The failure sequence described is consistent with several of the eyewitness accounts. The surviving witness working at column E4.8 at the time of the collapse noted that after he heard the loud bang, the ceiling directly over his head (underside of slab 9) was cracking just like ice breaking. Loss of support at E3.8 and/or E4.8 would account for this. Another witness (#11 in figure 4.3.1) located approximately 100 yd (91 m) south of the site heard several loud noises in rapid succession prior to the collapse. Other witnesses in the building offered similar testimony. This succession of noises is consistent with the progression of the lifting assembly failures along E line.

Cracking of floor slabs 9/10/11 between the E line columns and cracking along the G line involves failure in the center portion of the building. This agrees with the discussion in Section 4.4.1 in which the debris formed a heap in the center of each tower. Note the post-tensioning cables also tend to pull the columns inward in this fashion. The following witness observations also relate to failure of the center portion:

1. Witness No. 10. - located on the southside of the building on the parking garage
  - o "The roof floors caved into the center of the slabs and they all fell on top of the other."
2. Witness No. 13 - jumped from ground floor and observed collapse while running from building
  - o Observed two columns, the column at the extreme west corner (C1) and the column next to it (C2) on the Washington Ave. side bend towards the center of the building. He then observed the center of the slab drop and the edges of the slab raise up.
3. Witness No. 15 - welding wedges on level 3 or 4 at southeast corner of the east tower.
  - o Heard a loud cracking sound like a rifle shot magnified
  - o Observed large pieces of flooring coming down in the west tower.

The concrete pump truck operator's observations given in Section 4.3 relate to the collapse of the upper floor slabs south of the G line. He noted the two uppermost slabs in the vicinity of the southwest corner (column H1) started downward and then slowed momentarily (struck slabs 9/10/11). The collapse then spread eastward and northeastward throughout the uppermost slabs and then the building collapsed vertically.

The most probable cause of the initiation of the collapse of the east tower is less clear. Several possibilities exist. The possibility that debris from the west tower attacked the columns along line 7 was considered. Observation of the columns did not indicate this occurred. Three other mechanisms appear equally possible. First, the pour strips in place at the time of collapse could have transmitted destructive forces from the west tower into the east tower. Counterclockwise twisting of several of the columns in the lower levels of the east tower and a force directed from west to east on the exterior shear wall on the south face of the east tower were noted in Section 4.4.1. These observations are consistent with this possibility. Second, falling debris near the west end of column line D could have damaged the tendon anchorages in the east tower floor slabs at this location. With loss of anchorage in one or more floor slabs, the progression of failure would have been very similar to that described for column line E in the west tower. One eyewitness, the concrete pump truck operator located near the southeast corner of the west tower, reported the east tower collapsed as a result of being struck by sections of the collapsing west tower. Third, forces exerted by falling debris from the west tower could have caused lateral displacements of the east tower large enough to overcome the restoring moments discussed in Section 7.4.2. Loss of wedges supporting the floor slabs would follow. This loss of support could propagate through the floor slabs in the east tower in a manner similar to that discussed for the slabs at level 9/10/11 in the west tower.

Collapse of the east tower could have involved a combination of these three possibilities. Clearly it becomes more difficult to identify the exact sequence of events as failure progresses and force redistribution within the structure becomes more complex. The probable cause of the collapse discussed in Section 9.3 and the eyewitness accounts make it clear, however, that the collapse started in the west tower and progressed to the east tower.



TABLE 9.2.1

SUMMARY OF RESERVE CAPACITIES FOR VARIOUS FAILURE MECHANISMS

Condition Investigated	Failure Mechanism	Reserve Capacity Range*
Floor slab dead weight	Punching shear (Section 7.2.2)	4.0-23.1
-----		
Lateral Earth Pressure on Basement Wall	Shear failure of Shear wall (Section 7.4.4)	1.4
	Connection between floor slab and shear wall (Section 7.4.4)	1.7 - 1.9
	Sliding of Shear wall footing (Section 7.4.4)	1.3-2.7
-----		
Stability	Buckling of Individual Column (Section 7.3)	2.2-7.8
	Lateral Stability of Frame (Section 7.4.2)	1.1 (5.6)** (East- West) 1.2 (North-South)
-----		
Loss of Support of floor slab	Jack rod failure, bottom nut sliding off (Section 5.5.5)	1.1-1.3
-----		

\* Calculated or measured ultimate load

-----  
Applied load on structure

\*\* based on restoring moment effect



Figure 9.3.1 Indentation in top of column E4.8



Figure 9.3.2 Indentations in underside of lifting angles, column E4.8, level 9



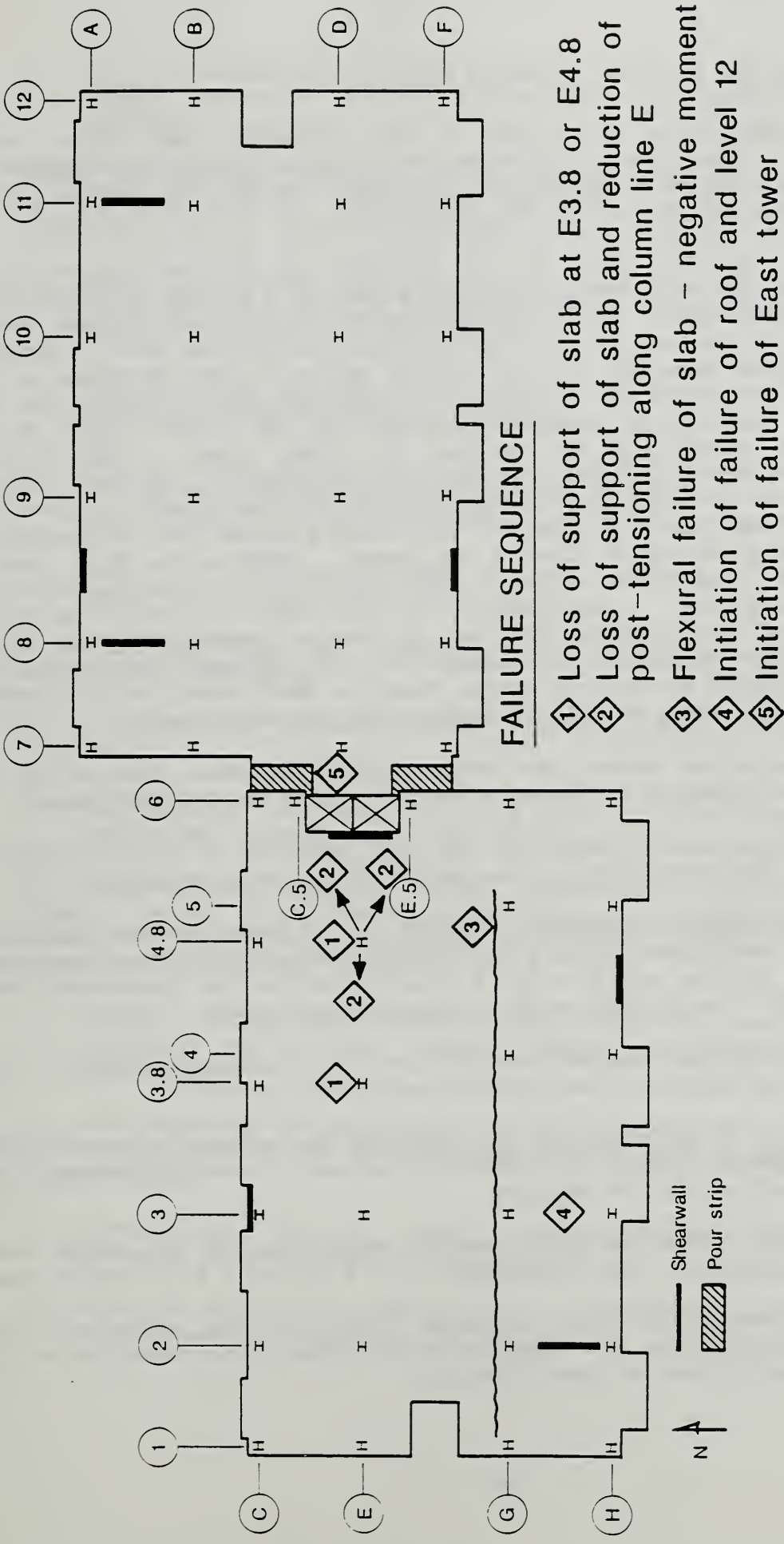
Figure 9.3.3 Indentations in underside of lifting angles, column E3.8, level 9



Figure 9.3.4 Indentation in underside of lifting angle, column E3.8, level 10



Figure 9.3.5 Indentation in underside of lifting angle, column E3.8, level 11



- FAILURE SEQUENCE**
- ① Loss of support of slab at E3.8 or E4.8
  - ② Loss of support of slab and reduction of post-tensioning along column line E
  - ③ Flexural failure of slab - negative moment
  - ④ Initiation of failure of roof and level 12
  - ⑤ Initiation of failure of East tower

Figure 9.4.1 Probable failure sequence

## 10. CONCLUSIONS

The following conclusions are based on the laboratory and field tests, computer analyses, the witness interviews and review of the project documentation conducted by the National Bureau of Standards during the course of the L'Ambiance Plaza building collapse investigation:

1. The most probable cause of the collapse was failure of the lifting system in the west tower during placement of a package of three upper level floor slabs. The failure most probably began below the most heavily loaded jack (column E4.8) or an adjacent jack (column E3.8). Excessive deformations occurred in the lifting angle of the shearhead at the location of the initial failure. This was followed by one of the jack rods in the lifting assembly slipping off the lifting angle in the shearhead supporting the package of three slabs. This failure mechanism was duplicated in laboratory experiments. The local failure propagated as loads were redistributed and the remaining jack rods along column line E slipped off the lifting angles and the package of three slabs failed in flexure and shear. These slabs fell, causing the lower level slabs to fail. This resulted in the collapse of the entire west tower. Consequently, the east tower collapsed due to one or more of the following factors: (a) forces transmitted to it by the west tower collapse, (b) damage to the unbonded post-tensioning tendons caused by falling debris from the west tower, or (c) lateral instability caused by falling debris from the west tower.
  - (a) Calculations showed that these supports (hydraulic jacks at the time of collapse) were the most heavily loaded in the west tower.
  - (b) An eyewitness account of the slab behavior at this location at the time of failure is consistent with loss of support.
  - (c) This failure mechanism occurred in laboratory tests simulating the conditions existing in the structure at the time of collapse. The failure resulted in a loud noise in the laboratory tests which is consistent with the eyewitness reports.
  - (d) The computed reserve capacity for this failure mechanism is one of the lowest of the possible mechanisms analyzed.
2. The quality of materials in the structure was generally in accordance with the project plans and specifications and did not play a significant role in initiating the collapse.
  - (a) Tensile properties and chemical composition of the column steel satisfied the ASTM requirements for A 36 and A 572 Grade 50 steel.
  - (b) The results of tests of cores from the floor slabs and shear walls indicated the compressive strengths of the concrete met the project plans and specifications.



- (c) Yield strength and breaking strength values of the post-tensioning strand generally satisfied the ASTM requirements for steel strand.
3. There were a number of deviations from the project plans and specifications in the structure as built, but the investigation indicated these deviations did not play a significant role in initiating the collapse.
- (a) Data from borings and test pits indicated a number of footings rest on layers of fill and disintegrated rock rather than "rock of suitable quality" or lean concrete.
  - (b) The strength of some of the welds was less than the strength implied in the structural drawings.
  - (c) Column splice details shown on the plans do not meet the requirements of the AISC Specification or of the AWS Structural Welding Code for prequalified complete-penetration groove-welds.
  - (d) Lack of joint penetration and large amounts of porosity were observed in some of the field welds.
4. It is unlikely that the horizontal jack used to plumb the structure initiated the collapse.
- (a) Displacements produced by the jack in plumbing the building were small.
  - (b) The maximum load the jack could apply to the structure was not sufficient to cause inelastic action.
5. The reserve capacity against lateral instability was small. It does not appear, however, that lateral instability was the initial cause of the collapse. Inadequate resistance to lateral instability may have caused the collapse of the east tower.
- (a) Deadmen and guy cables whose purpose would have been to plumb the building and provide lateral bracing were not used in the construction.
  - (b) The height of the structure above the cast top of the shear walls at the time of collapse was greater than three equivalent floors of height.
  - (c) Eyewitnesses did not report seeing or feeling any lateral movement at initiation of the collapse.
  - (d) Observations of the debris did not indicate any overall lateral displacements or drift in the collapse.

6. It is unlikely that lateral earth pressure acting against the basement wall on the north side of the structure caused the building to collapse.
  - (a) Calculations indicated that the capacities of: (1) the connections between the floor slabs and shearwalls, (2) the shearwalls and (3) the resistance of the shearwalls to sliding over their base were sufficient to resist the lateral soil pressure.
  
7. It is unlikely that differential foundation settlements caused the building to collapse.
  - (a) Data from the subsurface explorations indicate that differential foundation settlements not exceeding  $3/4$  in (19 mm) could have occurred during construction. These are not considered excessive for this type of structure. The greater part of these settlements occurred early in the erection process.

## 11. ACKNOWLEDGEMENTS

Regional and area officers of the Occupational Safety and Health Administration provided continued support throughout this investigation. The OSHA team posted in Bridgeport, Connecticut following the collapse were very helpful in handling the logistics for the NBS investigation, obtaining documents relating to the collapse and dealing with legal issues. The support of John Miles, Regional Administrator, Ronald Morin and John Stanton, Area Directors and the following OSHA staff: Joseph Normand, Edward Eagan, William Freeman, Romas Bossone, Thomas Guilmartin and Kang Yi is gratefully acknowledged.

The Department of Public Safety of the State of Connecticut provided copies of the documents relating to the construction including construction logs, testing reports, design drawings and shop drawings. Lieutenant Edmund Dunstone, Executive Officer, Bureau of State Fire Marshal and Safety Services and Leo Belval, State Building Inspector supplied this information and provided copies of video tapes of the collapse site taken during the rescue efforts and interviews of witnesses taken by the State Police during the subsequent investigation.

Morris Schupack, Mario G. Suarez, Dr. Randall W. Poston and Daniel J. McCarthy of Schupack Suarez Engineers Inc. in Norwalk, Connecticut participated with NBS in conducting the investigation. They provided field support in data collection, interpretation of design and construction practices relating to lift slab construction and analysis of the post-tensioned concrete slabs.

Clive DeVault from Schnabel Engineering Associates conducted the subsurface exploration, and together with Raymond deStephen, prepared the geotechnical engineering report in Appendix B. Connecticut Test Borings, Inc. performed the test borings and J. E. Barrett and Sons dug the test pits.

Neil Moreton, N.S.M. Co. Inc., provided an assessment of the welding practices and quality of the welding details.

T. Robert Shives, Dr. Richard J. Fields, Charles E. Brady, Leonard C. Smith and Dr. Thomas Siewert of the NBS Institute for Materials Science and Engineering and John Norris of the National Measurement Laboratory provided assessments of the material properties of welding details. Dr. William Stone assisted in developing the computer models and in conducting the structural analyses. Stuart Foltz prepared the drawings of the column deformations in Chapter 4. Frank Rankin, Jim Little and Herb Wechsler assisted in performing the structural laboratory tests. Dr. Nicholas J. Carino and Dr. H. S. Lew provided a comprehensive review of the report. Nancy Fleegle typed the report with great care.

## 12. REFERENCES

1. Lew, H.S., Fattal, S. G., Shaver, J. R., Reinhold, T. A., Hunt, B. J., "Investigation of Construction Failure of Reinforced Concrete Cooling Tower at Willow Island," West Virginia, NBSIR 78-1578, National Bureau of Standards, Washington, D.C., November, 1979.
2. "Building Code Requirements for Reinforced Concrete," ACI 318-83, American Concrete Institute, Detroit, MI, 1983.
3. "Lift Slab - The Modern Construction Method, Quality-Speed-Economy," Texstar Construction Corporation Publication, undated.
4. Carino, N. J., and Lew, H. S., "Re-examination of the Relation Between Splitting Tensile and Compression Strength of Normal Weight Concrete," ACI Journal, Proceedings Vol. 79, No. 3, May-June 1982, pp. 214-219.
5. "L'Ambiance Plaza Residential Apartment Building, Project Manual," TPM International Inc., Darien, CT, undated.
6. "Annual Book of ASTM Standards," Vols. 01.01, 01.04 AND 04.02, American Society for Testing and Materials, Philadelphia, PA, 1986, 1987.
7. Manual of Steel Construction, American Institute of Steel Construction, 8th Edition, Chicago, IL, 1981.
8. Load and Resistance Factor Design Specification for Structural Steel Buildings, American Institute of Steel Construction, 1st Eddition, Chicago, IL., September 1, 1986.
9. "Stress Analysis Module Primer," Publication #D005, PDA Engineering, 1560 Brookhollow Drive, Santa Ana, CA, Jan. 1985.
10. Lin, T. Y., "Load-Balancing Method for Design and Analysis of Prestressed Concrete Structures," Journal of the American Concrete Institute, Proceedings, V. 60, No. 6, Detroit, MI, June 1963, pp. 719-742.
11. "PATRAN User's Guide," PDA Engineering Software Products Division, 1560 Brookhollow Drive, Santa Ana, CA, undated.
12. Gross, J. L., Hambacher, D. G., "Analysis of Partially Erected Structurers", Proceedings of the 8th Conference on Electronic Computation, ASCE, Houston, Texas, American Soc. of Civil Eng., New York, NY, Feb. 1983.
13. Correspondence from structural engineer to general contractor dealing with inspection of shop welded steel, dated March 3, 1987.
14. American National Standard A58.1-1982, "Minimum Design Loads for Buildings and Other Structures," American National Standards Institute, 1430 Broadway, New York, NY 10018.

15. Russillo, Michael A., "Lift Slab Construction: Its History, Methodology, Economics and Applications", unpublished draft report.
16. Deere, D. U. and Miller, R. P., "Classification and Index Properties of Intact Rock," Tech. Special Report AFWL-TR-65, AF Special Weapons Center, Kirtland AFB, 1966.
17. Gardner, W.S., "Design of Drilled Piers in the Atlantic Piedmont, Foundations and Excavations in Decomposed Rock of the Piedmont Province," Geotechnical Special Publication No. 9, ASCE, New York, NY, April 1987.
18. Martin, R. E., "Settlement of Residual Soils, Foundations and Excavations in Decomposed Rock of the Piedmont Province," Geotechnical Special Publication No. 9, ASCE, New York, NY, April 1987.
19. Bowles, J. E., "Elastic Foundation Settlements on Sand Deposits," J. of Geotechnical Engineering, ASCE, Vol. 113, No. 8, August, 1987, p. 854.
20. deMello, V., "The Standard Penetration Test - A State-of-the-Art Report," 4th Pan Am. Conference on Soil Mechanics and Foundation Engineering, Puerto Rico, 1971.
21. Meyerhof, C. G., "Penetration and Bearing Capacity in Cohesive Soils," J. Soil Mechanics and Foundation Div. ASCE, Vol. 82, No. SMI, Jan. 1956.
22. "Lift-Slab Concrete Construction," Data Sheet 514, Revision A, National Safety Council, 444 North Michigan Avenue, Chicago, IL, 1974.
23. Jaky, J., "Pressure In Silos," 2nd Conference of ICSMFE, Vol. 2, pp 103-107, 1948.
24. Bowles, J. E., Foundation Analysis and Design, 3rd Edition, McGraw Hill, 1982.
25. "Recommendations for Concrete Members Prestressed with Unbonded Tendons," ACI-ASCE Committee 423, ACI 423.3R-83, 1983, 16 pp.
26. ANSI/AWS D1.1-83, Structural Welding Code-Steel, American Welding Society, Miami, Fla.

APPENDIX A

Detailed Observations of Stage IV Columns - West Tower

## APPENDIX A

### DETAILED OBSERVATIONS OF STAGE IV COLUMNS - WEST TOWER

COLUMN NO - C1  
 SECTION - HP 10X42  
 SHEARHEAD TYPE - A50  
 LENGTH - 19'-9" (FRACTURED AT STAGE III/IV SPLICE)  
 MARK - 1C  
 TACK WELDS - 1 SET ABOVE TOP WELD BLOCK  
 SHEARHEADS - NONE  
 COMMENTS: GRADUAL BEND TO SOUTH ABOUT WEAK AXIS AT LEVEL OF TOP SEAL BLOCK. SHEARHEADS 9-R APPEAR TO HAVE SLID OFF TOP OF COLUMN. UPWARD (NORTH SIDE) AND DOWNWARD (SOUTH SIDE) BITE MARKS ON FLANGE EDGES NEAR TOP OF COLUMN DUE TO SHEARHEAD RACKING. COLUMN BUCKLED APPROX 3 FT ABOVE LEVEL 1. LIFTING NUT INDENTED WEB ON SOUTH SIDE (NORTH SIDE WAS NOT INSPECTED). THREAD MARKS FROM JACK ROD ON NORTH SIDE OF WEB AT COLUMN TIP AND JACK FOOTPRINT ON TOP OF COLUMN INDICATE JACK ROLLED OFF OF COLUMN TOP TO THE SOUTH. NO VISIBLE DAMAGE TO WEDGE CONTACT SURFACES ON UPPER WELD BLOCKS.

COLUMN NO - C2  
 SECTION - HP 12X53  
 SHEARHEAD TYPE - C50  
 LENGTH - 19'-2"  
 MARK - 2C  
 TACK WELDS - 1 SET ABOVE TOP WELD BLOCK  
 SHEARHEADS - 5 IN PLACE (9-R)  
 COMMENTS: TWO SHEARHEADS ARE LOCATED BETWEEN THE TACK WELDS AND COLUMN TOP. THREE SHEARHEADS ARE LOCATED DIRECTLY BELOW TACK WELDS. COLUMN BUCKLED APPROX 3 FT ABOVE LEVEL 2. SLIGHTLY DEFORMED HEADER CHANNEL OF SHEARHEAD AT LEVEL 11 SUGGESTS CANTILEVER ACTION OF FLOOR SLAB. MARKS FROM LIFTING NUTS ARE VISIBLE ON UNDERSIDE OF SHEARHEAD AT LEVEL 9. EAST SIDE HAS ONLY A ROUND MARK (NO INDENTATION) WHILE THE WEST SIDE IS INDENTED SOMEWHAT LESS THAN 1/16 INCH. EAST SIDE OF WEB INDICATES SOME SCRAPING BY LIFTING NUT, BUT CONTAINS NO CLEARLY DEFINED INDENTATION DUE TO IMPACT. A JACK FOOTPRINT IS VISIBLE ON THE TOP SURFACE, ALONG WITH SMALL GOUGES ON WHAT IS BELIEVED TO BE THE NORTH FLANGE.

COLUMN NO - C3  
 SECTION - W 12X65  
 SHEARHEAD TYPE - W50  
 LENGTH - 20'-8"  
 MARK - 3C-4L-11  
 TACK WELDS - 1 SET ABOVE TOP WELD BLOCK  
 SHEARHEADS - 3 IN PLACE (9-11)  
 COMMENTS: COLUMN IS BENT ABOUT STRONG AXIS APPROX 1 FT ABOVE THE STAGE III/IV SPLICE. GRADUAL BEND TO EAST ABOUT WEAK AXIS NEAR TOP OF SEAL BLOCK. THE THREE SHEARHEADS (9, 10, 11) ARE CLUSTERED BETWEEN TOP WELD BLOCK AND LEVEL 6. SHEARHEADS 12 & R APPEAR TO HAVE SLID OFF TOP OF COLUMN. GOUGES IN NORTH FLANGE START AT TOP OF

SEAL BLOCK AND EXTEND UPWARD 7 3/8 INCHES. THESE APPEAR TO HAVE BEEN CAUSED BY THE LEVEL 10 SLAB DURING LIFTING. THE HEADER CHANNEL ON THE NORTH SIDE OF ALL THREE SHEARHEADS IS BENT OUTWARD, INDICATING CANTILEVER ACTION OF THE FLOOR SLABS. THE THIRD SHEARHEAD FROM THE TOP (LEVEL 9) SHOWS IMPRINTS OF THE LIFTING NUTS IN UNDERSIDE OF THE LIFTING ANGLES. THE EAST SIDE OF THE SHEARHEAD SHOWS A DOUBLE NUT IMPACT AS THE LIFTING NUT WORKED TOWARD THE EDGE OF THE LIFTING ANGLE. THE WEST SIDE SHOWS A CONTINUOUS GROOVE CAUSED AS THE LIFTING NUT SLID OFF THE LIFTING ANGLE. THE TIPS OF THE WEST ROD SLOT ARE BENT UPWARD APPROX 1/2 INCH. ALL THREE SHEAR HEADS HAVE A TEAR IN THE WELD BETWEEN THE LIFTING ANGLE AND THE HEADER CHANNEL. JACK ROD INDENTATION IS VISIBLE AT THE JUNCTURE OF THE WEST SIDE OF THE WEB AND THE NORTH FLANGE. FOUR UPWARD GOUGES AND FOUR DOWNWARD GOUGES ON EDGES OF FLANGES BETWEEN TOP WELD PLATE AND TOP OF COLUMN DUE TO SHEARHEAD RACKING. COLUMN BUCKLED JUST BELOW LEVEL 2.

COLUMN NO - C3.8  
SECTION - W 12X65  
SHEARHEAD TYPE - G50  
LENGTH - 6'-2"  
MARK -  
TACK WELDS - 1 SET ABOVE TOP WELD BLOCK  
SHEARHEADS - 3 IN PLACE

COMMENTS: DEFORMED SHAPE OF COLUMN SUGGESTS CANTILEVER ACTION BY SLABS 9-11 WHILE SLABS 12-R REMAINED IN PLACE. THE TOP OF THE COLUMN CONTAINS A JACK FOOTPRINT, DEEPER ON THE EAST SIDE THAN ON THE WEST. THERE ARE NO VISIBLE INDENTATIONS IN THE WEB DUE TO LIFTING NUT IMPACT.

COLUMN NO - C4.8  
SECTION - HP 12X53  
SHEARHEAD TYPE - C50 (ROOF - L50)  
LENGTH - 17'-6"  
MARK - C  
TACK WELDS - 1 SET ABOVE TOP WELD BLOCK  
SHEARHEADS - 4 IN PLACE (9-12)

COMMENTS: TWO SETS OF GOUGE MARKS ON NORTH FLANGE AT SEAL BLOCK AND JUST ABOVE SEAL BLOCK ARE ASSUMED TO HAVE BEEN CAUSED BY SLABS 9 AND 10 DURING JACKING OPERATION. FOUR SHEARHEADS REMAIN ON THIS SECTION, TWO BELOW THE SEAL BLOCK AND TWO ABOVE. LOCAL BENDING OF COLUMN FLANGES AND HEADER CHANNEL DUE TO CANTILEVER ACTION OF SLABS 9-11. THIS RESULTED IN GRADUAL BEND IN COLUMN ABOUT THE STRONG AXIS AT LEVEL 6. TOP SECTION WAS RESTRAINED BY SLABS 12-R, PRODUCING A REVERSED CURVATURE ABOVE LEVEL 6. THE FOURTH SHEARHEAD FROM TOP SHOWS MARKS FROM LIFTING NUTS AND IS BELIEVED TO BE LEVEL 9. NUT IMPRINT ON BOTTOM OF SHEARHEAD 9 ON EAST SIDE IS CLEAR. NUT DOES NOT APPEAR TO HAVE SLIPPED OFF. NUT ON WEST SIDE APPEARS TO HAVE SLIPPED OFF IN DIRECTION OF WEB. SHEARHEAD FROM LEVEL 11 BIT INTO EDGE OF FLANGE DURING RACKING. FOUR FT SECTION OF JACK ROD RUNS FROM TOP OF COLUMN DOWN TO SEAL BLOCK AND IS COMPLETE WITH LIFTING NUT AND SLEEVE. UPPER END OF ROD HAS



BEEN FLAME-CUT. TOP OF COLUMN SHOWS INDENTATION FROM JACK ROTATING ABOUT WEAK AXIS OF COLUMN. MARKS INDICATE JACK ROLLED TO EAST AS IT LEFT TOP OF COLUMN. THERE ARE NO VISIBLE INDENTATIONS IN THE WEB DUE TO LIFTING NUT IMPACT.

COLUMN NO - C6  
SECTION - W 8X35  
SHEARHEAD TYPE - J50  
LENGTH - COLUMN TOP NOT IDENTIFIED

COLUMN NO - C.5  
SECTION - W 12X65  
SHEARHEAD TYPE - L50  
LENGTH - 5 FT  
MARK - V  
TACK WELDS - 1 SET ABOVE WELD BLOCK  
SHEARHEADS - NONE

COMMENTS: JACK FOOTPRINT IS CLEARLY VISIBLE IN TOP OF COLUMN. THERE ARE NO VISIBLE INDENTATIONS IN THE WEB DUE TO LIFTING NUT IMPACT.

COLUMN NO - E1  
SECTION - W 10X60  
SHEARHEAD TYPE - B50  
LENGTH - 23 FT  
MARK - 1E  
TACK WELDS - 1 SET ABOVE TOP WELD BLOCK  
SHEARHEADS - 5 IN PLACE (9-R)

COMMENTS: GOUGE MARK LOCATED ON WEST FLANGE BEGINS AT TOP OF UPPER SEAL BLOCK AND APPEARS TO HAVE BEEN CAUSED BY SHEARHEAD 10 DURING LIFTING. COLUMN HAS GRADUAL BEND TO THE NORTH ABOUT WEAK AXIS APPROX 11 FT BELOW COLUMN TOP. WEST FLANGE HAS LOCAL DAMAGE THAT APPEARS TO HAVE BEEN CAUSED BY CANTILEVER ACTION OF SLABS 10 AND 11. SOUTH JACK ROD MADE CHAMFER MARK AT TOP OF THE WEB AND THE LIFTING NUT LEFT INDENTATIONS AT THE TIPS OF THE ROD SLOT IN SHEARHEAD 9. THIS SAME LIFTING NUT LEFT IMPACT MARK ON SOUTH SIDE OF WEB. NORTH LIFTING NUT INDENTED THE UNDERSIDE OF THE SHEARHEAD BUT LEFT NO MARKS INDICATING KICKOUT OF NUT. FOOTPRINT OF JACK VISIBLE ON TOP OF COLUMN INDICATES BOTH JACK RODS WERE HEAVILY LOADED. COLUMN BUCKLED TO EAST APPROX 4 FT BELOW THE STAGE III/IV SPLICE.

COLUMN NO - E2  
SECTION - W 12X106  
SHEARHEAD TYPE - P50 (ROOF - AA51)  
LENGTH - 14'-1"  
MARK - U  
TACK WELDS - 1 SET ABOVE TOP WELD BLOCK  
SHEARHEADS - NONE

COMMENTS: THIS SECTION IS VERY STRAIGHT WITH NO GOUGE MARKS ON FLANGES AND THERE IS NO CLEAR SIGN OF A JACK FOOTPRINT ON THE COLUMN TOP. IMPACT OF THE LIFTING NUTS CAUSED INDENTATIONS ON EACH SIDE OF THE WEB. THE UPPER SEAL BLOCKS WERE DAMAGED BY THE SHEARHEADS AS THEY SLID DOWN THE COLUMN. THE NEXT LOWER COLUMN SEGMENT WAS IDENTIFIED BY MATCHING THE CUTOFF SURFACES. THIS SEGMENT IS 12'-

10" LONG (5'-7" FROM STAGE IV AND 7'-3" FROM STAGE III) AND CONTAINS FOUR SHEARHEADS IDENTIFIED AS LEVELS 10,11,12, R.

COLUMN NO - E3  
SECTION - W 12X120  
SHEARHEAD TYPE - X51  
LENGTH - 11'-3"  
MARK - 3E  
TACK WELDS - 1 SET ABOVE TOP WELD BLOCK  
SHEARHEADS - NONE

COMMENTS: THIS SECTION IS BENT SLIGHTLY TO THE SOUTH ABOUT THE WEAK AXIS. NO UPWARD SCRAPING MARKS OR GOUGES ARE VISIBLE. ANOTHER SECTION OF THIS COLUMN IS LOCATED ADJACENT TO THE TOP SECTION. IT ALSO IS BENT ABOUT THE WEAK AXIS AND CONTAINS 14 SHEARHEADS. THE 14 SHEARHEADS ARE STACKED AT LEVEL C AND INCLUDE LEVEL 12. THE UNDERSIDE OF SHEARHEAD 9 HAS A DEEP TRACK ON THE SOUTH LIFTING ANGLE WHERE THE LIFTING NUT SLID OFF AND THE SOUTH SIDE OF THE WEB CONTAINS AN IMPACT MARK FROM THE LIFTING NUT. THE LIFTING ANGLE ON THE NORTH SIDE EXHIBITS A DOUBLE SET OF LIFTING NUT INDENTATIONS AND THE WEB EXHIBITS 3 NUT IMPACT MARKS AT 50 TO 53 INCHES FROM THE TOP OF THE COLUMN.

COLUMN NO - E3.8  
SECTION - W 12X120  
SHEARHEAD TYPE - X51  
LENGTH - COLUMN TOP NOT IDENTIFIED

COMMENTS: A COLUMN SEGMENT FROM STAGE II OF COLUMN E3.8 WAS LOCATED. ITS LENGTH IS 9'-3" AND THIS SECTION CONTAINS 11 SHEARHEADS (LEVELS 1-11). THE LOWER THREE LEVELS WERE FULLY WELDED. NUMBER 9 SHEARHEAD CONTAINS MARKS FROM THE LIFTING NUTS AND EVIDENCE THAT BOTH NUTS KICKED OUT FROM UNDER THE LIFTING ANGLES. IT APPEARS THAT ONE NUT GLANCED OFF THE WEB AND CAUGHT BOTH THE NUMBER 10 AND NUMBER 11 SHEARHEADS AS THEY WERE MOVING DOWNWARD.

COLUMN NO - E4.8  
SECTION - W 12X106  
SHEARHEAD TYPE - P50 (ROOF - R51)  
LENGTH - 14'-10"  
MARK - Y  
TACK WELDS - 1 SET ABOVE TOP WELD BLOCK  
SHEARHEADS - NONE

COMMENTS: INDENTATIONS IN THE TOP OF THIS COLUMN SHOW SIGNS OF THE JACK ROTATING ABOUT THE WEAK AXIS OF THE COLUMN. ONE EDGE OF THE FLANGE NEAR UPPER END OF THE COLUMN HAS BEEN INDENTED BY THE JACK ROD THREADS. ON THIS SAME SIDE OF THE COLUMN THE WEB HAS BEEN CHAMFERED BY THE JACK ROD AND THE WEB CONTAINS A LIFTING NUT IMPACT MARK. A SIMILAR MARK, BUT LESS PRONOUNCED, IS LOCATED ON THE OTHER SIDE OF THE WEB. A SEGMENT OF STAGE III OF THIS COLUMN WAS IDENTIFIED BY ITS COLUMN MARKINGS, ITS SECTION SIZE AND ITS COMBINATION OF MARK P50 AND MARK R51 SHEARHEADS. THE SEGMENT IS 12'-18" LONG AND CONTAINS SIX SHEARHEADS IDENTIFIED WITH LEVELS 8-R.

COLUMN NO - E.5  
SECTION - W 12X72  
SHEARHEAD TYPE - U51  
LENGTH - 6'-7"  
MARK - T  
TACK WELDS - 2 LEVELS AT UPPER WELD BLOCKS  
SHEARHEADS - 1  
COMMENTS: THE WEST FLANGE SHOWS SIGNS OF LOCAL BENDING DUE TO CANTILEVER ACTION OF FLOOR SLABS 9 TO R.

COLUMN NO - G1  
SECTION - W 10X60  
SHEARHEAD TYPE - B50  
LENGTH - 11'-4"  
MARK - 5-7  
TACK WELDS - 2 LEVELS AT UPPER WELD BLOCKS  
SHEARHEADS - NONE  
COMMENTS: THIS COLUMN SECTION IS VERY STRAIGHT WITH NO SIGNS OF SCRAPING OR GOUGING. COLUMN BUCKLED DIRECTLY ABOVE LEVEL 1. A LOWER SECTION OF THIS COLUMN IS A W 10X60 AND CONTAINS 10 B50 SHEARHEADS.

COLUMN NO - G2  
SECTION - W 12X106  
SHEARHEAD TYPE - P50 (ROOF - AA51)  
LENGTH - 19'-9"  
MARK -  
TACK WELDS - 2 LEVELS AT UPPER WELD BLOCKS  
SHEARHEADS - NONE  
COMMENTS: COLUMN SECTION IS STRAIGHT AND CLEAN WITH NO SIGNIFICANT SCRAPES OR GOUGES. SHEARHEADS APPEAR TO HAVE SLID STRAIGHT DOWN WITHOUT DAMAGING THE UPPER LEVEL WELD BLOCKS OR THE WEDGE CONTACT SURFACES.

COL NO - G3 OR G4  
SECTION - W 12X136  
SHEARHEAD TYPE - Y51  
LENGTH - 9'-10"  
MARK - 1-1 P  
TACK WELDS - 2 LEVELS AT UPPER WELD BLOCKS  
SHEARHEADS - NONE  
COMMENTS: LITTLE OR NO DAMAGE TO FLANGES NEAR TOP. NOTCH OBSERVED IN THE TOP OF ONE UPPER WELD BLOCK.

COLUMN NO - G3 OR G4  
SECTION - W 12X136  
SHEARHEAD TYPE - Y51  
LENGTH - 10 FT  
MARK - X  
TACK WELDS - 2 LEVELS AT UPPER WELD BLOCKS  
SHEARHEADS - NONE  
COMMENTS: INDENTATION (SCRAPING) IN ONE FLANGE JUST ABOVE TOP WELD BLOCK.

COLUMN NO - G5  
SECTION - W 12X106  
SHEARHEAD TYPE - P50 (ROOF - AA51)  
LENGTH - 18 FT  
MARK - XX  
TACK WELDS - 2 LEVELS AT UPPER WELD BLOCKS  
SHEARHEADS - NONE  
COMMENTS: SECTION IS PRACTICALLY STRAIGHT WITH NO SIGNIFICANT SCRAPES OR MARKS. NO VISIBLE DAMAGE TO UPPER WELD BLOCKS OR WEDGE CONTACT SURFACES. A LOWER SEGMENT OF THIS COLUMN CONTAINS SHEARHEADS FROM LEVELS 2 TO R.

COLUMN NO - G6  
SECTION - HP 12X53  
SHEARHEAD TYPE - C50  
LENGTH - 15'-10"  
MARK - WW  
TACK WELDS - 2 LEVELS AT UPPER WELD BLOCKS  
SHEARHEADS - 4 IN PLACE (9-12)  
COMMENTS: THE FOUR SHEARHEADS ON THIS COLUMN DID NOT GET PAST THE WEDGES UNDER SHEARHEAD 9. ROOF SHEARHEAD APPEARS TO HAVE SLID OFF TOP OF COLUMN. JACK RODS ARE STILL IN PLACE. FLANGES HAVE LOCAL DAMAGE AT SHEARHEAD POSITIONS AND COLUMN SEGMENT HAS BEEN TWISTED CLOCKWISE APPROXIMATELY 45 DEGREES.

COLUMN NO - H1  
SECTION - HP 10X42  
SHEARHEAD TYPE - A50  
LENGTH - 7'-10"  
MARK - K  
TACK WELDS - 2 LEVELS AT UPPER WELD BLOCKS  
SHEARHEADS - 4 IN PLACE (9-12)  
COMMENTS: COLUMN BUCKLED DIRECTLY ABOVE GND LEVEL. THERE ARE BITE MARKS IN THE FLANGE EDGES CAUSED BY RACKING OF THE SHEARHEADS. ALSO, THE FLANGES IN THE VICINITY OF THE SHEARHEADS HAVE UNDERGONE LOCAL BENDING WHICH INDICATES CANTILEVER ACTION BY THE FLOOR SLABS.

COLUMN NO - H2  
SECTION - W 12X65  
SHEARHEAD TYPE - D50  
LENGTH - 13 FT  
MARK - G  
TACK WELDS - PROBABLY 2 LEVELS AT UPPER WELD BLOCKS  
SHEARHEADS - 4 IN PLACE (9-12)  
COMMENTS: TOP SHEARHEAD APPEARS TO HAVE SLID OFF TOP OF COLUMN. THERE IS SIGNIFICANT LOCAL BENDING OF THE FLANGES NEAR THE TOP OF THE COLUMN DUE TO RACKING OF SHEARHEADS 9-12. A SEGMENT OF ONE OF THE JACK RODS RUNS DOWN THROUGH THE SHEARHEADS. THE COLUMN BUCKLED APPROX 2 FT ABOVE THE BOTTOM END OF THIS SEGMENT. ANOTHER SEGMENT OF THIS COLUMN FROM STAGE III CONTAINS SHEARHEADS FROM LEVELS 3 TO 8 WITH LEVEL 3 BEING FULLY WELDED.

COLUMN NO - H3  
SECTION - W 12X79  
SHEARHEAD TYPE - N50 (ROOF - E50)  
LENGTH - 30 FT  
MARK - ZZ  
TACK WELDS - 2 LEVELS AT UPPER WELD BLOCKS  
SHEARHEADS - NONE  
COMMENTS: THIS COLUMN SEGMENT HAS A GRADUAL AND UNIFORM BEND ABOUT WEAK AXIS. SHEARHEADS APPARENTLY SLID DOWN COLUMN WITHOUT DOING SIGNIFICANT DAMAGE.

COLUMN NO - H4  
SECTION - W 12X79  
SHEARHEAD TYPE - N50 (ROOF - E50)  
LENGTH - 19'-9" (FRACTURE AT STAGE III/IV SPLICE)  
MARK - Z  
TACK WELDS - 2 LEVELS AT UPPER WELD BLOCKS  
SHEARHEADS - NONE  
COMMENTS: THIS COLUMN SEGMENT IS RELATIVELY FREE OF SCRAPES AND GOUGES AND THE WELD BLOCKS AND WEDGE CONTACT SURFACES EXHIBIT VERY LITTLE DAMAGE. STAGE III OF THIS COLUMN CONTAINS SHEARHEADS FROM LEVELS 2 TO 12. SHEARHEAD 12 SHOWS MINIMAL DAMAGE AT THE POINT OF WEDGE CONTACT WHILE NUMBER 9 SHOWS SOME DISTORTION. THIS COLUMN SEGMENT BUCKLED JUST ABOVE THE STAGE II/III SPLICE.

COLUMN NO - H5  
SECTION - W 12X65  
SHEARHEAD TYPE - D50  
LENGTH - 12'-7"  
MARK - YY  
TACK WELDS - 2 LEVELS AT UPPER WELD BLOCKS  
SHEARHEADS - NONE  
COMMENTS: COLUMN H5 IS STRAIGHT AND SHOWS VERY LITTLE IN THE WAY OF MARKS OR SCRAPES. THERE IS A SLIGHT ROUNDING OF THE EDGES OF THE WEDGE CONTACT SURFACES AT THE UPPER WELD BLOCKS.

COLUMN NO - H6  
SECTION - HP 10X42  
SHEARHEAD TYPE - A50  
LENGTH - 8'-8"  
MARK - 5-2 D  
TACK WELDS - 2 LEVELS AT UPPER WELD BLOCKS  
SHEARHEADS - NONE  
COMMENTS: THIS SECTION HAS A GRADUAL BEND TO THE WEST JUST BELOW THE UPPER SEAL BLOCKS. THERE IS SOME LOCAL BENDING OF THE WEST FLANGE THAT APPEARS TO HAVE BEEN CAUSED BY THE SHEARHEADS. THE LOWER SECTION OF THE STAGE IV COLUMN IS IDENTIFIED BY THE SHOP NUMBER. ITS LENGTH ABOVE THE STAGE III/IV SPLICE IS 11'-1" AND 4'-6" BELOW THE SPLICE. THE SECTION IS BENT ABOUT THE WEAK AXIS APPROX 3 FT ABOVE THE STAGE III/IV SPLICE. NEITHER OF THESE TWO SECTIONS CONTAINS SHEARHEADS.

APPENDIX B

Geotechnical Engineering Investigation

Prepared by: Schnabel Engineering  
Consulting Engineers Associates  
and Geologists,  
West Chester, PA

GEOTECHNICAL ENGINEERING INVESTIGATION  
L'AMBIANCE PLAZA BUILDING COLLAPSE  
WASHINGTON AVENUE  
BRIDGEPORT, CONNECTICUT

Outline

Page

1. Summary of Conclusions	1
2. Description of Site and Background Information	2
3. Field Investigation	4
4. Soil and Rock Material Properties	9
5. Foundation Analysis	13
6. Lateral Earth Pressure Analysis	16

Appendix A

Summary of Soil Laboratory and In Situ Tests  
Gradation Test Curves (4)  
Proctor Test Curve  
Direct Shear Test Curves (2)  
Pressuremeter Test Procedures  
Pressuremeter Test Curve

Appendix B

Subsurface Exploration Data

Identification of Soil Samples

General Notes for Test Boring and Test Pit Logs

Test Boring Logs: B-1, B-2, B-2H, B-2HA, B-3E, B-4.8E, B-6H,  
B-9D, B-10D, B-10F

Test Pit Logs: TP-1H (east face), TP-1H (south face),  
TP-2H (west face), TP-2H (south face),  
TP-2H (east face), TP-10D (south face),  
TP-10F (north face), TP-10F (west face),  
TP-2

Test Boring and Test Pit Location Plan

Appendix C

Previous Test Borings by Others

Logs of PS-1, PS-2, PS-3, 1, 2, 3, 4, 5, 6, 7, 8, 9, 17

Location Plan of Previous Borings

Appendix D

Bibliography

## 1. CONCLUSIONS

Based on the information contained in this report, the following summary of conclusions is presented:

1. On-site soils and rock encountered in our field investigation consisted of fill materials, residual soils formed by the in-place weathering of parent bedrock and schist bedrock. The bedrock is believed to be a metamorphic rock of the Prospect Formation.

2. Footings were not supported on rock in some cases, as up to about 2.0 ft of probable fill and/or very compact residual soil was encountered beneath footings.

3. Due to the relatively shallow depth of soil beneath footings, we do not believe the bearing capacities of the footings examined were exceeded.

4. Estimated settlements for the footings investigated varied from negligible to 1/4 inch based on estimated column loads at the time of failure.

5. There may be a subgrade material beneath Footing 10F which could compress more than the estimated settlement as discussed herein.

6. Generally loose, but variable density silty sand backfill was encountered behind the north building wall. Upper and lower bound limiting earth pressure distributions on the north wall prior to collapse based on at-rest and active conditions are indicated on Sheets 2 and 3, respectively.



## 2. DESCRIPTION OF SITE AND BACKGROUND INFORMATION

### a. Site Description

The L'Ambiance Plaza site is located south of Washington Avenue and west of the entrance ramp to Route 8 in Bridgeport, Connecticut. It was to consist of a thirteen-story apartment tower with three basement parking levels. The building tower was divided into an east and west section, each about 62.5 x 112.0 ft (19 x 34 m) in plan view. A five-story parking garage was also being built as a part of the complex south of the apartment building. The structures were being built using the lift slab method.

The collapse occurred in the east and west sections of the building tower. At the time of our field investigation, some of the rubble had been cleared. Columns were cut off at varying lengths. Concrete slab debris was piled on the basement slab of the east and west sections. The basement slab remained intact. This slab had an architectural drawing elevation of EL -27.33, and this grade was used as a reference grade in this study. The footings, some shear walls, and the east, west, and north basement walls were also still in place during our study. The estimated loads on columns at the time of the building collapse are noted on Sheet 1.

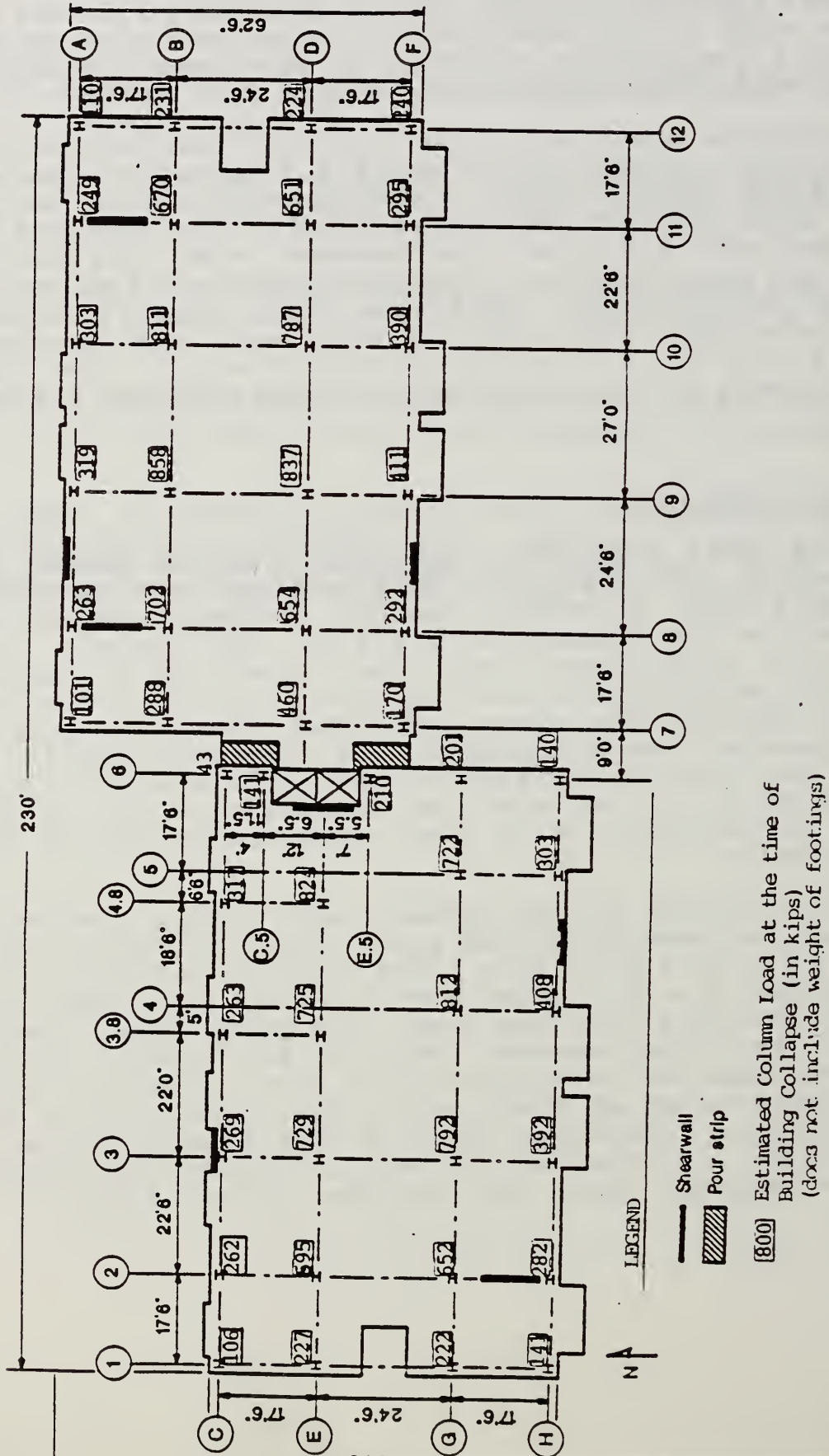
### b. Contract Drawings

The building tower loads were supported on spread footing foundations. Footings in the east and west sections were designed for a 7 tsf (670.3 kPa) allowable bearing pressure, as noted and dimensioned on the foundation plans for the project. General notes for the foundations in the plans specified an undisturbed rock footing subgrade suitable for this bearing pressure. An additional note on the plans indicated that if an unsuitable subgrade material was encountered, the contractor should either: a) remove the unsuitable material and replace with an approved engineered fill, b) increase the footing size per structural engineer's instructions, or c) lower footings to soil of suitable bearing capacity.

The lower two levels of the basement wall forming the north side of the tower had been backfilled prior to the collapse. This wall is about 18 ft in height above Floor Level E, and plans indicate it is supported on a 2 ft wide footing except at column locations where wider footings have been used. The garage level floor slabs were keyed into these basement walls on two levels, "C" and "D". Walls below grade were also cast on the east and west sides of the site but backfilling of these walls was incomplete. Project plans indicate a foundation drain at the exterior base of the basement walls. A layer of porous fill or bank run gravel was required as backfill behind the walls per project plans.

ESTIMATED COLUMN LOADS AT TIME  
OF FAILURE, IN KIPS (1K = 454 kg)

L'AMBIANCE PLAZA  
BUILDING COLLAPSE  
INVESTIGATION  
BRIDGEPORT, CT



c. Original Geotechnical Engineering Study

A geotechnical engineering report was provided for this project by Heynen Engineers, Clinton, Connecticut. Test boring information obtained from this report is included in Appendix C, along with a Location Plan. In the report it was recommended that all footings in the tower be founded on rock and dimensioned for a bearing pressure of 7 tsf. Settlements were calculated based on elastic solutions discussed in Schmertman (9) and Martin (5). Total settlements for an 8.5 x 8.5 footing were calculated assuming the 7 tsf bearing pressure and were conservatively estimated to range from < 0.5 to 1.5 inches (13 to 38 mm).

Recommendations by Heynen Engineers for the lateral earth pressures on the building walls appear to be based on Rankine active and passive lateral earth pressure coefficients, and an at-rest coefficient. The coefficients listed in the report are  $K_a = 0.3$  (active),  $K_p = 3.5$  (passive), and  $K_o = 0.5$  (at-rest). The lateral earth pressure recommended for use in design was a triangular earth pressure distribution with an ordinate at the base of 45H psf (1 psf = 47.88 Pa). Recommended resistance to lateral loading by footings was to be calculated from a reduced passive pressure coefficient,  $K_p = 1.9$  and a coefficient of sliding friction of 0.45.

d. Construction Observations by Others

Construction observations performed by Fairfield Testing Laboratories, Stamford, Connecticut, were reported in letters dated from July 10, 1986 through March 12, 1987 provided to us. These reports indicate footing subgrades in the tower were observed and consisted of bedrock, and/or a broken rock and earth fill. The fill was noted as compacted with a backhoe bucket and vibratory compaction, but there were no records of testing for in-place density. Backfill around the footings was tested on a spot-check basis and results indicated compaction to 95 percent of maximum dry density per Modified Proctor ASTM D-1557. From the records, the backfill material appears to be a poorly graded sand with silt and gravel, and maximum dry densities had been estimated at 124.3 to 127.6 pcf.

Project plans provided to us are Sheets S101, S201, S202, S203, S301, S302, A1, A11, and A12 dated January 1, 1986, for L'Ambiance Plaza by TPM Architects Inc.; and Texstar Construction Corporation Lift Slab Plan, Sheet TCC-1 with latest revision dated February 14, 1986. Estimated building loads at the time of failure were provided by NBS.

### 3. FIELD INVESTIGATION

Six test borings and two probe holes were drilled at footing locations selected by NBS personnel. In addition, two borings were performed within the north building wall backfill. All borings were performed by Connecticut Test Borings, Inc. of Seymour, Connecticut, under our inspection from May 28 to June 1, 1987.

Test pits were excavated adjacent to four footings, three of which were adjacent to test boring locations. These are designated by column location. A test pit was also excavated north of the building wall, and is designated Test Pit TP-2. These test pits were excavated by J.E. Barrett & Sons, Inc., on June 1 and 17, 1987. Test boring and test pit logs are included in Appendix B along with the Test Boring Location Plan, Sheet 2. The following is a summary of the field observations.

#### a. Geology

We understand the site was originally blanketed with surface layers of existing fill placed during previous development; and sand, gravel, cobble, and silt sedimentary deposits, probably from a glacial outwash. These materials were removed during the general excavation for the planned L'Ambiance Plaza construction. The soils observed during our field exploration consisted of fill materials placed during construction, residual soils, and bedrock.

Material described on our test boring and test pit logs as "probable fill" appears to be composed of the on-site residual soils and bedrock and is designated Stratum A. Backfill materials, designated Stratum A1, are generally sandy soils, and are probably a mixture of both residual and sedimentary soils.

The residual soils, designated Strata B and C herein, are soil materials formed by the in-place physical and chemical weathering of parent bedrock. The silty sands of Stratum B have undergone more advanced weathering and typically will exhibit none or very little of the relic structure from the parent bedrock. The disintegrated rock of Stratum C is less weathered and may exhibit certain rock-like qualities. In this report, disintegrated rock is defined as a very compact density, undisturbed, naturally occurring residual soil with Standard Penetration Test "N" values in excess of 60 blows/ft.

We believe the parent bedrock, designated Stratum D herein, is the Golden Hill schist of the Prospect Formation of Ordovician age. This schist bedrock is generally medium to coarse-grained containing quartz, mica in the form of muscovite and biotite, plagioclase and garnet, in order of decreasing mineral quantity. It is interlayered with fine to medium-grained gneiss with similar mineral composition. The schist bedrock appears to have an East North-East strike and a very steep dip to the north. These directions are referenced to north on project plans. Core

drilling of rock was started after SPT "N" values in excess of 100 blows over 6 inches or less of penetration were recorded.

b. Groundwater

Water levels were not initially noted for borings at footing locations because the water circulated during coring would have caused a superficial level. Follow up readings are noted on the boring logs, but indicate the borings were dry to cave depths of about 4.0 to 4.4 ft (1.2 to 1.3 m) up to 16 days after completion. In Borings B-1 and B-2, water was not encountered and the holes were dry upon completion to depths of caving at 10 to 12 ft.

An apparent water level was observed as noted in test pits adjacent to footings 2H and 10F. The water levels at these locations were comparable and relatively constant over a 16 day period. In the excavation at Footing 2H a flow was observed through fissures in the bedrock. The water levels indicated by this data is about EL -32.2 to -32.7.

Water level readings which were obtained in the field investigation are noted on the boring and test pit logs. The water table should be expected to fluctuate with variations in precipitation, surface runoff, leaking nearby utilities, pumping, and evaporation.

c. Footing Subgrade Conditions

Bearing conditions for selected footings were observed in some test pits and borings. The test pits were excavated to footing subgrade, and deeper if possible, to expose a cross section consisting of the side of the footing, the contact line between the footing concrete and subgrade materials, and underlying materials. It was apparent in the test pit excavations that footings had been formed rather than poured neat. The lateral over-excavation was typically a minimum 1.5 to 2 ft beyond the footing at the bearing grade and sloped wider toward ground surface. Test borings were cored through the footings to probe underlying subgrade materials.

Footing subgrade materials observed consisted of disintegrated rock and bedrock, and also probable fill materials. Materials labelled as probable fill were a mixture of silts, sands, mica, and rock fragments from on-site natural soils. No foreign matter, such as wood, construction debris, glass, paper, or similar was observed in the material to indicate a man-made deposit. However, the particle orientation in the probable fill stratum did not indicate any relic structure of a residual soil. In addition, construction records indicate similar materials were placed and compacted beneath footings.

### Footing 1H

The entire east face of this footing, and about 3 ft of the south face, was exposed down to bearing grade. Bearing material along the exposed footing perimeter consisted of schist bedrock. This bedrock was hard, slightly weathered and thinly bedded as observed in the bottom of the test pit adjacent to the footing perimeter. Contact between the footing and bedrock appeared to be continuous.

### Footing 2H-G

Generally the southern half of this 31'-10" (9.7 m) long footing was exposed by test pit excavations. Observations in the test pit indicated relatively continuous contact between the bottom of the footing and schist bedrock. Bedrock, as observed, was a hard, slightly to moderately weathered schist. However, test Boring B-2HA indicated 11 inches (279 mm) of disintegrated rock immediately underlying the footing.

A joint face was exposed along the west wall of Test Pit TP-2H (west face). The rock material at the face of the joint is slightly weathered and rust stained. There are discontinuous cracks in the joint face which extend generally vertically across the face. Rust stains were not present and these cracks were jagged and irregular. One crack extended across the bottom of the test pit and to the edge of the footing where access prevented further observation. Water was flowing from the cracks as noted on the test pit log.

### Footing 3E

The test boring performed through Footing 3E indicated that the footing may be underlain by up to 2 ft (0.6 m) of soil and disintegrated rock. One foot of a compact density, silty sand material was encountered immediately beneath the footing. The silty sand was underlain by 11.5 inches (292 mm) of disintegrated rock before hard, gray schist bedrock was encountered. We believe the compact silty sand is a fill material because the sampled material appeared to have been mixed.

### Footing 4.8E

About 5.5 inches (140 mm) of very compact density disintegrated rock was encountered immediately beneath Footing 4.8E in our test boring. The soil was underlain by a fresh, hard, gray schist.

### Footing 6H

The SPT test taken immediately below this footing indicated a very compact disintegrated rock material with an "N" value in excess of 100 blows per foot. However, the 6 inch (152 mm)

seating interval indicated a considerably less compact layer (12 blows/6 inches), and we do not believe this lower blowcount was due entirely to disturbance from boring procedures. The 6 inch (152 mm) layer just underlying the footing may be silty sand fill placed beneath the footing. Bedrock was encountered at a depth of 17 inches below the footing.

#### Footing 9D

This footing was cored with an Nx core barrel which could not be removed after breaking through the bottom of the footing. In the process of trying to remove the core barrel, it was bumped with the 140 pound (63.6 kg) donut hammer, as controlled by a rope with several wraps around the cathead. The core barrel penetrated the materials beneath the footing relatively easily, to a depth of about 6 inches (152 mm), indicating the material was not bedrock.

#### Footing 10D

About 6 ft (2 m) of the south face of Footing 10D was exposed by a test pit to the bearing grade. Observations in this test pit indicated a continuous contact between the footing and the bedrock, which was observed to be moderately hard, moderately weathered gray schist. The test boring in the footing indicated 9 inches (228 mm) of very compact disintegrated rock between the bottom of the footing and bedrock.

#### Footing 10F

Variable bearing conditions were observed beneath this footing. The test boring indicated up to 2.2 ft (670 mm) of soil beneath the footing. Of this 2.2 ft, less than the lowest 0.5 ft (152 mm) may have been disintegrated rock, overlying schist bedrock. However, in the split spoon sample recovered, we could not observe any residual rock structure and the material has been listed as a probable fill.

The test pits excavated along the north and west faces of the footing exposed continuous contact between the footing and bedrock along the west face, but a bedrock surface sloping to a grade up to about 1.5 ft (457 mm) below the footing on the north face. The subgrade materials are described in detail on the test pit log. In part, exposed materials on the north face appeared to be disintegrated rock or residual soil materials; however, the materials may have been partially disturbed from a natural orientation. There were gaps between natural planes of rock fragments up to 1/2 inch (13 mm). The materials could also be easily removed by hand and the excavation was extended about 6 to 8 inches (150 to 200 mm) back under the footing.

d. North Building Wall

Two borings, B-1 and B-2, and one test pit were performed within the backfill placed adjacent to the north building wall. The subsurface sampling and testing indicated a loose to compact density silty sand backfill to a depth of 13.5 to 18.5 ft (4.1 to 5.6 m). The variable density fill was underlain by compact to very compact residual soils to the depths of boring penetration at 16 to 20 ft (4.5 to 6.1 m).

Cracks in the ground surface were observed behind the wall adjacent to the east tower. These cracks were generally parallel to the wall and about 11 to 15 ft north of it. The cracks were up to about 1 inch wide.



#### 4. SOIL AND ROCK MATERIAL PROPERTIES

Seven jar samples, two tube samples, and one bulk sample were tested in the soils laboratory for plasticity characteristics and grain size distribution. The bulk sample was also remolded and tested for shear strength parameters. Pressuremeter and field density tests were performed at the site during the field investigation. Results of the laboratory and in situ testing are shown on the Summary and Graphs of Appendix A. All samples were tested in accordance with applicable ASTM standards. Properties of the soil and rock materials are discussed below by stratum.

##### Stratum A1: Backfill behind North Building Wall

Stratum A1 materials placed for floor slab support were not tested in our soils laboratory. The backfill behind the retaining wall was tested for plasticity indices, and the tested portion of the material was non-plastic. The tested samples contained silt to gravel-size particles; however, the grain-size distribution indicates a poorly graded material. About 16.9 to 25.8 percent of the samples were finer than the No. 200 sieve. The materials classified as silty sand with rock fragments, SM in accordance with ASTM D-2487.

SPT "N" values, field density tests, and dry densities performed on tube samples indicate the backfill is generally loose. Density tests performed by sandcone methods indicated dry densities of 87.4 and 109.6 pcf (1.40 and 1.76 ton/m<sup>3</sup>) with respective moisture contents of 23.5 and 7.8 percent. In place dry densities obtained on five samples within two undisturbed tubes were low, varying from 84.2 to 104.0 pcf (1.35 to 1.67 ton/m<sup>3</sup>). The above densities correspond to 67.2 to 87.5 percent of maximum dry density per ASTM D-1557. We believe these densities are generally representative of the backfill.

One pressuremeter test was performed on the representative loose density fill in Boring B-2 between 6 to 8 ft (1.8 to 2.4 m) depths. The test results were inconclusive. The material was so loose that the correction for probe membrane stiffness masked the resistance being measured in the soil backfill.

The backfill material appeared to be predominantly an excavated residual soil and rock fragment mixture. Since these materials are remolded, we believe the relic mineral bonds, generating an apparent cohesion within a natural residual soil, have been broken. The materials are also non-plastic, indicating no significant attraction between particles. Therefore, it is our opinion that this sample has no significant cohesion.

Direct shear tests were performed to determine the internal angle of friction for the mixture. These tests indicated a high angle of friction  $\phi = 37^\circ$ . We believe this angle is not representative of the actual value for the loose density materials and may, in part, be attributed to particle interlocking associated with the

constant volume direct shear test. We believe the shear stresses which can be obtained at lower strains with each test series are less likely to be biased by the constant volume test constraint and are probably more representative. For shear displacements of 0.2 inches and less, the angle of internal friction is accordingly,  $\phi \leq 33^\circ$ .

Based on the low "N" values and natural densities obtained in testing, we estimate the average friction angle in the backfill to vary between  $28^\circ$  and  $32^\circ$  based on Meyerhof's  $\phi$ -N correlation (6).

#### Stratum A: Probable Fill Beneath Footings

Tests indicated these materials are non-plastic. There was a predominant quantity of weathered rock fragments in these samples, ranging from sand to gravel in particle sizes. Gravel size rock fragments comprised about 34 to 58 percent of the tested samples. These particles were in a relatively advanced stage of weathering and therefore friable. In our opinion, repeated handling of the particles would have caused significant changes in grain size distribution, but ultimately the material would have broken down to a silty sand or sand with silt material. Therefore, we have classified the probable fill in accordance with plasticity and the relative silt and sand content. Thus, materials were classified silty sandy with rock fragments, or poorly graded sand with silt and rock fragments, SM in accordance with ASTM D-2487.

The probable fill soils are not considered to have cohesion for the same reason discussed previously on Stratum A1 backfill. The internal angle of friction was estimated from the standard penetration values obtained in the test borings based on Meyerhof  $\phi$ -N correlations (6). Accordingly, a range of values from about  $31^\circ$  to  $34^\circ$  is estimated for a range of "N" values from 16 to 24.

It was possible to run only one pressuremeter test on the probable fill encountered beneath footings. The pressuremeter test was performed beneath Footing 10F, where about 2 ft of probable fill material was encountered. The test indicated a Pressuremeter Modulus ( $E_p$ ) of 80 tsf and a Limit Pressure ( $P_L$ ) of 7.0 tsf. Elsewhere rock or disintegrated rock was encountered at a shallower depth below footing subgrade, and the test could not be performed.

We believe the rheologic factor relating the pressuremeter modulus to the Deformation Modulus for the silty sand materials is between 1.0 and 2.0. Therefore, the estimated Deformation Modulus,  $E_s$ , for the probable fill tested is between 80 and 160 tsf. The higher value corresponds closely with an empirical formula developed by Bowles (2) to relate "N" values to  $E_s$  for cohesionless materials. This formula

$$E_s = 5 [N + 15] \text{ tsf}$$

has been used to estimate the Modulus of Deformation beneath the other footings where pressuremeter tests could not be run. As estimated by this formula, the probable fill beneath two other footings, 3E and 6H, had upper bound Deformation Moduli of  $E_s = 155$  and  $195$  tsf, respectively. Lower bound moduli were estimated from these values, reduced by 50 percent to correspond to a rheologic factor of 1.0. This estimated range of moduli was used in our settlement calculations. The "N" values must be extrapolated for the estimate because layer thickness was less than 18 inches and included the six inch seating interval of the SPT test, which probably also contains less compact material than the underlying layers.

#### Stratum B: Residual Soil

Residual soil of Stratum B was encountered in only one boring, B-2, near the depth of penetration at 13.5 ft. The SPT "N" values indicate a compact density material which was visually classified as a silty sand, SM in accordance with ASTM D-2487. This material was not encountered elsewhere and was not examined further.

#### Stratum C: Disintegrated Rock

The very compact density residual materials of Stratum C are characterized by SPT "N" values greater than 60 and less than  $100/6$ ". One jar sample of materials was classified using a sieve analysis, plasticity indices, and a rationale similar to that applied to Stratum A1. This material was similarly non-plastic and contained a predominant portion of weathered rock fragments, classified as a poorly graded sand, with rock fragments (SP-SM).

The disintegrated rock material has not undergone the in-place physical and chemical weathering to the extent that all relic bonds are broken. Published data on strength and deformability characteristics of similarly weathered micaceous schist and gneiss has been related to "N" values between 60 and  $100/2$ ". The effective cohesion (c) has been measured at 0.2 to 2.5 tsf with the lower bound corresponding to the lower SPT values and cohesion increasing with density as indicated by higher "N" values, Gardner (3). The friction angle ( $\phi$ ) similarly was found to vary between 29 and 36°. Deformability of the disintegrated rock has also been related to a similar range of SPT "N" values from a data base developed in piedmont residual materials. It ranges from about 300 tsf to 1200 tsf, Martin (5). We believe these strength and deformation parameters are reasonably representative of the on-site disintegrated rock material for purposes of this study. Straight line interpolation has been used for estimating strength parameters over the range of "N" values. These parameters have been used in our investigation calculations.

Stratum D: Schist (Prospect Formation)

The schist bedrock cored in the test borings for this investigation was generally slightly weathered and moderately hard or better. Joint faces did not exhibit much more extensive weathering and were rust stained, but exposed moderately hard rock. Published data indicates a peak friction angle  $\phi$  between  $43^\circ$  and  $50^\circ$  for this type of rock, Gardner (3). Similarly, the cohesion can be correlated to the friction angle by

$$c = \frac{q_u}{2 \tan (45 + \phi/2)}$$

where  $q_u$  is the compressive strength of the rock. We have used the compressive strengths observed by Heynen Engineers to estimate the cohesion of on-site rock. Accordingly, the range in cohesion varies considerably from about 150 to 2100 psi.

The Deformation Modulus for intact rock will be greater than the upper values discussed for Stratum C materials because less weathering has occurred. For the purpose of this investigation, such a modulus indicates that, as a matter of practical consideration, the intact rock is not deformable within the stress range being considered. Any deformation would occur along joint faces with more advanced stages of weathering. However, our investigation did not indicate the presence of highly weathered material to significant depths below footings.

## 5. FOUNDATION ANALYSIS

The plan dimensions, estimated axial loads, and resulting bearing pressures of those footings examined during our field investigation are tabulated below.

### Column Loads and Bearing Pressures at Time of Failure for Tested Footings

<u>Footing</u>	<u>Plan Dimensions</u>	<u>Estimated Load (1) at Failure (kips)</u>	<u>Bearing Pressure (2) at Failure (ksf)</u>
1H	4' 6" x 4' 6" x 1' 9"	146	7.2
2H-2G	31' 10" x 10' 0" x 5' 0"	282 + 652 + 338 (combined load)	3.99 (average stress)
3E	10' 0" x 10' 0" x 3' 6"	782	7.82
4.8E	10' 0" x 10' 0" x 3' 6"	877	8.77
6H	5' 6" x 5' 6" x 2' 1"	150	4.95
9D	10' 0" x 10' 0" x 3' 6"	890	8.9
10F	7' 6" x 7' 6" x 2' 8"	413	7.33
10D	10' 0" x 10' 0" x 3' 6"	839	8.39

These values were used in our analysis as discussed below. Other footings were not considered in this analysis.

- 
- (1) 1 kip = 4.448 kN  
(2) 1 ksf = 47.88 kPa

a. Bearing Capacity of Footings

Based on the estimated loads at the time of failure, footing contact pressures were about 4.0 to 8.9 ksf for the footings investigated during this study. Under these loads a bearing capacity failure is considered very unlikely because of the high shear strength of the rock which was encountered in most cases at bottom of footing grades. Where soil was encountered beneath footings, its relatively shallow depth and granular nature precluded general bearing capacity failure. Similarly, punching or local bearing capacity failure is not considered likely as the footing/rock geometry does not lend itself to this failure mode.

We have conservatively estimated the bearing capacity for footings observed during our field investigation using factors for local shear, Bowles (1). In accordance with standard practice, a safety factor of three is generally used for calculating the allowable capacity. The lowest safety factors against local shear were calculated for Footings 10D, 3E and 10F, and were between 1.3 and 2.0 based on contact pressures listed in the preceding table. However, as noted, these calculated factors of safety are considered to be unrealistically low.

b. Footing Settlement

Settlement of the footings has been estimated using elastic solutions. We have considered the approach developed by Schmertmann (9), as modified by Martin (5) for residual soils, to be the most applicable. This method can account for subsoil layers, the effect of time, and strain distribution. The concentration of loads in a relatively narrow, compressible zone overlying bedrock has also been considered as discussed by Martin (5). We have assumed the bedrock is incompressible for the stress range considered. Additional methods based on elastic theory would have been considered in more detail to evaluate the relative effects of various parameters, had the estimated settlements been significant. However, our estimate for the worst case conditions observed during our field investigation, at Footing 10F, indicates less than 1/4 inch total settlement could have been anticipated. We note that this is much less than the settlement estimated in the design report calculations. However those design calculations were based on higher loads and, more significantly, on a lower quality designation for the underlying bedrock than that determined for the cores taken in our investigation. There was, at most, a 2 ft thick depth of relatively compressible material observed beneath the investigated footings.

The estimated settlement beneath Footing 10F was based on the 2 ft layer of compressible materials sampled in the test boring. We note that the test pit exposed bedrock on one side of the footing and soil on the other. Thus, an angular distortion of between 0.001 and 0.003 has been estimated for this footing based on the differential settlement across the footing.

However, beneath Footing 10F, the highly weathered rock observed on the east side of the test pit had open joints and gaps along foliation planes. In addition to the advanced stage of weathering, these voids could have allowed for appreciable deformation. This deformation would be impossible to quantify with any accuracy, because of the random geometry and unknown extent. A better indication of the extent of this condition could be obtained by removing the footing or examining the other two sides from adjacent test pits.

Settlement estimated at the footings examined in this study range between negligible for Footings 1H and 2H, and less than 1/4 inch for Footing 10F. Settlement beneath Footings 4.8E, 3E, 10D and 6H were estimated to be less than 1/10 inch. We believe a major portion of the estimated settlement for the applied loads listed herein had occurred prior to building collapse.

## 6. LATERAL EARTH PRESSURE ANALYSIS

Estimates of the lateral earth pressure acting on the north building wall below grade must take into account the soil behind the wall, and the deflections which the wall had likely undergone prior to collapse. The highly variable fill conditions behind the wall complicate estimates of soil parameters. It is estimated on the basis of the data obtained on the backfill that, in general, the backfill is in a loose state representative of a low angle of internal friction,  $\phi = 28$  to  $30^\circ$ . An average moist unit soil weight of 110 pcf is considered to be applicable. Back calculation of a failure wedge corresponding to the tension cracks observed in the backfill assuming a Rankine active failure state also indicates  $\phi$  values of about  $30^\circ$  and less.

We believe the cracks visible in the soil behind the north building wall resulted from a displacement of the wall, but this displacement could have occurred after the collapse, possibly during rescue efforts. If the partially constructed building wall afforded enough rigidity to prevent wall movement prior to the collapse, then an at-rest pressure condition would have been approached. However, we have noted from project plans that this wall would have been supported by transmitting the loads through the building shear walls to spread footing foundations. For this support to have been mobilized in the foundations, some strain must have occurred. Therefore, an estimate of the pressure distribution would be limited by the lower bound of an active pressure distribution and an upper bound of an at-rest pressure distribution.

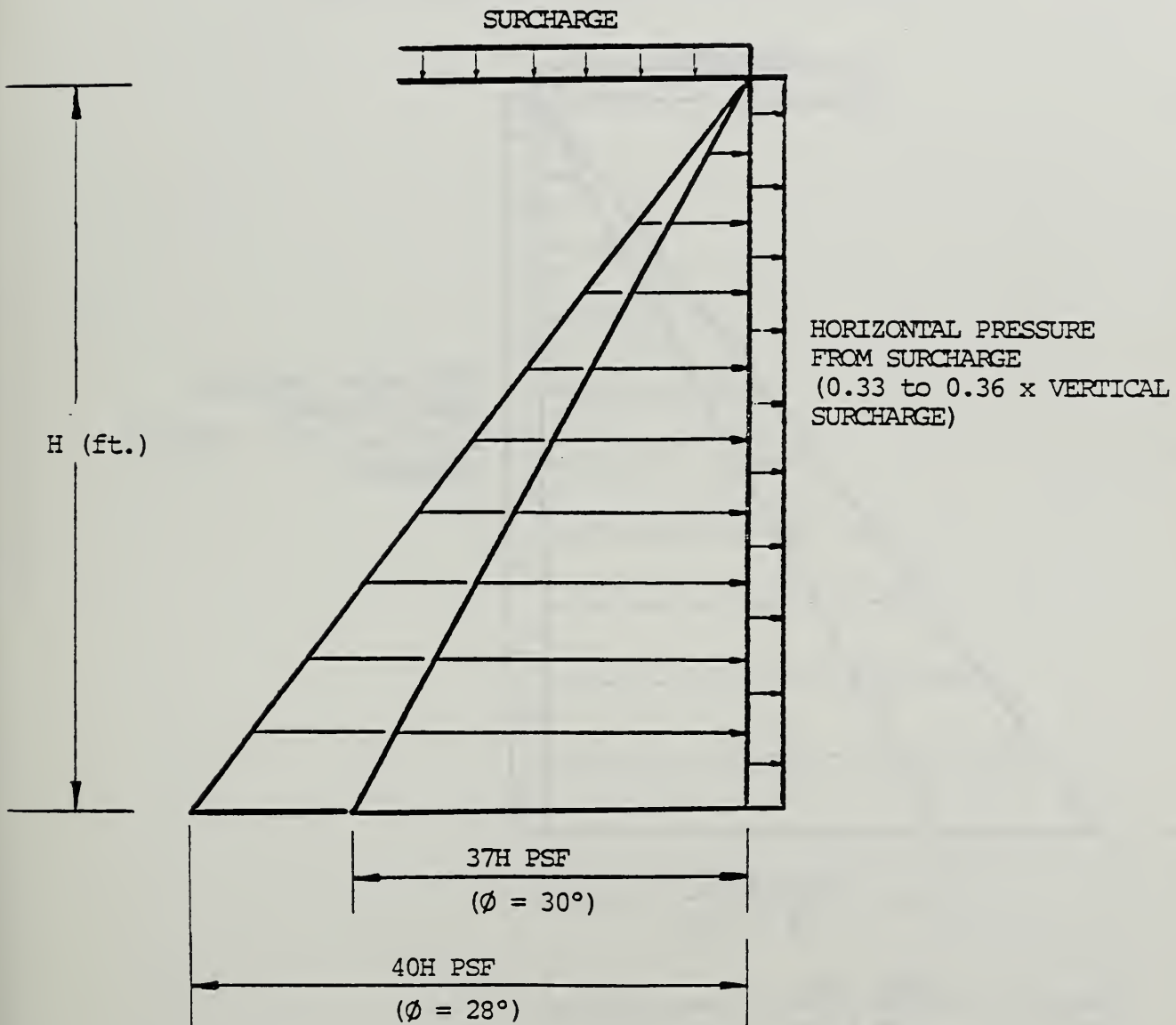
An active earth pressure coefficient  $K_a = 0.33$  to  $0.36$  is considered applicable for the wall. The estimated range of equivalent fluid pressures acting on the wall assuming active conditions is shown on Sheet 2.

A similar equivalent fluid pressure distribution for the at-rest condition has been estimated using Jaky's approximation (Winterkorn and Fang, 11) of the at-rest coefficient estimated as  $K_a = 0.5$  to  $0.53$ . The estimated range of equivalent fluid pressures acting on the wall assuming at-rest conditions is shown on Sheet 3.



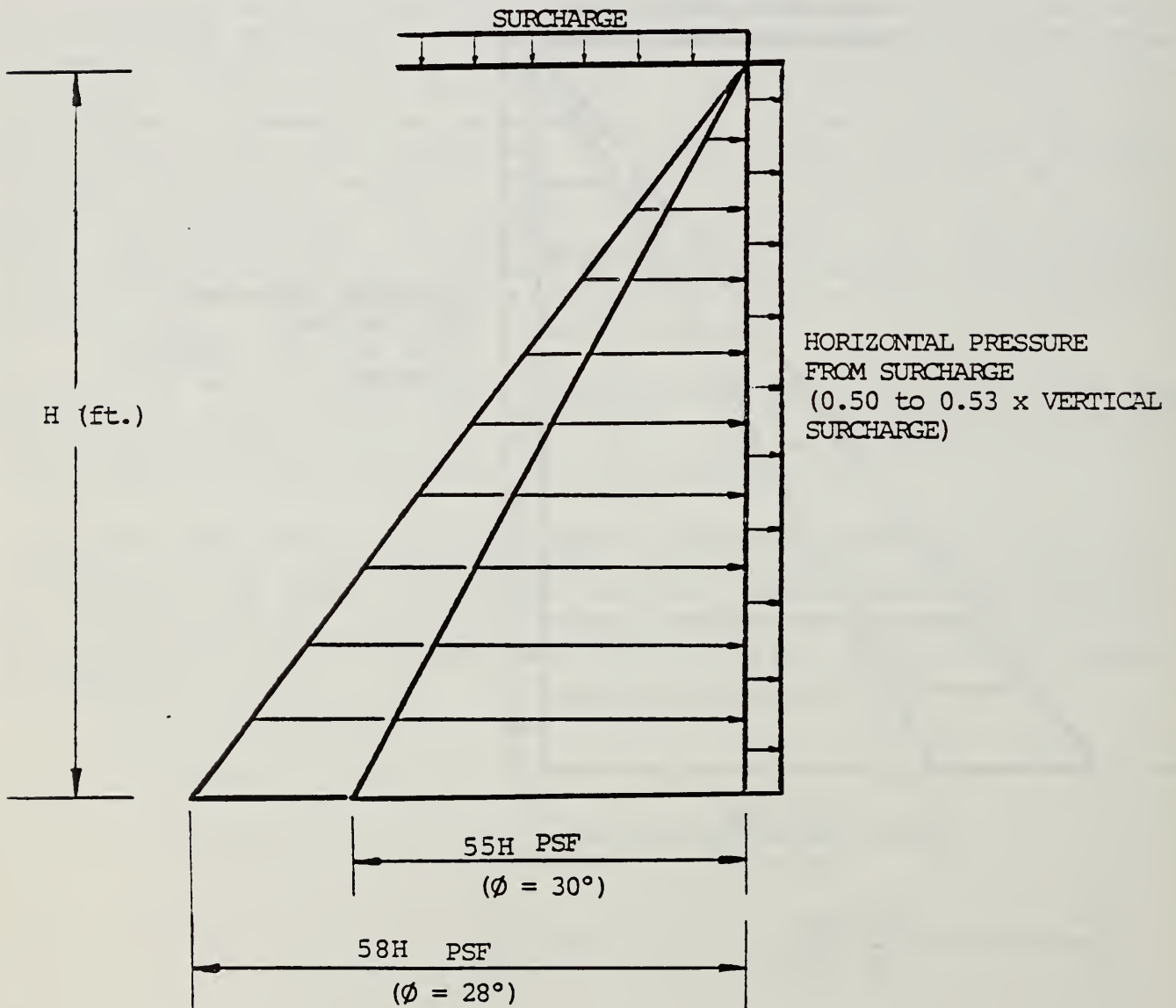
ESTIMATED LATERAL EARTH PRESSURES  
ASSUMING ACTIVE CONDITIONS

L'AMBIANCE PLAZA  
BUILDING COLLAPSE  
INVESTIGATION  
BRIDGEPORT, CT



ESTIMATED LATERAL EARTH PRESSURES  
ASSUMING AT-REST CONDITIONS

L'AMBIANCE PLAZA  
BUILDING COLLAPSE  
INVESTIGATION  
BRIDGEPORT, CT



SOIL LABORATORY AND IN SITU TESTS

SUMMARY OF SOIL LABORATORY TESTS

Boring No.	Sample Depth Elev.	Sample Type	Description of Soil Specimen	Stratum	Natural Density pcf		Atterberg Limits			Natural Moisture (%)	% Passing No. 200 Sieve	Max. Dry Density pcf	Remarks
					Wet	Dry	LL	PL	PI				
B-1	12.0' -21.3	JAR	SILTY SAND WITH ROCK FRAGMENTS (SM)	A1	--	--	NP	NP	NP	9.4	16.9	--	See gradation test curve
TP-2	5.0' -15.3	BULK	SILTY SAND WITH WEATHERED ROCK FRAGMENTS AND GRAVEL, CONTAINS MICA, WOOD, GLASS, AND BRICK FRAGMENTS, GRAY (SM)	A1	*	*	NP	NP	NP	--	25.8	125.3	See gradation test curve See direct shear test curves * φ = 37° See proctor curve
	5.0' -15.3	TUBE	SILTY SAND WITH WEATHERED ROCK FRAGMENTS AND GRAVEL - BROWN (SM)	A1	118.5 115.0 106.4	104.0 102.3 96.3	NP	NP	NP	14.0 12.4 10.3	--	125.3	Natural densities taken on successive 6" segments of tube See proctor curve
	5.0' -15.3	TUBE	SILTY SAND WITH WEATHERED ROCK FRAGMENTS AND GRAVEL - BROWN (SM)	A1	106.6 96.5	92.2 84.2	NP	NP	NP	15.6 14.7	--	125.3	Natural densities taken on successive 6" segments of tube See proctor curve

Notes: 1. Soil tests in accordance with applicable ASTM Standards

2. Soil classifications in accordance with Unified Soil Classification System

3. Key to abbreviations: LL=Liquid Limit; PL=Plastic Limit; PI=Plasticity Index; NP=Non-Plastic

4. Soil Tests were conducted by: C. Graves, J. Mann, B. Flick

SUMMARY OF SOIL LABORATORY TESTS

Boring No.	Sample Depth Elev.	Sample Type	Description of Soil Specimen	Stratum	Natural Density pcf		Atterberg Limits			Natural Moisture (%)	% Passing No. 200 Sieve	Max. Dry Density pcf	Remarks
					Wet	Dry	LL	PL	PI				
TP-2	5.0' -15.3	FIELD TEST	SILTY SAND WITH WEATHERED ROCK FRAGMENTS AND GRAVEL - BROWN (SM)	AI	108.0	87.4	--	--	--	23.5	--	125.3	See proctor curve
	5.0' -15.3	FIELD TEST	SILTY SAND WITH WEATHERED ROCK FRAGMENTS AND GRAVEL - BROWN (SM)	AI	118.2	109.6	--	--	--	7.8	--	125.3	See proctor curve
B-2	6.0' -16.3	JAR	SILTY SAND WITH ROCK FRAGMENTS, BROWN (SM)	AI	--	--	NP	NP	NP	10.7	25.6	--	See gradation test curve
B-3E	5.0' -32.0	JAR	SILTY SAND WITH ROCK FRAGMENTS, BROWN (SM)	A	--	--	NP	NP	NP	14.1	14.3	--	See gradation test curve
	6.0' -33.0	JAR	POORLY GRADED SAND WITH SILT AND ROCK FRAGMENTS, BROWN (SP-SM)	A	--	--	NP	NP	NP	8.3	9.6	--	See gradation test curve

Notes: 1. Soil tests in accordance with applicable ASTM Standards

2. Soil classifications in accordance with Unified Soil Classification System

3. Key to abbreviations: LL=Liquid Limit; PL=Plastic Limit; PI=Plasticity Index; NP=Non-Plastic

4. Soil Tests were conducted by: C. Graves, J. Mann, B. Flick

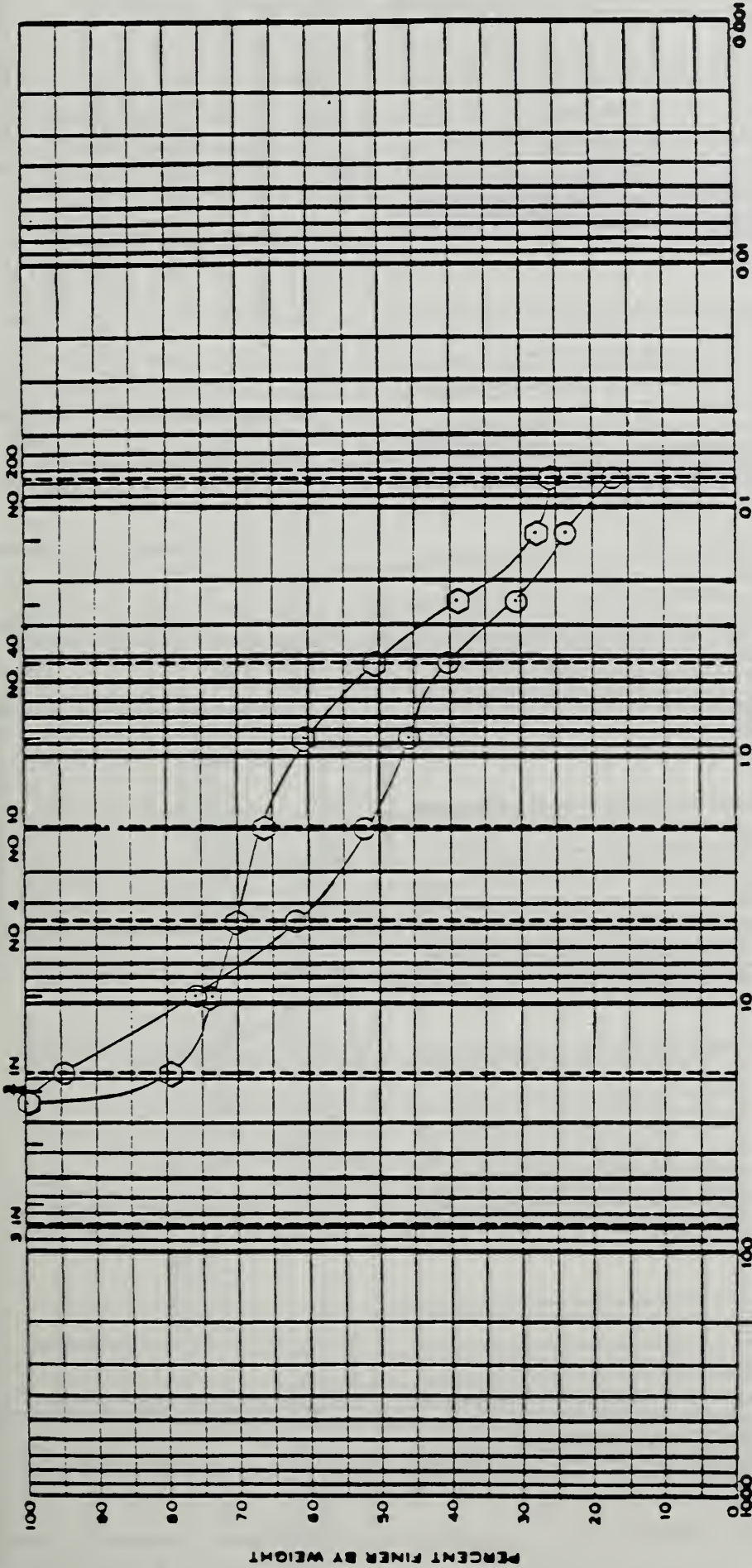
SUMMARY OF SOIL LABORATORY TESTS

Boring No.	Sample Depth Elev.	Sample Type	Description of Soil Specimen	Stratum	Natural Density pcf		Atterberg Limits			Natural Moisture (%)	% Passing No. 200 Sieve	Max. Dry Density pcf	Remarks
					Wet	Dry	LL	PL	PI				
	7.0' -34.0	JAR	POORLY GRADED SAND WITH SILT AND ROCK FRAGMENTS, BROWN (SP-SM)	C	--	--	NP	NP	NP	11.1	7.8	--	See gradation test curve
B-10F	4.0' -31.4	JAR	POORLY GRADED SAND WITH SILT AND ROCK FRAGMENTS, BROWN, (SP-SM)	A	--	--	NP	NP	NP	12.4	9.1	--	See gradation test curve See pressuremeter test curve P <sub>M</sub> = 80 tsf; P <sub>L</sub> = 7 tsf
	6.0' -33.4	JAR	POORLY GRADED SAND WITH SILT AND ROCK FRAGMENTS, BROWN (SP-SM)	A	--	--	NP	NP	NP	11.8	12.0	--	See gradation test curve

- Notes: 1. Soil tests in accordance with applicable ASTM Standards
2. Soil classifications in accordance with Unified Soil Classification System

3. Key to abbreviations: LL=Liquid Limit; PL=Plastic Limit; PI=Plasticity Index; NP=Non-Plastic
4. Soil Tests were conducted by: C. Graves, J. Mann, B. Flick

U S STANDARD SIEVE SIZE



COBBLES	GRAVEL		SAND		SILT OR CLAY
	Coarse	Fine	Medium	Fine	

KEY	BORING	DEPTH	DESCRIPTION OF SOIL SAMPLE TESTED	CLASSIF	M.C.	LL	PI
○	B-1	12'	SILTY SAND WITH ROCK FRAGMENT'S	SM	9.4	NP	NP
◊	B-2	6'	SILTY SAND WITH ROCK FRAGMENT'S	SM	10.7	NP	NP

SCHNABEL ENGINEERING ASSOCIATES

GRADATION CURVES

PROJECT: L'AMBIANCE PLAZA

BRIDGEPORT, CT

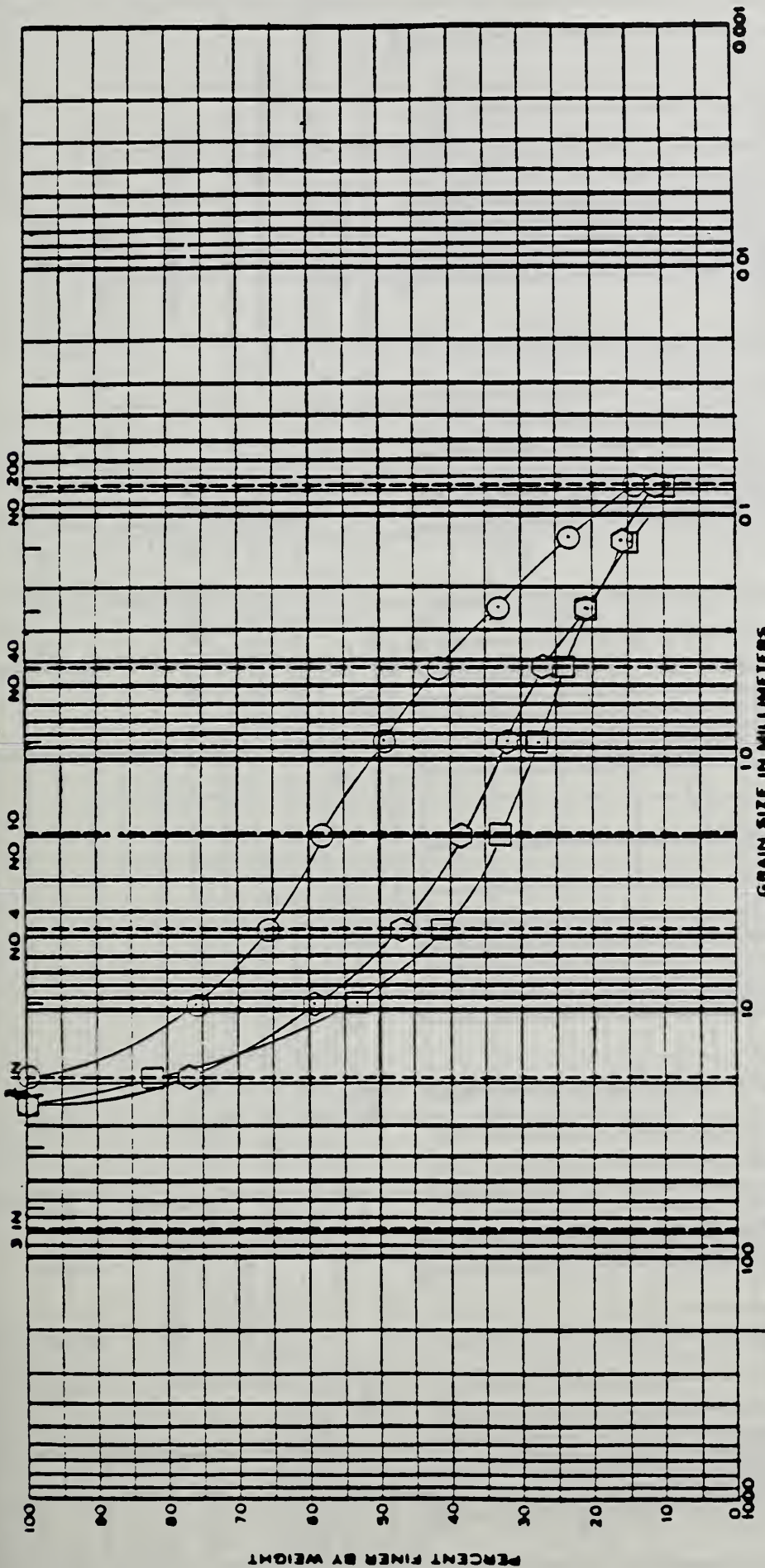
DATE: 8-25-87

CONTR. NO. CT870587





U S STANDARD SIEVE SIZE



GRAIN SIZE IN MILLIMETERS

SILT OR CLAY

COBBLES

GRAVEL

SAND

Medium

Coarse

Fine

Fine

KEY	BORING	DEPTH	DESCRIPTION OF SOIL SAMPLE TESTED	CLASSIF	M C	LL	PI
○	B-3E	5'	SILTY SAND WITH ROCK FRAGMENTS	SM	14.1	NP	NP
◇	B-3E	7'	POORLY GRADED SAND WITH SILT AND ROCK FRAGMENTS	SP-SM	11.1	NP	NP
□	B-3E	6'	POORLY GRADED SAND WITH SILT AND ROCK FRAGMENTS	SP-SM	8.3	NP	NP

SCHNABEL ENGINEERING ASSOCIATES

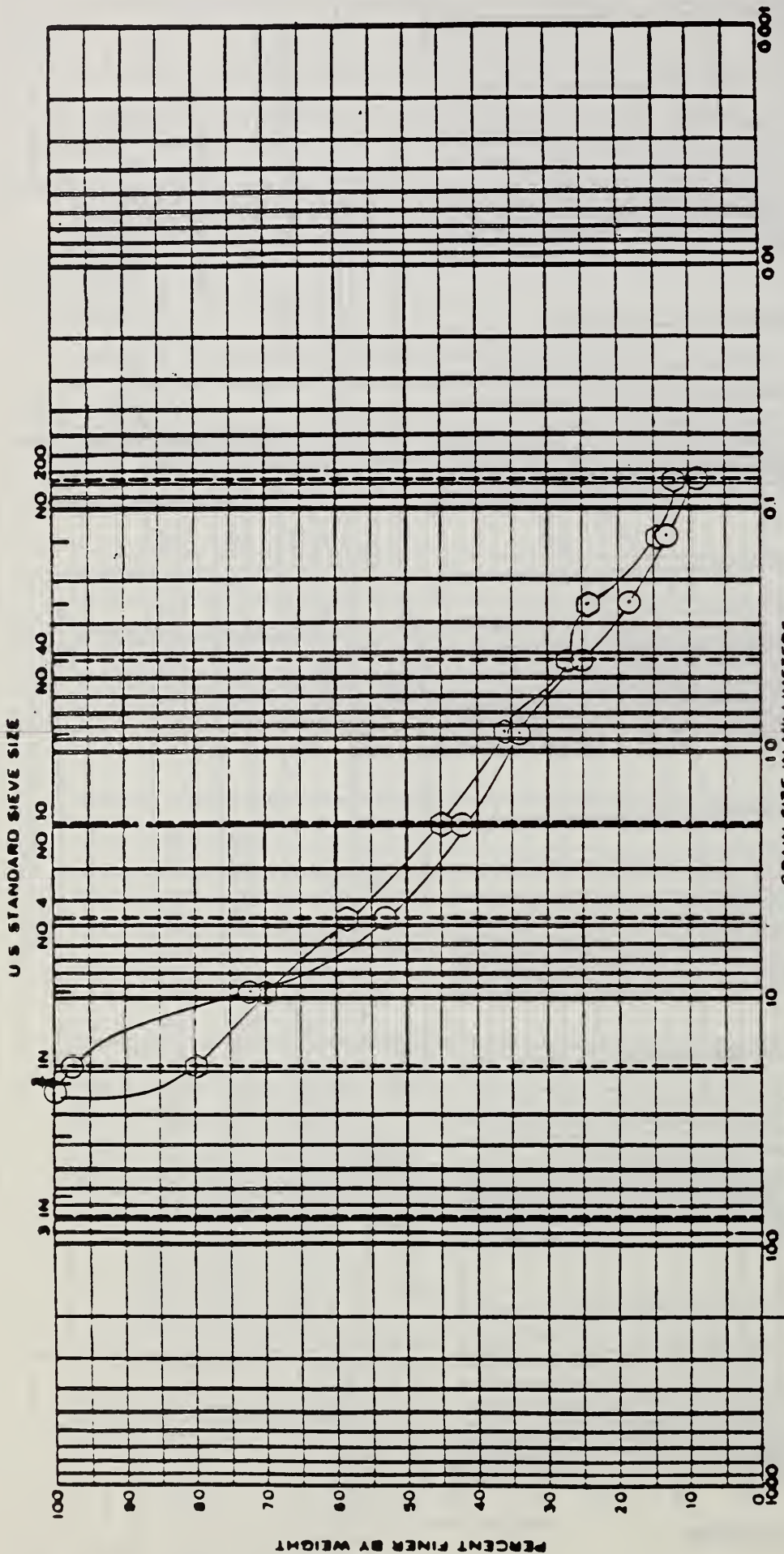
GRADATION CURVES

PROJECT: L'AMBANCE PLAZA

BRIDGEPORT, CT

DATE: 8-25-87

CONTR. NO CT1870587



COBBLES	GRAVEL		SAND		SILT OR CLAY
	Coarse	Fine	Coarse	Fine	

KEY	BORING	DEPTH	DESCRIPTION OF SOIL SAMPLE TESTED	CLASSIF	M C	LL	PI
○	B-10F	4'	POORLY GRADED SAND WITH SILT AND ROCK FRAGMENTS	SP-SM	12.4	NP	NP
◊	B-10F	6'	POORLY GRADED SAND WITH SILT AND ROCK FRAGMENTS	SP-SM	11.8	NP	NP

SCHNABEL ENGINEERING ASSOCIATES

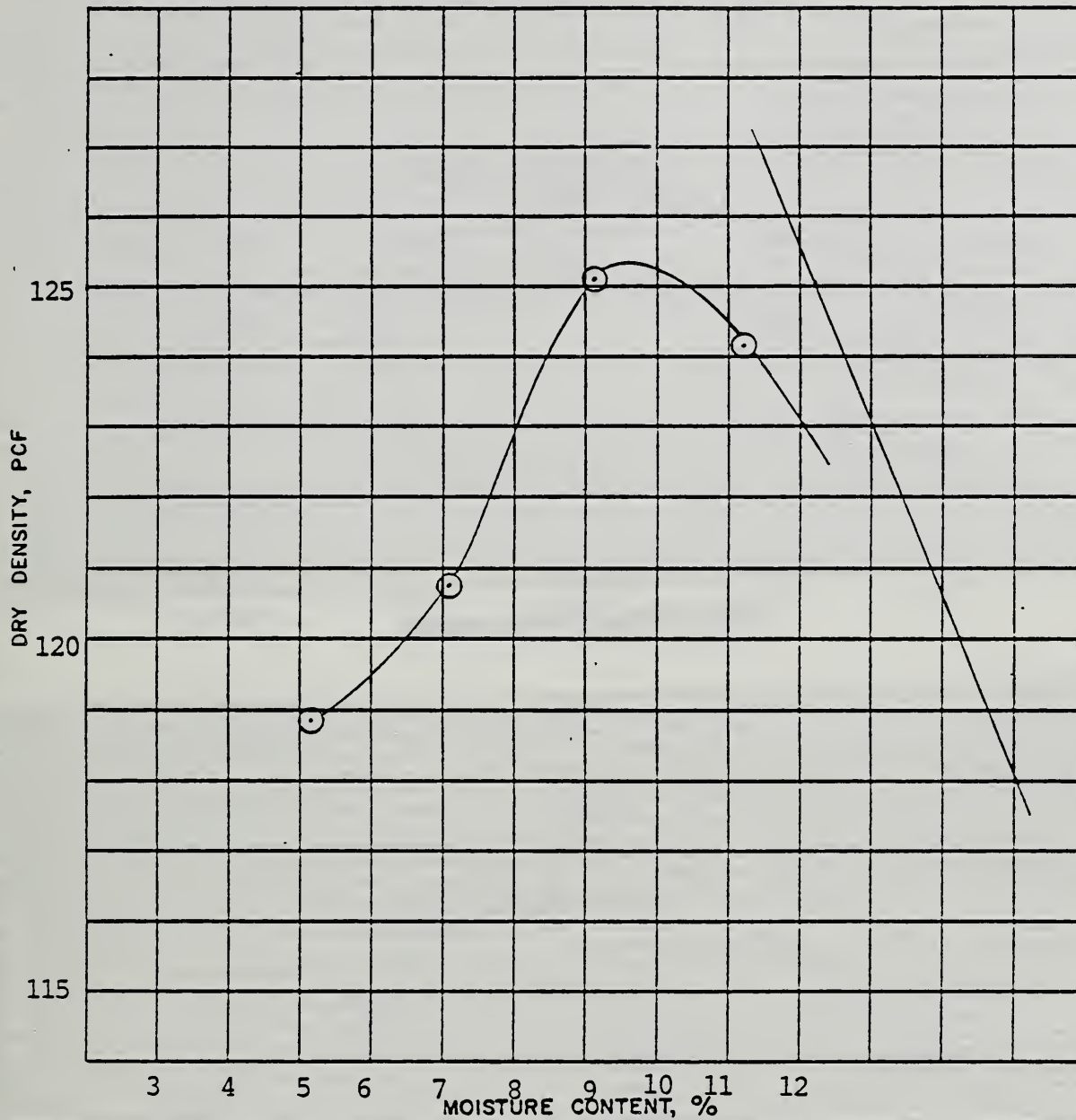
GRADATION CURVES

PROJECT: L'AMBIANCE PLAZA

BRIDGEPORT, CT

DATE 8-25-87

CONTR. NO.: CT870587



SPECIFIC GRAVITY 2.65

SPECIFICATION: ASTM D-1557  
METHOD:

DESCRIPTION OF SAMPLE  
SILTY SAND WITH WEATHERED ROCK FRAGMENTS,  
BROWN

SCHNABEL ENGINEERING  
ASSOCIATES

CLASSIFICATION: SM

MOISTURE DENSITY  
RELATION

SAMPLE NO.: TP-2 / 5.0'

LIQUID LIMIT: NP

SOURCE: ON-SITE

PLASTICITY INDEX: NP

L'AMBIANCE PLAZA  
BRIDGEPORT, CONNECTICUT

% PASSING 3/4" SIEVE

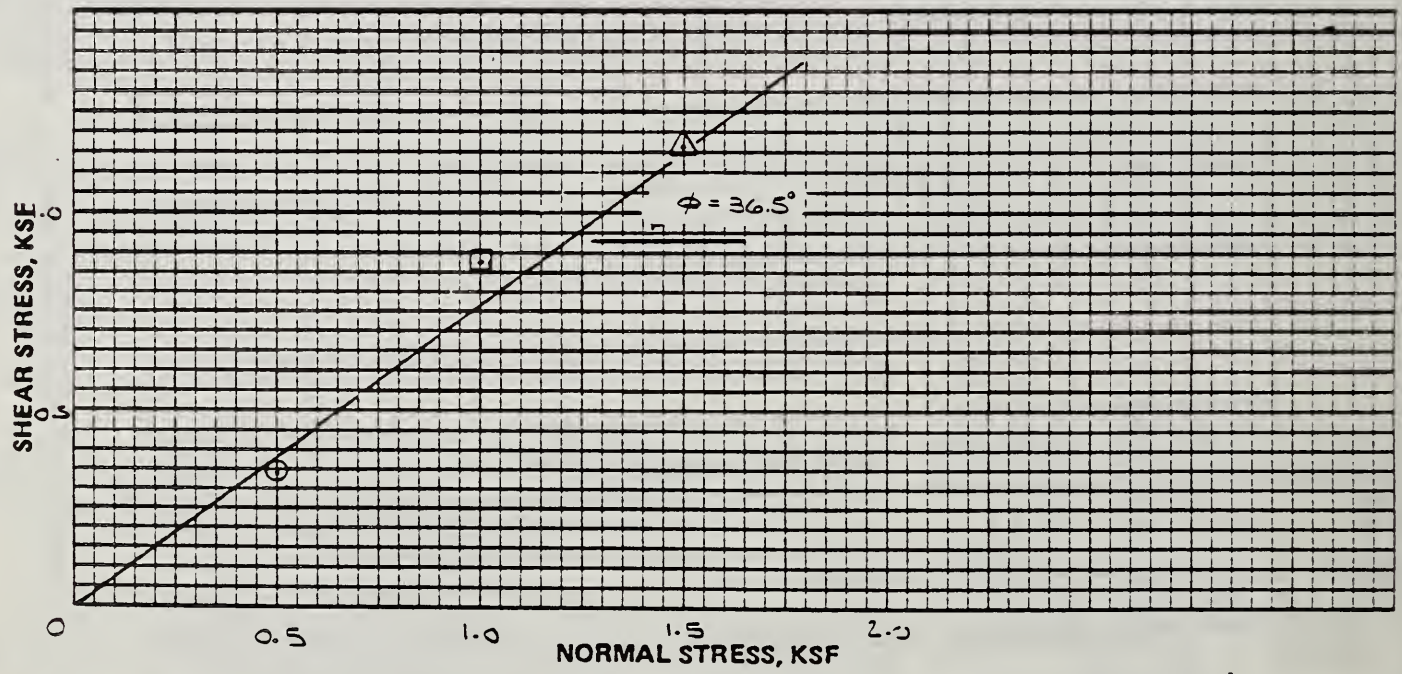
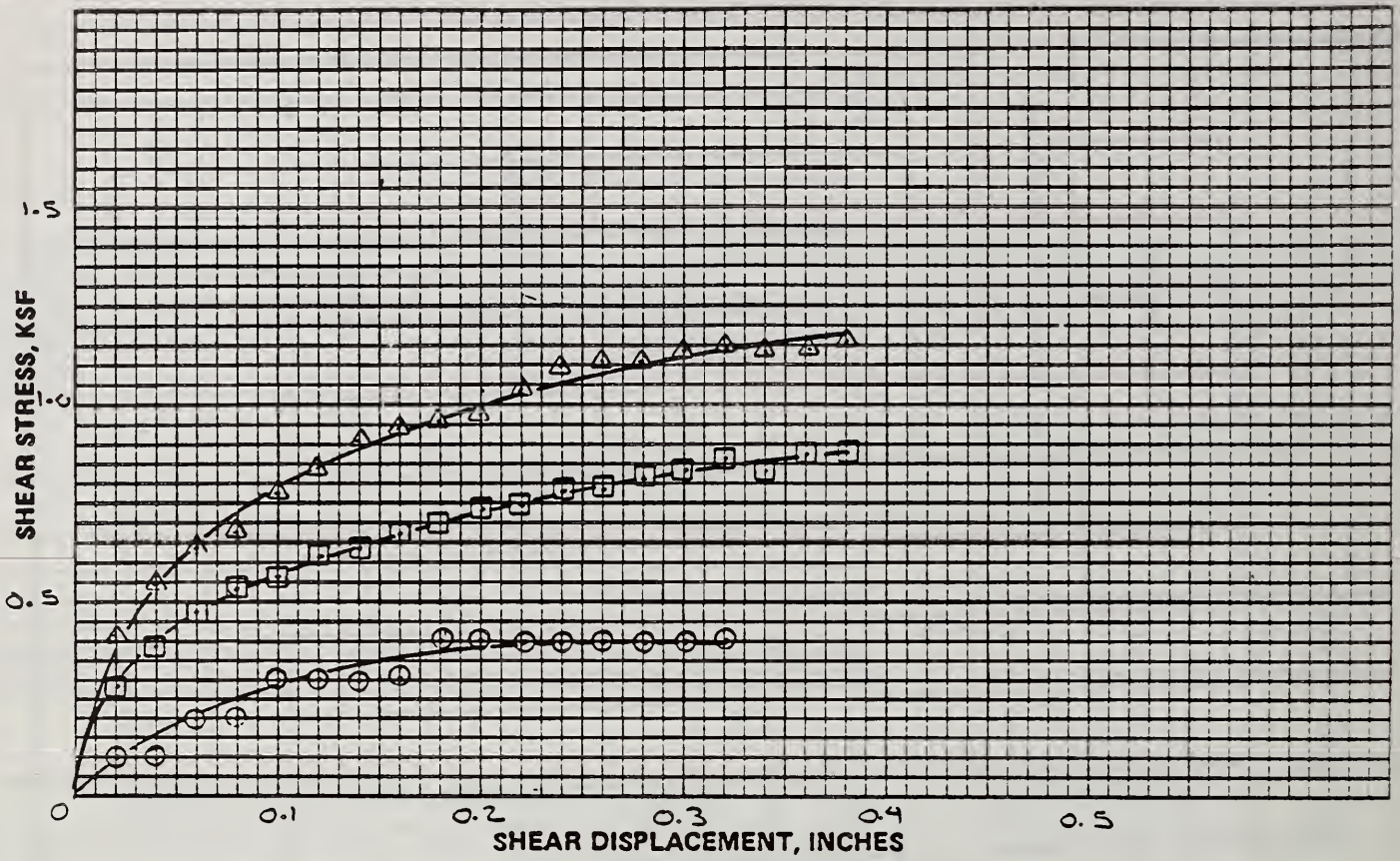
MAX DRY DENSITY 125.3 PCF

DATE  
8-25-87

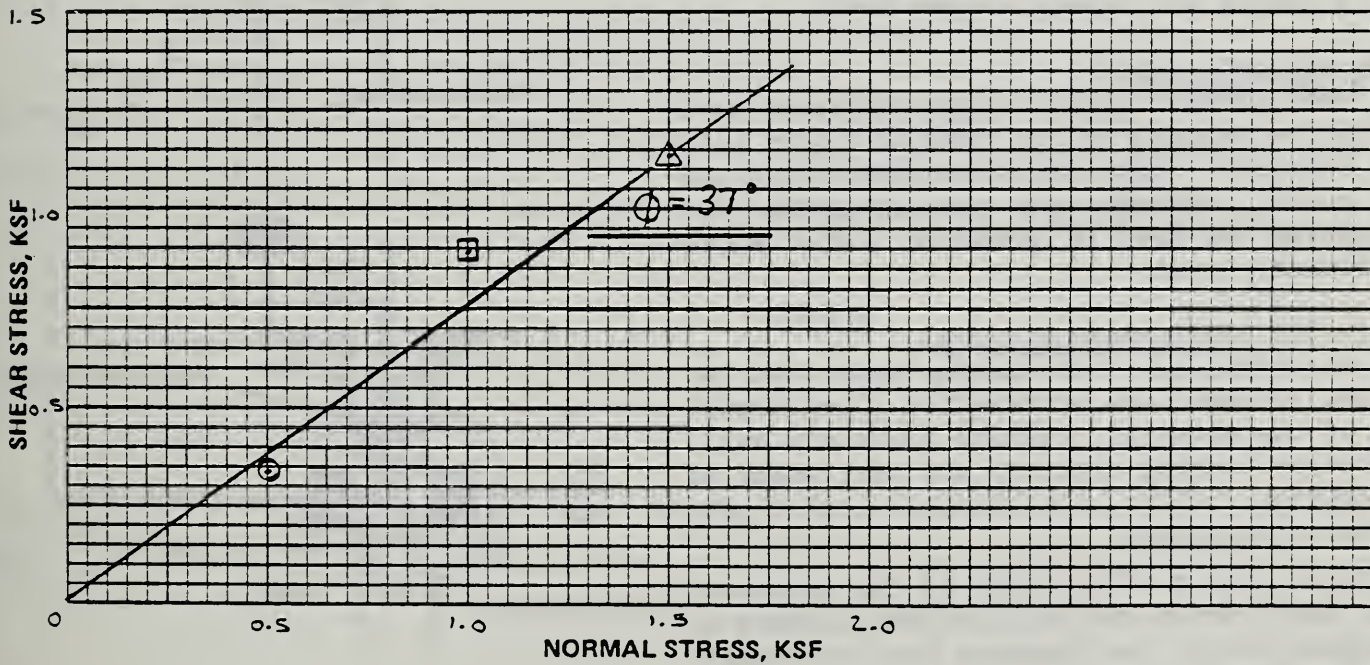
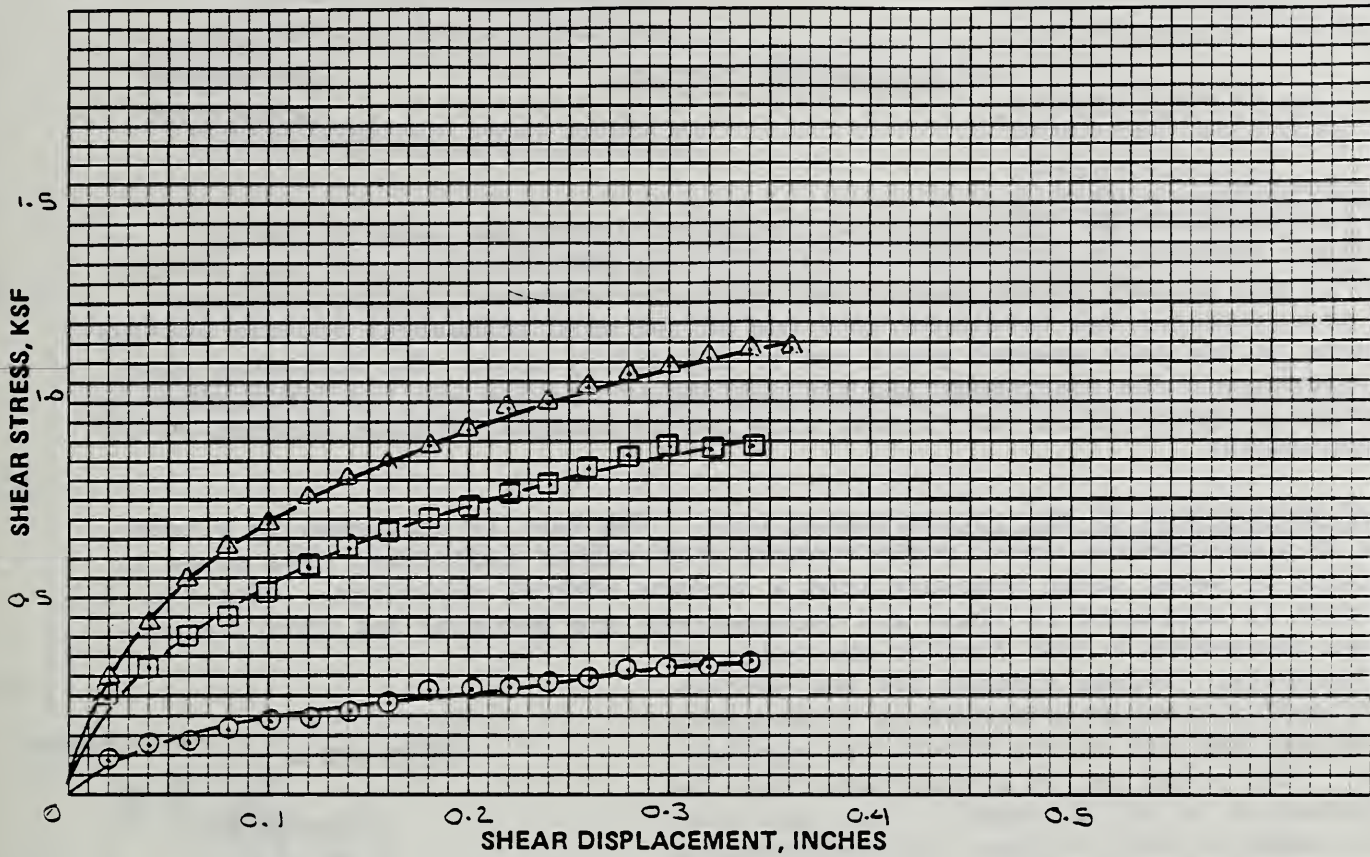
CONTRACT NO.  
CT870587

% PASSING NO. 4 SIEVE

OPT. MOISTURE 9.5 %



DESCRIPTION OF SOIL SAMPLE TESTED								SCHNABEL ENGINEERING ASSOCIATES	
								DIRECT SHEAR TEST	
KEY	BORING NO.	DEPTH FT.	NORMAL STRESS (KSF)	MOIST. CONT. %		DENSITY, PCF		TYPE OF TEST: CONSOLIDATED, UNDRAINED	
				INITIAL	FINAL	DRY	WET	RATE OF SHEAR: 0.03-0.05 INCHES/MINUTE	
○	TP-2	5.0	0.5	18.5	18.4	88.4	104.8	PROJECT: L'AMBIANCE BUILDING	
□	TP-2	5.0	1.0	18.5	18.7	96.6	114.5	PLAZA DAMAGE STUDY	
△	TP-2	5.0	1.5	18.7	18.7	93.4	110.9	DATE: 8-25-87	CONTR. NO.: CT870587



DESCRIPTION OF SOIL SAMPLE TESTED							SCHNABEL ENGINEERING ASSOCIATES		
							<b>DIRECT SHEAR TEST</b>		
							TYPE OF TEST: UNCONSOLIDATED, UNDRAINED		
							RATE OF SHEAR: 0.03 INCHES / MINUTE		
							PROJECT: L'AMRIANCE BUILDING		
							DAMAGE STUDY		
							DATE: 8-25-87	CONTR. NO.: CS70587	
KEY	BORING NO.	DEPTH FT.	NORMAL STRESS (KSF)	MOIST. CONT. % INITIAL	MOIST. CONT. % FINAL	DENSITY, PCF DRY	DENSITY, PCF WET		
○	TP-2	5.0	0.5	15.2	16.2	93.4	107.6		
□	TP-2	5.0	1.0	16.2	16.6	93.6	108.8		
△	TP-2	5.0	1.5	16.4	17.3	95.3	110.9		

Introduction

The pressuremeter developed by Louis Menard of France has been in use by Schnabel Engineering Associates since 1967. We were first to use this instrument in the eastern United States and offer pressuremeter testing services. The pressuremeter has developed into one of the more successful in-situ testing methods in the past several years and is now widely used. The following short description of the instrument and the outline of its use and its limitations is intended to familiarize our clients with the advantages of field testing by the pressuremeter.

Brief description of the pressuremeter test: The test is performed in a borehole by a cylindrical metal probe covered with rubber membranes. The probe is inflated by water under pressure from a surface control apparatus. (See Fig. 1.) Pressure is increased in steps and deformations are recorded and thus the procedure represents a load test on the walls of the borehole. Volume changes for one particular loading step are recorded at 15 seconds, 30 seconds and one minute after load application. The probe may be lowered and tests be performed up to 100 ft depth. Tests are generally made in test borings and some special equipment and techniques are required to prepare a boring for pressuremeter tests.

Areas of application

The pressuremeter test may be considered most useful in residual soils, granular soils with some cohesion, very stiff to hard clays and soft rock. Methods are also available for conducting the test in granular soils below groundwater level.

Results of pressuremeter tests

The test furnishes information as to the undrained strength and deformation characteristics of the material. Results provide a basis to predict bearing capacity and settlement of foundations, slope stability and other soil mechanics problems.

The basic result of the test is the pressuremeter curve which indicates volume increase of the probe versus the pressure applied considering readings at the end of each loading step. This curve also represents the deformation of the soil under lateral radial stresses. (See Fig. 2.) The initial portion represents the adjustments of the probe to the bore hole and further the restoration of the original horizontal pressures. Then a straight line portion of the curve follows which is the elastic deformation of the subsoil and can be measured by the slope of the line, resulting in the pressuremeter modulus  $E_p$ . This modulus is evaluated for each test and is shown in the units of tons per square foot ( $kg/cm^2$ ). The pressuremeter modulus is similar to the modulus of elasticity except it is measured in the horizontal direction. Corrections for anisotropy are necessary in most soils to obtain elasticity in the

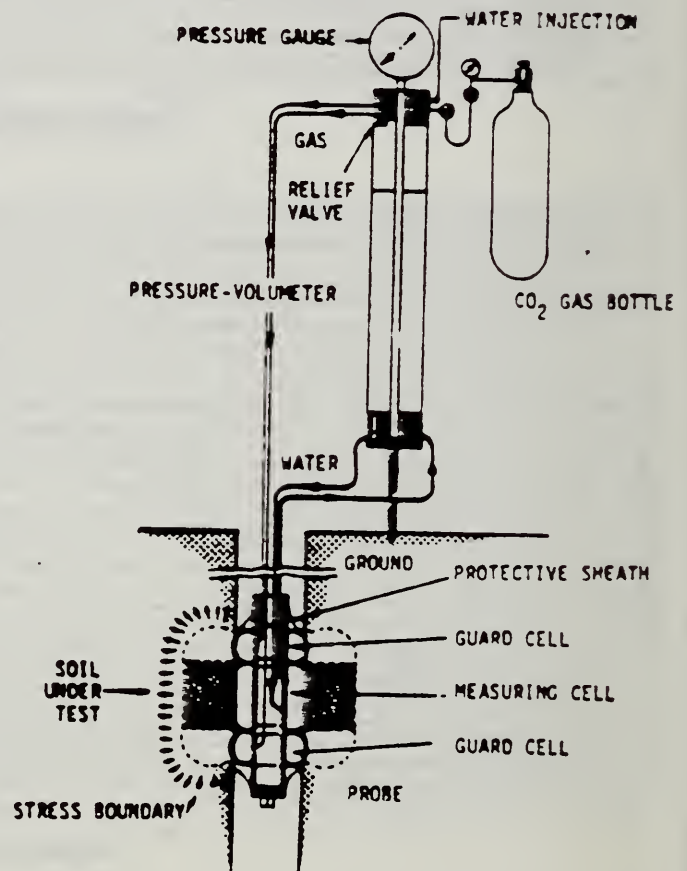
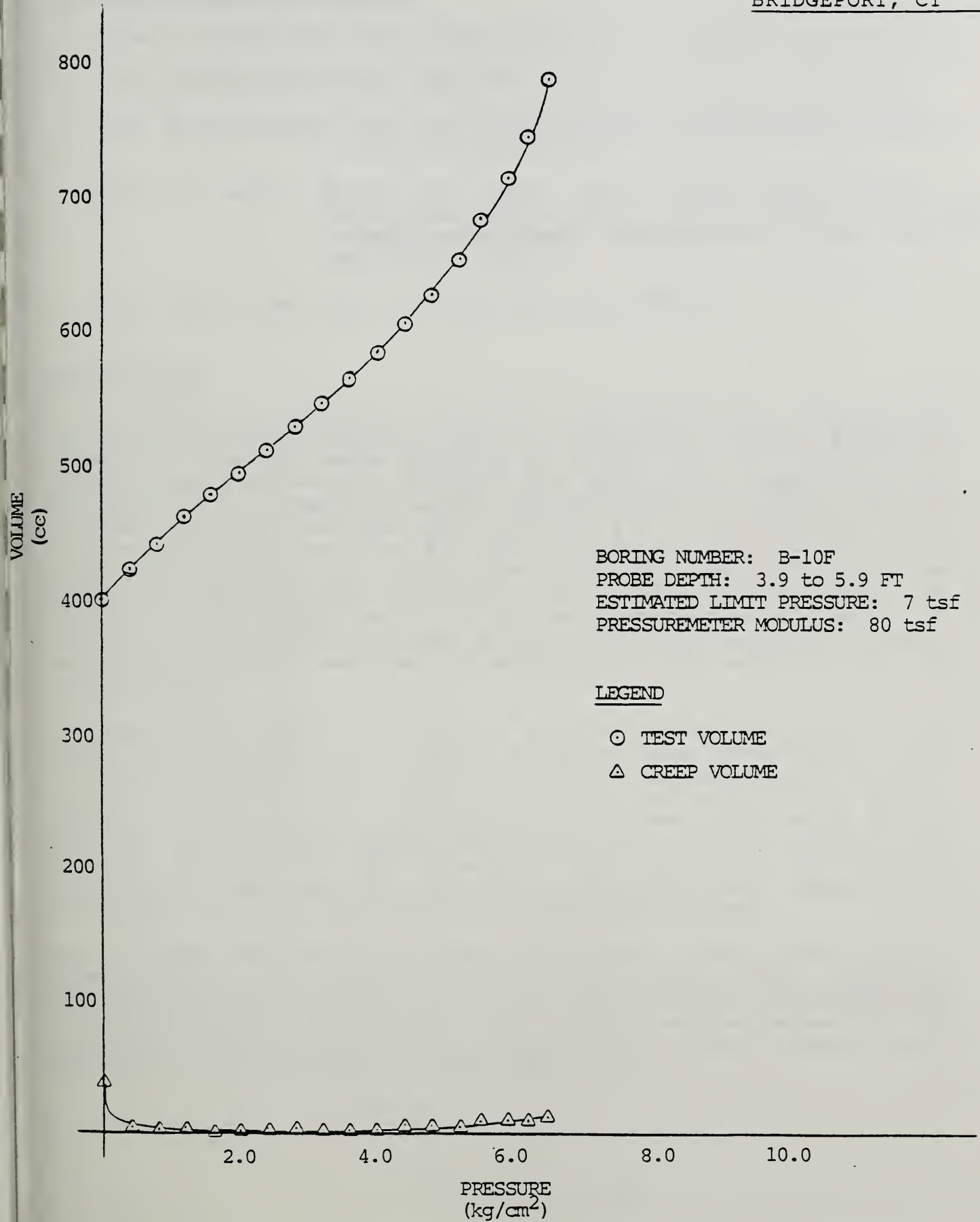


Figure 1

PRESSUREMETER TEST RESULTS

L'AMBIANCE PLAZA  
BUILDING COLLAPSE  
INVESTIGATION  
BRIDGEPORT, CT



BORING NUMBER: B-10F  
PROBE DEPTH: 3.9 to 5.9 FT  
ESTIMATED LIMIT PRESSURE: 7 tsf  
PRESSUREMETER MODULUS: 80 tsf

LEGEND  
○ TEST VOLUME  
△ CREEP VOLUME

SUBSURFACE EXPLORATION DATA



SUBSURFACE EXPLORATION DATA

General Notes for Test Boring Logs

Identification of Soil Samples

Test Boring Logs: B-1, B-2, B-2H, B-2HA, B-3E, B-4.8E, P-6H,  
B-9D, B-10D, B-10F

Test Pit Logs: TP-1H (east face), TP-1H (south face), TP-2H  
(west face), TP-2H (south face), TP-2H (east face),  
TP-10D (south face), TP-10F (north face), TP-10F  
(west face), TP-2

Test Boring and Test Pit Location Plan, Sheet 2

Test Borings

Test borings at footing locations were advanced through the footings to allow sampling and/or testing of actual subgrade materials. Borings were advanced by coring into the floor slab, footing, and intermediate backfill for floor slab support with an HW core barrel. The core barrel was advanced to within 2 inches of plan footing bottom and through all reinforcing steel encountered. A three inch tri-cone roller bit was used to break apart the concrete and flush the concrete cuttings until the bottom of the footing was penetrated. Reinforcing steel was removed with a magnet before breaking through the bottom of the footing. The roller bit was immediately removed and Standard Penetration Testing was used to sample and test materials to the rock surface.

To sample the underlying bedrock once encountered, the HW core barrel was advanced to the depth of split spoon penetration. The tri-cone roller bit and circulated water was used to cut to this depth. At Footing 10-F the roller bit was advanced about 0.2 ft further to seat in the rock surface. Rock was cored using double tube NX core barrels, except at Footing 10-D where a single tube NX core barrel was used because it was the only core barrel available at the time the test coring was performed. Percentages of recovery and RQD are indicated on the boring logs.

Test borings north of the building wall were drilled using hollow-stem augers. The augers were advanced with a plug inserted. Continuous sampling using the driven split spoon was performed following removal of the plug. The sampling was performed in 2 ft intervals as indicated on the Test Boring Logs. Augers were advanced following two successive samplings.

The driven split spoon was used to obtain the Standard Penetration Test resistance "N" values in soil materials. "N" values were determined as the number of blows required to drive a 2 inch O.D., 1-3/8 inch I.D. sampling spoon one foot using an automatic SPT hammer system. The driving force is provided by a 140 pound hammer falling 30 inches. In accordance with ASTM D-1556, the "N" value is taken after seating the sampler 6 inches in the bottom of the hole. The driving force provided by the automatic hammer has been studied by Riggs, Mathes and Rassieur (8), and results indicate "N" values in the lower range of those produced by using the standard cathead and rope method, with two wraps.


### Test Pits

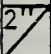

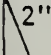
Most test pits were excavated with a crawler mounted, hydraulic backhoe. Some less accessible areas of the test pits and TP-2H (south face) were excavated with a rubber-tire backhoe/loader.

### Test Boring/Pit Location and Elevation Survey

Test borings and test pits were located by taping from existing building features as shown on Sheet 2. These locations should be considered accurate to 1 ft +. Elevations at footing locations were measured from the top of the footing and were referenced to plan top of footing elevations. Test pit and boring elevations north of the building wall were referenced to plan top of wall elevations. The elevations should be considered accurate to the nearest 0.5 ft + from the referenced feature.

GENERAL NOTES FOR TEST BORING LOGS

1. NUMBERS IN "SAMPLE SPOON" COLUMN INDICATE BLOWS REQUIRED TO DRIVE A 2 INCH O.D., 1-3/8 INCH I.D. SAMPLING SPOON 6 INCHES USING A 140 POUND HAMMER FALLING 30 INCHES ACCORDING TO ASTM D-1586.
2. VISUAL CLASSIFICATION OF SOIL IS IN ACCORDANCE WITH TERMINOLOGY SET FORTH IN "IDENTIFICATION OF SOIL." THE UNIFIED SOIL CLASSIFICATION SYMBOLS SHOWN IN PARENTHESES ARE BASED ON VISUAL INSPECTION.
3. ESTIMATED GROUNDWATER LEVELS INDICATED BY ; THESE LEVELS ARE ONLY ESTIMATES FROM AVAILABLE DATA AND MAY VARY WITH PRECIPITATION, POROSITY OF THE SOIL, SITE TOPOGRAPHY, ETC.
4. REFUSAL AT THE SURFACE OF ROCK, BOULDER, OR OBSTRUCTION IS DEFINED AS A PENETRATION RESISTANCE OF 100 BLOWS FOR 2 INCHES PENETRATION OR LESS.
5. THE BORING LOGS AND RELATED INFORMATION DEPICT SUBSURFACE CONDITIONS ONLY AT THE SPECIFIC LOCATIONS AND AT THE PARTICULAR TIME WHEN DRILLED. SOIL CONDITIONS AT OTHER LOCATIONS MAY DIFFER FROM CONDITIONS OCCURRING AT THESE BORING LOCATIONS. ALSO, THE PASSAGE OF TIME MAY RESULT IN A CHANGE IN THE SUBSURFACE SOIL AND GROUNDWATER CONDITIONS AT THESE BORING LOCATIONS.
6. THE STRATIFICATION LINES REPRESENT THE APPROXIMATE BOUNDARY BETWEEN SOIL AND ROCK TYPES AS DETERMINED FROM THE DRILLING AND SAMPLING OPERATION. SOME VARIATION MAY ALSO BE EXPECTED VERTICALLY BETWEEN SAMPLES TAKEN. THE SOIL PROFILE, WATER LEVEL OBSERVATIONS AND PENETRATION RESISTANCES PRESENTED ON THESE BORING LOGS HAVE BEEN MADE WITH REASONABLE CARE AND ACCURACY AND MUST BE CONSIDERED ONLY AN APPROXIMATE REPRESENTATION OF SUBSURFACE CONDITIONS TO BE ENCOUNTERED AT THE PARTICULAR LOCATION.
7. BORING LOG VERTICAL SCALE: 1/6 INCH = 1 FT.
8. TEST BORINGS DRILLED BY CONNECTICUT TEST BORINGS, INC., SEYMOUR, CONNECTICUT UNDER INSPECTION OF SCHNABEL ENGINEERING ASSOCIATES.
9. KEY TO SYMBOLS AND ABBREVIATIONS:

S	STANDARD PENETRATION TEST	*, NO SAMPLE RECOVERY
2" 	2" or 3" UNDISTURBED TUBE SAMPLE (RECOVERY SHOWN IN REMARKS COLUMN)	do, DITTO
	PRESSUREMETER TEST	RQD, ROCK QUALITY DESIGNATION
V	VANE SHEAR TEST	w, NATURAL MOISTURE CONTENT
C	STATIC CONE PENETRATION TEST	
2" 	NX OR 2 INCH O.D. ROCK CORE RUN (RECOVERY SHOWN IN REMARKS COLUMN)	

# SCHNABEL ENGINEERING ASSOCIATES

## Consulting Geotechnical Engineers

### IDENTIFICATION OF SOIL

#### I. DEFINITION OF SOIL GROUP NAMES

ASTM D-2487-83

		Symbol	Group Name
Coarse-Grained Soils More than 50% retained on No. 200 sieve	Gravels — More than 50% of coarse fraction retained on No. 4 sieve Coarse, 3/4" to 3" Fine, No. 4 to 3/4"	Clean Gravels Less than 5% fines	GW Well graded gravel
			GP Poorly graded gravel
		Gravels with Fines More than 12% fines	GM Silty gravel
			GC Clayey gravel
	Sands — 50% or more of coarse fraction passes No. 4 sieve Coarse, No. 10 to No. 4 Medium, No. 40 to No. 10 Fine, No. 200 to No. 40	Clean Sands Less than 5% fines	SW Well-graded sand
			SP Poorly graded sand
		Sands with Fines More than 12% fines	SM Silty sand
			SC Clayey sand
Fine-Grained Soils 50% or more passes the No. 200 sieve	Silts and Clays — Liquid Limit less than 50 Low to medium plasticity	Inorganic	CL Lean clay
			ML Silt
		Organic	OL Organic clay Organic silt
	Silts and Clays — Liquid Limit 50 or more Medium to high plasticity	Inorganic	CH Fat clay
			MH Elastic silt
		Organic	OH Organic clay Organic silt
Highly Organic Soils	Primarily organic matter, dark in color, and organic odor	PT	Peat

#### II. DEFINITION OF MINOR COMPONENT PROPORTIONS

Minor Component	Approximate Percentage of Fraction by Weight
<b>Adjective Form</b> Gravelly, Sandy	30% or more coarse grained
<b>With</b> Sand, Gravel	15% or more coarse grained
Silt, Clay	5% to 12% fine grained
<b>Trace</b> Sand, Gravel	Less than 15% coarse grained
Silt, Clay	Less than 5% fine grained

#### III. GLOSSARY OF MISCELLANEOUS TERMS

**SYMBOLS** — Unified Soil Classification Symbols are shown above as group symbols. Use A Line Chart for laboratory identification. Dual symbols are used for borderline classifications.

**BOULDERS & COBBLES** — Boulders are considered rounded pieces of rock larger than 12 inches, while cobbles range from 3 to 12 inch size.

**DISINTEGRATED ROCK** — Residual rock material with a standard penetration resistance (SPT) of more than 60 blows per foot, and less than refusal. Refusal is defined as a SPT of 100 blows for 2" or less penetration.

**ROCK FRAGMENTS** — Angular pieces of rock, distinguished from transported gravel, which have separated from original vein or strata and are present in a soil matrix.

**QUARTZ** — A hard silica mineral often found in residual soils

**IRONITE** — Iron oxide deposited within a soil layer forming cemented deposits

**CEMENTED SAND** — Usually localized rock-like deposits within a soil stratum composed of sand grains cemented by calcium carbonate or other materials.

**MICA** — A soft plate of silica mineral found in many rocks, and in residual or transported soil derived therefrom.

**ORGANIC MATERIALS** (Excluding Peat):

Topsoil - Surface soils that support plant life and which contain considerable amounts of organic matter:

Organic Matter - Soil containing organic colloids throughout its structure;

Lignite - Hard, brittle decomposed organic matter with low fixed carbon content (a low grade of coal).

**FILL** — Man made deposit containing soil, rock and often foreign matter.

**PROBABLE FILL** — Soils which contain no visually detected foreign matter but which are suspect with regard to origin

**LENSES** — 0 to 1/2 inch seam of minor soil component.

**LAYERS** — 1/2 to 12 inch seam of minor soil component.

**POCKET** — Discontinuous body of minor soil component

**COLOR SHADES** — Light to dark to indicate substantial difference in color.

**MOISTURE CONDITIONS** — Wet, moist, or dry to indicate visual appearance of specimen.

PROJECT: L'AMBIANCE PLAZA, BUILDING COLLAPSE INVESTIGATION

SHEET NO: 1 OF 1

CLIENT: NATIONAL BUREAU OF STANDARDS

JOB NO: CT870587

BORING CONTRACTOR: CONNECTICUT TEST BORINGS, INC. DRILL: CME55

ELEVATION: -9.3+

WATER LEVEL DATA

DRIVE SAMPLER

CASING SIZE:

	DATE	TIME	DEPTH	CAVED	TYPE	S. S.	DATE START:
ENCOUNTERED	5-30		DRY	---	DIA.	2" O.D.	5-30-87
AFTER CASING PULLED	5-30		DRY	12'	WT.	140#	DATE FINISHED: 5-30-87
HR. READING	BACKFILLED UPON COMPLETION				FALL	30"	DRILLER: J. DeANGELISS
							INSPECTOR: C. DeVAULT

STRATUM	DEPTH FT.	ELEV.	BLOWS ON SAMPLE SPOON PER 6"	SYMBOL	IDENTIFICATION	REMARKS	
		-9.3±					
A1		-20	4-3-		SILTY SAND FILL WITH CONCRETE FRAGMENTS IN NOSE OF SPOON FROM 0 TO 2 FT, MOIST - BROWN (SM)	BACKFILL	
			2-1	S			
			1-1-				
			1-1	S			
			WOR-1-				
			1-2	S			
			6-9-				
			10-16	S			DO, WITH ROCK FRAGMENTS AND BRICK
			5-3-				
			3-3	S			DO, WITH CINDERS
			3-4-				
			9-10	S			
			4-6-				
			10-11	S			DO, WITH ROCK FRAGMENTS IN NOSE OF SPOON
			4-3-				
	2-4	S	DO, WITH MICA - GRAY				
	3-2-						
	4-3	S					
C	18.5		5-7-		DISINTEGRATED ROCK WITH QUARTZ AND MICA, MOIST - GRAY	RESIDUAL	
	20.0		27-82	S	BORING TERMINATED AT 20'		

SCHNABEL ENGINEERING ASSOCIATES CONSULTING ENGINEERS	TEST BORING LOG	BORING NO: B-2					
PROJECT: L'AMBIANCE PLAZA, BUILDING COLLAPSE INVESTIGATION		SHEET NO: 1 OF 1					
CLIENT: NATIONAL BUREAU OF STANDARDS		JOB NO: CT870587					
BORING CONTRACTOR: CONNECTICUT TEST BORINGS, INC. DRILL: CME55		ELEVATION: -10.3±					
WATER LEVEL DATA							
	DATE	TIME	DEPTH	CAVED	DRIVE SAMPLER TYPE	S.S.	CASING SIZE:
ENCOUNTERED	6-1		DRY	—	DIA.	2" O.D.	DATE START: 6-1-87
AFTER CASING PULLED	6-1		DRY	10'	WT.	140#	DATE FINISHED: 6-1-87
HR. READING	BACKFILLED UPON COMPLETION				FALL	30"	INSPECTOR: C. DevAULT

STRATUM	DEPTH FT.	ELEV.	BLOWS ON SAMPLE SPOON PER 6"	SYMBOL	IDENTIFICATION	REMARKS
		-10.3±	5-3 -		SILTY SAND FILL WITH ROCK FRAGMENTS, MOIST-BROWN (SM)  DO, WITH BRICK	BACKFILL
A 1			6-7	S		
			6-4 -			
			4-4	S		
			2-2 -			
			2-1	S		
			1-2 -			
			1-2	S		
			0-3 -			
			5-3	S		
			2-1 -			
		1-2	S			
		3-1 -				
	13.5		3-12	S	SILTY SAND WITH MICA, MOIST - GRAY AND BROWN (SM)	RESIDUAL
B	16.0		17-20 -	S		
			29-43	S		
					BORING TERMINATED AT 16.0'	



SCHNABEL ENGINEERING ASSOCIATES CONSULTING ENGINEERS		TEST BORING LOG		BORING NO : B-2HA		
PROJECT: L'AMBIANCE PLAZA, BUILDING COLLAPSE INVESTIGATION				SHEET NO : 1 OF 1		
CLIENT: NATIONAL BUREAU OF STANDARDS				JOB NO: CT870587		
BORING CONTRACTOR: CONNECTICUT TEST BORINGS, INC				ELEVATION: -27.3±		
DRILL: CMB55				CASING SIZE:		
WATER LEVEL DATA			DRIVE SAMPLER		DATE START: 5-28-87	
	DATE	TIME	DEPTH	CAVED	TYPE	S. S.
ENCOUNTERED	5-30		SEE NOTE BELOW	DIA.	2" O.D.	DATE FINISHED: 5-28-87
AFTER CASING PULLED	5-31		-	-	WT.	DRILLER: J. DeANGELISS
7 HR. READING	6-17	CAVED AND DRY AT 48"	FALL	30"		INSPECTOR: C. DeVAULT

STRATUM	DEPTH FT.	ELEV.	BLOWS ON SAMPLE SPOON PER 6"	SYMBOL	IDENTIFICATION	REMARKS
		-27.3±			5-3/4" CONCRETE	FLOOR SLAB AND BACKFILL
A1	1.0				FINE TO COARSE SILTY SAND FILL WITH GRAVEL	
		-30			- BROWN (SM)	
					CONCRETE	FOOTING
	6.1					
C	7.0		103-125/5"	S	DISINTEGRATED ROCK WITH MICA, MOIST - BROWN	RESIDUAL
	7.5				AND GRAY	
			REC=100%	NX	SLIGHTLY WEATHERED, HARD, GRAY SCHIST,	PROSPECT FORMATION
D			RQD= 73%		MODERATELY FRACTURED	
	11.5				BORING TERMINATED AT 11.5'	a. ROLLER BIT TO 7.5 FT TO REMOVE REINFORCING STEEL
					NOTE:-WATER USED DURING CORING. THEREFORE WATER LEVEL IN BORING UNNATURALLY HIGH DURING AND UPON BORING COMPLETION	
					NOTE:-FINAL WATER LEVEL READING OBTAINED FROM TEST PIT ON EAST SIDE OF FOOTING 2H, LEVEL AT EL -32.2	
					NOTE:-WATER OBSERVED FLOWING INTO TEST PIT EXCAVATION ON THE WEST SIDE OF FOOTING 2H. WATER FLOWING IN THROUGH FISSURES IN ROCK AT OR UP TO ABOUT 6 INCHES BELOW BOTTOM OF FOOTING	



PROJECT: AMBIANCE PLAZA, BUILDING COLLAPSE INVESTIGATION

SHEET NO.: 1 OF 1

CLIENT: NATIONAL BUREAU OF STANDARDS

JOB NO.: CT870587

BORING CONTRACTOR: CONNECTICUT TEST BORINGS, INC. DRILL: CME55

ELEVATION: -27.0±

WATER LEVEL DATA

DRIVE SAMPLER

CASING SIZE:

	DATE	TIME	DEPTH	CAVED	TYPE	S.S.	DATE START:
ENCOUNTERED	5-30		SEE NOTE BELOW		DIA.	2" O.D.	5-30-87
AFTER CASING PULLED	5-30				WT.	140#	5-30-87
HR. READING	BORING BURIED IN RUBBLE UPON			FALL	30"		

DRILLER: J. DeANGELISS  
INSPECTOR: C. DeVAULT

STRATUM	DEPTH FT.	ELEV.	BLOWS ON SAMPLE SPOON, PER 6"	SYMBOL	COMPLETION IDENTIFICATION	REMARKS
		-27.0±			6.75" CONCRETE	FLOOR SLAB AND BACKFILL
A1	1.3				FINE TO COARSE SILTY SAND, FILL WITH GRAVEL - BROWN (SM)	BACKFILL
		-30			CONCRETE (FOOTING)	FOOTING
	4.8				SILTY SAND WITH ROCK FRAGMENTS, MOIST - BROWN (SM)	PROBABLE FILL
A	5.8		8-8-	S		
C	6.8		58-100/5.5		DISINTEGRATED ROCK, MOIST-BROWN AND GRAY	RESIDUAL
			REC=92% ROD=75%	NX	SLIGHTLY WEATHERED, HARD, GRAY SCHIST, SLIGHTLY TO MODERATELY FRACTURED	PROSPECT FORMATION
D	11.7					
					BORING TERMINATED AT 11.7'	
					NOTE:-WATER USED DURING CORING. THEREFORE WATER LEVEL IN BORING UNNATURALLY HIGH DURING AND UPON BORING COMPLETION	



SCHNABEL ENGINEERING ASSOCIATES CONSULTING ENGINEERS		TEST BORING LOG		BORING NO: B-6H	
PROJECT: L'AMBIANCE PLAZA, BUILDING COLLAPSE INVESTIGATION				SHEET NO: 1 OF 1	
CLIENT: NATIONAL BUREAU OF STANDARDS				JOB NO: CT870587	
BORING CONTRACTOR: CONNECTICUT TEST BORINGS, INC				ELEVATION: -27.3±	
DRILL: CME55				CASING SIZE:	
WATER LEVEL DATA		DATE		TIME	
ENCOUNTERED		5-31		SEE NOTE BELOW	
AFTER CASING PULLED		6-1		--	
6 DAY READING		6-17		CAVED AND DRY AT 51"	
DRIVE SAMPLER		TYPE		S.S.	
ENCOUNTERED		DIA.		2" O.D.	
AFTER CASING PULLED		WT.		140#	
6 DAY READING		FALL		30"	
				DATE START: 5-31-87	
				DATE FINISHED: 6-1-87	
				DRILLER: J. DeANGELISS	
				INSPECTOR: C. DeVAULT	

STRATUM	DEPTH FT.	ELEV.	BLOWS ON SAMPLE SPOON PER 6"	SYMBOL	IDENTIFICATION	REMARKS
		-27.3±			5" CONCRETE	FLOOR SLAB AND BACKFILL
A1	1.4	-30			FINE TO COARSE SILTY SAND, FILL WITH GRAVEL - BROWN (SM)	
	3.7				CONCRETE	FOOTING
A	4.2		12-61-		NOTE A	
C	5.3		100/5"	S	NOTE B	RESIDUAL
			REC=97%	NX	SLIGHTLY WEATHERED, HARD GRAY SCHIST, SLIGHTLY TO MODERATELY FRACTURED	PROSPECT FORMATION
D	8.3		ROD=86%			
					BORING TERMINATED AT 8.3'	NOTE: FROM 3.7' TO 4.1' MAY BE SOIL FILL MATERIAL
					NOTE A: -SILTY SAND, PROBABLE FILL WITH ROCK FRAGMENTS, MOIST - BROWN (SM)	
					NOTE B: -DISINTEGRATED ROCK WITH MICA, MOIST - GRAY AND BROWN	
					NOTE: -WATER USED DURING CORING. THEREFORE WATER LEVEL IN BORING UNNATURALLY HIGH DURING AND UPON BORING COMPLETION	

SCHNABEL ENGINEERING ASSOCIATES CONSULTING ENGINEERS				TEST BORING LOG			BORING NO: B-10D	
PROJECT: L'AMBIANCE PLAZA, BUILDING COLLAPSE INVESTIGATION						SHEET NO: 1 OF 1		
CLIENT: NATIONAL BUREAU OF STANDARDS						JOB NO: CT870587		
BORING CONTRACTOR: CONNECTICUT TEST BORINGS, INC						DRILL: CME55	ELEVATION: -27.3±	
WATER LEVEL DATA				DRIVE SAMPLER		CASING SIZE:		
	DATE	TIME	DEPTH	CAVED	TYPE	S.S.	DATE START: 5-28-87	
ENCOUNTERED	5-28		SEE NOTE BELOW		DIA.	2" O.D.	DATE FINISHED: 5-28-87	
AFTER CASING PULLED	5-28				WT.	140*	DRILLER: J. DeANGELISS	
20 DAY READING	6-17		CAVED AND DRY AT 48"		FALL	30"	INSPECTOR: C. DeVAULT	
STRATUM	DEPTH FT.	ELEV.	BLOWS ON SAMPLE SPOON PER 6"	SYMBOL	IDENTIFICATION		REMARKS	
		-27.3±			3.75" CONCRETE		FLOOR SLAB AND BACKFILL	
A1	1.0				FINE TO COARSE SILTY SAND FILL -			
		-30			BROWN (SM) CONCRETE		FOOTING	
	4.7							
C	5.4		30-110/3"	S	DISINTEGRATED ROCK, MOIST - GRAY AND BROWN		RESIDUAL	
D			REC=42% ROD=7%	NX	SLIGHTLY WEATHERED, HARD, GRAY SCHIST, MODERATELY FRACTURED		PROSPECT FORMATION	
	10.3				BORING TERMINATED AT 10.3'		NOTE: SINGLE TUBE CORE BARREL USED	
					NOTE:-WATER USED DURING CORING. THEREFORE WATER LEVEL IN BORING UNNATURALLY HIGH DURING AND UPON BORING COMPLETION			
					NOTE:-WATER LEVEL MEASURED AT 62 INCHES BELOW THE FLOOR SLAB IN THE TEST PIT BETWEEN FOOTINGS 10F and 10D ON 6-1-87 AND 6-17-87, WATER LEVEL AT EL -32.5			

SCHNABEL ENGINEERING ASSOCIATES CONSULTING ENGINEERS		TEST BORING LOG		BORING NO: B-10F		
PROJECT: L'AMBIANCE PLAZA, BUILDING COLLAPSE INVESTIGATION				SHEET NO: 1 OF 1		
CLIENT: NATIONAL BUREAU OF STANDARDS				JOB NO: CT870587		
BORING CONTRACTOR: CONNECTICUT TEST BORINGS, INC.				ELEVATION: -27.4±		
DRILL: CMSS				CASING SIZE:		
WATER LEVEL DATA			DRIVE SAMPLER		DATE START: 5-28-87	
	DATE	TIME	DEPTH	CAVED	TYPE	S.S.
ENCOUNTERED	5-28		SEE NOTE BELOW		DIA.	2" O.D.
AFTER CASING PULLED	5-29		--	--	WT.	140#
9 DAY READING	6-17		CAVED AND DRY AT 48"	FALL	30"	INSPECTOR: C. DeVAULT

STRATUM	DEPTH FT.	ELEV.	BLOWS ON SAMPLE SPOON PER 6"	SYMBOL	IDENTIFICATION	REMARKS
		-27.4±			7" CONCRETE	FLOOR SLAB AND BACKFILL
A1	0.9				FINE TO COARSE SILTY SAND FILL -	
		-30			BROWN (SM) CONCRETE	FOOTING
	3.9					
A	5.9		5-6-10-39	S	POORLY GRADED SAND WITH SILT AND ROCK FRAGMENTS, TRACE MICA, MOIST - BROWN (SP-SM)	PROBABLE FILL
	6.1			S		
D			REC=93% ROD=74%	NX	SLIGHTLY WEATHERED, MODERATELY HARD TO HARD GRAY SCHIST, MODERATELY FRACTURED MODERATELY FRACTURED	PROSPECT FORMATION
	11.1				BORING TERMINATED AT 11.1'	a. ROLLER BIT TO 6'1" PRIOR TO CORING
					NOTE:-WATER USED DURING CORING. THEREFORE WATER LEVEL IN BORING UNNATURALLY HIGH DURING AND UPON BORING COMPLETION	
					NOTE:-WATER LEVEL MEASURED AT 62 INCHES BELOW THE FLOOR SLAB IN THE TEST PIT BETWEEN FOOTINGS 10F AND 10D ON 6-1-87 AND 6-17-87, WATER LEVEL AT EL -32.5	

SCHNABEL ENGINEERING ASSOCIATES  
 GEOTECHNICAL CONSULTANTS  
 WEST CHESTER, PA.  
 TEST PIT LOG

Contract No. CT870587 Date Started: 6-1-87 Date Ended: 6-1-87  
 Test Pit No. TP-1H (EAST FACE) Surface Elevation: -27.3  
 Project: L'AMBIANCE PLAZA BLDG. Groundwater Elevation: DRY  
COLLAPSE INVESTIGATION  
 Location: WASHINGTON AND Equipment for Excavation: RUBBERTIRE BACKHOE/  
COURTLAND, BRIDGEPORT, CT SEA Representative: C. DeVAULT  
LOADER

Depth	Elev. -27.3	Stratum	Description of Soil and Observations	Remarks
1'			5" CONCRETE FINE TO COARSE SILTY SAND FILL WITH GRAVEL, MOIST - BROWN (SM)	FLOOR SLAB AND BACKFILL
2.75'			CONCRETE	FOOTING

BACKHOE REFUSAL ON ROCK AT FOOTING SUBGRADE @ 2.75'      Entire east face  
of footing exposed  
(4.5 ft N to S)

Notes on materials at bottom of test pit:

- 1) Gray, hard, slightly weathered schist rock, thinly bedded.
- 2) ENE strike, very steep dip (appears to be greater than 70° north).
- 3) Backhoe barely able to gouge rock surface.
- 4) Contact between footing concrete and bedrock continuous.

SCHNABEL ENGINEERING ASSOCIATES  
 GEOTECHNICAL CONSULTANTS  
 WEST CHESTER, PA.  
 TEST PIT LOG

Contract No. CT870587 Date Started: 6-1-87 Date Ended: 6-1-87  
 Test Pit No. TP-1H (SOUTH FACE) Surface Elevation: -27.3  
 Project: L'AMBIANCE PLAZA BLDG. Groundwater Elevation: DRY  
COLLAPSE INVESTIGATION  
 Location: WASHINGTON AND Equipment for Excavation: RUBBERTIRE BACKHOE/  
COURTLAND, BRIDGEPORT, CT LOADER  
 SEA Representative: C. DeVAULT

Depth	Elev.	Stratum	Description of Soil and Observations	Remarks
	-27.3			
1'			5" CONCRETE FINE TO COARSE SILTY SAND FILL WITH GRAVEL, MOIST - BROWN (SM)	FLOOR SLAB AND BACKFILL
2.75'			CONCRETE	FOOTING

BACKHOE REFUSAL ON ROCK AT FOOTING SUBGRADE @ 2.75'

About 3 ft of  
south face exposed  
extending from SE  
corner

Notes on materials at bottom of test pit:

- 1) Gray, hard, slightly weathered schist rock, thinly bedded.
- 2) ENE strike, very steep dip (appears to be greater than 70° north).
- 3) Contact between footing concrete and bedrock continuous.





- 7) Water being pumped from test pit during our observations. Did not reach a stable level while we were on-site.
- 8) See TP-2H (east face) for water level.
- 9) Strand of yellow wire extending about 3 inches from beneath footing at a point about 13 ft north of SW corner.
- 10) Contact between footing concrete and bedrock continuous and tight except near mentioned crack area. Along a 2 to 2.5 ft strip there were loose rock fragments which could be pulled from beneath the footing, leaving up to 6 inches deep pit beneath footing subgrade. Pulled fragments from as far as 6 inches back from side face of footing.



SCHNABEL ENGINEERING ASSOCIATES  
 GEOTECHNICAL CONSULTANTS  
 WEST CHESTER, PA.  
 TEST PIT LOG

Contract No. CT870587 Date Started: 6-1-87 Date Ended: 6-1-87  
 Test Pit No. TP-2H (EAST FACE) Surface Elevation: -27.3  
 Project: L'AMBIANCE PLAZA BLDG. Groundwater Elevation: -32.2 (SEE NOTES)  
COLLAPSE INVESTIGATION  
 Location: WASHINGTON AND Equipment for Excavation: CRAWLER MOUNTED  
COURTLAND, BRIDGEPORT, CT HYDRAULIC BACKHOE  
 SEA Representative: C. DeVAULT

Depth	Elev.	Stratum	Description of Soil and Observations	Remarks
	-27.3			
1'			5-6" CONCRETE FINE TO COARSE SILTY SAND FILL WITH GRAVEL, MOIST - BROWN (SM)	FLOOR SLAB AND BACKFILL
			CONCRETE	FOOTING
6'				

BACKHOE REFUSAL ON ROCK AT FOOTING SUBGRADE @ 6'

About 12 ft of east face of footing exposed extending north from SE corner.

Notes on materials at bottom of test pit:

- 1) Water in test pit at time of observations. Not removed entirely by sumps during observations.
- 2) Water level assumed to be perched in rock surface from coring water and recent test boring work.
- 3) Follow-up observations 6-17-87, water level at 4.9 ft depth, EL -32.2. Water noted flowing into west face of test pit through fissures.
- 4) With water in test pit, observations of subgrade made by probing and feeling materials and interface between footing and rock.
- 5) Hard rock at bottom of test pit elevation comparable to footing subgrade.
- 6) Contact between footing concrete and bedrock feels continuous.

SCHNABEL ENGINEERING ASSOCIATES  
 GEOTECHNICAL CONSULTANTS  
 WEST CHESTER, PA.  
 TEST PIT LOG

Contract No. CT870587 Date Started: 6-1-87 Date Ended: 6-1-87  
 Test Pit No. TP-10D (SOUTH FACE) Surface Elevation: -27.3  
 Project: L'AMBIANCE PLAZA BLDG. Groundwater Elevation: DRY  
COLLAPSE INVESTIGATION  
 Location: WASHINGTON AND Equipment for Excavation: CRAWLER MOUNTED  
COURTLAND, BRIDGEPORT, CT SEA Representative: C. DeVAULT

Depth	Elev.	Stratum	Description of Soil and Observations	Remarks
1'	-27.3		4" CONCRETE FINE TO COARSE SILTY SAND FILL WITH GRAVEL, MOIST - BROWN (SM)	FLOOR SLAB AND BACKFILL
			CONCRETE	FOOTING
4.5'				

BACKHOE REFUSAL ON ROCK AT FOOTING SUBGRADE AT ABOUT 4.5'

About 6 ft of south face exposed extending from SW corner

Notes on materials at bottom of test pit:

- 1) Gray, moderately hard, moderately weathered schist.
- 2) ENE strike, very steep dip (appears to be 85° + north).
- 3) Contact between footing concrete and rock continuous.
- 4) Water at 4.6 ft depth (6-1-87).
- 5) Subgrade dry 6-17-87.





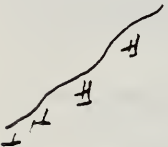
- Gray, moderately weathered, medium to moderately hard schist.
- Highly fractured, both vertically and horizontally. Rock fragments/blocks can easily be removed by hand.
- Void spaces between rock bedding planes and fractures up to 1/2 inch width probed to 3 inch depth.
- Rock fragments appear to have been loosened from natural orientation.



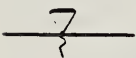
- Silt, sand rock fragment fill, moist - brown.



- Golf-ball size gravel piece.



- Gray, slightly weathered, hard schist.
- ENE strike, very steep dip (nearly vertical).



- Water level measured at EL -32.5 (18 inches below bottom of footing).

SCHNABEL ENGINEERING ASSOCIATES  
 GEOTECHNICAL CONSULTANTS  
 WEST CHESTER, PA.  
 TEST PIT LOG

Contract No. CT870587 Date Started: 6-1-87 Date Ended: 6-1-87  
 Test Pit No. TP-10F (WEST FACE) Surface Elevation: -27.3  
 Project: L'AMBIANCE PLAZA BLDG. Groundwater Elevation: DRY  
COLLAPSE INVESTIGATION  
 Location: WASHINGTON AND Equipment for Excavation: CRAWLER MOUNTED  
COURTLAND, BRIDGEPORT, CT SEA Representative: C. DeVAULT  
HYDRAULIC BACKHOE

Depth	Elev.	Stratum	Description of Soil and Observations	Remarks
- 1' -	-27.3		6" CONCRETE FINE TO COARSE SILTY SAND FILL WITH GRAVEL, MOIST - <u>BROWN</u>	FLOOR SLAB AND BACKFILL
- 3.7' -			CONCRETE	FOOTING

BACKHOE REFUSAL ON ROCK AT FOOTING SUBGRADE @ 3.7'

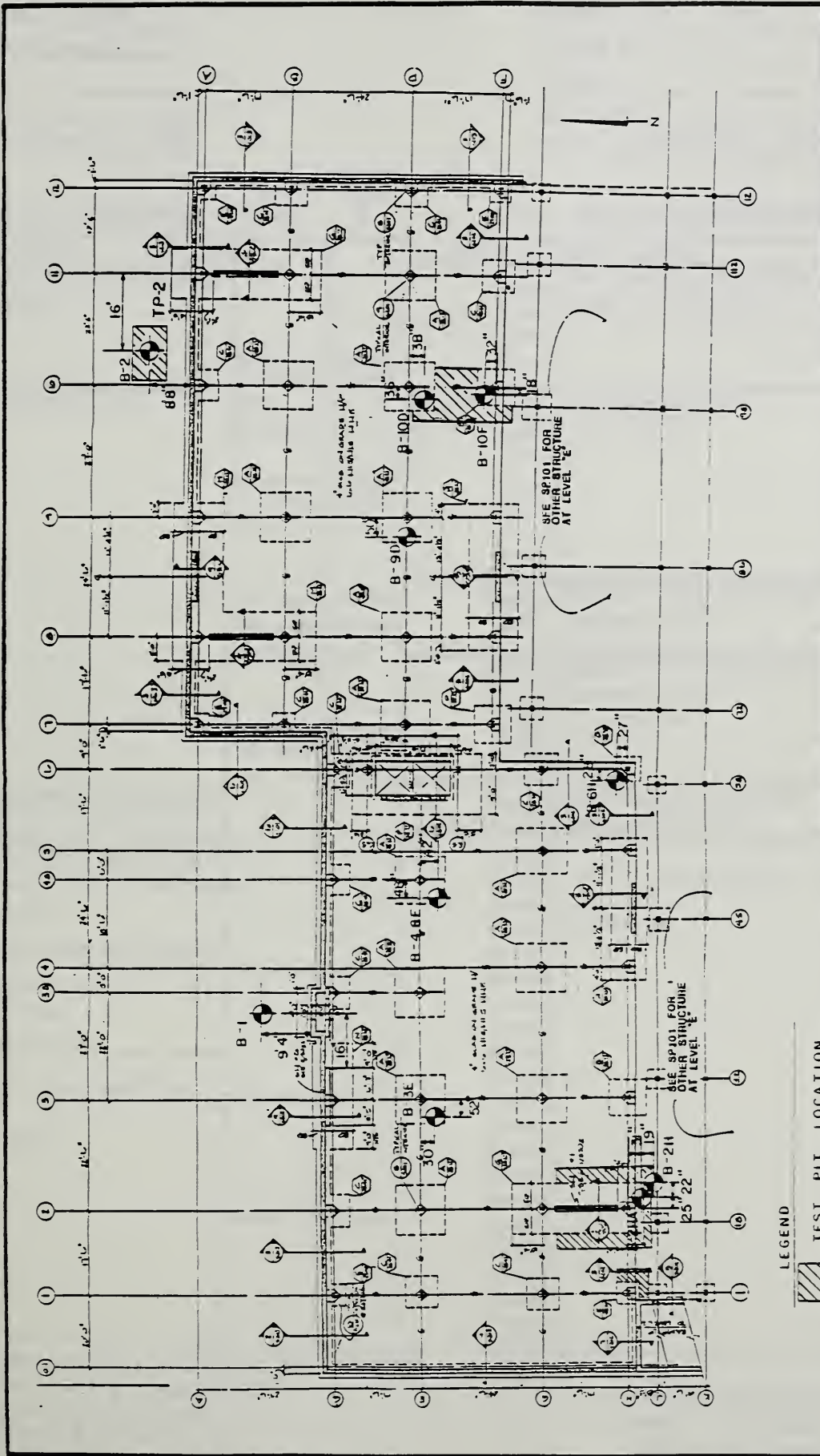
About 4 to 4.5 ft  
of west face ex-  
posed extending  
from NW corner.

Notes on materials at bottom of test pit:

- 1) Gray, hard to moderately hard, slightly to moderately weathered schist, thinly bedded.
- 2) ENE strike, very steep dip.
- 3) Contact between footing concrete and bedrock continuous.

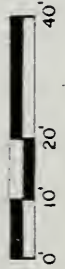








**SCHINABEL**  
ENGINEERING  
ASSOCIATES  
CONSULTING GEOLOGICAL ENGINEERS AND GEOGRAPHERS  
17 LAMBANCE PLAZA, WASHINGTON AND COURTLAND  
STREETS, BRIDGEPORT, CONNECTICUT  
TEST BORING AND  
TEST PIT  
LOCATION PLAN  
CIR 0587

DATE: 11-20-64  
DRAWN BY: JIG  
CHECKED BY: JIG  
SCALE: 1"=20'



- LEGEND**
-  TEST PIT LOCATION
  -  TEST BORING LOCATION

PREVIOUS TEST BORINGS BY OTHERS

**TEST BORING REPORT**

PROJ. \_\_\_\_\_  
 CLIENT T P M INTERNATIONAL, INC.

BORING NO. PS-1  
 LINE & STA. \_\_\_\_\_  
 OFFSET \_\_\_\_\_  
 GR. ELEV. \_\_\_\_\_  
 DATE October 23, 1985

BORING NO. PS-2  
 LINE & STA. \_\_\_\_\_  
 OFFSET \_\_\_\_\_  
 GR. ELEV. \_\_\_\_\_  
 DATE October 22, 1985

A STRATUM DESCRIPTION		DENSITY OR CONSIST.	BLOWS PER 6" B
3	Bit. Concr.		
	Br. M-F Sand & Grav., Cobbles.		
	"	V. Comp Dry	10-21 35
0	Decomposed Rock		
	"	V. Comp Dry	23-31 36
	"	No sample due to C. material	
	"	No sample due to C. material	
3.5	Run#1: 23.5 to 25.0 Recovery: 12" Fractured.		
	Run#2: 25.0 to 28.5 Recovery: 54" Fractured Phyllite		
5	Run#3: 28.5 to 33.5 Recovery: 21" Fractured		
5	End of Boring-33.5 GWO-None		

A STRATUM DESCRIPTION		DENSITY OR CONSIST.	BLOWS PER 6" B
0.2	Bit. Concr.		
	Br. M-F Silty Sand, some C-F Grav.		
	"	M. Comp Dry	7-10 13
	Decomposed Rock		
	"	Dense Dry: Rec: 0"	50/2"
	Run#1: 14.0 to 17.0 Recovery: 23"		
	Phyllites		
	Run#2: 17.0 to 22.5 Recovery: 72" Fractured		
	Run#3: 22.5 to 24.0 Recovery: 13"		
	End of Boring-24.0 GWO-None		

- 1 COL. A Blows on Casing \* DRILL TIME PER FOOT
- 2 COL. B Blows on 1 1/2" Sampler (I.D.)
- 3 HAMMER = 140#, FALL 30"
- 4 SAMPLER = O. D. SPLIT SPOON
- 5 GWO = GROUND WATER OBSERVATIONS

**FIELD — % CONTENT**  
 AND — 40 to 50%  
 SOME — 10 to 40%  
 TRACE — 0 to 10%



**TEST BORING REPORT**

BORING NO. 1  
 LINE & STA. \_\_\_\_\_  
 OFFSET \_\_\_\_\_  
 GR. ELEV. \_\_\_\_\_  
 DATE July 18, 1985

BORING NO. 3  
 LINE & STA. \_\_\_\_\_  
 OFFSET \_\_\_\_\_  
 GR. ELEV. \_\_\_\_\_  
 DATE July 11, 1985

A STRATUM DESCRIPTION		DENSITY OR CONSIST.	BLOWS PER 6" B
1.0	Topsoil		
	Red Br. M-F Silty Sand, some F. Grav.		
	"	Comp Dry	16-17 21
11.0	"	Dense Dry	13-10 50
14.0	Decomp. Rock		
19.0	10 Gneiss 12 Run#1: 14.0 to 19.0 12 Recovery: 12" 11 Fractured & Seamy 12		
	End of Boring-19.0 GWO-None		

A STRATUM DESCRIPTION		DENSITY OR CONSIST.	BLOWS PER 6" B
	Br. M-F Sand, Tr. M-F Grav., Tr. Decomp. Rock, Rock Frags.		
	"	Dense Dry	10-25 50
	"	Dense Dry	50/1"
	"	Dense Dry	50
20.0	10 Gneiss 12 Run#1: 20.0 to 25.0 15 Recovery: 20 " 15 Fractured & Seamy		
25.0	10		
	End of Boring-25.0 GWO-None		

- 1 COL. A Blows on Casing \* DRILL TIME PER FOOT
- 2 COL. B Blows on 1 3/8" Sampler (I.D.)
- 3 HAMMER = 140#, FALL 30"
- 4 SAMPLER = O. D. SPLIT SPOON
- 5 GWO = GROUND WATER OBSERVATIONS

FIELD — % CONTENT  
 AND — 40 to 50%  
 SOME — 10 to 40%  
 TRACE — 0 to 10%

**TEST BORING REPORT**

BORING NO. 2  
 LINE & STA. \_\_\_\_\_  
 OFFSET \_\_\_\_\_  
 GR. ELEV. \_\_\_\_\_  
 DATE June 26, 1985

BORING NO. 17  
 LINE & STA. \_\_\_\_\_  
 OFFSET \_\_\_\_\_  
 GR. ELEV. \_\_\_\_\_  
 DATE June 26, 1985

A STRATUM DESCRIPTION		DENSITY OR CONSIST.	BLOWS PER 6" B
0.2	Bit. Concr.		
3.0	Blk. M-F Silty Sand		
	Br. M-F Silty Sand, some M-C Grav., Tr. Mica	V. Comp Dry	17-30 21
	"	V. Comp Dry	18-25 26
12.0	Decomposed Rock Fragm. Br. M-F Sand.		
16.0	"	Dense Dry	50/5"
	17 Gneiss		
	17 Run#1: 16.0 to 21.0		
	19 Recovery: 18"		
	20 Fractured & Seamy		
21.0	19		
	End of Boring-21.0		
	GWO- None		

A STRATUM DESCRIPTION		DENSITY OR CONSIST.	BLOWS PER 6" B
0.1	Bit. Concr.		
2.5	Blk. M-F Silty Sand, some M-F Grav.		
4.0	Br. M-F Silty Sand		
5.0	Decomposed Rock		
	8 Gneiss		
	8 Run#1: 5.0 to 10.0		
	7 Recovery: 12"		
	10 Fractured & Seamy		
10.0	9		
	End of Boring-10.0		
	GWO-None		

- 1 COL. A Blows on Casing \* DRILL TIME PER FOOT
- 2 COL. B Blows on 1 3/8" Sampler (I.D.)
- 3 HAMMER = 140#, FALL 30"
- 4 SAMPLER = O. D. SPLIT SPOON
- 5 GWO = GROUND WATER OBSERVATIONS

FIELD — % CONTENT  
 AND — 40 to 50%  
 SOME — 10 to 40%  
 TRACE — 0 to 10%

TEST BORING REPORT

Apartment Complex, Washington Ave.  
 Bridgeport, Connecticut

PROJ. \_\_\_\_\_  
 CLIENT T P M INTERNATIONAL, INC.

BORING NO. 4  
 LINE & STA. \_\_\_\_\_  
 OFFSET \_\_\_\_\_  
 GR. ELEV. \_\_\_\_\_  
 DATE July 11, 1985

BORING NO. 5  
 LINE & STA. \_\_\_\_\_  
 OFFSET \_\_\_\_\_  
 GR. ELEV. \_\_\_\_\_  
 DATE July 16, 1985

A STRATUM DESCRIPTION		DENSITY OR CONSIST.	BLOWS PER 6" B
	Br. M-F Sand, Tr. M-F Grav., Tr. Decomp. Rock frags.		4.0
	"	M. Comp Dry	10-7 7
	"	Dense Dry	13-20 21
14.5			10.0
10	Gneiss		15.0
10	Run#1: 14.5 to 19.5		
12	Recovery: 31"		
10	Fractured & Seamy		
19.5			
	End of Boring-19.5		
	GWO- None		

A STRATUM DESCRIPTION		DENSITY OR CONSIST.	BLOWS PER 6" B
	Dark Br. M-F Silty Sand, some M-F Grav.		
	Decomp. Rock		
	"	Comp Dry	10-21 20
	Gneiss		7
	Run#1: 10.0 to 15.0		11
	Recovery: 22"		12
	Fractured & Seamy		10
			15
	End of Boring-15.0		
	GWO-None		

- 1 COL. A Blows on Casing \* DRILL TIME PER FOOT
- 2 COL. B Blows on 1 3/8" Sampler (I.D.)
- 3 HAMMER = 140#, FALL 30"
- 4 SAMPLER = O. D. SPLIT SPOON
- 5 GWO = GROUND WATER OBSERVATIONS

FIELD - % CONTENT  
 AND - 40 to 50%  
 SOME - 10 to 40%

**TEST BORING REPORT**

PROJ. Bridgeport, Connecticut  
 CLIENT T P M INTERNATIONAL, INC.

BORING NO. 6

LINE & STA. \_\_\_\_\_

OFFSET \_\_\_\_\_

GR. ELEV. \_\_\_\_\_

DATE July 16, 1985

BORING NO. 7

LINE & STA. \_\_\_\_\_

OFFSET \_\_\_\_\_

GR. ELEV. \_\_\_\_\_

DATE July 15, 1985

**A STRATUM DESCRIPTION**

DENSITY OR CONSIST. B

**A STRATUM DESCRIPTION**

DENSITY OR CONSIST. B

	STRATUM DESCRIPTION	DENSITY OR CONSIST.	B
	Dark Br. M-F Sand, some M-F Grav., Cobbles		
	"	Loose Dry	2-2 3
8.0			8.0
	Lt. Br. M-F Sand, some M-F Grav.		10.0
	"	Dense Dry	50
14.0			
12	Gneiss		15.0
12	Run#1:14.0 to 19.0		
10	Recovery:8.0		
10	Fractured & Seamy with decomp. rock		
19.0			
	End of Boring-19.0		
	GWO=None		

	STRATUM DESCRIPTION	DENSITY OR CONSIST.	B
	Black Ash, Glass, Brick Pcs., Fill Area.		
	"	Loose Dry	2-2 4
	Decomp. Rock		
11	Gneiss		
7	Run#1: 10.0 to 15.0		
13	Recovery: 24"		
10	Fractured & Seamy with Decomp. Rock		
19			
	End of Boring-15.0		
	GWO=None		

- 1 COL. A Blows on Casing \* DRILL TIME PER FOOT
- 2 COL. B Blows on 1 3/4" Sampler (I.D.)
- 3 HAMMER = 140#, FALL 30"
- 4 SAMPLER = O. D. SPLIT SPOON
- 5 GWO = GROUND WATER OBSERVATIONS

**FIELD — % CONTENT**  
 AND — 40 to 50%  
 SOME — 10 to 40%  
 TRACE — 0 to 10%



**TEST BORING REPORT**

Apartment Complex, Washington Ave.  
 Bridgeport, Connecticut  
 PROJ. \_\_\_\_\_  
 CLIENT T P M INTERNATIONAL, INC.

BORING NO. 8  
 LINE & STA. \_\_\_\_\_  
 OFFSET \_\_\_\_\_  
 GR. ELEV. \_\_\_\_\_  
 DATE July 15, 1985

BORING NO. 9  
 LINE & STA. \_\_\_\_\_  
 OFFSET \_\_\_\_\_  
 GR. ELEV. \_\_\_\_\_  
 DATE July 15, 1985

A STRATUM DESCRIPTION		DENSITY OR CONSIST.	BLOWS PER 6" B
	Br. M-F Sand & Grav., Cobbles.		
4.0			3.0
5.0	Decomp. Rock		
12	Gneiss		
12	Run#1: 5.0 to 10.0		
10	Recovery: 12"		7.5
10	Fractured & Seamy with Decomp. Rock		
10.0			
	End of Boring-10.0		
	GWO-None		12.5

A STRATUM DESCRIPTION		DENSITY OR CONSIST.	BLOWS PER 6" B
	Br. M-F Sand, some M-F Grav.		
	Decomp. Rock		
	"	Dense Bry	13-50
13	Gneiss		
11	Run#1: 7.5 to 12.5		
19	Recovery: 42"		
14	Fractured & Seamy		
12			
	End of Boring-12.5		
	GWO-None		

- 1 COL. A Blows on Casing \* DRILL TIME PER FOOT
- 2 COL. B Blows on 1 3/8" Sampler (I.D.)
- 3 HAMMER = 140#, FALL 30"
- 4 SAMPLER = O. D. SPLIT SPOON
- 5 GWO = GROUND WATER OBSERVATIONS

FIELD - % CONTENT  
 AND - 40 to 50%  
 SOME - 10 to 40%

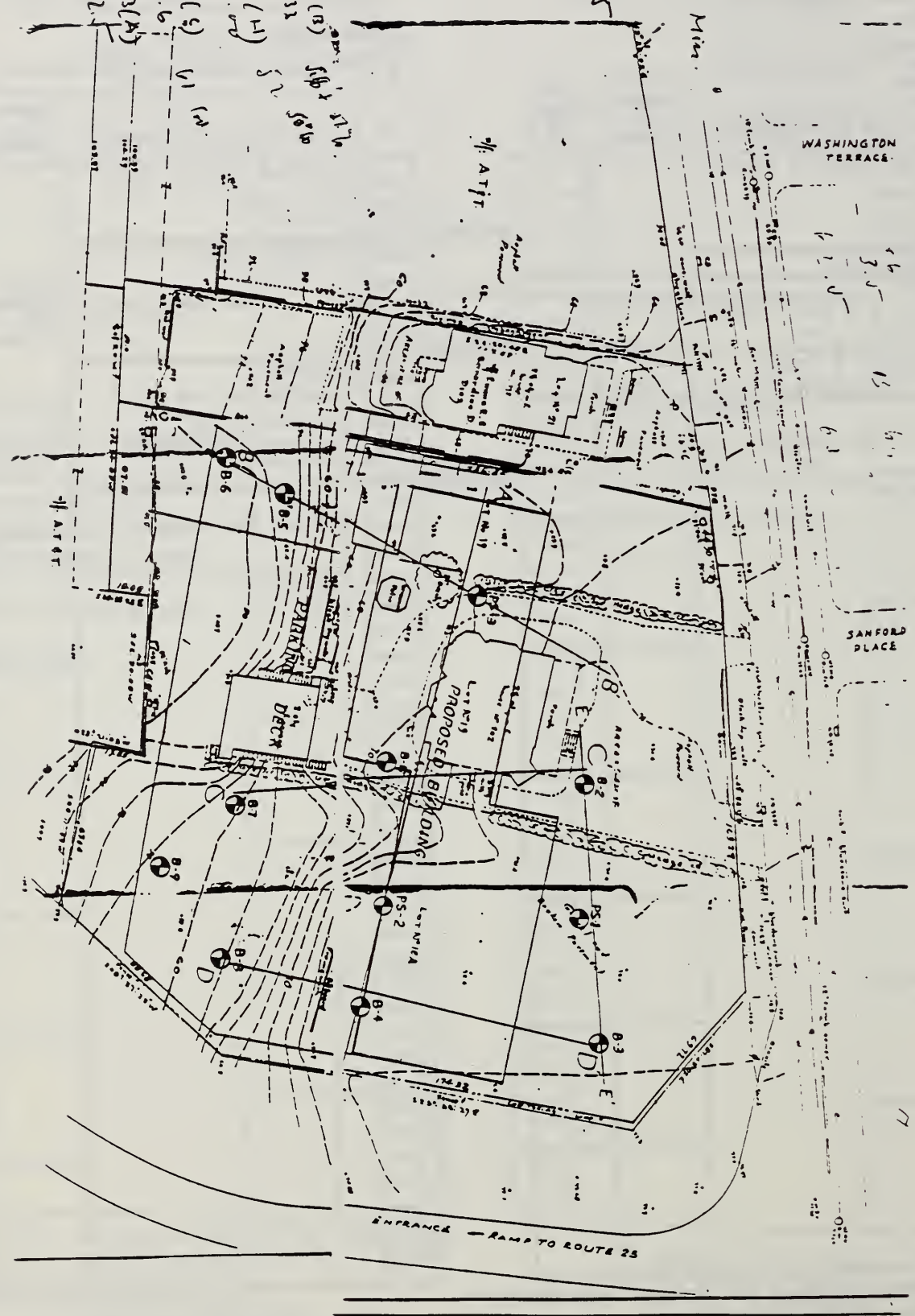
84.33  
-27.33

Slack 57.2  
3.33

1/2 of Ely 63.9  
Miles

A (incl.) 62.5

B-7 1/2 E-10 (B) 50.0  
1.5 50.0 52.33  
PS-2 16 F-19 (H) 51.0  
V2  
B-7 71 G-16 (S) V1 (A) 53.6  
66 10.0  
PS-13  
E-3 (A) 62.1



BIBLIOGRAPHY

BIBLIOGRAPHY

- (1) Bowles, Joseph E., (1968), Foundation Analysis and Design, McGraw Hill, New York, 659 pp.
- (2) Bowles, Joseph E., (1982), Foundation Analysis and Design, 3rd Edition, Table 5, McGraw Hill, New York.
- (3) Gardner, W.S., (1987), "Design of Drilled Piers in the Atlantic Piedmont", Foundations and Excavations in Decomposed Rock of the Piedmont Province, Geotechnical Special Publication No. 9, ASCE, April 28, 1987, pp. 62-86.
- (4) Lambe, T. William, and Whitman, Robert V., (1969), Soil Mechanics, John Wiley and Sons, New York, 553 pp.
- (5) Martin, R.E., (1987), "Settlement of Residual Soils", Foundations and Excavations in Decomposed Rock of the Piedmont Province, Geotechnical Special Publication No. 9, ASCE, April 28, 1987, pp. 1-14.
- (6) Meyerhof, C.G., (1956), "Penetration and Bearing Capacity in Cohesive Soils", Journal of Soil Mechanics and Foundation Division, ASCE, Vol. 82, No. SM 1.
- (7) NAVFAC DM-7.1, (1982), Soil Mechanics, Department of the Navy, Alexandria.
- (8) Riggs, Charles O., Mathes, Gary M., and Rassieur, Charles L., (1984), "A Field Study of an Automatic SPT Hammer System", reprint from Geotechnical Testing Journal, September 1984.
- (9) Schmertmann, J.H., Hartman, J.P., and Brown, P.R., "Improved Strain Influence Factor Diagrams", Journal of the Geotechnical Division, ASCE, Vol. 104, No. GT8, August 1978, pp. 1131-1135.
- (10) Sowers, George F., (1979), Soil Mechanics and Foundations: Geotechnical Engineering, MacMillan Publishing Co., New York, 621 pp.
- (11) Winterkorn, Hans F., and Fang, Hsai-Yang, Editors, (1975), Foundation Engineering Handbook, Van Nostrand Reinhold Company, New York, 751 pp.

APPENDIX C

Resistance Criteria for Columns and Floor Slabs

APPENDIX C

RESISTANCE CRITERIA FOR COLUMNS AND FLOOR SLABS

Columns

AISC - Reference 8

$$P_n = A_g F_{cr}$$

for  $\lambda_c \leq 1.5$

$$F_{cr} = (0.658 \frac{\lambda_c^2}{c}) F_y$$

for  $\lambda_c \geq 1.5$

$$F_{cr} = \left[ \begin{array}{c} 0.877 \\ \text{---} \\ 2 \\ \text{---} \\ c \end{array} \right] F_y$$

where

$$\lambda_c = \frac{Kl}{r\pi} \sqrt{\frac{F_y}{E}}$$

$P_n$  = nominal axial strength

$A_g$  = gross area of member, in.<sup>2</sup>

$F_y$  = specified yield stress, ksi

$E$  = modulus of elasticity, ksi

$K$  = effective length factor

$l$  = unbraced length of member, in.

$r$  = governing radius of gyration about plane of buckling, in.

Floor Slabs

ACI - Reference 2

Punching Shear

$$V_n = V_c = (3.5\sqrt{f'_c} + 0.3f_{pc})b_o d + V_p$$

where  $V_n$  = nominal shear force

$f'_c$  = specified compressive strength of concrete, psi

$f_{pc}$  = average value of effective stress at centroid of section

$b_o$  = perimeter of critical section

$d$  = structural depth of slab at support

$V_p$  = vertical component of effective prestress forces, taken as zero for this analysis.

Alternatively, for exterior columns having a slab edge distance less than four times the slab thickness, shear capacity is calculated as for a nonprestressed slab, where:

$$V_c = (2 + 4/\beta_c) \sqrt{f'_c} b_o d$$

where  $\beta_c$  = ratio of lengths of long, short sides of reaction area  
 $b_o$  = perimeter of critical section  
 $d$  = structural depth of slab at critical section

#### Moment Capacity

$M_N$  =  $A_{ps} f_{ps} (d-a/2)$   
 $M_N$  = Nominal moment capacity of unit width strip of slab  
 $A_{ps}$  = area of prestressing strand  
 $f_{ps}$  = effective stress in prestressing strand  
 $d$  = depth from extreme compression fiber to centroid of prestressing strand at location where moment is evaluated  
 $a$  = depth of uniform compression stress block at nominal moment capacity based on ACI assumptions of stress block

U.S. DEPT. OF COMM. <b>BIBLIOGRAPHIC DATA SHEET</b> <i>(See instructions)</i>	1. PUBLICATION OR REPORT NO. NBSIR 87-3640	2. Performing Organ. Report No.	3. Publication Date
4. TITLE AND SUBTITLE INVESTIGATION OF L'AMBIANCE PLAZA BUILDING COLLAPSE IN BRIDGEPORT, CONNECTICUT			
5. AUTHOR(S) Charles G. Culver, Charles F. Scribner, Richard D. Marshall, Felix Y. Yokel, John L. Gross, Charles W. C. Yancey, Erik M. Hendrickson			
6. PERFORMING ORGANIZATION <i>(If joint or other than NBS, see instructions)</i> <b>NATIONAL BUREAU OF STANDARDS          U.S. DEPARTMENT OF COMMERCE          GAITHERSBURG, MD 20899</b>		7. Contract/Grant No. 8. Type of Report & Period Covered	
9. SPONSORING ORGANIZATION NAME AND COMPLETE ADDRESS <i>(Street, City, State, ZIP)</i> The Occupational Safety & Health Administration Department of Labor Washington, D.C. 20001			
10. SUPPLEMENTARY NOTES  <input type="checkbox"/> Document describes a computer program; SF-185, FIPS Software Summary, is attached.			
11. ABSTRACT <i>(A 200-word or less factual summary of most significant information. If document includes a significant bibliography or literature survey, mention it here)</i>  Results from an investigation to determine the cause of the collapse of the L'Ambiance Plaza building on April 23, 1987 are presented. The building was being constructed using the lift-slab method; collapse occurred during construction. The investigation included on-site inspections immediately following the collapse, review of eyewitness accounts of the collapse, review of project documentation, laboratory and field tests and analyses of the structure. Several potential failure mechanisms were investigated. The most probable cause of the collapse was determined to be loss of support at a lifting jack in the west tower during placement of an upper level package of three floor slabs. The loss of support was likely due to excessive deformation of the lifting angle in a shearhead followed by a lifting nut slipping off the lifting angle of the shearhead. The postulated failure mechanism was duplicated in laboratory experiments. The local failure propagated as loads were redistributed. The remaining jack rods along column line E supporting the package of floor slabs slipped off the lifting angles and the slabs failed in flexure and shear. These slabs fell causing the lower level slabs to fail.			
12. KEY WORDS <i>(Six to twelve entries; alphabetical order; capitalize only proper names; and separate key words by semicolons)</i> building; collapse, concrete; construction failure; lift-slab construction; post-tensioned concrete; progressive collapse.			
13. AVAILABILITY <input checked="" type="checkbox"/> Unlimited <input type="checkbox"/> For Official Distribution. Do Not Release to NTIS <input type="checkbox"/> Order From Superintendent of Documents, U.S. Government Printing Office, Washington, D.C. 20402. <input checked="" type="checkbox"/> Order From National Technical Information Service (NTIS), Springfield, VA. 22161		14. NO. OF PRINTED PAGES 314 15. Price	





